

UNIVERSITY OF SOUTHAMPTON

Approaches Towards the Automated Interpretation and  
Prediction of ES-MS/MS Spectra of Non-Peptidic,  
Pharmaceutical, Combinatorial Compounds

Aikaterini Maria Klagkou

Doctor of Philosophy

Faculty of Science

School of Chemistry

September 2003

UNIVERSITY OF SOUTHAMPTON

ABSTRACT

FACULTY OF SCIENCE

CHEMISTRY

Doctor of Philosophy

Approaches Towards the Automated Interpretation and Prediction of ES-MS/MS Spectra of Non-Peptidic, Pharmaceutical, Combinatorial Compounds

by Aikaterini Maria Klagkou

Electrospray tandem mass spectrometry is currently widely used in protein sequencing. The knowledge of the dissociation trends of peptidic molecules allows detailed identification of the amino acid residues and to a certain extent successful characterisation of unknown peptidic compounds. The process of protein identification is frequently aided by interpretive AI software packages that offer fast and simple ways for manipulating the ES-MS/MS data.

Identification of non-peptidic molecules using a similar automated approach is, at the moment, a challenge. The dissociation pathways of non-peptidic compounds vary for each class of molecules and general rules have not been established. The ionisation and fragmentation mechanisms taking place under ES-MS/MS conditions have also not been identified and therefore electron ionisation rules are often employed by the AI packages in order to overcome this problem. This approach leads to a very low success rate when it comes to identifying an unknown non-peptidic molecule from its ES-MS/MS spectrum.

The aim of this investigation was to develop existing interpretive software packages such that they take account of the specific fragmentation pathways and mechanisms involved in ES-MS/MS. Sub-libraries of non-peptidic, combinatorial molecules were studied and specific rules for their dissociation were established. This allowed pattern recognition methods to be used. Throughout this work, detailed mechanisms and fragmentation pathways together with the sites of ionisation have been investigated. Incorporation of the findings into an AI software package should enable the rapid characterisation of the components of combinatorial libraries using ES-MS/MS only.

---

**Contents**

	Page Number
<b>List of Figures</b> .....	<b>1</b>
<b>List of Tables</b> .....	<b>5</b>
<b>Preface</b> .....	<b>7</b>
<b>Acknowledgements</b> .....	<b>8</b>
<b>Abbreviations</b> .....	<b>9</b>
<b>Chapter 1: Introduction</b>	
1a. Overview.....	<b>11</b>
1b. Instrumentation.....	<b>15</b>
1c. Mass Frontier.....	<b>23</b>
<b>Chapter 2: The Fragmentation Patterns of Six Groups of Non-Peptidic Compounds</b>	
2a. Introduction.....	<b>29</b>
2b. Experimental.....	<b>29</b>
2c. Results and Discussion.....	<b>30</b>
<i>The Fragmentation Pathway of Carnitines</i> .....	<b>30</b>
<i>The Fragmentation Pathway of Pheniramines and Disopyramides</i> .....	<b>33</b>
<i>The Fragmentation Pathway of Purines</i> .....	<b>33</b>
<i>The Fragmentation Pathway of Benzimidazoles</i> .....	<b>36</b>
<i>The Fragmentation Pathway of Amphetamines</i> .....	<b>38</b>
<i>The Fragmentation Pathway of 3-Alkylamino-imidazo-[1,2-<math>\alpha</math>]azines</i> .....	<b>39</b>
2d. Conclusion.....	<b>40</b>
<b>Chapter 3: The Fragmentation Pattern of an Array of Amino Acids</b>	
3a. Introduction.....	<b>42</b>
3b. Experimental.....	<b>42</b>
3c. Results and Discussion.....	<b>43</b>
3d. Conclusion.....	<b>56</b>
<b>Chapter 4: The Fragmentation Pattern of a Combinatorial Library</b>	
4a. Introduction.....	<b>58</b>
4b. Experimental.....	<b>58</b>
4c. Results and Discussion.....	<b>59</b>
<i>The Fragmentation Pathway of Amino-Sulphonamides</i> .....	<b>60</b>
<i>The Fragmentation Pathway of Acetylated Amino-Sulphonamides</i> .....	<b>66</b>
<i>The Fragmentation Pathway of Methyl-Sulphonamides</i> .....	<b>67</b>
<i>The Fragmentation Pathway of Non-Substituted Benzenesulphonamides</i> .....	<b>70</b>
<i>The Fragmentation Pathway of a Group of Various Sulphonamides</i> .....	<b>73</b>
4d. Molecular Modelling Calculations.....	<b>74</b>
4e. Conclusion.....	<b>75</b>

---

---

<b>Chapter 5: Identification of Unknown Non-Peptidic Molecules From Their ES-MS/MS Spectra: Automated Approach and Limitations</b>	
5a. Introduction.....	77
5b. Experimental .....	77
5c. Results and Discussion .....	78
5d. Conclusion .....	86
<b>Chapter 6: Comparison of the Fragmentation Patterns Observed for Three Sets of Compounds on Different Trap Instruments</b>	
6a. Introduction.....	87
6b. Experimental .....	87
6c. Theory of Operation of the Linear Trap .....	88
6d. Results and Discussion.....	90
6e. Conclusion .....	91
<b>Chapter 7: Conclusion and Further Applications</b> .....	93
<b>Appendix 1</b> .....	97
<b>Appendix 2</b> .....	107
<b>Appendix 3</b> .....	115
<b>Appendix 4</b> .....	124
<b>Appendix 5</b> .....	130
<b>List of References</b> .....	140

---

## Figures

	Page Number
<b>Chapter 1, Figure 1:</b> The Split and Mix approach is combinatorial chemistry .....	12
<b>Chapter 1, Figure 2:</b> The common types of background ions arising from backbone cleavages of protonated linear peptides.....	14
<b>Chapter 1, Figure 3:</b> The basic components of any mass spectrometer.....	15
<b>Chapter 1, Figure 4:</b> Schematic representation of electrospray ionisation.....	16
<b>Chapter 1, Figure 5:</b> The quadrupole ion trap.....	18
<b>Chapter 1, Figure 6:</b> Schematic representation of the cubic analyser cell .....	19
<b>Chapter 1, Figures 7a, 7b and 7c:</b> The three fundamental motions of the ion in the analyser cell .....	21
<b>Chapter 1, Figure 8:</b> Ion excitation and detection in the analyser cell .....	22
<b>Chapter 1, Figure 9:</b> Mass Frontier-Spectra Manager .....	24
<b>Chapter 1, Figure 10:</b> Mass Frontier-Structure Editor.....	24
<b>Chapter 1, Figure 11:</b> Mass Frontier-Fragments and Mechanisms .....	25
<b>Chapter 1, Figure 12:</b> Mass Frontier-Spectra Classifier and Spectra Projector.....	25
<b>Chapter 1, Figure 13:</b> Plot of two mass spectra in a three-dimensional space, based on multivariate statistics .....	26
<b>Chapter 1, Figure 14:</b> Geometrical interpretation of PCA .....	27
<b>Chapter 2, Figure 15:</b> The ES-MS/MS spectrum of propionylcarnitine .....	30
<b>Chapter 2, Figure 16:</b> The main fragment ions of carnitines.....	31
<b>Chapter 2, Figure 17:</b> The ES-MS/MS spectrum of valeryl carnitine butyl ester.....	31
<b>Chapter 2, Figure 18:</b> The main fragment ions of carnitine butyl esters .....	32
<b>Chapter 2, Figure 19:</b> The main fragment ions produced by pheniramines and disopyramides .....	33
<b>Chapter 2, Figure 20:</b> The ES-MS/MS spectrum of proxiphylline .....	35
<b>Chapter 2, Figure 21:</b> The main fragment ions observed for purines with aliphatic chains attached .....	35
<b>Chapter 2, Figure 22:</b> The ES-MS/MS spectrum of thiabendazole.....	36
<b>Chapter 2, Figure 23:</b> The ES-MS/MS spectrum of carbendazim.....	36
<b>Chapter 2, Figure 24:</b> The ES-MS/MS spectrum of d-labelled carbendazim .....	37
<b>Chapter 2, Figure 25:</b> The tautomeric structures of benzimidazoles with a carbamate substituent attached on the 2'-position of the benzimidazole ring.....	37
<b>Chapter 2, Figure 26:</b> The main fragment ions produced by amphetamines under ES-MS/MS conditions.....	38
<b>Chapter 2, Figure 27:</b> The ES-MS/MS spectrum of 2-(4-methoxyphenyl)-N-(1,1,3,3-tetramethyl butyl)imidazo[1,2- $\alpha$ ]-puridin-3-amine.....	39
<b>Chapter 2, Figure 28:</b> The main fragment ions produced by the group of 3-alkylamino-imidazo-[1,2- $\alpha$ ]azines studied.....	40

<b>Chapter 3, Figure 29:</b> The ES-MS/MS spectrum of valine.....	<b>43</b>
<b>Chapter 3, Figure 30:</b> The ES-MS/MS spectrum of 3,4-dihydroxyphenylalanine.....	<b>44</b>
<b>Chapter 3, Figure 31:</b> The three main mechanisms leading to the loss of 46 Da, as proposed in literature .....	<b>46</b>
<b>Chapter 3, Figure 32:</b> The mechanism proposed by Rogalewicz <i>et al</i> for the loss of 46 Da from amino acids under ES-MS/MS conditions .....	<b>46</b>
<b>Chapter 3, Figure 33:</b> The ES-MS/MS spectra obtained for valine, methionine, phenylalanine and tyrosine on the LCQ ion trap with wideband excitation off.....	<b>47</b>
<b>Chapter 3, Figure 34:</b> The ES-MS/MS spectra of valine, methionine, tyrosine and phenylalanine obtained during d-labelling experiments.....	<b>48</b>
<b>Chapter 3, Figure 35:</b> The ES-MS/MS spectrum of 3,4-dihydroxyphenylalanine butyl ester .....	<b>49</b>
<b>Chapter 3, Figure 36:</b> The ES-MS/MS spectrum of threonine methyl ester.....	<b>50</b>
<b>Chapter 3, Figure 37:</b> The ES-MS/MS spectrum of fully labelled threonine methyl ester ... ..	<b>51</b>
<b>Chapter 3, Figure 38:</b> The ES-MS/MS spectrum of threonine butyl ester.....	<b>51</b>
<b>Chapter 3, Figure 39:</b> Spectra obtained for the methyl ester protected amino acids during d-labelling experiments.....	<b>53</b>
<b>Chapter 3, Figure 40:</b> Application of the mechanism proposed by Meot-Ner to protected amino acids.....	<b>54</b>
<b>Chapter 3, Figure 41:</b> Application of the mechanism proposed by Tsang and Harrison and Rogalewicz <i>et al</i> to protected amino acids .....	<b>55</b>
<b>Chapter 3, Figure 42:</b> Application of the mechanism proposed by Kulik and Herma and Beranová <i>et al</i> to protected amino acids .....	<b>55</b>
<b>Chapter 3, Figure 43:</b> The mechanisms proposed for the loss of formic acid and butyl formate from amino acids and butyl ester amino acids respectively.....	<b>56</b>
<b>Chapter 4, Figure 44:</b> The core structures of the five main sub-groups of the sulphonamide library .....	<b>60</b>
<b>Chapter 4, Figure 45:</b> The ES-MS/MS spectrum of 4-amino- <i>N</i> -(5-methyl-2-pyridinyl)-benzenesulphonamide .....	<b>60</b>
<b>Chapter 4, Figure 46:</b> The ES-MS/MS spectrum of sulphamerazine, acquired on the LCQ ion trap .....	<b>61</b>
<b>Chapter 4, Figure 47:</b> The ES-MS/MS spectrum of sulphadiazine, acquired on the LCQ ion trap .....	<b>61</b>
<b>Chapter 4, Figure 48:</b> The ES-MS/MS spectrum of sulphamethazine, acquired on the LCQ ion trap .....	<b>62</b>
<b>Chapter 4, Figure 49:</b> The ES-MS/MS spectrum of sulphamerazine, acquired on the TSQ triple quadrupole .....	<b>63</b>
<b>Chapter 4, Figure 50:</b> The ES-MS/MS spectrum of sulphadiazine, acquired on the TSQ triple quadrupole .....	<b>63</b>

<b>Chapter 4, Figure 51:</b> The ES-MS/MS spectrum of sulphamethazine, acquired on the TSQ triple quadrupole .....	<b>63</b>
<b>Chapter 4, Figure 52:</b> The ES-MS/MS spectrum of the fully labelled 4-amino- <i>N</i> -(5-methyl-2-pyridinyl)-benzenesulphonamide.....	<b>65</b>
<b>Chapter 4, Figure 53:</b> Mechanisms proposed for the formation of some of the common fragment ions of the amino-sulphonamides.....	<b>65</b>
<b>Chapter 4, Figure 54:</b> The ES-MS/MS spectrum of <i>N</i> -[4-[(5-methyl-2-pyridinyl)amino]sulphonyl]phenyl]-acetamide.....	<b>66</b>
<b>Chapter 4, Figure 55:</b> The ES-MS/MS spectrum of 4-methyl- <i>N</i> -(5-methyl-2-pyridinyl)-benzenesulphonamide .....	<b>67</b>
<b>Chapter 4, Figure 56:</b> The ES-MS/MS spectrum of the fully labelled 4-methyl- <i>N</i> -(5-methyl-2-pyridinyl)-benzenesulphonamide.....	<b>69</b>
<b>Chapter 4, Figure 57:</b> Mechanisms proposed for the formation of some of the common fragment ions of the methyl-sulphonamides.....	<b>70</b>
<b>Chapter 4, Figure 58:</b> The ES-MS/MS spectrum of <i>N</i> -(5-methyl-2-pyridinyl)-benzenesulphonamide .....	<b>70</b>
<b>Chapter 4, Figure 59:</b> The ES-MS/MS spectrum of the fully labelled <i>N</i> -(5-methyl-2-pyridinyl)-benzenesulphonamide .....	<b>72</b>
<b>Chapter 4, Figure 60:</b> Mechanisms proposed for the formation of some of the common fragment ions of the non-substituted benzenesulphonamides.....	<b>73</b>
<b>Chapter 4, Figure 61:</b> The ES-MS/MS spectrum of 4-fluoro- <i>N</i> -2-pyridinyl-benzenesulphonamide .....	<b>73</b>
<b>Chapter 5, Figure 62:</b> Classification of three groups of compounds using PCA .....	<b>80</b>
<b>Chapter 5, Figure 63:</b> The ES-MS/MS spectra of three isomeric sulphonamides.....	<b>81</b>
<b>Chapter 5, Figure 64:</b> The core structure of the ergopeptine alkaloids studied .....	<b>82</b>
<b>Chapter 5, Figure 65:</b> Example of the types of fragment ions and mechanisms generated by Mass Frontier to interpret the spectra of fused ring systems .....	<b>84</b>
<b>Chapter 5, Figure 66:</b> The core structures of sulphonamides and sulphonylureas.....	<b>85</b>
<b>Chapter 5, Figure 67:</b> The ES-MS/MS spectrum of metsulphuron methyl.....	<b>85</b>
<b>Chapter 6, Figure 68:</b> Schematic representation of the linear trap .....	<b>89</b>
<b>Chapter 6, Figure 69:</b> Axial and radial trapping of the ions in the linear trap .....	<b>89</b>
<b>Chapter 6, Figure 70:</b> The ES-MS/MS spectra of a methyl-sulphonamide obtained on the Q Trap using three different scan modes .....	<b>91</b>
<b>Chapter 7, Figure 71:</b> The known metabolites of sulphadiazine .....	<b>95</b>
<b>Chapter 7, Figure 72:</b> General strategy for the use of MS/MS for the detection and identification of metabolites.....	<b>95</b>
<b>Appendix 3, Figure 1:</b> The structures of sulphamerazine, sulphadiazine and sulphamethazine .....	<b>115</b>
<b>Appendix 3, Figure 2:</b> The structure of the “model” sulphonamide used to carry out <i>ab initio</i> calculations .....	<b>115</b>

---

<b>Appendix 3, Figure 3:</b> ES-MS/MS spectra obtained on the LCQ ion trap for samples of sulphamerazine prepared in acetonitrile and methanol .....	117
<b>Appendix 3, Figure 4:</b> ES-MS/MS spectra obtained on the LCQ ion trap for samples of sulphadiazine prepared in acetonitrile and methanol .....	118
<b>Appendix 3, Figure 5:</b> ES-MS/MS spectra obtained on the LCQ ion trap for samples of sulphamethazine prepared in acetonitrile and methanol .....	118
<b>Appendix 3, Figure 6:</b> Summary of the results of the <i>ab initio</i> calculations carried out on <i>N</i> -(5-methyl-2-pyridinyl)-benzenesulphonamide .....	123
<b>Appendix 4, Figure 1:</b> The ES-MS/MS spectra of the library of ergopeptine alkaloids studied .....	125
<b>Appendix 4, Figure 2:</b> The ES-MS/MS spectra of the four aflatoxins studied .....	127
<b>Appendix 5, Figure 1:</b> ES-MS/MS spectra obtained for a methyl-sulphonamide on the two conventional bench-top ion traps and on the FTMS .....	134
<b>Appendix 5, Figure 2:</b> ES-MS/MS spectra obtained for albendazole on the two conventional bench-top ion traps and on the FTMS .....	135
<b>Appendix 5, Figure 3:</b> ES-MS/MS spectra obtained for thiophensulphuron methyl on the two conventional bench-top ion traps and on the FTMS .....	136
<b>Appendix 5, Figure 4:</b> Comparison between the ES-MS/MS spectra obtained for a methyl-sulphonamide on a conventional, spherical, quadrupole ion trap and on the linear ion trap .....	137
<b>Appendix 5, Figure 5:</b> Comparison between the ES-MS/MS spectra obtained for albendazole on a conventional, spherical, quadrupole ion trap and on the linear ion trap .....	138
<b>Appendix 5, Figure 6:</b> Comparison between the ES-MS/MS spectra obtained for thiophensulphuron methyl on a conventional, spherical, quadrupole ion trap and on the linear ion trap .....	139

## Tables

## Page Number

<b>Chapter 2, Table 1:</b> The main fragment ions produced by four purines with no aliphatic chains in their structures .....	<b>34</b>
<b>Chapter 2, Table 2:</b> The structural components of the group of 3-alkylamino-imidazo-[1,2- $\alpha$ ]azines studied.....	<b>39</b>
<b>Chapter 3, Table 3:</b> Structures proposed for the fragment ions observed in the ES-MS/MS spectrum of tyrosine.....	<b>44</b>
<b>Chapter 3, Table 4:</b> Structures proposed for the fragment ions observed in the spectra of tyrosine methyl ester and tyrosine butyl ester.....	<b>52</b>
<b>Chapter 4, Table 5:</b> Structures proposed for the common fragment ions and neutral losses produced by the amino-sulphonamides.....	<b>61</b>
<b>Chapter 4, Table 6:</b> Summary of the results of the exact mass analysis carried out on sulphamerazine, sulphadiazine and sulphamethazine .....	<b>62</b>
<b>Chapter 4, Table 7:</b> Summary of the results of the MS <sup>3</sup> experiments carried out on 4-amino- <i>N</i> -(5-methyl-2-pyridinyl)-benzenesulphonamide.....	<b>64</b>
<b>Chapter 4, Table 8:</b> Structures proposed for the main fragment ions and neutral losses produced by the acetylated amino-sulphonamides .....	<b>66</b>
<b>Chapter 4, Table 9:</b> Structures proposed for the common fragment ions and neutral losses produced by the methyl-sulphonamides.....	<b>68</b>
<b>Chapter 4, Table 10:</b> Summary of the results of the MS <sup>3</sup> experiments carried out on 4-methyl- <i>N</i> -(5-methyl-2-pyridinyl)-benzenesulphonamide .....	<b>68</b>
<b>Chapter 4, Table 11:</b> Structures proposed for the common fragment ions and neutral losses produced by the non-substituted benzenesulphonamides .....	<b>71</b>
<b>Chapter 4, Table 12:</b> Summary of the results of the MS <sup>3</sup> experiments carried out on <i>N</i> -(5-methyl-2-pyridinyl)-benzenesulphonamide.....	<b>72</b>
<b>Chapter 4, Table 13:</b> Structures proposed for the main fragment ions and neutral losses produced by the five sulphonamides studied with various groups attached on the benzene ring ....	<b>74</b>
<b>Chapter 5, Table 14:</b> Identification of the functionalities present in the structure of an unknown sulphonamide based on the <i>m/z</i> values observed in the spectrum .....	<b>79</b>
<b>Chapter 5, Table 15:</b> Summary of the results of the MS <sup>3</sup> experiments carried out on the isomeric sulphonamides .....	<b>81</b>
<b>Appendix 1, Table 1:</b> The structures of the carnitines studied.....	<b>97</b>
<b>Appendix 1, Table 2:</b> The structures of the carnitine butyl esters studied .....	<b>99</b>
<b>Appendix 1, Table 3:</b> The structures of the pheniramines and disopyramides studied.....	<b>100</b>
<b>Appendix 1, Table 4:</b> The structures of the purines studied .....	<b>101</b>
<b>Appendix 1, Table 5:</b> The structures of the benzimidazoles studied.....	<b>102</b>
<b>Appendix 1, Table 6:</b> The structures of the amphetamines studied.....	<b>103</b>

---

<b>Appendix 1, Table 7:</b> The structures of the 3-alkylamino-imidazo-[1,2- $\alpha$ ]azines studied....	<b>105</b>
<b>Appendix 2, Table 1:</b> The structures of the unprotected amino acids studied .....	<b>107</b>
<b>Appendix 2, Table 2:</b> Summary of the exact mass analysis results for the unprotected amino acids.....	<b>109</b>
<b>Appendix 2, Table 3:</b> The structures of the protected amino acids studied .....	<b>110</b>
<b>Appendix 2, Table 4:</b> Correlation between the spectra of the butyl ester and the methyl ester amino acids .....	<b>113</b>
<b>Appendix 2, Table 5:</b> Summary of the exact mass analysis results for the methyl ester amino acids.....	<b>114</b>
<b>Appendix 3, Table 1:</b> The structures of the amino-sulphonamides studied .....	<b>116</b>
<b>Appendix 3, Table 2:</b> The structures of the acetylated amino-sulphonamides studied .....	<b>119</b>
<b>Appendix 3, Table 3:</b> The structures of the methyl-sulphonamides studied .....	<b>120</b>
<b>Appendix 3, Table 4:</b> The structures of the non-substituted benzenesulphonamides studied .....	<b>121</b>
<b>Appendix 3, Table 5:</b> The structures of the five sulphonamides studied with various substituents attached on the benzene ring .....	<b>122</b>
<b>Appendix 4, Table 1:</b> The structures of the library of ergopeptine alkaloids studied ....	<b>124</b>
<b>Appendix 4, Table 2:</b> The structures of the four aflatoxins studied .....	<b>126</b>
<b>Appendix 4, Table 3:</b> The structures of the library of sulphonylureas studied .....	<b>128</b>
<b>Appendix 5, Table 1:</b> The structures of the sulphonylureas analysed .....	<b>130</b>
<b>Appendix 5, Table 2:</b> The structures of the sulphonamides analysed .....	<b>132</b>
<b>Appendix 5, Table 3:</b> The structures of the benzimidazoles analysed .....	<b>133</b>

## Preface

I declare that this thesis is the result of work carried out wholly by myself with the exception of the following experiments:

- Analysis of the three groups of compounds on the Q Trap Linear Trap (MDS Sciex, Concord, ON, Canada) was carried out by Paula Wiebkin (Applied Biosystems).
- The molecular modelling calculations were carried out under the guidance of Dr Alexander Alex (Pfizer) and Dr Colin Edge (GSK).

Parts of the thesis that have been published:

“Approaches Towards the Automated Interpretation and Prediction of Electrospray Tandem Mass Spectra of Non-Peptidic Combinatorial Compounds”

Klagkou K, Pullen F, Harrison M, Organ A, Firth A, Langley GJ. *Rapid Commun. Mass Spectrom.* 2003; **17**: 1163.

“The Fragmentation Pathway of Sulphonamides Under ES-MS/MS Conditions”

Klagkou K, Pullen F, Harrison M, Organ A, Firth A, Langley GJ. *Rapid Commun. Mass Spectrom.* 2003; **17**: 2373.

“Τα περάσαμε όμορφα, όμορφα, όμορφα,  
τα περάσαμε όμορφα, όμορφα, παιδιά...”  
Hellenic Children's Song

## Acknowledgements

I would like to thank the following people for their contributions to this project:

John Langley for his time and guidance throughout this investigation.

Frank Pullen, Andy Organ, Mark Harrison and Alistair Firth for their time and their input in case meetings.

Julie Herniman for her help in the lab.

Alexander Alex and Colin Edge for their advice with the molecular modelling calculations.

Paula Wiebkin and Anneke Lubben for the analysis of samples on their instruments.

Alistair Firth, Andy Osprey, Paul Desmond and Paul Scullion for letting me use their lab and for their efforts with the metabolism work.

Mark Harrison and the people in Thermo Finnigan (Hemel Hempstead) for letting me use their instruments and for their help and their ideas with the d-labelling experiments and the adduct studies.

Terry Threlfall for the synthesis of the sulphonamide library.

George Perkins and Sally-Ann Fancy for letting me use their trap and for the analysis of the azine group.

Robert Mistrik for his help with Mass Frontier.

---

**Abbreviations**

Å	Angstrom
AC	Alternating Current
AI	Artificial Intelligence
API	Atmospheric Pressure Ionisation
a.u.	Arbitrary Units
B	Magnetic Field
CE	Capillary Electrophoresis
CI	Chemical Ionisation
CID	Collision Induced Dissociation
CLND	Chemiluminescent Nitrogen Detector
D, d	Deuterium
Da	Dalton
dB	Decibel
DBE	Double Bond Equivalents
DC	Direct Current
EI	Electron Ionisation
ELSD	Evaporative Light Scattering Detector
ES	Electrospray
eV	Electron Volt
f	Frequency
$f_c$	Cyclotron Frequency
FAB	Fast Atom Bombardment
$F_c$	Centrifugal Force
$F_L$	Lorentz Force
FIA	Flow Injection Analysis
FT	Fourier Transform
FTICR	Fourier Transform Ion Cyclotron Resonance
FTICRMS	Fourier Transform Ion Cyclotron Resonance Mass Spectrometry
FTNMR	Fourier Transform Nuclear Magnetic Resonance
GC	Gas Chromatography
HPLC	High-Performance Liquid Chromatography
HTS	High-Throughput Screening
Hz	Hertz
Kcal	Kilocalories
kV	Kilo-Volt
L	Litre

---

LC	Liquid Chromatography
M, m	Mass
MALDI	Matrix Assisted Laser Desorption Ionisation
min	Minute
mL	Millilitre
mm	Millimetre
MS	Mass Spectrometry
MS/MS	Tandem Mass Spectrometry
nm	Nanometre
NMR	Nuclear Magnetic Resonance
OA	Open-Access
PCA	Principal Component Analysis
ppm	Parts Per Million
psi	Pressure
QMI	Quasi-Molecular Ion
r	Radius
r.i.	Relative Intensity
RF, Rf	Radio-Frequency
RMM	Relative Molecular Mass
sec	Second
SIM	Single Ion Monitoring
T	Tesla
UV	Ultra-Violet
V	Volt
v	Velocity
z	Charge
μg	Micro-gram
μsec	Micro-seconds
π	Pi
ω	Angular Velocity
3D	Three-Dimensional
°C	Degrees Celsius

## 1. Introduction

### 1a. Overview

The process of drug discovery has evolved over many centuries. Historically, people have turned to nature to find cures for human diseases and thus the first treatments available were typically plant or animal product extracts based on water or alcohol.<sup>1</sup> Organic chemistry, as it is known today, first appeared towards the end of the 19<sup>th</sup> Century and the first synthetic drugs, aspirin and antipyrine, were produced.<sup>2</sup> However, drug discovery remained a crude process and depended entirely on trial-and-error. This picture was only changed through the development of biological and biochemical approaches, when the advances in these areas finally led to the first steps towards rational drug design.

In the 1940s the understanding of the immune system resulted in the discovery of the first antibiotics.<sup>2</sup> By the 1960s, the knowledge into enzymatic reactions had increased and synthetic targets were set for the medicinal chemists based on the new information about drug-receptor interactions. In the 1970s and 1980s, the development of computer science and analytical techniques such as Nuclear Magnetic Resonance (NMR) spectroscopy and X-ray crystallography allowed the characterisation of proteins and revealed their function. Drug design became the new trend in the pharmaceutical industry and efforts were focused on the synthesis of specific molecules designed to interact with specific enzymes. The decade of the 1990s is characterised by the advances in molecular biology and gene research as well as the evolution of more powerful informatics tools. Thousands of new potential biological targets, enzymes and receptors, were discovered. An opportunity then appeared to increase the number of compounds identified as biologically active (leads).<sup>3,4</sup> High-throughput screening (HTS) methodologies were developed for the rapid evaluation of biological activity, whilst synthesis became the rate-limiting step in the drug discovery process.<sup>5,6</sup> Medicinal chemists realised that the classical way of carrying out synthesis could not cope with the numbers of compounds needed for HTS. As a result, the 1990s saw the development of a new trend in the pharmaceutical industry, combinatorial chemistry.<sup>7</sup>

The strategy which forms the basis of combinatorial chemistry is extremely simple, namely the combination of chemical building blocks, potentially in all combinations and variations.<sup>3</sup> Two main strategies are currently available: the solid-phase synthesis of libraries resulting in mixtures of compounds and the parallel synthesis of compounds either on solid-support or in solution, resulting in a large number of discrete samples.<sup>8,9</sup> Combinatorial libraries are synthesised either with the aim of screening against various biological targets (lead discovery) or with the aim of improving the structure of an already identified lead so that it would fulfil certain specifications (lead optimisation). Therefore their size and composition is dictated by their function in the drug discovery process.<sup>10,11</sup>

The synthesis of combinatorial libraries of mixtures is usually carried out using the methodology initiated by Merrifield.<sup>12-14</sup> A resin is employed as solid support for the compound being synthesised and completion of reactions is achieved using excess of reagents, which are finally washed away at the end of each synthetic step.<sup>15</sup> Geysen,<sup>16</sup> Furka,<sup>17</sup> Houghten,<sup>18</sup> and Lam<sup>19</sup> applied the information available on solid-phase synthesis and developed a unique method for

Initially, libraries containing thousands of compounds were synthesised but due to problems of identification of the active compound, the numbers of compounds per library have now decreased. Currently, preference is given to parallel synthesis of discrete compounds that are easily detected over the traditional Split and Mix approach. The relative ease of automation of parallel synthesis led to a great increase in the number of compounds identified as leads that require further optimisation.<sup>13,14</sup>

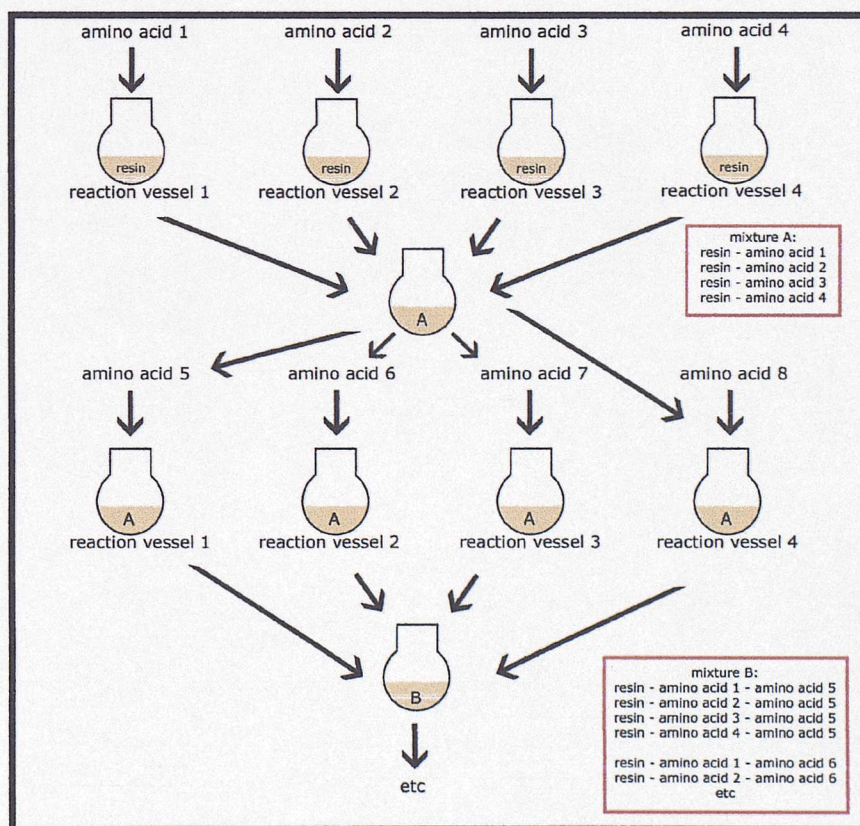


**Figure 1:** The Split and Mix approach in combinatorial chemistry.

The use of combinatorial chemistry and HTS accelerated the processes of synthesis and biological testing. On the other hand, analytical characterisation of the combinatorial libraries became the new bottleneck in drug development.<sup>4,13</sup> Structure and purity confirmation for the library components has to take place in the same manner as for products obtained *via* traditional synthesis. However, due to time constraints, the small amounts of compounds synthesised and the large numbers of samples associated with combinatorial synthesis, analytical characterisation of libraries by classical methods is rendered impractical and slow. Analytical techniques needed to become faster and more accurate to keep up with the pace of the new methodologies.

Mass spectrometry (MS) played the leading role in the analysis of combinatorial libraries.<sup>21-23</sup> Atmospheric Pressure Ionisation (API) became the default ionisation technique with electrospray (ES) at the forefront. **(Section 1b)** The technique is fast, sensitive, accurate, capable of automation and compatible for coupling with other analytical techniques such as high-performance liquid chromatography (HPLC) and capillary electrophoresis (CE). All these advantages made ES-MS an ideal method for the analysis of combinatorial libraries. The wide range of applications of mass spectrometry in combinatorial chemistry is reflected by the large number of relevant literature published in this area.<sup>24-37</sup>

The sample is most commonly introduced for MS analysis by using either flow injection analysis (FIA) or HPLC.<sup>4</sup> Since analysis speed is the major concern, flow injection analysis is usually advantageous compared to HPLC. However, in-source discrimination effects, such as signal suppression, can occur because of the co-elution of bi-products, residual reagents and salts. Additionally, clear information on sample purity is not always obtained. These drawbacks are successfully addressed when the sample is introduced by HPLC. A further advantage of HPLC-MS is the possibility of working simultaneously with one or more types of detector e.g. ultra-violet detector (UV), Chemiluminescent Nitrogen Detector (CLND) and Evaporative Light Scattering Detector (ELSD), connected in series or in parallel with the mass spectrometer.

As FIA-MS and HPLC-MS became more pervasive in the analysis of combinatorial libraries, open access (OA) instrumentation was increasingly used in combinatorial laboratories.<sup>21,34,38,39</sup> For OA-MS complete descriptors of the samples and mass spectrometry analysis methods are entered into the data system.<sup>40</sup> The samples are then queued in an HPLC autosampler and subsequently injected into the mass spectrometer to automatically produce the corresponding mass spectra. Automation of data acquisition, processing, interpretation and reporting is possible. Modules for processing mass spectra data with the aim to characterise the components of combinatorial libraries were also produced.<sup>32</sup> These usually involved a correlation between measured and predicted mass spectra, providing a rapid means to confirm library products, identify synthesis errors and estimate overall library integrity.

The subsequent coupling of ES-MS with tandem MS (MS/MS) resulted in a new powerful method of analysis since it provides information about the molecular weight of compounds as well as information about their structural components. As a result ES-MS/MS became a key technology for the characterization of peptidic compounds.<sup>41,42</sup> It provides a rapid and sensitive means of determining the amino acid sequence of peptides and offers various advantages over the

traditional sequencing methods.<sup>43,44</sup> Firstly, it generally works well for the naturally occurring amino acids as well as for modified or unusual amino acid residues and secondly, it is not necessary for the peptide of interest to be exhaustively purified. Finally, the process of spectrum acquisition takes a finite time regardless of the composition of the peptide.

The fragmentation pathway of peptides is well-documented.<sup>45,46</sup> The protonated molecules fragment along the peptide backbone and also produce some side chain fragmentation. The three types of bonds that can fragment along the amino acid backbone are the NH-CH, CH-CO and CO-NH bonds. **(Figure 2)** Dissociation of each bond results in a charged and a neutral species, while the charge can stay on either side of the molecule after fragmentation depending on the chemistry and the relative proton affinity of the two resulting species.<sup>47</sup> For each amino acid residue six main fragment ions are possible. As shown in **Figure 2**, a, b and c ions have the charge retained on the N-terminal fragment ion and x, y and z ions have the charge retained on the C-terminal fragment ion. The most common cleavage sites are the CO-NH bonds, which give rise to the b and/or y ions. The extent of side chain fragmentation detected depends on the type of analyser used in the mass spectrometer.<sup>47</sup>

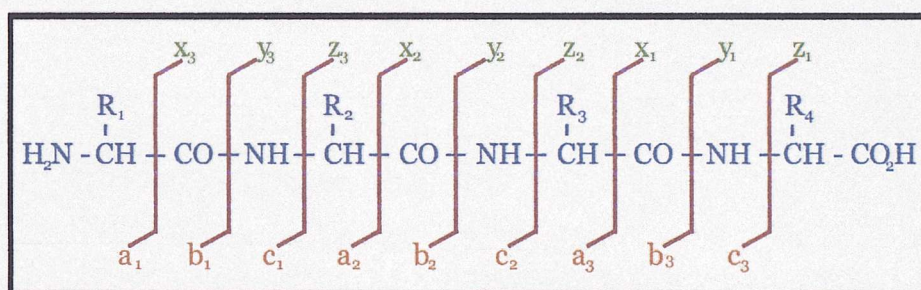


**Figure 2:** The common types of background ions arising from backbone cleavages of protonated linear peptides.

Knowledge of the facile cleavage sites of peptides makes interpretation of MS/MS spectra very efficient. Moreover, the ability to predict the pattern has led to the development of algorithms for automatic data handling.<sup>48</sup> Various computer programs have been developed, that allow rapid characterisation of unknown peptidic compounds from their electrospray MS/MS spectra. Unfortunately, the same advances have not also taken place in the field of non-peptidic, combinatorial compounds. Although the fragmentation pathways of various classes of molecules have been described under electron ionisation (EI) conditions,<sup>49-51</sup> their dissociation routes have not been explored when ES-MS/MS is used. Consequently, existing artificial intelligence (AI) software packages employ EI fragmentation rules to achieve spectra prediction. Though sometimes helpful, this approach is flawed, mainly because the processes taking place in EI involve the formation of odd electron molecular ions, whilst under ES conditions even electron species are formed. As a result, the interpretation of MS/MS spectra of non-peptidic, combinatorial molecules in the pharmaceutical industry is required to be addressed by the highly trained specialist. This can be time consuming and is not an approach amenable to the requirements of a high-throughput automated environment.

The aim of this project is to improve the speed and accuracy of ES-MS/MS spectra interpretation and prediction for non-peptidic, combinatorial, pharmaceutical compounds. Our goal is to recognise the functionalities that dominate dissociation under ES-MS/MS conditions and identify the ionisation mechanisms and dissociation processes that take place. This should allow general rules to be established and lead to identification of unknown drug molecules from their ES-MS/MS spectra with the use of improved algorithms. To achieve this we have studied the dissociation pathways of various classes of drug molecules under ES-MS/MS conditions. A library of 1000 spectra obtained on an ion trap instrument was used.<sup>52</sup> The common fragment ions and neutral mass losses for each class were identified. Additional studies were carried out to explore the ionisation and fragmentation mechanisms taking place when ES-MS/MS is used. As an aid in our studies, an artificial intelligence (AI) predictive package, Mass Frontier (Thermo Finnigan, San Jose, CA, USA) has been used. Observation of the limitations of the software, with respect to fragment ion prediction, allows identification of the areas that require optimisation. The ultimate aim of this work is the incorporation of these findings into the software package in order to achieve rapid characterisation of the components of non-peptidic, combinatorial libraries using the ES-MS/MS technology already available in the combinatorial laboratory.

### 1b. Instrumentation

Mass spectrometry uses the difference in mass to charge ratio of ionised atoms or molecules in order to separate them from each other.<sup>2</sup> Regardless of the type of instrument or the type of analysis, a mass spectrometer is made up of five separate systems: inlet, ion source, mass analyser, detector and recorder. **(Figure 3)** Various technologies have been developed for each of these fundamental components. The method of choice for analysis depends on the sample under investigation and the type of analysis required. For the needs of this project, all samples were analysed on a quadrupole ion trap instrument using electrospray ionisation. In addition, exact mass measurements were carried out using electrospray Fourier Transform Ion Cyclotron Resonance Mass Spectrometry (ES-FTICRMS).

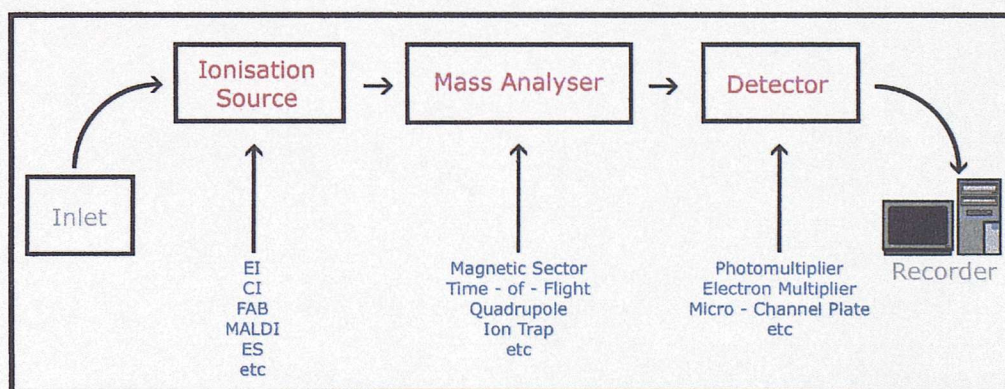


**Figure 3:** The basic components of any mass spectrometer.

Currently electrospray ionisation is widely applied in the pharmaceutical industry. It is an atmospheric pressure ionisation technique and it is well suited for the analysis of polar molecules

ranging from less than 100 Da to more than 70,000 Da in molecular weight.<sup>47</sup> During electrospray, the sample is dissolved in a polar, volatile solvent and pumped through a narrow stainless steel capillary.<sup>53-58</sup> A high potential difference of 3 to 5 kV is applied between the tip of the capillary and a counter electrode. As a consequence of the strong electric field created, the sample emerging from the tip is dispersed into an aerosol of highly charged droplets, a process that is aided by a nebulising gas, that is flowing co-axially around the outside of the capillary. This gas usually nitrogen, helps to direct the spray emerging from the capillary tip towards the mass spectrometer. **(Figure 4)** The charged droplets diminish in size by solvent evaporation, assisted by a warm flow of nitrogen gas known as the drying gas, which passes across the front of the ionisation source. At a certain point, desolvation is aided by repulsive Coulombic forces overcoming the cohesive forces of the droplet.<sup>47,59</sup> Eventually, charged sample ions, free from solvent are released from the droplets, some of which pass through a sampling cone into the intermediate vacuum region and from there through an orifice into the analyser of the mass spectrometer which is held under vacuum.

The formation of gas phase ions from the small charged droplets is not yet fully understood.<sup>48</sup> Two mechanisms have been proposed. The original idea was that the solvent evaporates and the droplets break up, until those with only a single analyte ion are created.<sup>60</sup> Evaporation continues until a gas phase ion is formed and this process is usually referred to as the charged-residue model. An alternative mechanism, the ion evaporation model, was later suggested.<sup>61</sup> According to this theory, droplets with a radius less than 10 nm can allow field desorption, *i.e.* direct emission of gaseous ion. The charge state of the ion will depend upon the number of charges that are transferred from the droplet surface to the ion during desorption. The gas phase ion formation processes are still under debate and while the ion evaporation theory might be the most accepted, a mechanism related to the charged-residue process may account for the formation of gaseous protonated macromolecules.<sup>48</sup>

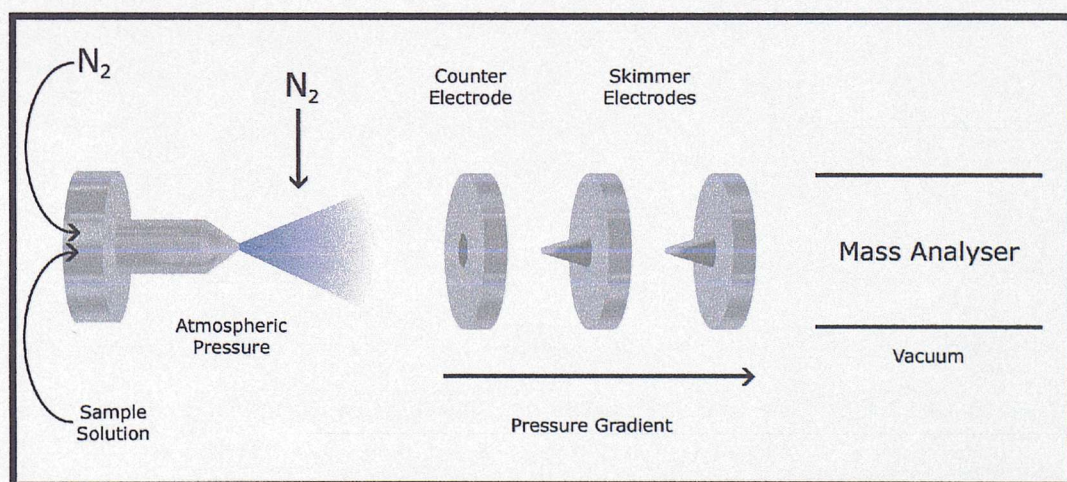


**Figure 4:** Schematic representation of electrospray ionisation.

Electrospray is considered to be one of the softest ionisation techniques available since little energy is transferred to the molecules other than that required for ionisation. Thus protonated,

deprotonated or cationised molecules, that undergo very little fragmentation, can be generated even from highly polar, thermolabile molecules.<sup>47</sup> A second advantage of the technique is the ease of coupling with HPLC or CE. Since electrospray is a solvent-based method, various interfaces have been developed so that samples can undergo chromatography *en route* to the ionisation source. As a result, electrospray became the method of choice for a wide range of applications and is currently the norm in most open access systems in the pharmaceutical industry.

Nowadays, ion trap mass spectrometers are also extensively used. This is mainly because of their operating and structural simplicity, sensitivity, high efficiency in performing multiple MS/MS experiments and their relative low price-performance ratio.<sup>62</sup> The quadrupole ion trap functions as an ion storage device, which confines gaseous ions for a period of time. With the advent of atmospheric pressure ionisation and its subsequent coupling to the ion trap, the range of applications of the instrument became enormous.<sup>63-68</sup>

The quadrupole ion trap analyser consists of three hyperbolic electrodes: the ring electrode, the entrance end cap electrode and the exit end cap electrode, which form a cavity in which it is possible to store and analyse ions.<sup>58,69</sup> The end cap electrodes have a small hole in their centres through which the ions travel. The ring electrode is located halfway between the two end cap electrodes. **(Figure 5)** For single stage MS experiments, ions formed in the ion source enter the cavity of the trap through the entrance end cap electrode, while various voltages are applied to the electrodes to trap and eject ions according to their different  $m/z$  ratios.<sup>69</sup> As a result, a three dimensional (3D) quadrupolar potential field is generated within the trap cavity. Because of this, the ions entering the trap are confined in a stable oscillating trajectory both in the axial and radial direction. This trajectory depends on the trapping potential and the  $m/z$  ratio of each ion. The ions fill most of the space of the interior of the trap and have the tendency to increase the radius of their motion because of the electrostatic repulsion of equally charged particles. In order to avoid ion loss by collisions with the electrodes the ion motion is dampened with the use of an inert gas.<sup>66</sup> The cavity of the trap is filled with helium or argon and collisions between the gas atoms and the ions result in the latter losing their momentum and move to trajectories closer to the centre of the trap. As an outcome of repeated collisions the ions become a focused cloud near the trap centre. This improves mass resolution because all the ions occupy a small space (limited spatial distribution) and field imperfection is minimal at the centre of the trap. Scanning is accomplished by altering the electrode system potential to produce instabilities to the ion trajectories and thus eject the ions in the axial direction. The ions are ejected in order of increasing  $m/z$  ratio and focused by the exit lens into the detector.<sup>58,66,69</sup>

To obtain structural information on a particular ion, MS/MS experiments can be carried out.<sup>58,70-72</sup> Once the ions are stored in the cavity of the trap, the voltages of the electrodes can be changed to eliminate all but the desired ion in order to carry out MS/MS experiments.<sup>69</sup> The radio frequency (RF) voltage is then adjusted to stabilise the isolated ion (precursor ion) and capture the ions generated during the MS/MS experiment (product ions). For the purposes of tandem MS, the internal energy of the isolated ions in the trap is increased by application of a supplemental voltage to the end cap electrodes to cause dissociating collisions with the inert gas. This is known as

Collision Induced Dissociation (CID). The analyser is then scanned following the same process as described for the single MS experiment and a full spectrum of the product ions is produced.

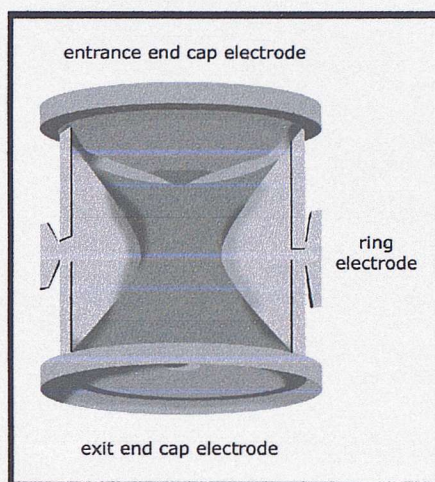


**Figure 5:** The quadrupole ion trap.

The use of the quadrupole ion trap has enabled highly reproducible MS/MS spectra to be obtained and has led to the generation of the first searchable MS/MS library.<sup>52</sup> This was achieved with the introduction of wideband excitation and normalised collision energy. The ion trap has a limited product ion mass range and less energy is imparted to the precursor ion than in a quadrupole instrument. For this reason, the loss of water is often the main dissociation process observed after fragmentation of the quasi-molecular ion (QMI) by CID. The resulting fragment ions can then be further dissociated with the use of MS<sup>3</sup> experiments in order to obtain the required structural information. A direct approach for obtaining the desired level of dissociation is with the use of wideband excitation (pseudo-MS<sup>3</sup>). Using this method, excitation is carried out automatically to 20 mass units below the selected precursor ion mass, thereby further fragmenting any  $[M+H-H_2O]^+$  ions formed. This mechanism provides richer product ion mass spectra for various types of compounds.<sup>52</sup> A further property of ion traps is that the effective imported energy decreases as the mass of the parent ion increases. A linear relationship has been found between the mass and energy transferred, so that a mass-dependant correction can be automatically applied to the collision energy to give the so-called "normalised collision energy". The developments of wideband excitation and normalised collision energy led to the creation a searchable MS/MS library by Baumann *et al.*<sup>52</sup> This library was donated to us, courtesy of Thermo Finnigan, and spectra were used for the purposes of this project.

FTICRMS attracts attention because of its combination of high to ultrahigh mass resolution and very high mass accuracy and precision.<sup>73</sup> All Fourier Transform (FT) MS instruments have four main components in common.<sup>74,75</sup>

1. The magnet.

The magnetic field necessary for the operation of the instrument is provided either by a permanent magnet, an electromagnet or a super-conducting magnet. Since the performance of

the instrument increases as the strength of the magnetic field increases, a super-conducting magnet is most commonly used.

## 2. The analyser cell.

The cell is the heart of the FTMS, where ions are stored, mass analysed and detected, and it is situated in the centre of the magnet. Although different cell designs are available, *e.g.* cylindrical, orthorhombic *etc.*, its function is best demonstrated by the cubic cell. **(Figure 6)** Six plates are arranged in the shape of a cube, oriented in the magnetic field in such a way that one opposing pair of plates is orthogonal to the direction of the field and two pairs of plates lie parallel to the field. The plates that are perpendicular to the field are called the trapping plates. It is common that the trapping plates have small holes that permit electrons or ions to enter all along the magnetic field lines. The four remaining plates are used for ion excitation and detection.

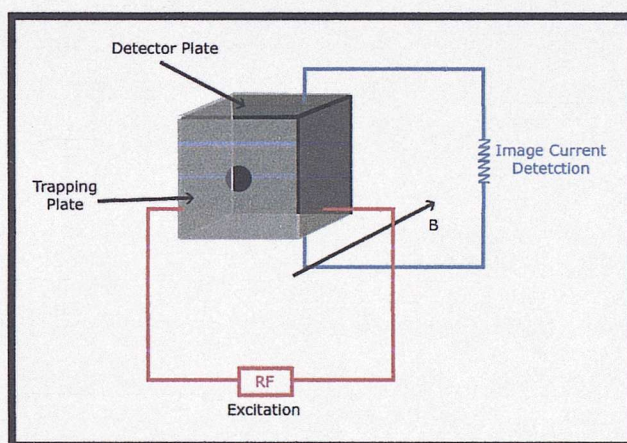


**Figure 6:** Schematic representation of the cubic analyser cell.

## 3. The ultra-high vacuum system.

The FTICRMS is more sensitive to pressure than other instruments. Long dwell times of ions in the cell are only possible in a very high vacuum because residual gas from air disturbs the motion of the ions and shortens the time for analysis and direction. Turbomolecular pumps provide the vacuum required. In the cases where ES is employed and ionisation takes place under atmospheric pressure, several pumping stages are required to overcome the enormous pressure difference from ion introduction to ion detection.

## 4. The sophisticated data system.

Similar components as those used for FTNMR are employed. These include a frequency synthesiser, delay pulse generator, broadband RF amplifier, a fast transient digitiser and a computer to co-ordinate all the electronic devices during the acquisition of data.

In most mass spectrometers the different events happen in different parts of the instrument, simultaneously and continuously. In the FTICRMS, most functions happen in the cell, at different times, *i.e.* sequentially.<sup>74</sup> The following sequence of events takes place:

1. Quench.
2. Ionise.

3. Excite.
4. Detect.

During the process of quenching, the cell is cleaned of ions from previous experiments. Voltages are applied on the trapping plates and the ions present are ejected from the cell. When ES is used as the method of ionisation, the ions are generated in the ion source and RF and electrostatic voltages are applied in order to transfer the ions in the cell. In the case of other ionisation techniques, such as EI, ions can also be generated inside the cell.<sup>74</sup>

Once the ions enter the cell, they perform three discrete forms of motion: trapping motion, cyclotron motion and magnetron motion.<sup>74-77</sup> The electric field created between the two trapping plates forces the ions to undergo simple harmonic oscillation between the two plates along the axis of the magnetic field (trapping motion). Simultaneously, ions in the analyser cell are also exposed to the strong magnetic field and undergo a stable cyclic motion in a plane perpendicular to the magnetic field, the "so-called" cyclotron motion.

The principle of the cyclotron motion can be described as follows.<sup>58,74-78</sup> An ion of charge  $z$ , moving with velocity  $v$ , in a static magnetic field  $B$ , is subjected to a force  $F_L$  that is proportional to the magnitude of the charge and the speed of the ion and is perpendicular to the velocity of the ion.

$$F_L = z * v * B \quad (\text{Equation 1})$$

When the velocity of the ion is perpendicular to the magnetic field, the ion is forced to move in a circular orbit. The Lorentz force  $F_L$  is then directed inward and is counterbalanced by the centrifugal force  $F_C$  which is directed outward. According to Newton's second law:

$$F_C = (m * v^2) / r \quad (\text{Equation 2})$$

where  $r$  is the radius of the circular orbit and  $m$  is the mass of the ion.  
By equating equations 1 and 2 we obtain:

$$v / r = (B * z) / m \quad (\text{Equation 3})$$

The angular frequency  $\omega$  of the ion is:

$$\omega = v / r = 2 * \pi * f \quad (\text{Equation 4})$$

where  $f$  is the oscillating frequency of the ion.

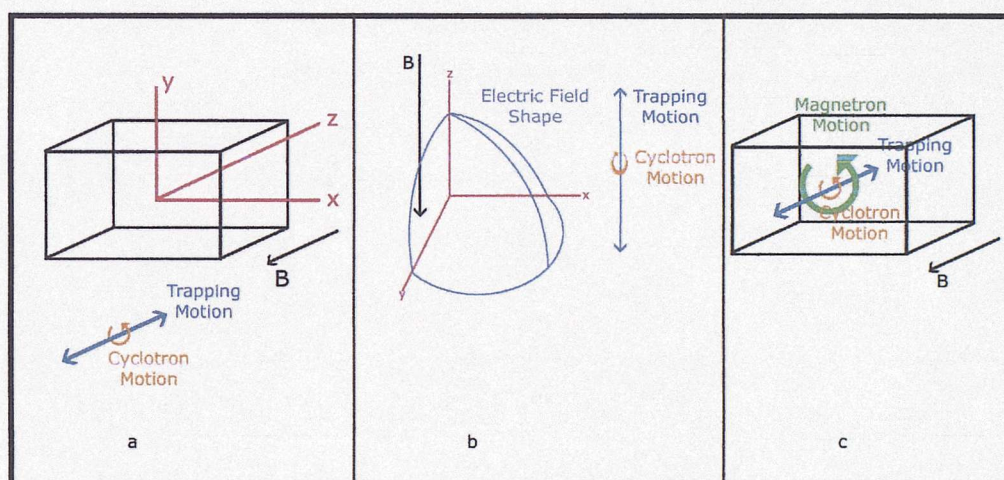
By substitution of the equation 4 in equation 3 we get:

$$2 * \pi * f = (B * z) / m \text{ and finally } f_C = (B * z) / (2 * \pi * m) \quad (\text{Equation 5})$$

The cyclotron frequency  $f_C$  characterises the cyclotron motion of each ion of a certain  $m/z$ .

Trapping motion and cyclotron motion are not coupled, thus it would seem that the magnetic and electric fields operate on the ions in an independent fashion. However, the combination of the magnetic field and the electric field together introduce a third fundamental motion of the ions, called the magnetron motion.<sup>74</sup>

To understand the magnetron motion, it is necessary to consider the shape of the electric field in the analyser cell.<sup>74,75</sup> A rectangular co-ordinate system can be defined with the z-axis parallel to the magnetic field and the centre of the cell as the origin. The motion of the ion due to the magnetic field occurs in the x and y plane, while the trapping potential constrains the ion motion along the z-axis. **(Figure 7a)** The electric potential in the cell reaches a maximum at the trapping plates and has a minimum at the centre of the cell. **(Figure 7b)** The shape of the trapping potential provides a restoring force that traps ions along the z-coordinate, but repels ions in the x and y plane. Essentially the electric field acts to drive ions away from the centre of the analyser cell, while the magnetic field prevents ions from being accelerated into the walls of the analyser cell. The electric and magnetic fields combine to produce magnetron motion, a precession of the guiding centre of the cyclotron motion of an ion around the centre of the cell. **(Figure 7c)**



**Figures 7a, 7b and 7c:** The three fundamental motions of the ion in the analyser cell.

After the ions are formed and trapped in the analyser cell, they only have a small amount of kinetic energy and the radius of the cyclotron orbit is usually small compared with the dimensions of the cell. In order to collect a signal it is necessary to excite the ions of a given  $m/z$  as a coherent package to a larger orbital radius by applying a sinusoidal voltage to the excitation plates.<sup>74</sup> The ion spirals outwards when its cyclotron frequency is in resonance with the frequency of the applied RF electric field. When the kinetic energy of the ion increases, the velocity of the ion increases as well and therefore, its radius also has to increase in order to maintain the same frequency. If the RF voltage is applied continuously, the ions that absorb energy will spiral outward until they strike an excitation or detection plate where they will be neutralised. This feature can be used to remove mass-selected ions from the analyser cell.<sup>74</sup> If the field is turned off before the ions strike the cell plates, they undergo cyclotron motion on the larger radius. **(Figure 8)** All ions of the same  $m/z$

ratio are excited coherently, which means that they are grouped as tightly after excitation as they were initially and undergo cyclotron motion as a packet. As they pass the cell's electrodes, the packet attracts electrons first to one and then the other of the two detection plates through the external circuit that joins them. This alternating current is called image current.<sup>73</sup> The periodic cyclotron motion of the ions produces a sinusoidal image signal, which can be amplified, digitised and stored for processing by a computer. The frequency of the detected sinusoid is equal to the difference between the cyclotron and the magnetron frequencies of the ions.

Ions of many masses can be detected simultaneously with FTICRMS and image current detection is non-destructive. To accomplish simultaneous detection of many ions, many frequencies are applied during the excitation event using a rapid frequency sweep.<sup>74</sup> This will cause all ions with cyclotron frequencies in this range to be excited into large cyclotron orbits of the same radius. The image current that results from ions of several  $m/z$  ratios is a composite of sinusoids of different frequencies and amplitudes. The frequency components of the signal are obtained by applying a Fourier Transform (FT) to the time domain transient and the FT of any portion of this transient would show the same group of ions. However, mass resolution improves in direct proportion to the length of transient that is recorded. The amplitude of the transient signal decays with time as collisions between the ions and neutrals, in the analyser cell, destroy the coherence of the ion packet. Thus FTICRMS works best at ultra-high vacuum, where the collision frequency is lowest.

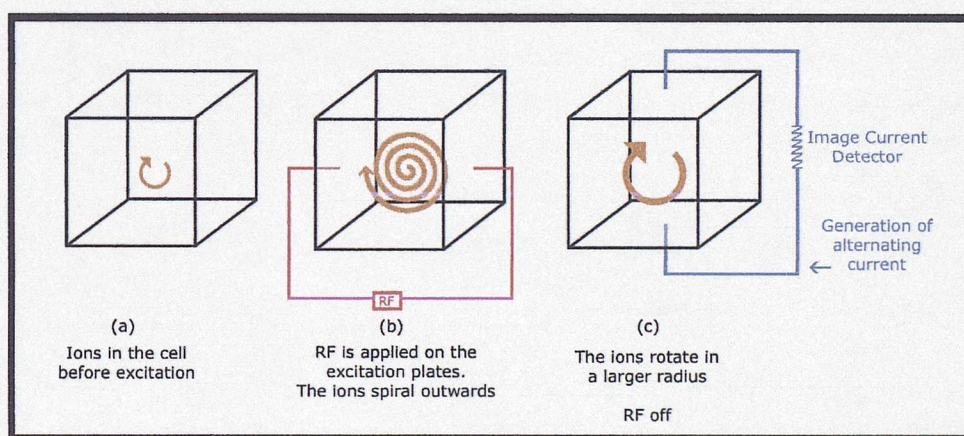


**Figure 8:** Ion excitation and detection in the analyser cell.

The increasing number of articles relating FTICRMS to combinatorial chemistry indicates the importance of this MS technique for the analysis of complex mixtures.<sup>79,80</sup> Throughout this project, FTICRMS is used for carrying out exact mass experiments. Based on the  $m/z$  values present in the spectra, the molecular formula of each fragment ion and its number of double bond equivalents\* can be calculated and this is a valuable tool for fragment ion identification and structure recognition.

\* For any compound  $C_xH_yN_zO_n$ , the number of double bond equivalents is given by the equation:

### 1c. Mass Frontier<sup>81</sup>

Mass Frontier is an AI software package that deals primarily with the interpretation and prediction of mass spectra of small organic molecules. The software features various modules that can potentially be used towards the automatic identification of non-peptidic, combinatorial compounds. The five main modules used for data manipulation are as follows.

- The main work platform (Spectra Manager) provides a convenient way for organising and processing spectra, chemical structures and libraries utilising a user-friendly spreadsheet format. **(Figure 9)**
- In a similar way, the GC/LC/MS Processor has been designed for users of MS coupled techniques such as liquid chromatography (LC) MS and gas chromatography (GC) MS.
- The Structure Editor allows chemical structure drawing. It is a simple, full-featured structure drawing tool that offers the advantage over similar packages of automatic calculation of the mass of a selected fragment ion and the corresponding mass loss. **(Figure 10)**
- The Fragments and Mechanisms module is a system for fragment ion identification. Detailed fragment ions and mechanisms can be generated for the active structure in the Spectra Manager or the compound drawn in the Structure Editor. In this way, the module can be used to predict the fragment ions a compound will generate and to interpret the spectrum of a known compound. **(Figure 11)**
- The Spectra Classifier employs classification methods in order to organise spectra into different groups. **(Figure 12)** The primary goal of spectra classification is to find correlation between the properties of compounds and their mass spectra. Because the physical and chemical properties and the biological activities of chemical compounds are to a large extent a function of molecular structure, the results of classification analysis reflect structural features that are determined by fragment ions appearing in a mass spectrum.<sup>81</sup> Together with library search and fragmentation prediction methods, classification provides a powerful tool for compound identification.

---

DBE=  $x-0.5y+0.5z+1$ . Whole numbers of DBE (e.g. 1,2,3, etc...) indicate that the species under investigation has an odd number of electrons. Even electron species produce half numbers (e.g. 1.5, 2.5, 3.5, etc...).

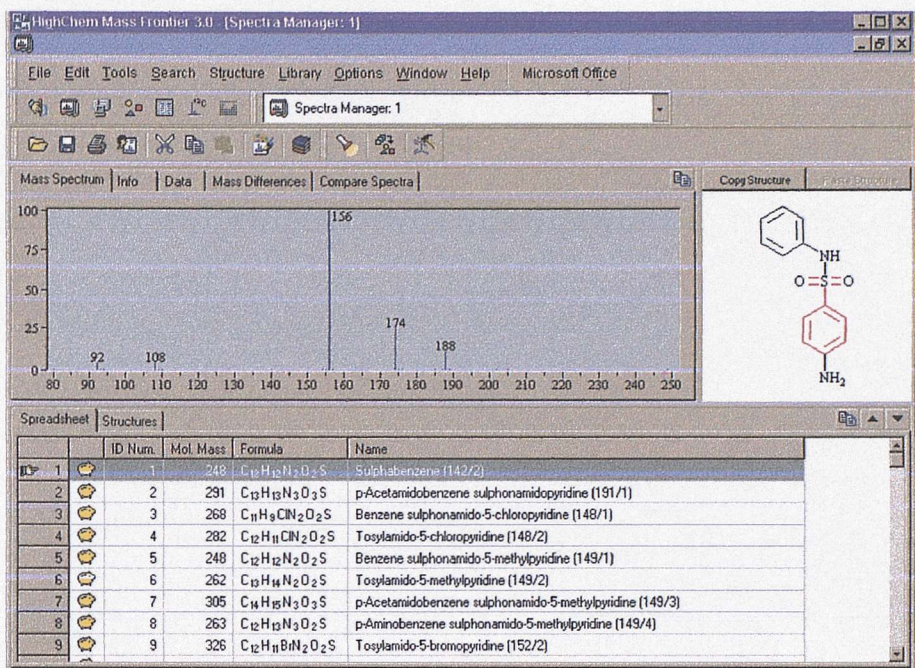


Figure 9: Mass Frontier-Spectra Manager.

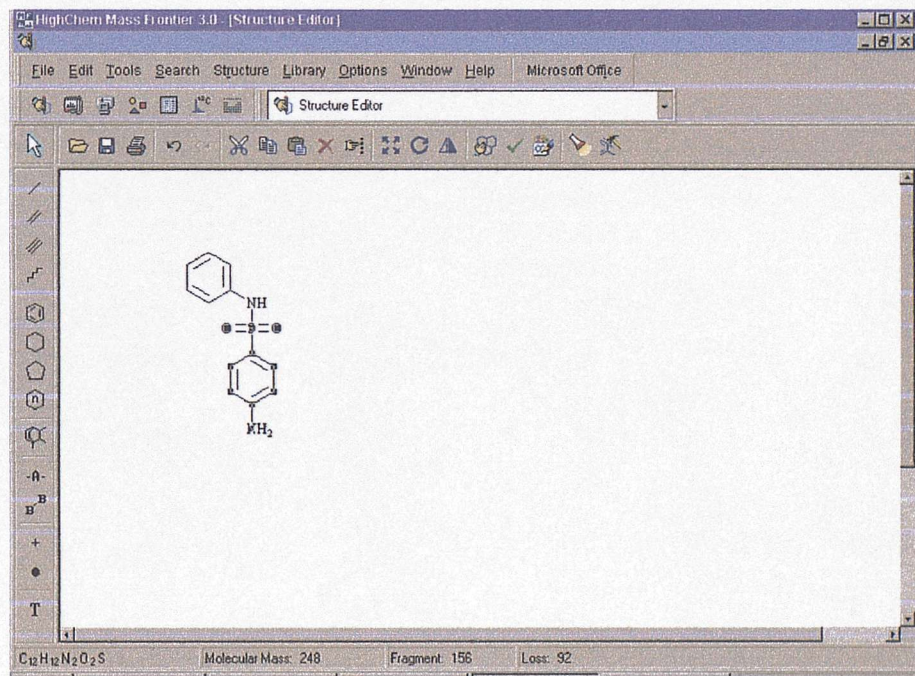


Figure 10: Mass Frontier-Structure Editor.

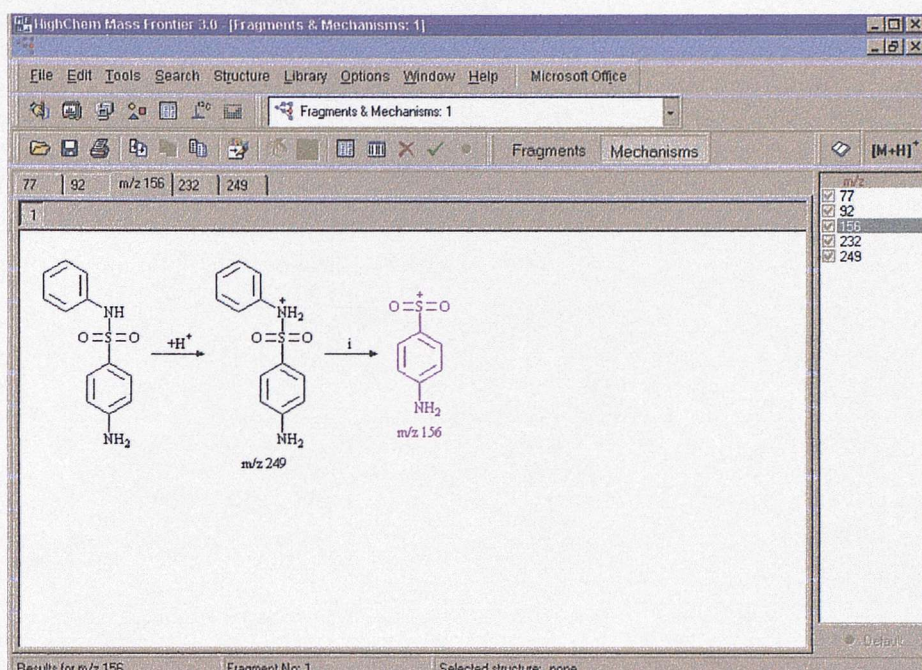


Figure 11: Mass Frontier-Fragments and Mechanisms.

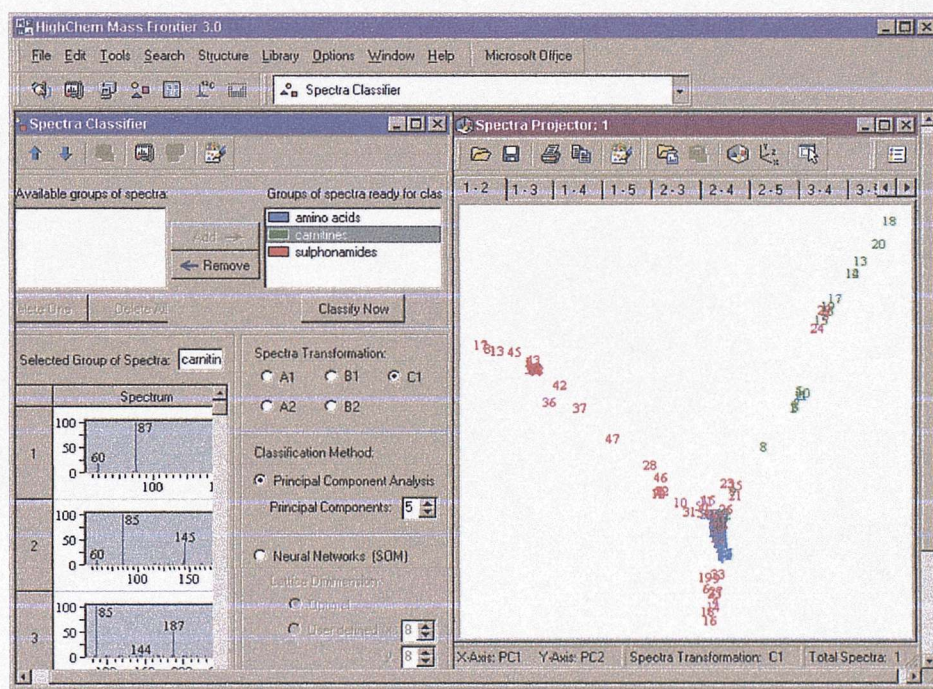
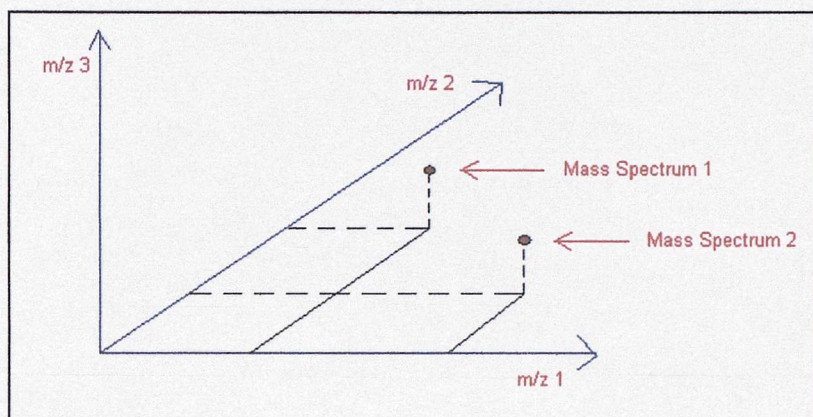


Figure 12: Mass Frontier-Spectra Classifier and Spectra Projector.

Mass Frontier contains two classification methods: Principal Component Analysis (PCA) and Neural Networks. These methods are based on different principles. PCA uses multivariate statistics, while Neural Networks are based on competitive learning. The classification method we have used for the purposes of this project is PCA.

In multivariate statistics, each spectrum can be considered as a single point in an  $n$ -dimensional space, with the intensities being the coordinates of this point.<sup>81</sup> (Figure 13) A dimension (axes) of

that space represents an  $m/z$  ratio of a considered ion. Therefore, the dimensionality is determined by the highest  $m/z$  value in the spectrum. For example, the EI spectrum of hydrogen exhibits two ions, at  $m/z=1$  (2%) and at  $m/z=2$  (100%). This spectrum can be viewed as a point in a two dimensional space with the coordinates  $[2, 100]$ .<sup>81</sup>



**Figure 13:** Plot of two mass spectra in a three-dimensional space, based on multivariate statistics.<sup>81</sup>

The basic hypothesis of multivariate statistical methods is the assumption that the distance between points (spectra) in an  $n$ -dimensional space is related to a relevant property of the compounds, which represent those points. If the points are close to form a cluster or a separate region, we can assume that the compounds that correspond to these points, exhibit common or similar properties.<sup>81</sup> To ensure the results of classification have statistical significance, usually one or more groups of 10 to 1000 spectra, should be placed in the same dimensional space. Then, these points (spectra) can be evaluated using multivariate statistical methods like PCA. The objective of any classification process is to separate the points (spectra) into two or more classes according to the desired structural or other properties.<sup>81</sup>

The central idea of Principal Component Analysis (PCA) is to reduce the dimensionality of a data set, in which there are a large number of interrelated (*i.e.* correlated) variables, while retaining as much as possible of the variation present in the data set.<sup>81-84</sup> In the case of mass spectrometry, the data set consists of the mass spectra of different compounds. The mass spectra are expressed as the intensities of individual  $m/z$  ratios (*i.e.* variables). The aim of PCA is to find a new coordinate system that can be expressed as the linear combination of the original variables ( $m/z$  ratios), so that the major trends in the data are described. **(Figure 14)** Mathematically, PCA relies upon eigenvalue/eigenvector decomposition of the covariance or the correlation matrix of the original variables. PCA decomposes the data matrix  $\mathbf{X}$ , as the multiplication of two matrices,  $\mathbf{P}$ , the matrix of new coordinates of data points and  $\mathbf{T}'$ , the transposition of the coefficients matrix of the linear combination of the original variables.<sup>81</sup>

$$\mathbf{X} = \mathbf{P} * \mathbf{T}' \text{ (Equation 6)}$$

Generally, it is found that the data can be adequately described using far fewer coordinates, which are called principal components, than original variables. The first principal component is the combination of variables that explains the greatest amount of variation. The second principal component defines the next largest amount of variation and is independent to the first principal component. There can be as many principle components as there are variables. The process can be viewed as a rotation of the existing axes to new positions in the space defined by the original variables. In this new rotation, there is no correlation between the new variables defined by the rotation. The first new variable contains the maximum amount of variation, the second new variable contains the maximum amount of variation unexplained by the first and is orthogonal to the first and so on.<sup>82-84</sup> PCA also serves as a data reduction method and a very good visualisation tool. When the data points are plotted in the new coordinate system, the relationships and clusters are often more apparent than when the data points are plotted with the original coordinates.<sup>81</sup>

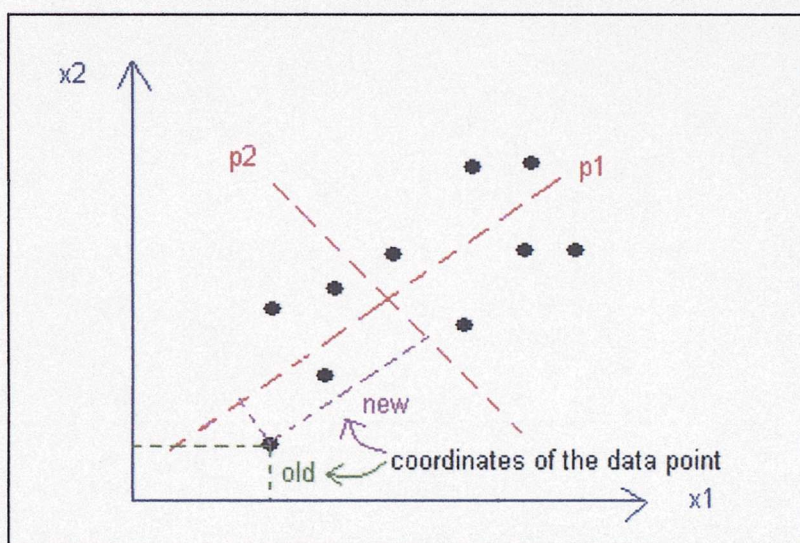


**Figure 14:** Geometrical interpretation of PCA. The axes of the new coordinate system (principal components p1 and p2) are created as the linear combination of the original axes.<sup>81</sup>

Despite the advanced modules Mass Frontier offers, its success rate with respect to fragment ion prediction when ES-MS/MS is used is rather low. This is due to certain limitations of the software that mainly involve the Fragments and Mechanisms module. The software predicts reaction pathways that are based on general fragmentation and rearrangement rules, originating from electron ionisation. Compound specific mechanisms that cannot be applied generally are not included. Additionally, fragment ions can only be generated from bond cleavages since bond creation is not supported and therefore, ring contractions, cyclisations, skeletal and non-hydrogen rearrangements, that often occur, are not included in the fragmentation generation module. For example, although the ion at  $m/z$  149 in an EI mass spectrum produced by phthalates is a well-known impurity ion, it cannot be recognised by Mass Frontier because it is formed *via* a series of rearrangements. General rules for the dissociation pathways of non-peptidic compounds have not yet been established for ES-MS/MS. The primary sites of ionisation and the fragmentation mechanisms taking place have also not been identified. Therefore the approaches Mass Frontier

employs for fragment ion generation are not ideal for compounds analysed using ES-MS/MS. Incorporation of the findings of this project into Mass Frontier should improve the ion prediction mode. This, in combination with the other modules the software features, should permit use of the program for rapid characterisation of combinatorial libraries.

## 2. The Fragmentation Patterns of Six Groups of Non-Peptidic Compounds

### 2a. Introduction

If the dissociation of non-peptidic molecules under ES-MS/MS conditions was taking place in a random manner, *i.e.* each compound produced compound specific fragment ions only, it would not be possible to identify which functional groups play an important role in dissociation and subsequently establish general fragmentation rules. Based on this, the first step in this investigation was to prove that the formation of fragment ions in ES-MS/MS depends on the structures of the molecules analysed and therefore show that compounds with common substructures follow common dissociation pathways.

To demonstrate the existence of fragmentation patterns, the spectra of six groups of non-peptidic compounds were studied. For each class of compounds, the common fragment ions and neutral losses were identified. Structures were assigned to the  $m/z$  values observed in the spectra with the aid of Mass Frontier and literature references. In certain cases, additional investigations were carried out, with respect to the ionisation and dissociation mechanisms taking place for fragment ion formation.

The results show that the groups of molecules studied follow unique dissociation routes, *i.e.* a distinct fragmentation pattern is identified for each class of compounds.

### 2b. Experimental

#### Materials

- The fragmentation pathways of benzimidazoles, carnitines, amphetamines, pheniramines, disopyramides and purines were determined using spectra available in the MS/MS library.<sup>52</sup>
- The library of 3-alkylamino-imidazo-[1,2- $\alpha$ ]azines was synthesised in house<sup>85</sup> and used without further purification.
- The benzimidazoles used in the d-labelling experiments were purchased from Sigma-Aldrich, Gillingham, UK.
- Methanol, HPLC grade, was purchased from Fisher, Loughborough, UK.
- Formic acid, analytical grade 98-100%, was purchased from Sigma-Aldrich, Gillingham, UK.
- Deuterated methanol ( $\text{CH}_3\text{OD}$ , 99%) and deuterated acetic acid ( $\text{CD}_3\text{COOD}$ , 99.5%) used for the d-labelling experiments were purchased from Qmx Laboratories Ltd, Thaxted, UK.

#### Sample Preparation

- Solutions of all compounds analysed were prepared in methanol and 0.1% formic acid. Concentration: 10  $\mu\text{g/mL}$ .
- For the d-labelling experiments, all compounds were dissolved in deuterated methanol and 0.1% deuterated acetic acid. Concentration: 10  $\mu\text{g/mL}$ .

### Instrumentation and Conditions Used

- All samples were analysed on an LCQ Deca Ion Trap (Thermo Finnigan, San Jose, CA, USA) under standard conditions: Capillary Temperature: 200 °C, Sheath Gas Flow: 35 au, Auxiliary Gas Flow: 10 au, Source Voltage: 4.5 kV. Nitrogen was used as the sheath and the auxiliary gas and helium was the collision gas.

MS/MS parameters: Isolation Width: 18, Collision Energy: 35%.

- Exact mass measurements were carried out using an Apex III FTICRMS (Bruker, Billerica, MA, USA): Capillary: -4.5 kV, End Plate: -3.8 kV, Capillary Exit: 102 V, Skimmer 1: 8.26 V, Skimmer 2: 7.64 V, Offset: 1.00, Rf Amplitude: 550.00 Hz, Dry Gas Temperature: 130°C. Nitrogen was used as the drying gas and argon was used as the collision gas.

MS/MS parameters: corr sweep pulse length: 1000  $\mu$ sec, corr sweep attenuation: 30.0 dB, ejection safety belt: 3000 Hz, user pulse length: 5000  $\mu$ sec, ion activation pulse length: 250000  $\mu$ sec, ion activation attenuation: 49.5 dB, frequency offset from activation mass: -500 Hz, user delay length: 3 sec.

- D-labelling experiments were carried out on an LCQ Deca Ion Trap (Thermo Finnigan, San Jose, CA, USA) using the following conditions: Capillary Temperature: 200 °C, Sheath Gas Flow: 5 au, Auxiliary Gas Flow: 20 au, Source Voltage: 4.5 kV. Nitrogen was used as the sheath and the auxiliary gas and helium was the collision gas.

MS/MS parameters: Isolation Width: 1, Collision Energy: 35%.

## 2c. Results and Discussion

### The Fragmentation Pathway of Carnitines

Spectra of twelve carnitines (**Appendix 1, Table 1**) and ten carnitine butyl esters (**Appendix 1, Table 2**) were available in the MS/MS library. The fragmentation pathway of the compounds under ES-MS/MS conditions was investigated and the main fragment ions produced by the compounds were identified.

Carnitines produced common fragment ions at  $m/z$  85,  $m/z$  144 and also due to the loss of 59 Da. *E.g.* the spectrum of propionylcarnitine is shown in **Figure 15**.

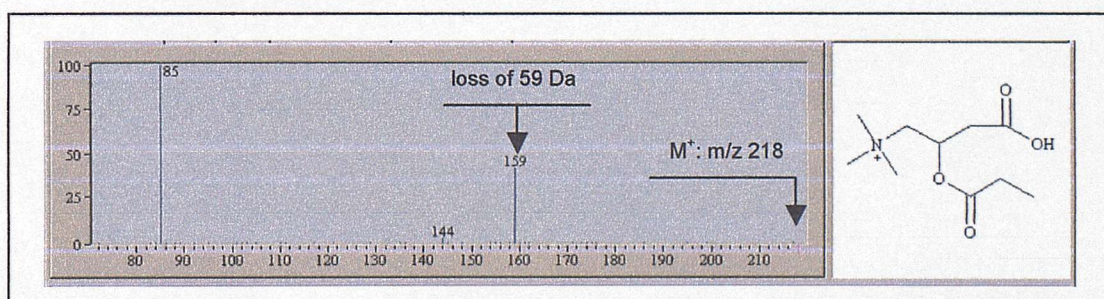


**Figure 15:** The ES-MS/MS spectrum of propionylcarnitine.

The loss of 59 Da corresponds to the loss of trimethylamine.<sup>86-95</sup> (**Figure 16, Scheme A**) Additional loss of XCOOH from the molecules leads to the most abundant ion in the spectra, at

$m/z$  85. (**Figure 16, Scheme B**) This ion is produced by most carnitines and is frequently reported in literature<sup>86-101</sup>, as it is commonly used in Single Ion Monitoring (SIM) experiments aimed at the detection of carnitines at low concentration levels. Both ions at  $m/z$  85 and due to the loss of 59 Da are stabilised by cyclisation and form lactones.<sup>88,96</sup> The ion at  $m/z$  144 is formed after the loss of XCOOH, but this time the trimethylamine moiety remains on the molecule.<sup>89-91,95</sup> (**Figure 16, Scheme C**) Finally, carnitines with long alkyl chains (X) produce an additional fragment ion that corresponds to  $^+\text{COX}$  as shown in **Figure 16, Scheme D**. The  $m/z$  value of this fragment ion varies depending on the size of the alkyl chain.

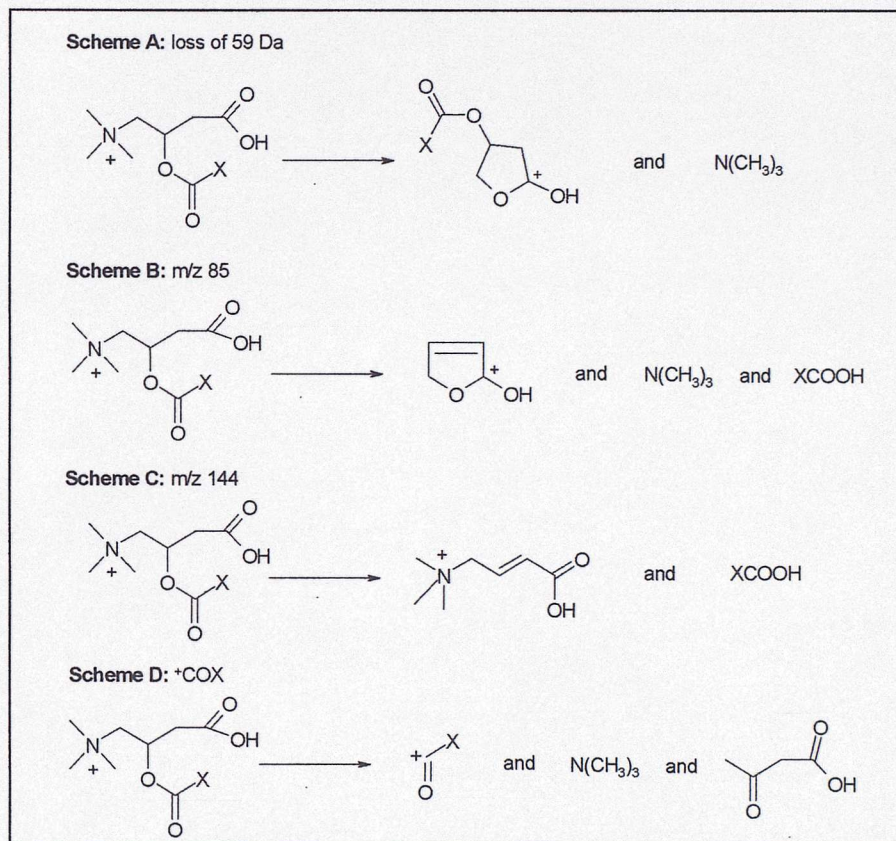
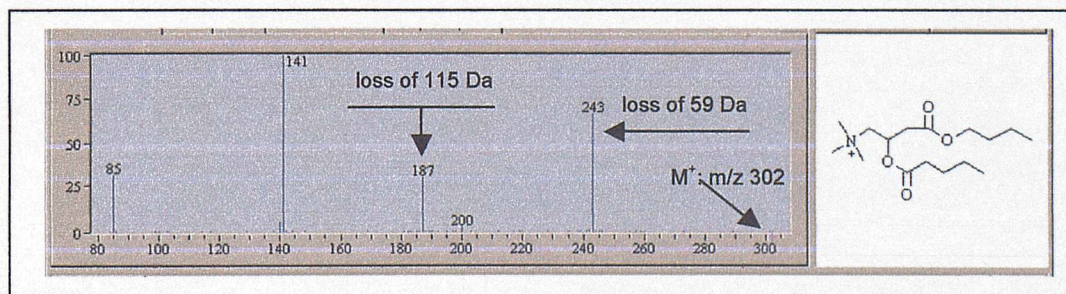


**Figure 16:** The main fragment ions of carnitines.

Carnitine butyl esters dissociate in a similar manner as the unprotected molecules. Common fragment ions appear at  $m/z$  85,  $m/z$  140,  $m/z$  141 and  $m/z$  200 and due to the losses of 59 Da and 115 Da. *E.g.* the spectrum of valerylcarnitine butyl ester is shown in **Figure 17**.



The dissociation pattern previously described for carnitines is also maintained for the butyl protected molecules, but additional fragment ions are observed due to the new functionality present in the structures. The loss of 59 Da involves loss of the trimethylamine only, (**Figure 18, Scheme A**) while the loss of 115 Da corresponds to the loss of the trimethylamine followed by the loss of butene.<sup>91,102</sup> (**Figure 18, Scheme B**) In a similar fashion, the fragment ion at  $m/z$  141 is formed after the trimethylamine and XCOOH are lost from the molecules, (**Figure 18, Scheme C**) while additional loss of butene results in the formation of the fragment ion at  $m/z$  85. (**Figure 18, Scheme D**) The structures of all the ions mentioned above are again stabilised through cyclisation and lactones are formed.<sup>88,96</sup> The fragment ion at  $m/z$  200 corresponds to the ion previously observed for carnitines at  $m/z$  144. It involves loss of XCOOH from the compounds, while the trimethylamine and the butyl group remain attached. (**Figure 18, Scheme E**) Finally, the structure of the fragment ion at  $m/z$  140 was not identified. Although this ion is present in the spectra of most carnitine butyl esters, its abundance was always less than 10% and its presence was never reported in literature references.

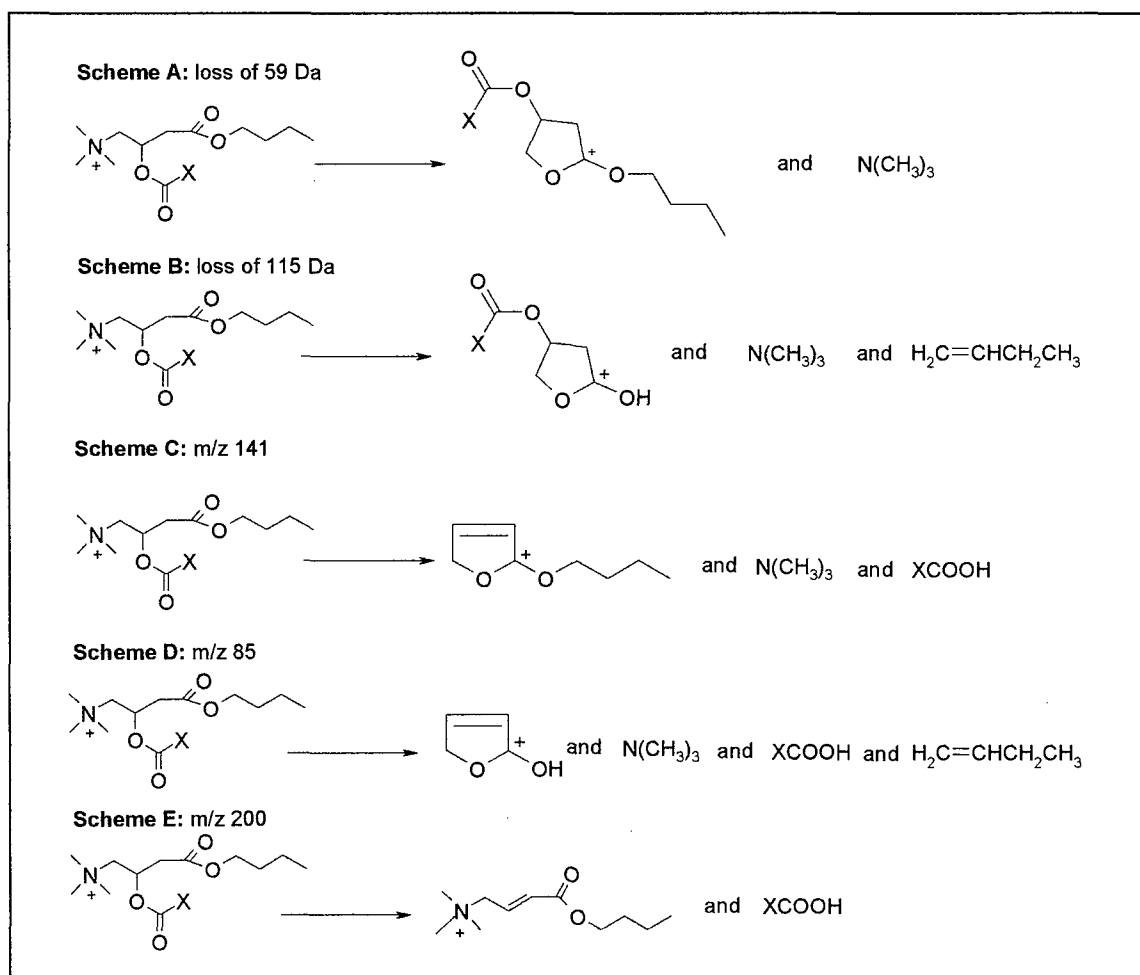


**Figure 18:** The main fragment ions of carnitine butyl esters.

The spectra obtained both for carnitines and their butyl esters clearly indicate that a common route is followed by all the compounds studied within this group.

### The Fragmentation Pathway of Pheniramines and Disopyramides

The structures of the five compounds studied are shown in **Appendix 1, Table 3**. All compounds consist of the substructure of pheniramine with additional substituents attached at various sides of the molecules. The five compounds dissociate in a common manner and form only one fragment ion due to cleavage of the tertiary amine, which leads to the loss of the secondary amine  $(\text{CH}_3)_2\text{NH}$ .

In the case of the three pheniramines, this corresponds to the loss of 45 Da<sup>103,104</sup> (**Figure 19, Scheme A**), while for the two disopyramides the loss corresponds to 101 Da. (**Figure 19, Scheme B**) Halogen substituents present on the benzene ring of the compounds play no role in dissociation. Similarly, the addition of the amide group in the structures of the disopyramides causes no additional fragment ions to be formed. The tertiary amine is the only part of the molecules that fragments.

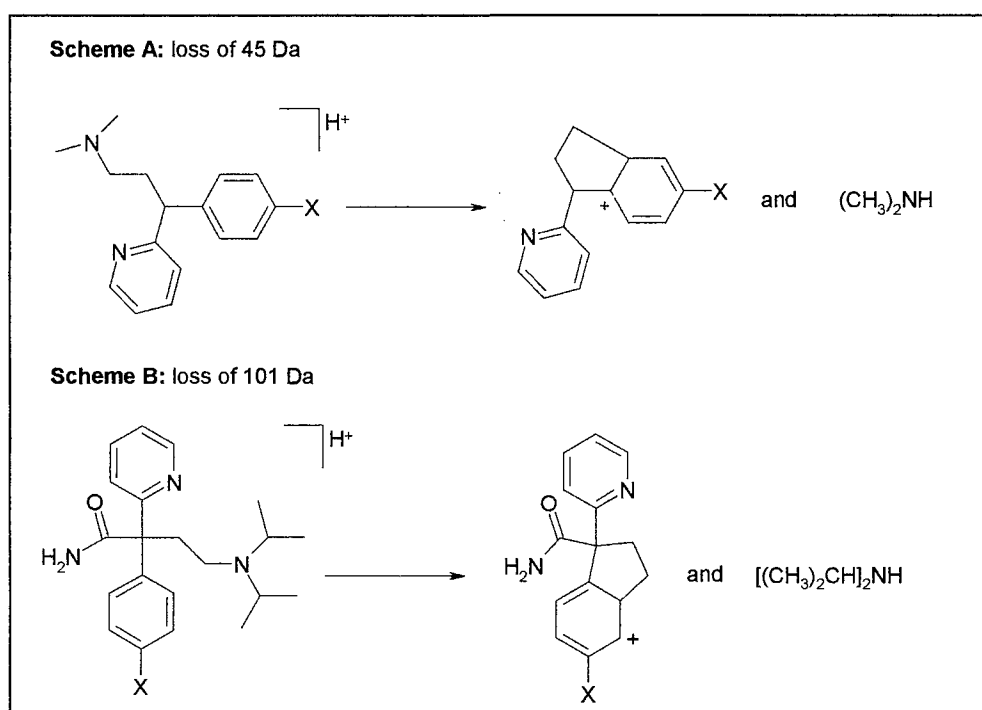


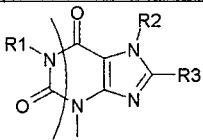
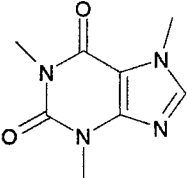
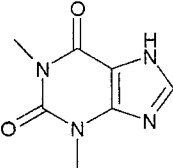
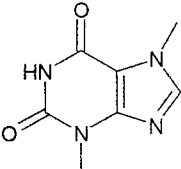
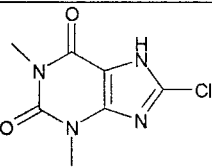
**Figure 19:** The main fragment ions produced by pheniramines and disopyramides.

### The Fragmentation Pathway of Purines

The spectra of nine purines (**Appendix 1, Table 4**) were available in the MS/MS library. The structures of caffeine, theophylline, theobromine and 8-chlorotheophylline consist only of the purine ring system, whilst on the rings of proxiphylline, diprophylline, bamiphylline, etamiphylline and etophylline additional aliphatic chains are attached. This difference in the structures results in the compounds following markedly different dissociation routes.

The main fragmentation pathway followed by caffeine and its homologues involves loss of part of the six-member ring of the purine system, as shown in **Table 1**.<sup>50,51,105-111</sup> The  $m/z$  value of the resulting fragment ion and the corresponding neutral loss vary, depending on the substituents on

the rings. Most compounds produced additional compound specific ions, the majority of which were of low abundance.

Compound	Common Neutral Loss
	
 Caffeine	m/z 138 loss of CH <sub>3</sub> NCO (loss of 57 Da)
 Theophylline	m/z 124 loss of CH <sub>3</sub> NCO (loss of 57 Da)
 Theobromine	m/z 138 loss of NHCO (loss of 43 Da)
 8-Chlorotheophylline	m/z 158 loss of CH <sub>3</sub> NCO (loss of 57 Da)

**Table 1:** The main fragment ion produced by the four purines with no aliphatic chains in their structures.

In the cases of proxyphylline, diprophylline, bamiphylline, etamiphylline and etophylline, the purine ring system does not fragment. Fragment ions are only formed due to dissociation taking place on the aliphatic chains. Each compound produced one fragment ion, which was always due to cleavage of some part of the aliphatic fraction of the structure. *E.g.* the spectrum of proxyphylline is shown in **Figure 20**.

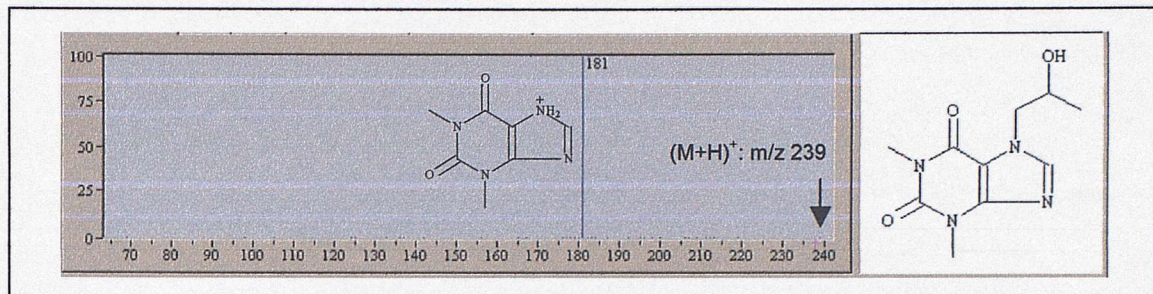


**Figure 20:** The ES-MS/MS spectrum of proxyphylline.

The fragment ion at  $m/z$  181, which is observed in the spectra of proxyphylline, diprophylline and etophylline is formed after the whole aliphatic chain is cleaved. (**Figure 21, Scheme A**) On the other hand, in the cases of bamiphylline and etamiphylline, where a tertiary amine is included in the chain, dissociation results in cleavage of the tertiary amine only. (**Figure 21, Schemes B and C**)

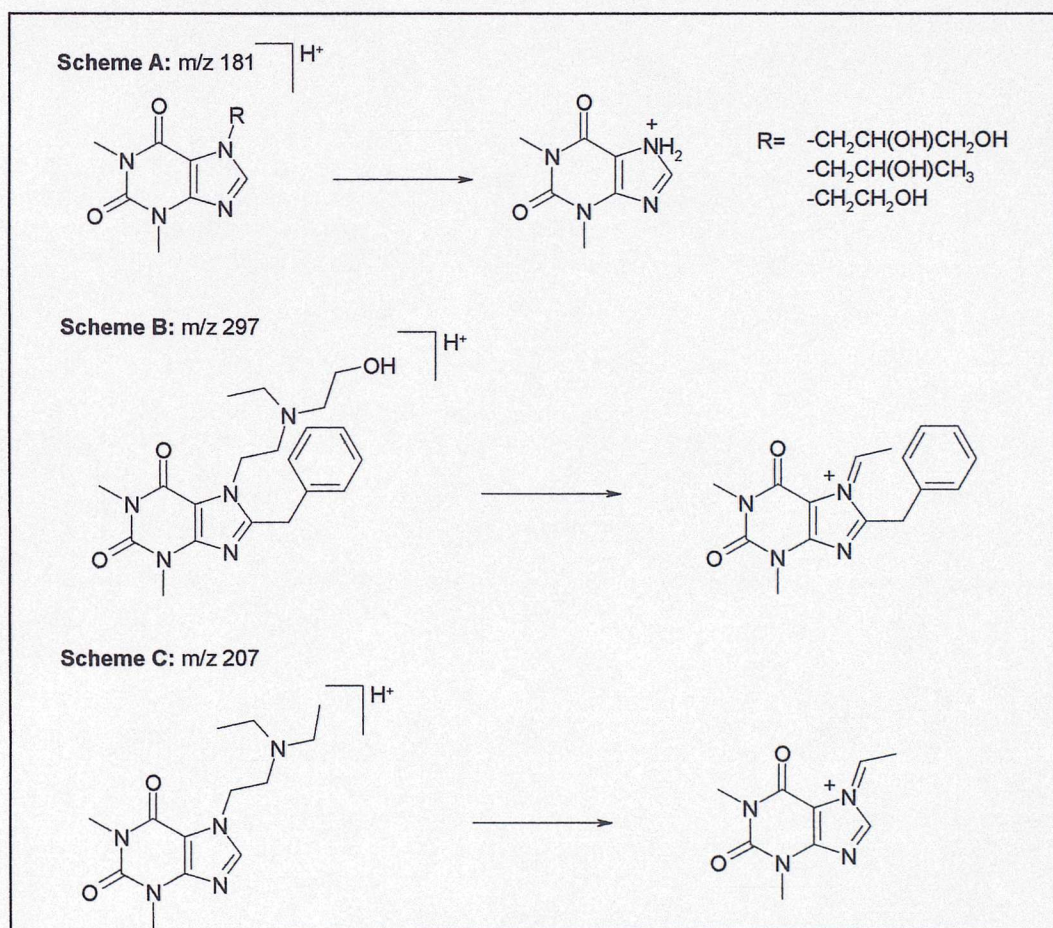


**Figure 21:** The main fragment ions observed for purines with aliphatic chains attached.

The dissociation pathways followed by the nine purines provide a clear example of how the different functionalities in the structures affect fragmentation under ES-MS/MS conditions. Dissociation for caffeine and its homologues takes place on the ring system and the bonds easiest to cleave, after protonation, are the ones indicated in **Table 1**. When aliphatic chains are added to

the structures, fragmentation takes place on the aliphatic part of the molecules and if an amine functionality is present, the bond easiest to break, after protonation, is the one next to the amine group. This example provides an indication of the types of functionalities that dominate dissociation in ES-MS/MS and shows that if a hierarchy of influence were established, fragment ion prediction based on molecular structure would be possible.

### The Fragmentation Pathway of Benzimidazoles

The structures of a small group of benzimidazoles studied are shown in **Appendix 1, Table 5**. The only compound without a carbamate substituent attached on the 2'-position of the benzimidazole ring is thiabendazole, which has a thiazole ring attached instead. Thiabendazole produces only one fragment ion at  $m/z$  175 due to the loss of HCN (27 Da) from the thiazole ring.<sup>112</sup> (**Figure 22**) Fragment ions due to dissociation taking place on the benzimidazole rings were not observed.

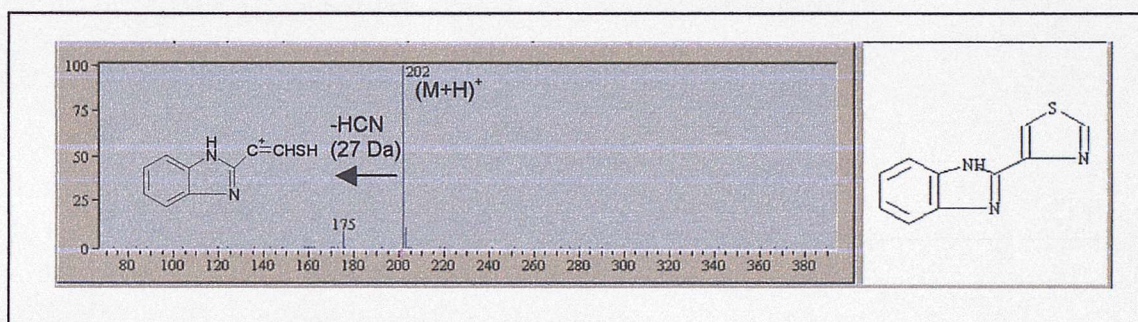


**Figure 22:** The ES-MS/MS spectrum of thiabendazole.

A single ion due to the loss of 32 Da was observed in the spectra of all other compounds and corresponds to the loss of  $CH_3OH$  from the carbamate group.<sup>113-122</sup> *E.g.* the spectrum of carbendazim is shown in **Figure 23**. It appears that for this class of compounds dissociation is limited to the most labile substituent attached to the benzimidazole rings, whilst the ring structure is stable and does not fragment.

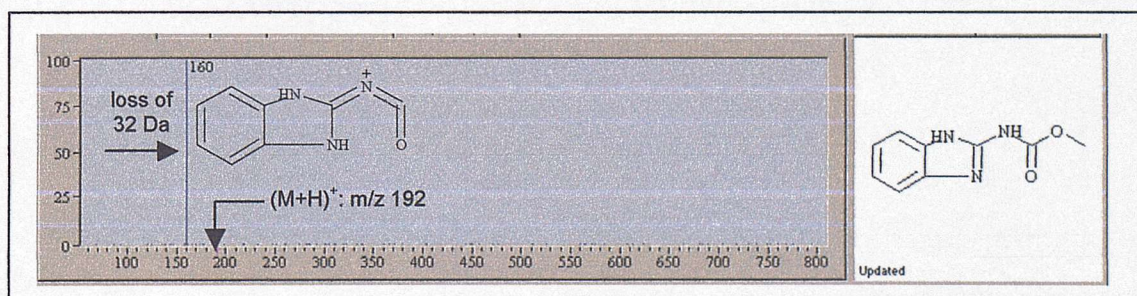


**Figure 23:** The ES-MS/MS spectrum of carbendazim.

In order to investigate the mechanism leading to the loss of  $\text{CH}_3\text{OH}$  from the benzimidazoles, d-labelling experiments were carried out on five of the compounds producing this loss\*. All the MS/MS spectra obtained for the fully d-labelled compounds, showed that only one fragment ion was present, due to the loss of 33 Da corresponding to the loss of  $\text{CH}_3\text{OD}$ . Therefore, the H involved in the loss of  $\text{CH}_3\text{OH}$  is an exchangeable hydrogen. This could be either the proton gained during ionisation or one of the two amine hydrogens present in the structure of the compounds. The spectrum of carbendazim obtained during the d-labelling experiments demonstrating the extra 1 Da loss is shown in **Figure 24**.

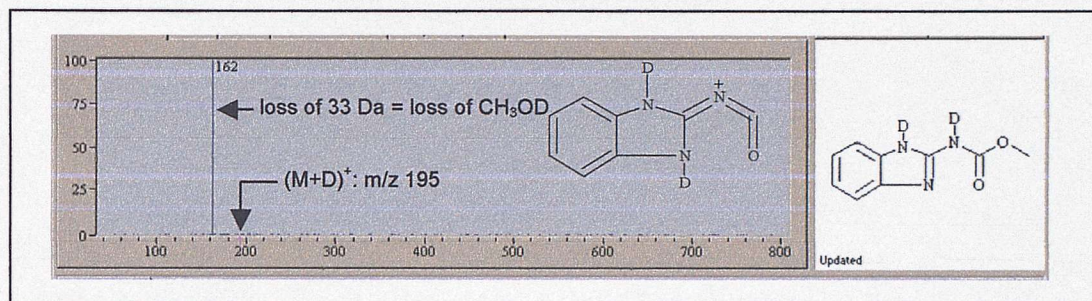


**Figure 24:** The ES-MS/MS spectrum of d-labelled carbendazim.

Although the structure of the resulting fragment ion due to the loss of  $\text{CH}_3\text{OH}$  can be predicted and the origin of the hydrogens involved in the mechanism is known, a detailed mechanistic pathway for ion formation cannot be proposed until the primary site of ionisation of the compounds is identified. In the case of this class of molecules, this is not an easy task. The three tautomeric structures of the benzimidazoles with the carbamate group attached are shown in **Figure 25**. Molecular modelling calculations at a high level of theory are required in order to determine which of the tautomers exist in the gas phase or whether all of them co-exist. Identification of the primary sites of ionisation for all the tautomers involved should then follow in order to cover all the mechanistic possibilities. The conformation of the compounds in the gas phase has to be revealed before a mechanism can be proposed. Such studies are out of the scope of this project and therefore this mechanistic pathway was not examined in any more depth.

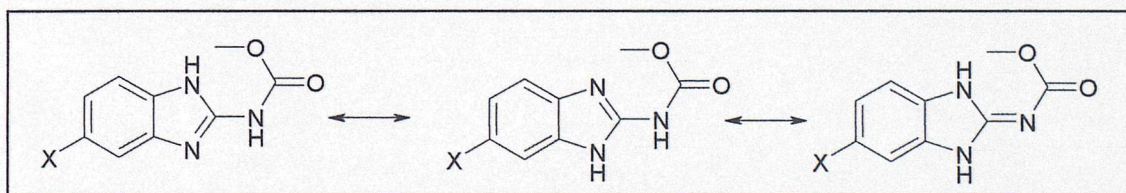


**Figure 25:** The tautomeric structures of benzimidazoles with a carbamate substituent attached on the 2'-position of the benzimidazole ring.

\* Oxfendazole is not commercially available.

### The Fragmentation Pathway of Amphetamines

Fifteen molecules consisting of the amphetamine substructure were available in the MS/MS library. (**Appendix 1, Table 6**) Their spectra were studied and the common fragment ions produced were identified.

Compounds with functional groups attached to the benzene ring and the amine group of amphetamine follow a common dissociation pathway based on straightforward bond cleavages. Protonation is known to occur on the amine functionality, as this was previously proven to be the most basic site of the structure.<sup>123</sup> Then the amine is cleaved to produce an ion at  $m/z$  119, when  $R_1=H$  and at appropriate  $m/z$  values consistent with the functional groups attached.<sup>123-127</sup> (**Figure 26, Scheme A**) Further loss of  $CH_2=CH_2$  results in a fragment ion at  $m/z$  91 or at higher  $m/z$  values depending again on the degree of substitution on the aromatic ring.<sup>123-128</sup> (**Figure 26, Scheme B**) Although some compounds produced additional compound specific ions, the common dissociation route described above was followed by all molecules studied.

Differences in the fragmentation pathway described are observed when compounds with hydroxyl or carbonyl substituents on the aliphatic part of the molecules are considered. Additional dissociation takes place at the hydroxyl and at the carbonyl group and a large number of compound specific fragment ions are formed for each compound. When a hydroxyl substituent is present on the molecules, the fragment ion previously observed at  $m/z$  119 is shifted at  $m/z$  117. This is due to an additional loss of  $H_2O$  taking place that results in the creation of the double bond. (**Figure 26, Scheme C**)

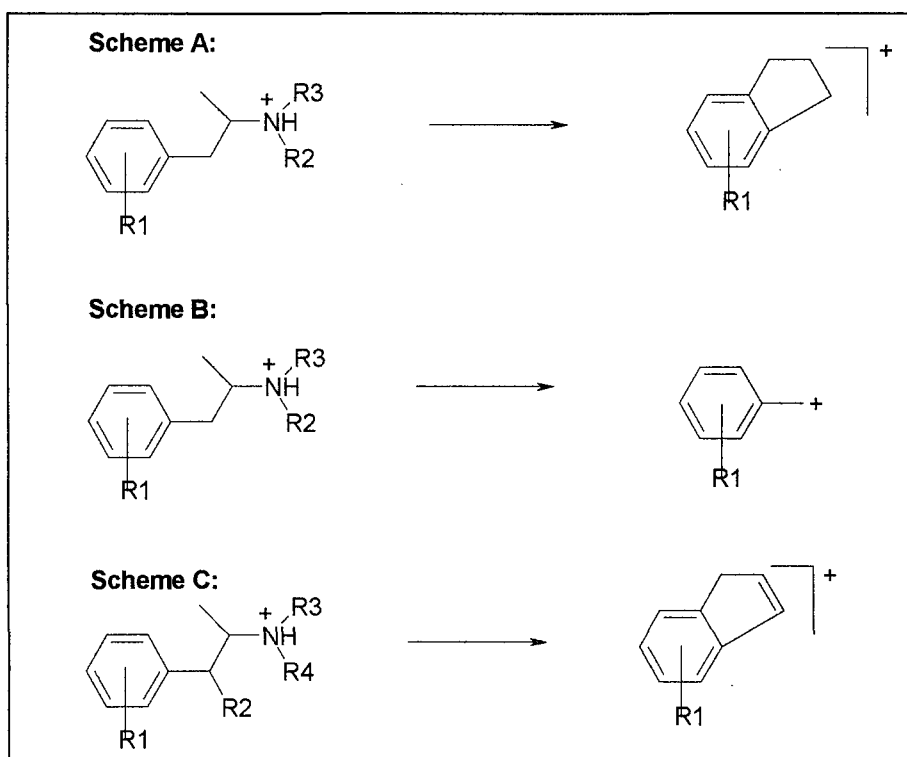


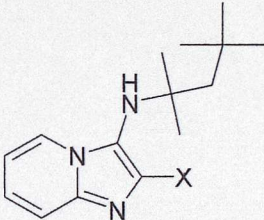
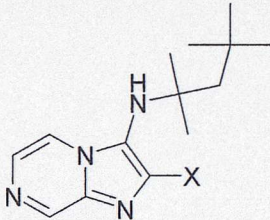
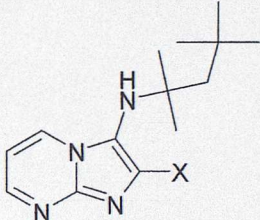
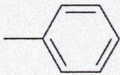
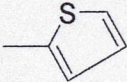
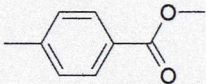
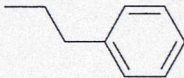

**Figure 26:** The main fragment ions produced by amphetamines under ES-MS/MS conditions.

Overall, a common fragmentation pattern is observed for all amphetamines and a number of common fragment ions are formed. However, the dissociation routes leading to the formation of those fragment ions differ depending on the functionalities present in the structures of the compounds. In addition, identification of the fragmentation pattern can be difficult due to the large number of individual compound specific ions produced by certain molecules.

### The Fragmentation Pathway of 3-Alkylamino-imidazo-[1,2- $\alpha$ ]azines

The library of 3-alkylamino-imidazo-[1,2- $\alpha$ ]azines was synthesised in the Combinatorial Centre of Excellence.<sup>85</sup> The structures of the individual compounds are shown in **Appendix 1, Table 7**.

Differences in the structures of the molecules exist with respect to the number of nitrogens and their position in the rings, as well as the various substituents X. The three core structures and the different substituents X are shown in **Table 2**.

Core Structures					
X Groups					

**Table 2:** The structural components of the group of 3-alkylamino-imidazo-[1,2- $\alpha$ ]azines studied.

Despite the differences in the structures, all compounds fragment in the same manner. Three common neutral losses were observed of 112 Da, 113 Da and 139 Da. *E.g.* the spectrum of one of the 3-alkylamino-imidazo-[1,2- $\alpha$ ]azines is shown in **Figure 27**.

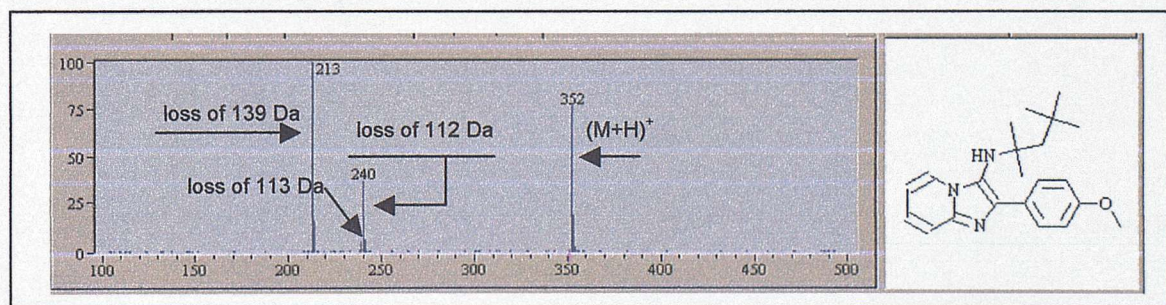


**Figure 27:** The ES-MS/MS spectrum of 2-(4-methoxyphenyl)-*N*-(1,1,3,3-tetramethylbutyl)imidazo[1,2- $\alpha$ ]pyridin-3-amine.

The loss of 112 Da corresponds to the loss of the tetramethylbutyl substituent, leading to the generation of an even electron species as shown in **Figure 28, Scheme A**. In a similar manner, the loss of 113 Da corresponds to the loss of the same substituent but the resulting ion is a radical cation **Figure 28, Scheme B**. This fragment ion is not observed for all compounds and its abundance in the spectra is always low. Finally, further loss of HCN or HNC (27 Da) from the fragment ion due to the loss of 112 Da results in the third common neutral loss observed for these compounds, corresponding to 139 Da **Figure 28, Scheme C**. Fragment ions that did not follow the general pattern observed for the group (compound specific) were not produced by any of the compounds in the library. All molecules generated very similar spectra and followed the same dissociation pathway.

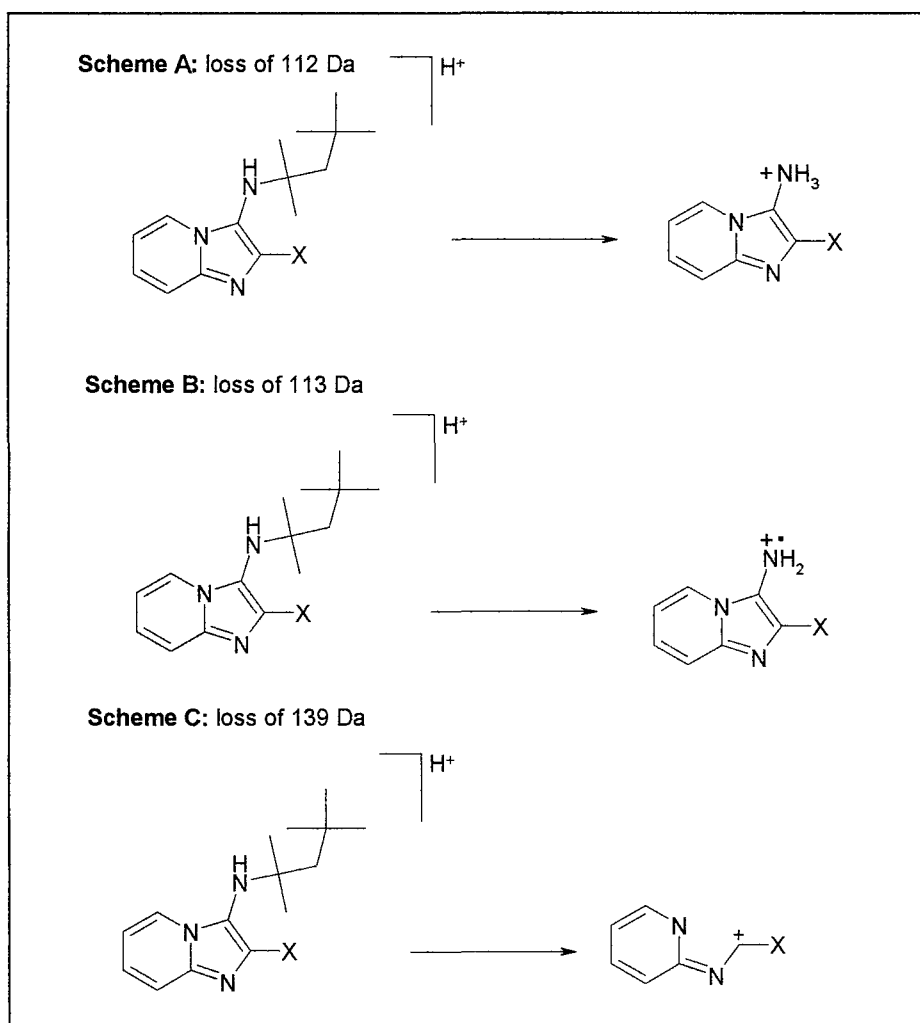


**Figure 28:** The main fragment ions produced by the group of 3-alkylamino-imidazo-[1,2- $\alpha$ ]azines studied.

## 2d. Conclusion

The fragmentation pathways of six groups of non-peptidic molecules under ES-MS/MS conditions were studied and the main fragment ions observed in the spectra were identified. The

results showed that dissociation under ES-MS/MS conditions is dependant upon the structures of the compounds and therefore compounds with similar structures follow similar dissociation routes. This renders identification of the bonds on the molecules likely to be cleaved possible and enables fragment ion prediction. Additional studies on the dissociation pathways of the various classes of non-peptidic molecules should provide further information about fragmentation by ES-MS/MS that in turn could be incorporated into an AI software package to aid the automated interpretation of data.

### 3. The Fragmentation Pattern of an Array of Amino Acids

#### 3a. Introduction

In order to establish that the observations made in **Chapter 2** about dissociation in ES-MS/MS remain valid when large groups of molecules are considered, the fragmentation routes of an array of amino acids were investigated. This array was chosen based on the facts that amino acids are often used in combinatorial synthesis, that they are structurally simple molecules and their way of dissociation has been studied in the past by many research groups, using a range of mass spectrometric techniques.<sup>98-100,129-150</sup>

The amino acids studied were divided into two groups of protected and unprotected molecules. For each group the main fragment ions formed were identified and mechanisms leading to their formation were investigated using exact mass measurements and d-labelling experiments. The results obtained were compared with those reported in literature and observations were made about the fragmentation processes followed by this type of compound under ES-MS/MS conditions.

#### 3b. Experimental

##### Materials

- The fragmentation pathways of the array of amino acids were determined using spectra available in the MS/MS library.<sup>52</sup>
- The amino acids used in the d-labelling experiments were purchased from Sigma-Aldrich, Gillingham, UK.
- Methanol, HPLC grade, was purchased from Fisher, Loughborough, UK.
- Formic acid, analytical grade 98-100%, was purchased from Sigma-Aldrich, Gillingham, UK.
- Deuterated methanol ( $\text{CH}_3\text{OD}$ , 99%) and deuterated acetic acid ( $\text{CD}_3\text{COOD}$ , 99.5%) used for the d-labelling experiments were purchased from Qmx Laboratories Ltd, Thaxted, UK.

##### Sample Preparation

- Solutions of all compounds analysed were prepared in methanol and 0.1% formic acid. Concentration: 10  $\mu\text{g/mL}$ .
- For the d-labelling experiments, all compounds were dissolved in deuterated methanol and 0.1% deuterated acetic acid. Concentration: 10  $\mu\text{g/mL}$ .

##### Instrumentation and Conditions Used

- All samples were analysed on an LCQ Deca Ion Trap (Thermo Finnigan, San Jose, CA, USA) under standard conditions: Capillary Temperature: 200 °C, Sheath Gas Flow: 35 au, Auxiliary Gas Flow: 10 au, Source Voltage: 4.5 kV. Nitrogen was used as the sheath and the auxiliary gas and helium was the collision gas.

MS/MS parameters: Isolation Width: 18, Collision Energy: 35%.

- Exact mass measurements were carried out using an Apex III FTICRMS (Bruker, Billerica, MA, USA): Capillary: -4.5 kV, End Plate: -3.8 kV, Capillary Exit: 157.85 V, Skimmer 1: 9.42 V, Skimmer 2: 6.17 V, Offset: 1.12, Rf Amplitude: 550.00 Hz, Dry Gas Temperature: 130°C. Nitrogen was used as the drying gas and argon was used as the collision gas.

MS/MS parameters: corr sweep pulse length: 1000  $\mu$ sec, corr sweep attenuation: 30.0 dB, ejection safety belt: 3000 Hz, user pulse length: 5000  $\mu$ sec, ion activation pulse length: 250000  $\mu$ sec, ion activation attenuation: 49.5 dB, frequency offset from activation mass: -500 Hz, user delay length: 3 sec.

- D-labelling experiments were carried out on an LCQ Deca Ion Trap (Thermo Finnigan, San Jose, CA, USA) using the following conditions: Capillary Temperature: 200 °C, Sheath Gas Flow: 5 au, Auxiliary Gas Flow: 20 au, Source Voltage: 4.5 kV. Nitrogen was used as the sheath and the auxiliary gas and helium was the collision gas.

MS/MS parameters: Isolation Width: 1, Collision Energy: 35%.

### 3c. Results and Discussion

An investigation into the ES-MS/MS spectra of forty amino acids (**Appendix 2, Table 1**) showed that common neutral losses together with compound specific fragment ions were present. Compound specific ions were mainly formed due to the various side chains attached on the compounds,<sup>129-136</sup> while the neutral losses originated from the amino acid core. The main ion produced by the aliphatic amino acids was due to the loss of 46 Da, literature reports this as corresponding to the loss of the elements of formic acid, H<sub>2</sub>, C, O<sub>2</sub>.<sup>44,129-147</sup> *E.g.* the spectrum of valine is shown in **Figure 29**. The loss of 46 Da was also observed in the spectra of the aromatic compounds and this ion was always of high abundance. Additional fragment ions were observed for the aromatic amino acids due to the loss of 35 Da, corresponding to the losses of NH<sub>3</sub> and H<sub>2</sub>O<sup>99,147</sup> and due to the loss of 63 Da, corresponding to H<sub>2</sub>CO<sub>2</sub> followed by the loss of NH<sub>3</sub>.<sup>99,147</sup> Finally, the loss of 59 Da was observed and this has not been previously reported in literature. *E.g.* the spectrum of 3,4-dihydroxyphenylalanine is shown in **Figure 30**.

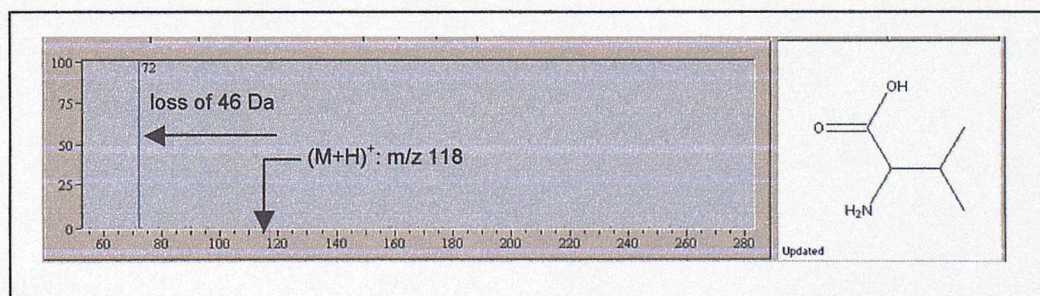


**Figure 29:** The ES-MS/MS spectrum of valine.

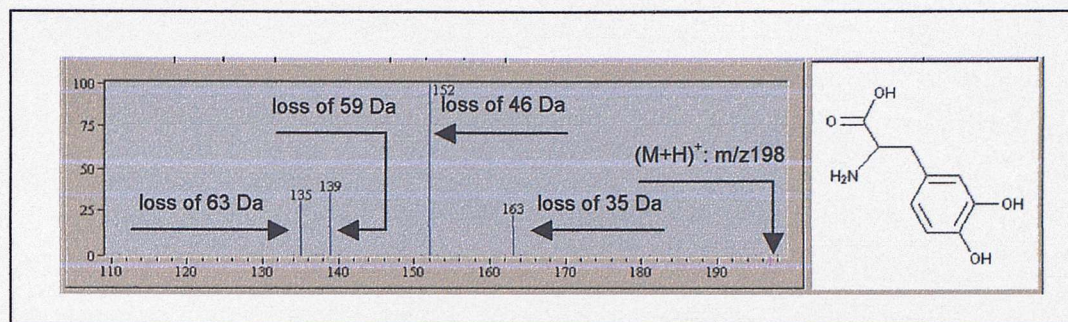


**Figure 30:** The ES-MS/MS spectrum of 3,4-dihydroxyphenylalanine.

Exact mass measurements by FTMS and d-labelling experiments were carried out, in order to confirm the identity of the neutral losses observed and also investigate the mechanism leading to the loss of 46 Da. Two aliphatic amino acids, valine and methionine, and two aromatic molecules, phenylalanine and tyrosine were randomly chosen to be used in these experiments. The results of the exact mass analysis are summarised in **Appendix 2, Table 2**. The identities of the neutral losses as proposed in literature were confirmed. The loss of 59 Da was only observed for tyrosine and was recognised to be the loss of  $C_2H_5NO$ . Formation of the resulting fragment ion possibly involves a rearrangement. Based on the results obtained and with the aid of Mass Frontier, structures can now be assigned to the ions formed due to the common neutral losses observed for the amino acids. *E.g.* the fragment ions formed by tyrosine are shown in **Table 3**.

Common Neutral Loss Observed	Identity of Neutral Loss	Structure of Resulting Fragment Ion
loss of 35 Da	$H_2O + NH_3$	
loss of 46 Da	$H_2CO_2$	
loss of 59 Da	$C_2H_5NO$	
loss of 63 Da	$H_2CO_2 + NH_3$	

**Table 3:** Structures proposed for the fragment ions observed in the ES-MS/MS spectrum of tyrosine.

The mechanism leading to the loss of 46 Da from amino acids has been an area of interest for many research groups. Milne *et al*<sup>129</sup> first proposed a dissociation route for aliphatic and aromatic amino acids under methane CI conditions. The neutral losses of 35, 46 and 63 Da were reported and two years later, they were further confirmed by Leclercq and Desiderio.<sup>130</sup> The first mechanism leading to the loss of 46 Da was proposed by Meot-Ner and Field,<sup>137</sup> (**Figure 31, Scheme A**) *i.e.* when the amino acids are analysed under isobutane CI conditions, the loss of formic acid occurs *via* an energetically favoured bi-cyclic intermediate, after protonation on the NH<sub>2</sub> group. In 1974, Tsang and Harrison<sup>131</sup> proposed a different route that involves the two-step loss of H<sub>2</sub>O and CO. (**Figure 31, Scheme B**) The ionisation methods used were methane and hydrogen CI and d-labelling experiments were used to contrast the results previously published by Meot-Ner and Field. Tsang and Harrison proposed that protonation takes place at various sites of the structure and intra-molecular transfer of the gained proton can occur before dissociation. In 1988, a third possible fragmentation route was proposed by Kulik and Herma.<sup>133</sup> Based on their experiments using FAB MS, the mechanism leading to the loss of 46 Da from amino acids can either be the two-step process suggested by Tsang and Harrison or the one-step loss of rapidly dissociating dihydroxycarbene. (**Figure 31, Scheme C**) Protonation is proposed on the amine group and then the proton is transferred to other sites for dissociation to occur. This fragmentation route, that involves the loss of a dihydroxycarbene, was also supported by Beranová *et al*<sup>140</sup>. The latter studied the mechanism in question using both methane CI and FAB MS and they concluded that different processes could occur under different ionisation conditions. For metastable ions formed using CI, the loss of H<sub>2</sub>O followed by CO is the energetically favoured route. On the other hand, ions formed using CID can dissociate following either the two-step process proposed by Tsang and Harrison or in one step as dihydroxycarbene. For the elimination of dihydroxycarbene, protonation is suggested on the carbonyl group.

Various other groups have investigated the same mechanism and depending on the ionisation method used, the results usually fit one of the proposed routes shown in **Figure 31**.<sup>132,134,135,138,139</sup> Additional minor processes were also reported,<sup>134</sup> as well as variations in the original mechanisms were proposed.<sup>132</sup> The three main dissociation routes were also investigated using *ab initio* calculations.<sup>148,149</sup> Evaluation of the energies of the cations formed after protonation on all the possible functional groups, as well as of the energies of the reaction intermediates leading to the final fragment ion, allows comparison of the total energy of each pathway and subsequent identification of the energetically favoured dissociation route. In most cases this was found to be the mechanism proposed by Tsang and Harrison, *i.e.* the two step process, whilst the loss of dihydroxycarbene was identified as a possible secondary process.

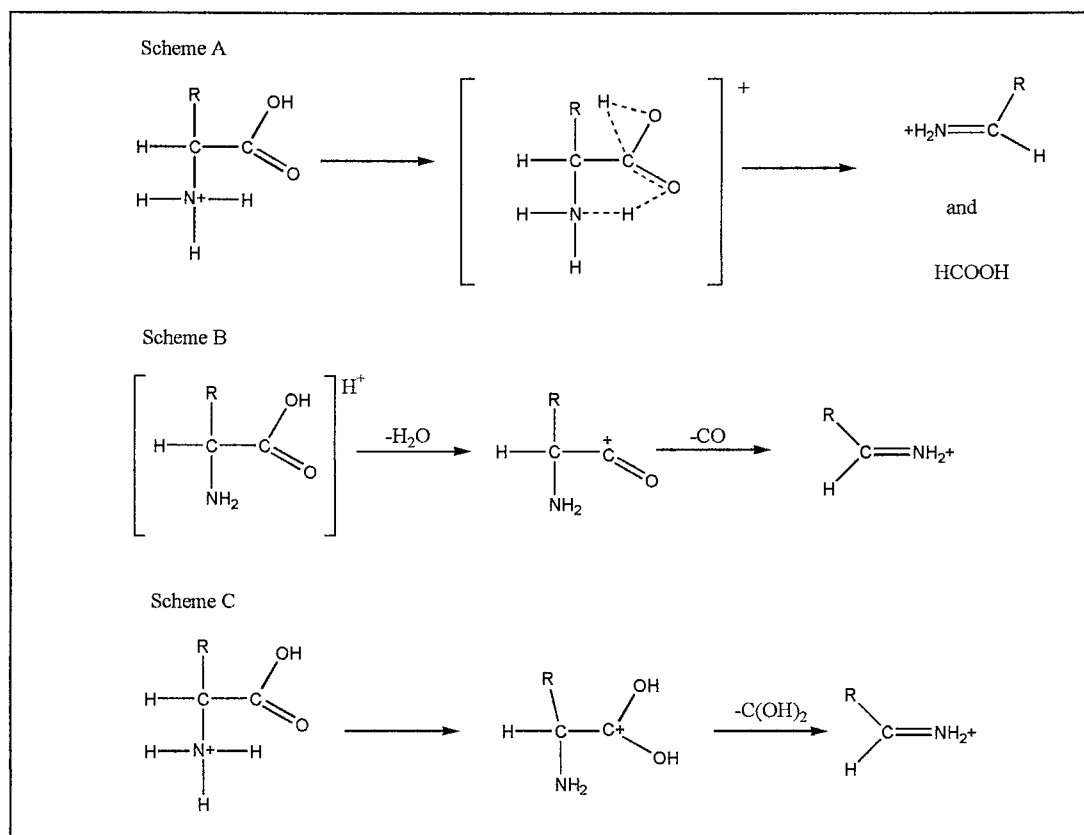


**Figure 31:** The three main mechanisms leading to the loss of 46 Da, as proposed in literature.<sup>131,133,137</sup>

The mechanism involved in the loss of 46 Da from amino acids, was studied under ES-MS/MS conditions by Rogalewicz *et al*<sup>136</sup> on a triple quadrupole instrument. D-labelling experiments and *ab initio* calculations carried out on all  $\alpha$ -amino acids allowed the authors to postulate a general mechanism for the loss of 46 Da. The sequential losses of H<sub>2</sub>O and CO, through protonation on the amine and further proton transfer to the hydroxyl group, were proposed. (**Figure 32**) In order to determine whether the same data would be obtained using ES-MS/MS on an ion trap instrument, experiments were carried out on the four amino acids chosen, valine, methionine, phenylalanine and tyrosine, and the results were compared with those reported in literature.

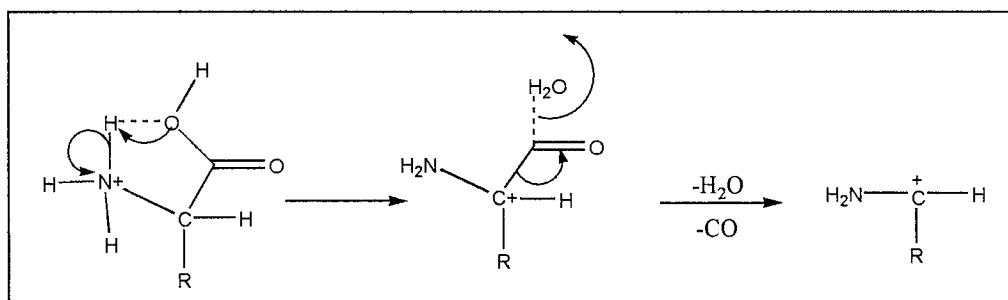


**Figure 32:** The mechanism proposed by Rogalewicz *et al*<sup>136</sup> for the loss of 46 Da from amino acids under ES-MS/MS conditions.

In order to observe fragment ions due to the losses of  $\text{H}_2\text{O}$  and  $\text{NH}_3$ , the MS/MS spectra of the four amino acids were initially recorded on the LCQ ion trap with the wideband excitation function turned off. The spectra obtained for the compounds are shown in **Figure 33**. The loss of 46 Da was present in all spectra, whilst the loss of  $\text{H}_2\text{O}$  suggesting a two-step process taking place was never observed.

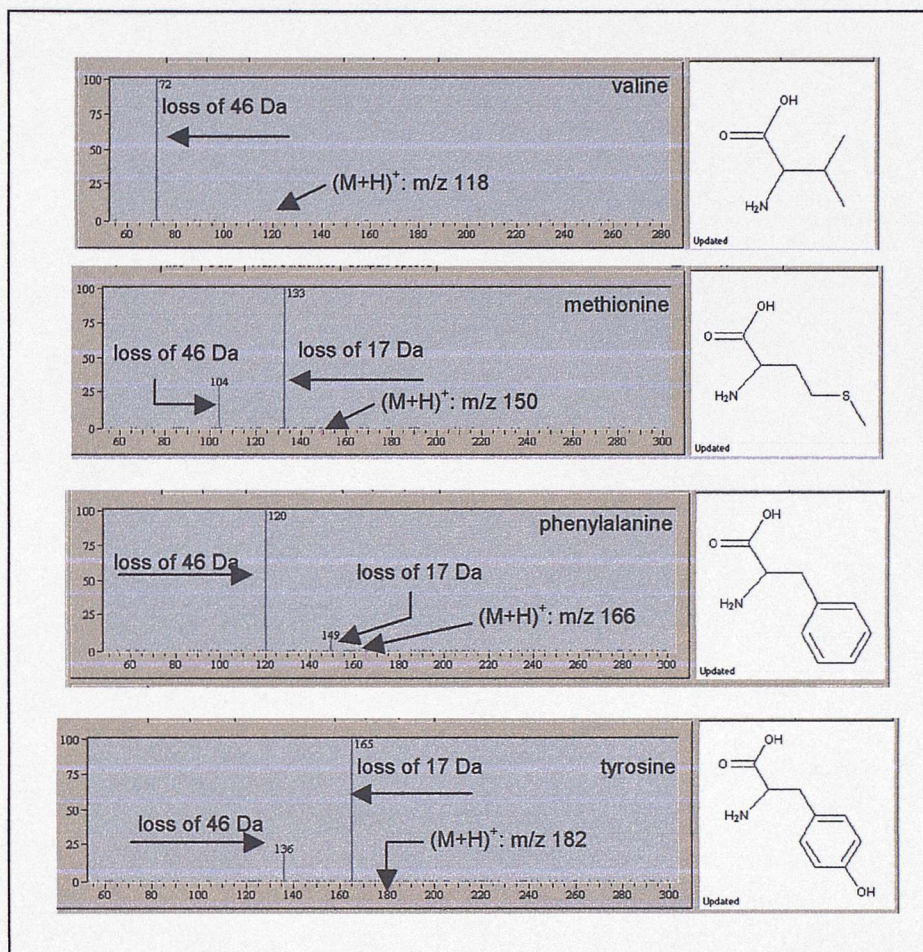


**Figure 33:** The ES-MS/MS spectra obtained for valine, methionine, phenylalanine and tyrosine on the LCQ ion trap with wideband excitation off.

To identify the origin of the hydrogens involved in the loss of 46 Da, d-labelling experiments were also carried out using the four compounds. MS/MS on the fully labelled valine, methionine and tyrosine showed that only exchangeable hydrogens are involved in the loss of  $\text{H}_2\text{CO}_2$ . These would be the hydrogen of the hydroxyl group in the acid functionality and one of the hydrogens of the protonated amine. Phenylalanine produced different results and a mixture of both exchangeable and non-exchangeable hydrogens appeared to be involved in this loss. (**Figure 34**) This result is in contrast with data reported by Rogalewicz *et al*, where the loss of exchangeable hydrogens only is observed from all  $\alpha$ -amino acids, including phenylalanine. Repeated d-labelling experiments for these compounds consistently showed that for phenylalanine both exchangeable and non-exchangeable hydrogens are involved in the loss of  $\text{H}_2\text{CO}_2$ .

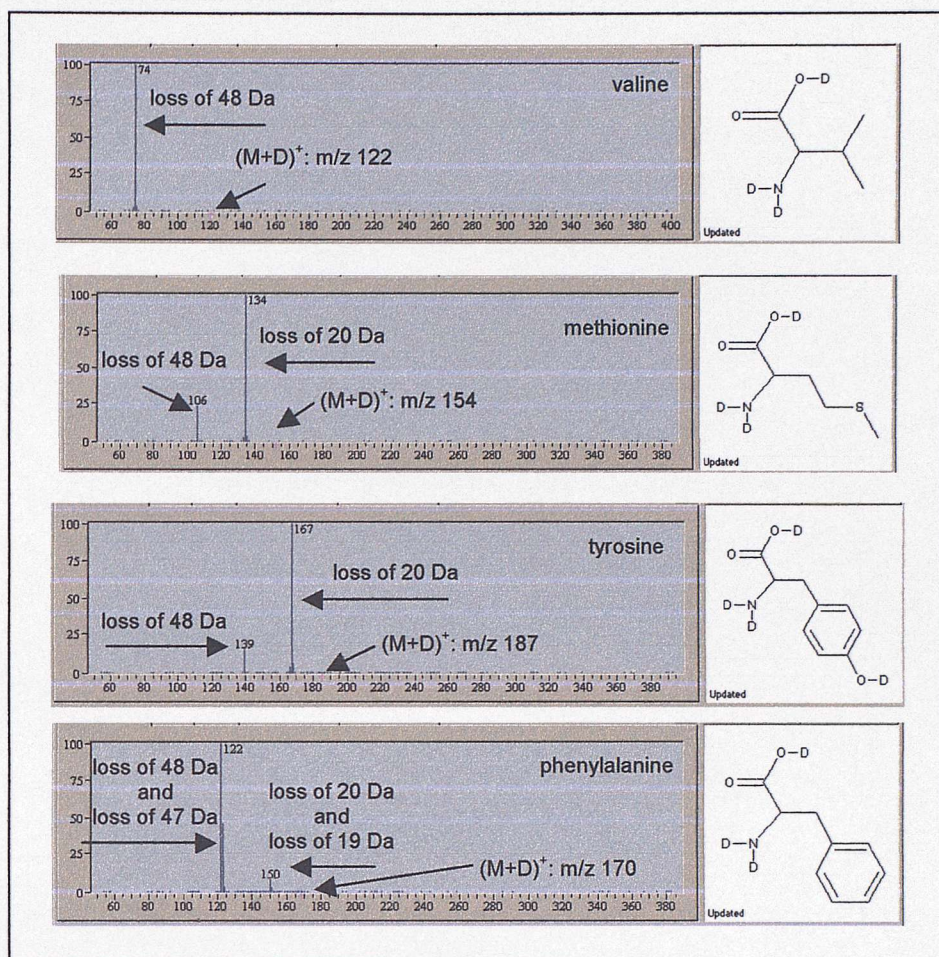


**Figure 34:** The ES-MS/MS spectra of valine, methionine, tyrosine and phenylalanine obtained during d-labelling experiments.

No evidence was found in any of the experiments performed, that the loss of 46 Da is a two-step process involving the sequential loss of H<sub>2</sub>O and CO. The loss of H<sub>2</sub>O was not observed in any of the MS/MS spectra obtained, even when the settings of the ion trap were optimised to ensure detection if such loss occurred (wideband excitation function: off). The results collected so far indicate that amino acids lose 46 Da in a one-step process that could be either the elimination of formic acid or of dihydroxycarbene. Additional studies carried out on the protected molecules, as described below, allowed further differentiation between the possible dissociation routes.

The spectra of 35 amino acids with a butyl ester group attached on the acid functionality (**Appendix 2, Table 3**) were investigated and the common neutral losses present in the spectra were identified. The loss of 102 Da resulted in a prominent fragment ion for most compounds, that corresponds to the loss of butyl formate.<sup>98,100,145,150</sup> The loss of 56 Da was also often observed and literature references propose this to be the loss of butene.<sup>150</sup> Additional losses of 73, 74 and 91 Da were present in many spectra, but their appearance has not been reported. Similarly, the loss of 59 Da previously observed for the unprotected amino acids was also encountered. This loss was identified, using tyrosine, as C<sub>2</sub>H<sub>5</sub>NO eliminated from the compound *via* a rearrangement.

The spectrum of 3,4-dihydroxyphenylalanine butyl ester, displaying the typical losses produced by this type of compounds, is shown in **Figure 35**.

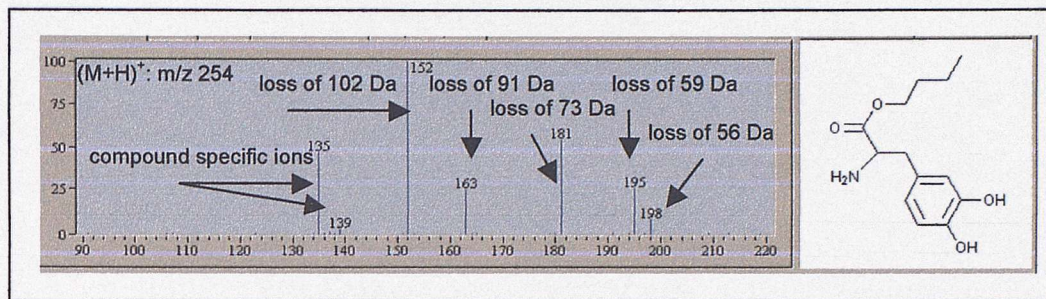


**Figure 35:** The ES-MS/MS spectrum of 3,4-dihydroxyphenylalanine butyl ester.

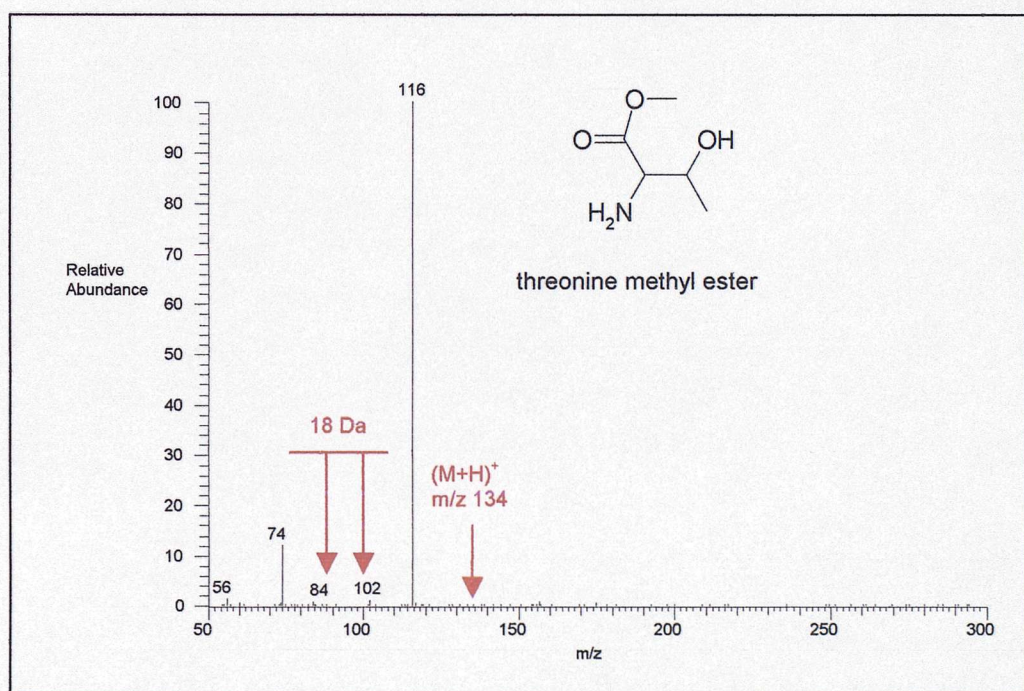
To confirm the identities of the common neutral losses as those proposed in literature and also obtain further information about those that have not been reported so far, exact mass measurement and d-labelling experiments were again carried out using four randomly chosen protected amino acids. Since the butyl esters of amino acids are not commercially available, methyl esters were used instead. Threonine methyl ester, methionine methyl ester, phenylalanine methyl ester and tyrosine methyl ester were employed with the aim to establish their dissociation routes.

ES-MS/MS spectra were obtained for the four methyl ester amino acids on the LCQ ion trap. Then, the neutral losses observed were correlated with those in the spectra of the butyl ester molecules. (**Appendix 2, Table 4**) The loss of 60 Da was observed in the spectra of all methyl ester compounds analysed and leads to the formation of the same ion as the loss of 102 Da, generated by the butyl ester amino acids. This loss of 60 Da should correspond to the loss of methyl formate.<sup>130,140</sup> An equivalent loss to the loss of 56 Da, which is believed to be butene, was not observed. This was expected since the loss of butene involves the formation of a six-centre intermediate<sup>50</sup>, which cannot take place in the presence of a methyl group. The loss of 32 Da for the methyl esters, that could correspond to the loss of  $\text{CH}_3\text{OH}$  was identified as the equivalent loss of 74 Da from the butyl esters, while the loss of 49 Da from the methyl esters led to the same ion as the corresponding loss of 91 Da from the butyl esters. Based on the above observations, further experiments were carried out using the methyl ester amino acids in order to identify the structures of the main fragment ions formed.

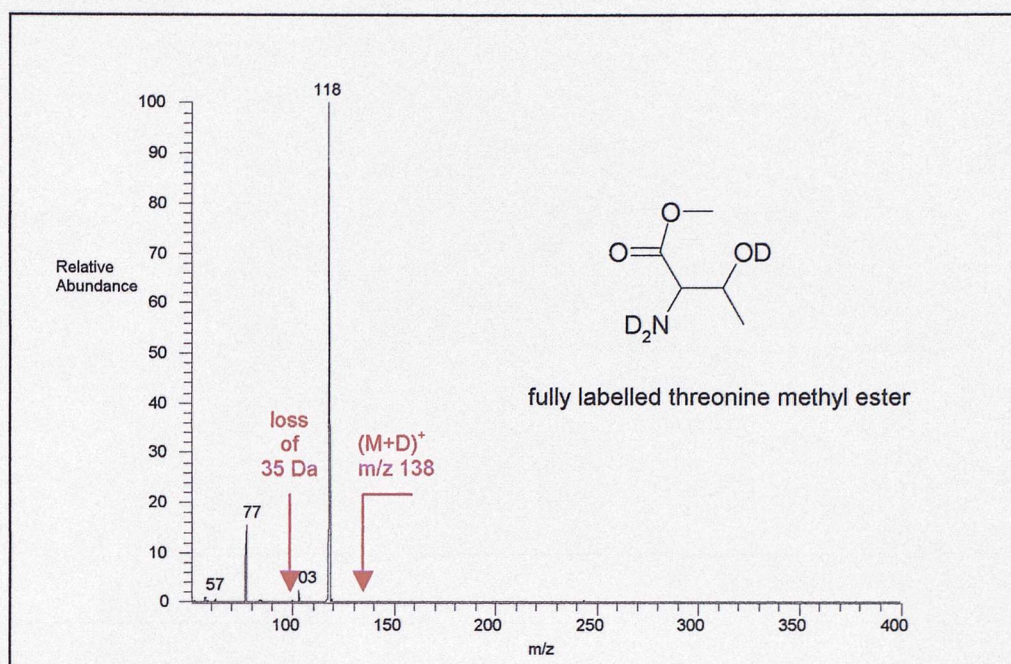
Initially, threonine methyl ester, methionine methyl ester, phenylalanine methyl ester and tyrosine methyl ester were analysed by FTMS and the molecular formulae of the fragment ions of interest were calculated. (**Appendix 2, Table 5**) Information was obtained about two fragment ions. The loss of 60 Da was confirmed to be the loss of  $\text{HCOOCH}_3$ , as reported in literature, and this implies that the loss of 102 Da present in the spectra of the butyl ester amino acids is the loss of  $\text{HCOOCH}_2\text{CH}_2\text{CH}_2\text{CH}_3$ . The loss of 49 Da was only observed in the spectrum of tyrosine methyl ester and was identified as the loss of  $\text{CH}_3\text{OH}$ , followed by  $\text{NH}_3$ . The corresponding loss of 91 Da for the butyl ester protected compounds should be the loss of  $\text{CH}_3\text{CH}_2\text{CH}_2\text{CH}_2\text{OH}$  and  $\text{NH}_3$ . Although the loss of 32 Da was not observed when the amino acids were analysed on the

FTICRMS, information about the resulting fragment ion was gained from d-labelling experiments carried out on the LCQ bench-top ion trap.

The MS/MS spectra of threonine methyl ester acquired during standard analysis and d-labelling experiments are shown in **Figures 36** and **37**. The fragment ion at  $m/z$  102 in the spectrum of the un-labelled compound was believed to be formed *via* the loss of  $\text{CH}_3\text{OH}$  (32 Da). In the spectrum of the labelled threonine methyl ester, the ion shows a mass shift to  $m/z$  103 and the corresponding loss is equivalent to 35 Da. This eliminates the possibility of the fragment ion being due to the loss of methanol from the methyl ester group, because from the fully labelled compound this loss should correspond to either 32 or 33 Da, depending on the type of hydrogen involved. Using a different interpretation, the ion at  $m/z$  102 could be a water-adduct of the fragment ion at  $m/z$  84, also present in the spectrum of threonine methyl ester. The two ions are 18 mass units apart. An in-depth investigation into the formation of adducts of fragment ions with solvents, in the ion trap, is described in **Chapter 4**. The existence of adducts in the spectra of a library of sulphonamides is proven and all evidence indicates that certain fragment ions of amino acids can also be explained in the same manner. The low abundance of  $m/z$  84 in the spectrum of threonine methyl ester (**Figure 36**) does not allow further experiments to be carried out in order to support this theory, but all  $m/z$  values observed appear to confirm it.

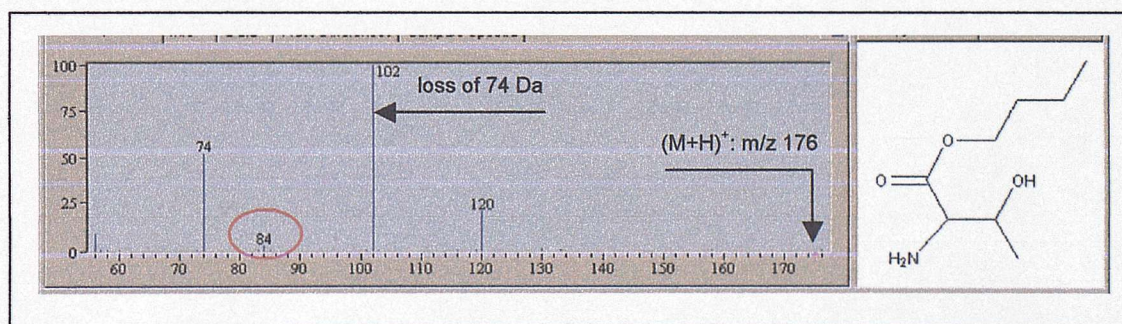


**Figure 36:** The ES-MS/MS spectrum of threonine methyl ester.



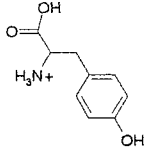
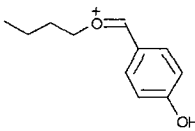
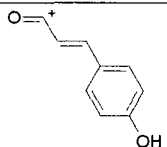
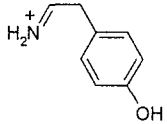
**Figure 37:** The ES-MS/MS spectrum of fully labelled threonine methyl ester.

Exact mass analysis by FTMS revealed that the fragment ion at  $m/z$  84 is formed due to the loss of  $\text{CH}_3\text{OH}$  and  $\text{H}_2\text{O}$ . This means that the equivalent ion in the spectra of the butyl ester compound would be formed due to the loss of  $\text{CH}_3\text{CH}_2\text{CH}_2\text{CH}_2\text{OH}$  and  $\text{H}_2\text{O}$  and would appear in the spectra due to the loss of 92 Da. The intensity of this ion in the spectrum of threonine butyl ester (**Figure 38**) is low, but its corresponding adduct with water, expected to appear due to the loss of 74 Da, is observed at high abundance. The loss of 74 Da has already been identified as a common neutral loss formed by protected amino acids and it is mainly observed in the spectra of compounds with functionalities in their side chains that can induce the loss of  $\text{H}_2\text{O}$ , e.g. hydroxyl groups. The fragment ion due to the common loss of 73 Da can also be explained in the same manner. It appears to be an adduct with water of the fragment ion due to the loss of 91 Da, previously identified as the loss of  $\text{CH}_3\text{CH}_2\text{CH}_2\text{CH}_2\text{OH}$  and  $\text{NH}_3$ .



**Figure 38:** The ES-MS/MS spectrum of threonine butyl ester.

Using all the data collected by exact mass analysis and d-labelling experiments for the identification of the fragment ions produced by the methyl ester and the butyl ester amino acids, structures can now be assigned to most of the  $m/z$  values observed in the spectra. *E.g.* the fragment ions generated by tyrosine methyl ester and tyrosine butyl ester are shown in **Table 4**.

Neutral Loss Observed for Tyrosine Butyl Ester	Neutral Loss Observed for Tyrosine Methyl Ester	Identity of Neutral Loss for Tyrosine Butyl Ester	Identity of Neutral Loss for Tyrosine Butyl Ester	Structure of Resulting Fragment Ion
loss of 56 Da	—	$\text{CH}_2\text{CHCH}_2\text{CH}_3$	—	
loss of 59 Da	—	$\text{C}_2\text{H}_5\text{NO}$	—	
loss of 73 Da	—	$\text{H}_2\text{O}$ adduct with the loss of 91 Da	—	—
loss of 91 Da	loss of 49 Da	$\text{CH}_3\text{CH}_2\text{CH}_2\text{CH}_2\text{OH} + \text{NH}_3$	$\text{CH}_3\text{OH} + \text{NH}_3$	
loss of 102 Da	loss of 60 Da	$\text{HCOOCH}_2\text{CH}_2\text{CH}_2\text{CH}_3$	$\text{HCOOCH}_3$	

**Table 4:** Structures proposed for the fragment ions observed in the spectra of tyrosine methyl ester and tyrosine butyl ester.

To obtain information about the mechanism leading, according to literature, to the formation of alkyl formates from protected amino acids, d-labelling experiments were carried out using the four amino acid methyl esters available. Similar results to those obtained when d-labelling was carried out on the unprotected molecules were observed. The ES-MS/MS spectra of fully labelled threonine methyl ester, methionine methyl ester and tyrosine methyl ester showed that the hydrogen required for the formation of the formate is an exchangeable one. (**Figure 39**) Conversely, phenylalanine methyl ester produced a mixture of results and both exchangeable and non-exchangeable hydrogens appeared to be involved in the mechanism. This observation is consistent with the data previously obtained for phenylalanine. The behaviour of this molecule differs from that of the other amino acids, even from that of the structurally similar tyrosine. The

effect of the extra hydroxyl group in the structures requires investigation in order to try to explain these results.

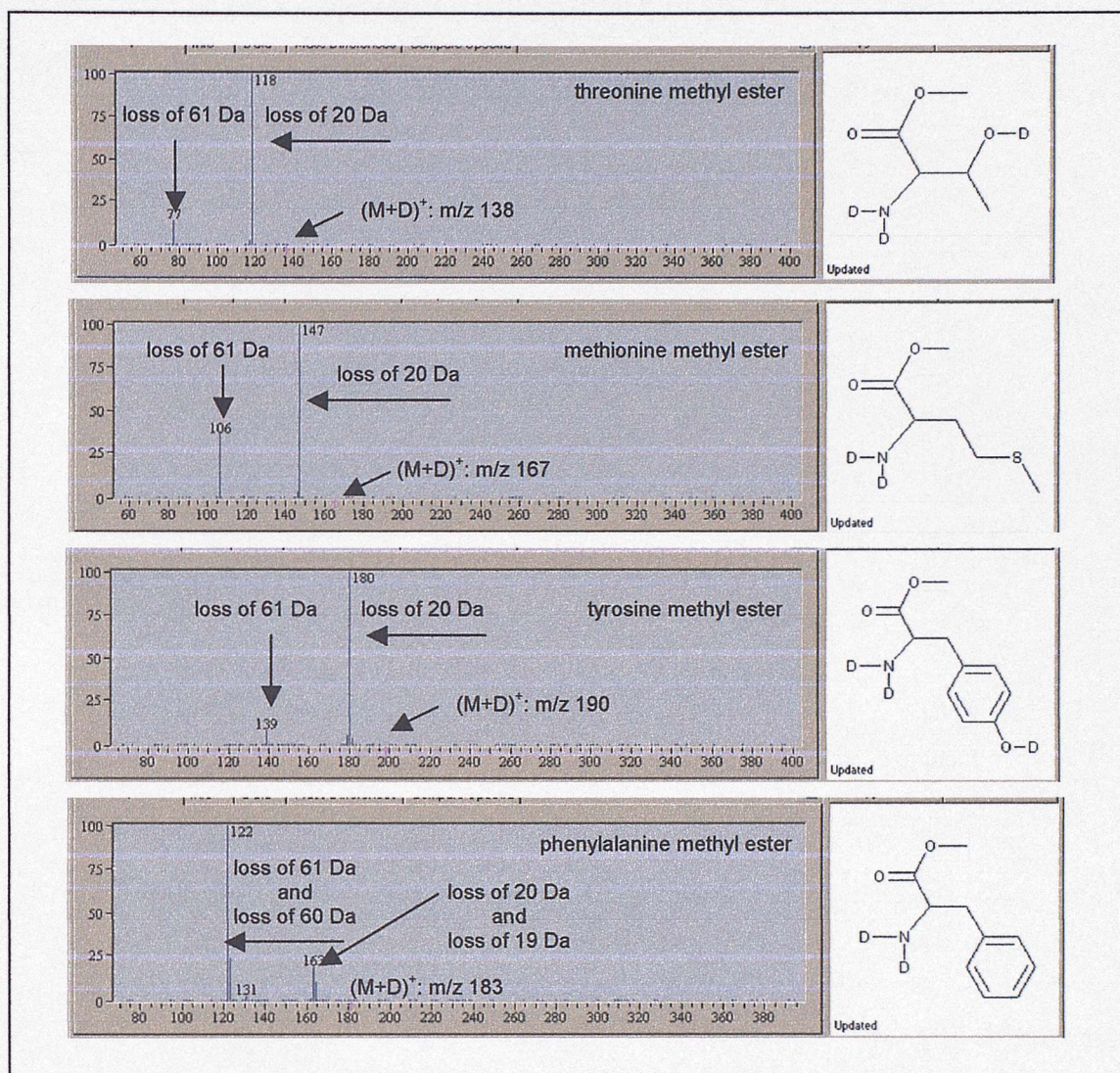


**Figure 39:** Spectra obtained for the methyl ester protected amino acids during d-labelling experiments.

The studies carried out on both the protected and the unprotected amino acids indicate that a common mechanism leads to the losses of 46, 60 and 102 Da. Based on this, the various mechanistic theories available in literature were tested against the results obtained for the six amino acids that produced consistent results in the d-labelling experiments, with the aim of identifying a suitable mechanism.

According to Meot-Ner and Field, the formation of formic acid occurs *via* a doubly cyclic intermediate. In this intermediate, the hydrogen of the hydroxyl group in the amino acid core becomes the hydrogen attached to the carbonyl carbon of formic acid. The hydroxyl group becomes a carbonyl and the carbonyl of the amino acid becomes the hydroxyl group. (**Figure 40**) This mechanism fits the data obtained for the unprotected amino acids but not for the protected

compounds. When a butyl ester or a methyl ester group is attached to the hydroxyl group of the amino acids, the intermediate proposed by Meot-Ner and Field would not be formed, since the hydrogen of the hydroxyl group would not be available. The mechanism could not occur for protected compounds and the loss of alkyl formate would not be observed. However, the losses of 60 Da and 102 Da are present in most of the spectra of the protected amino acids.

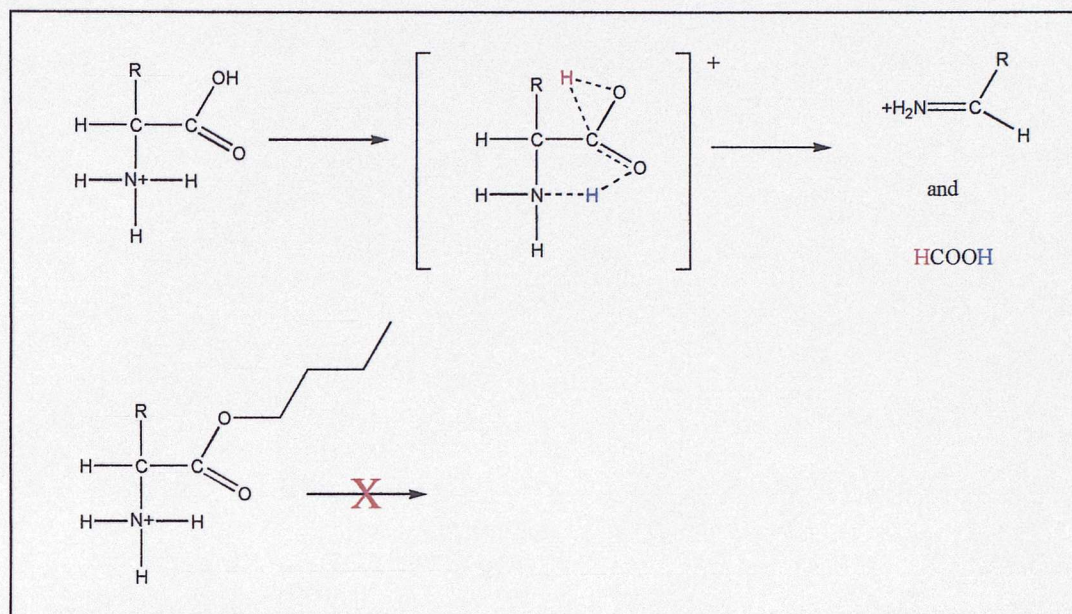


**Figure 40:** Application of the mechanism proposed by Meot-Ner to protected amino acids.

The mechanisms proposed by Tsang and Harrison and later on by Rolalewicz *et al*, that involve the sequential losses of H<sub>2</sub>O and CO, can also be eliminated. There is no indication in the ES-MS/MS spectra of amino acids that the loss of H<sub>2</sub>O occurs. Such loss would be easily detected in a quadrupole ion trap. However, the loss of 18 Da was only present in the spectrum of threonine methyl ester and it is known from literature to originate from the side chain of this amino acid.<sup>131,135,136</sup> Protonation on amino acids is also known from literature to occur on the NH<sub>2</sub> group.<sup>133,136-140,148,149</sup> For the mechanism proposed by the two research groups to take place, intramolecular transfer of a hydrogen from the site of protonation to the hydroxyl group is required. **(Figure 41)** Such transfer would be possible for unprotected amino acids and would lead to the loss of H<sub>2</sub>O. For protected molecules the oxygen ceases to be basic enough to attract the proton that would lead to the corresponding loss.<sup>138</sup> Therefore, the first step of the mechanism would not take place.

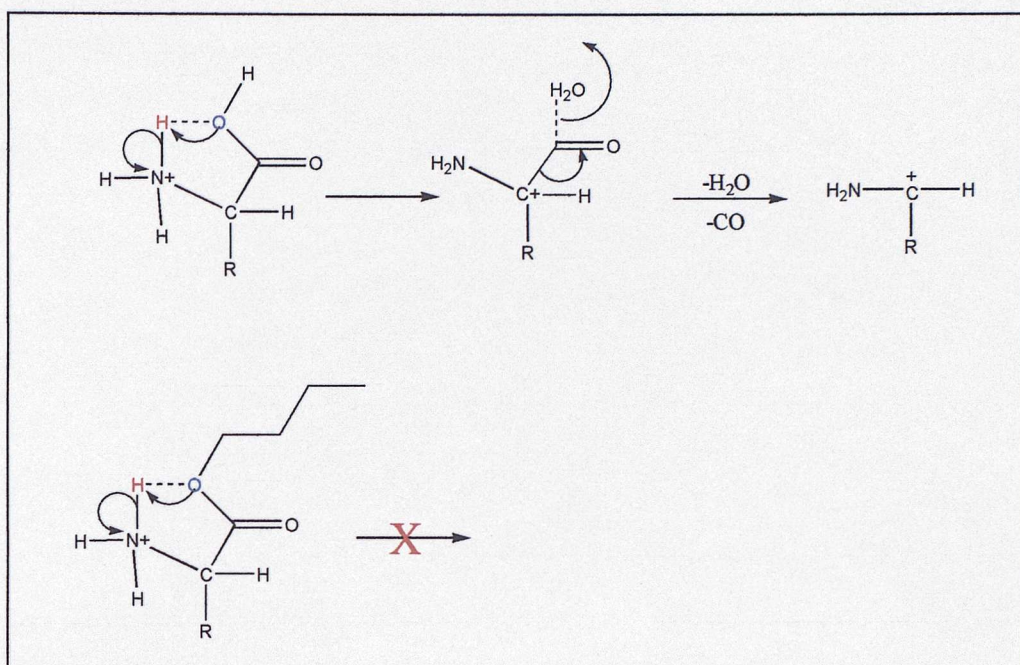


**Figure 41:** Application of the mechanism proposed by Tsang and Harrison and Rogalewicz *et al* to protected amino acids.

Finally, the mechanism proposed by Kulik and Herma and later by Beranová *et al*, that involves the elimination of dihydroxycarbene could potentially take place both for the unprotected and protected compounds. (**Figure 42**) However, the neutral fragments formed from the protected amino acids are not alkyl formates as reported in literature, but carbenes. This contradicts the published data of various research groups that support the generation of alkyl formates without reservation.

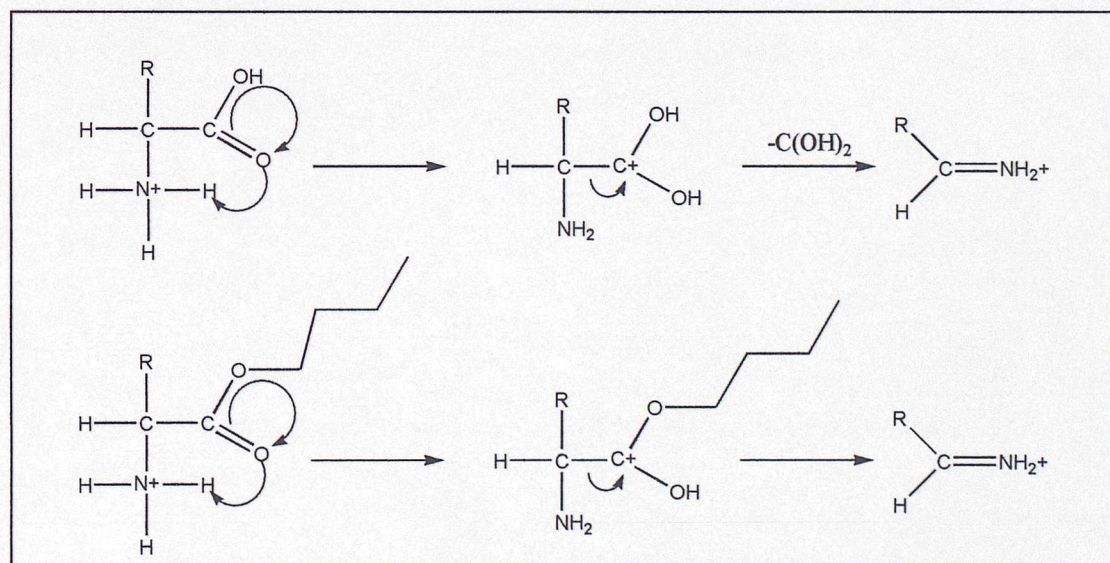


**Figure 42:** Application of the mechanism proposed by Kulik and Herma and Beranová *et al* to protected amino acids.

Based on the experimental data gathered during the investigation of amino acids and after the comparison with the mechanisms reported in literature for the formation of the main fragment ion for this set of compounds, a new mechanism can now be proposed leading to the loss of formic acid from amino acids and to the loss of alkyl formates from the protected molecules. (**Figure 43**) The mechanism can be applied to most compounds producing those losses, although possible additional fragmentation processes also take place that would justify the d-labelling experiments. In order to postulate a final mechanism for all amino acids, mechanistic studies using larger numbers of compounds are necessary.

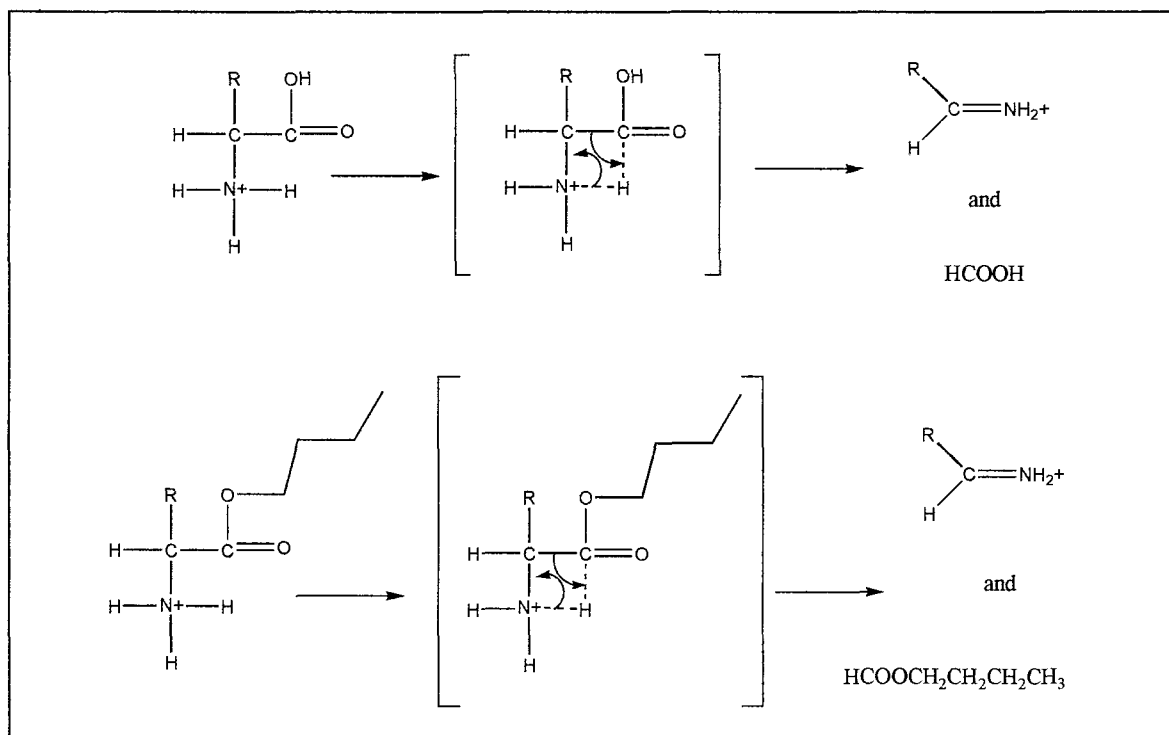


**Figure 43:** The mechanisms proposed for the loss of formic acid and butyl formate from amino acids and butyl ester amino acids respectively.

### 3d. Conclusion

The fragmentation pathway of an array of amino acids was investigated and it was established that all compounds produced the same neutral losses due to the amino acid core, as well as compound specific fragment ions due to the side chains attached on the amino acid core. A fragmentation pattern was established and it was proven to be followed by all molecules. These results suggest that fragmentation patterns can be identified for large numbers of compounds and are not limited to small groups only.

Valuable information about the ionisation and dissociation processes taking place in ES-MS/MS was gained through the studies into the mechanisms leading to the formation of the main fragment ion for this class of molecules. Mechanisms adapted from other ionisation techniques, e.g. EI, CI, FAB, cannot necessarily be directly applied to those observed in the dissociation processes following electrospray ionisation. This is demonstrated by the variation of literature reported

mechanisms for the same dissociation process of the loss of 46 Da. This point is important for the improvement of fragment ion prediction modes in software packages because it further emphasises the current flawed approach of existing AI programmes.

For the amino acid array, the mechanism leading to the loss of 46 Da from unprotected amino acids, as well as the losses of 60 Da and 102 Da from methyl ester and butyl esters, respectively, were investigated. A common dissociation route for all types of compounds was proposed. However, extensive studies on larger number of amino acids are required to confirm the suggested dissociation route and ensure its applicability to all the types of amino acid molecules.

## 4. The Fragmentation Pattern of a Combinatorial Library

### 4a. Introduction

The investigation into the fragmentation patterns of non-peptidic molecules was extended from small groups to an array of monomers and finally to a combinatorial library. A library of sulphonamides was studied and the common fragment ions and neutral losses generated by the different components were identified. Exact mass measurements, MS<sup>3</sup> and d-labelling experiments, as well as *ab initio* calculations, were employed in order to reveal the mechanisms leading to the formation of the main fragment ions. A clear fragmentation pathway was eventually identified for all the compounds in the library.

### 4b. Experimental

#### Materials

- Spectra of the sulphonamides were either available in the MS/MS library<sup>52</sup> or the compounds were synthesised in house and were analysed without further purification.
- Methanol, HPLC grade, was purchased from Fisher, Loughborough, UK.
- Acetonitrile, HPLC grade, was purchased from Fisher, Loughborough, UK.
- Formic acid, analytical grade 98-100%, was purchased from Sigma-Aldrich, Gillingham, UK.
- Deuterated methanol (CH<sub>3</sub>OD, 99%) and deuterated acetic acid (CD<sub>3</sub>COOD, 99.5%), used for the d-labelling experiments, were purchased from Qmx Laboratories Ltd, Thaxted, UK.

#### Sample Preparation

- Solutions of all compounds analysed were prepared in methanol and 0.1% formic acid. Concentration: 10 µg/mL.
- For the studies carried out into the formation of adducts of fragment ions with solvents, solutions of sulphamerazine, sulphamethazine and sulphadiazine (**Appendix 3, Figure 1**) were prepared in acetonitrile with 0.1% formic acid. Concentration: 10 µg/mL.
- For the d-labelling experiments, all compounds under study were dissolved in deuterated methanol and 0.1% deuterated acetic acid. Concentration: 10 µg/mL.

#### Instrumentation and Conditions Used:

- All samples were analysed on an LCQ Deca Ion Trap (Thermo Finnigan, San Jose, CA, USA) under standard conditions: Capillary Temperature: 200 °C, Sheath Gas Flow: 35 au, Auxiliary Gas Flow: 10 au, Source Voltage: 4.5 kV. Nitrogen was used as the sheath and the auxiliary gas and helium was the collision gas.
- MS/MS parameters: Isolation Width: 1, Collision Energy: 35%.
- Exact mass measurements were carried out using an Apex III FTICRMS (Bruker, Billerica, MA, USA): Capillary: -4.5 kV, End Plate: -3.8 kV, Capillary Exit: 102 V, Skimmer 1: 8.26 V,

Skimmer 2: 7.64 V, Offset: 1.00, Rf Amplitude: 550.00 Hz, Dry Gas Temperature: 130°C. Nitrogen was used as the drying gas and argon was used as the collision gas.

MS/MS parameters: corr sweep pulse length: 1000  $\mu$ sec, corr sweep attenuation: 30.0 dB, ejection safety belt: 3000 Hz, user pulse length: 5000  $\mu$ sec, ion activation pulse length: 250000  $\mu$ sec, ion activation attenuation: 49.5 dB, frequency offset from activation mass: -500 Hz, user delay length: 3 sec.

MS/MS/MS parameters: corr sweep pulse length: 500  $\mu$ sec, corr sweep attenuation: 30.0 dB, ejection safety belt: 0 Hz, user pulse length: 5000  $\mu$ sec, ion activation pulse length: 250000  $\mu$ sec, ion activation attenuation: 49.5 dB, frequency offset from activation mass: -500 Hz, user delay length: 6 sec.

- D-labelling experiments were carried out on an LCQ Deca Ion Trap (Thermo Finnigan, San Jose, CA, USA) using the following conditions: Capillary Temperature: 200 °C, Sheath Gas Flow: 5 au, Auxiliary Gas Flow: 20 au, Source Voltage: 4.5 kV. Nitrogen was used as the sheath and the auxiliary gas and helium was the collision gas.

MS/MS parameters: Isolation Width: 1, Collision Energy: 35%.

- Sulphamerazine, sulphamethazine and sulphadiazine were analysed on a TSQ Quantum Triple Quadrupole (Thermo Finnigan, San Jose, CA, USA) using the following conditions: Capillary Temperature: 200 °C, Sheath Gas Flow: 35 au, Auxiliary Gas Flow: 10 au, Source Voltage: 4.5 kV. Nitrogen was used as the sheath and the auxiliary gas, as well as the collision gas.

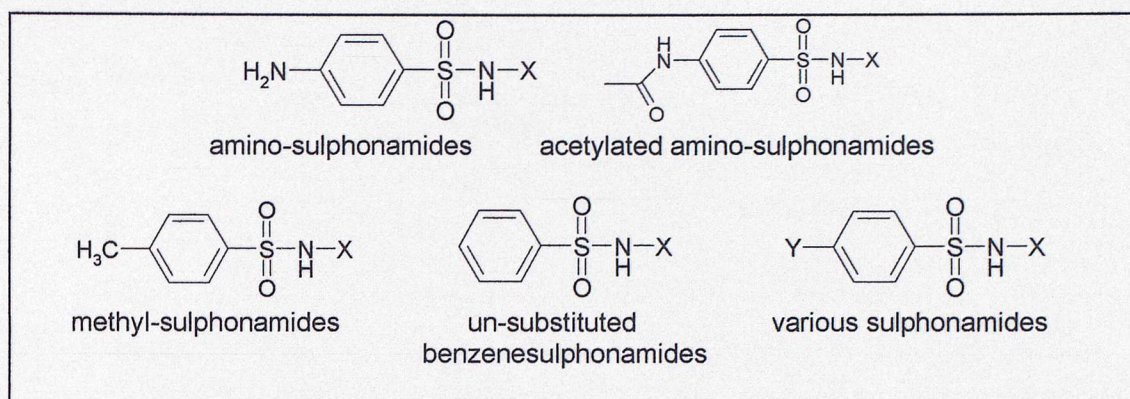
MS/MS parameters: Collision Energy: 30%.

#### Ab initio Calculations

Molecular modelling calculations were carried out on a "model" sulphonamide. *N*-(5-methyl-2-pyridinyl)-benzenesulphonamide was used for this purpose. (**Appendix 3, Figure 2**) The lowest energy conformers of the molecule in the gas phase were identified using semi-empirical AM1 calculations. The lowest energy conformers of all the possible protonated forms were also identified in the same way. Geometry optimisation for all chosen conformers was carried out at the B3LYP/ 6-31G\* density functional level.

#### **4c. Results and Discussions**

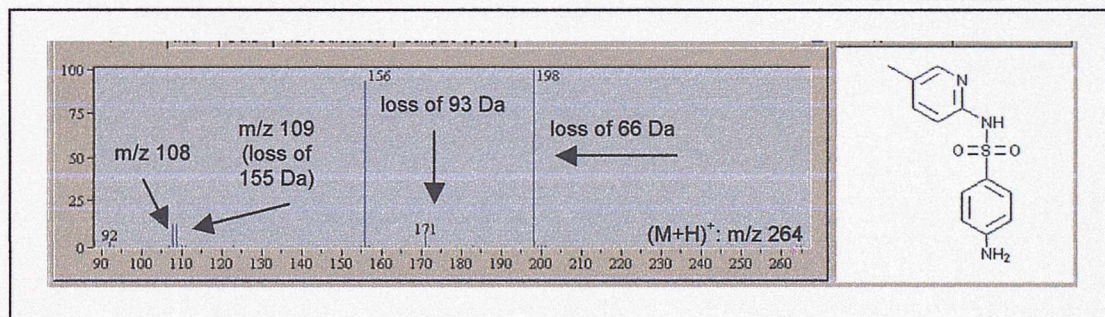
The library of sulphonamides was divided into five sub-groups based on the substituents attached on the benzene ring of the molecules. (**Figure 44**) The fragmentation pathway of each sub-group was investigated separately and observations were made about the role the various functionalities attached on the benzene ring play in the mechanisms leading to the main fragment ions. The fragmentation patterns produced by all sub-groups were eventually compared and a common dissociation route was established.



**Figure 44:** The core structures of the five main sub-groups of the sulphonamide library.

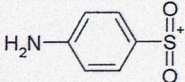
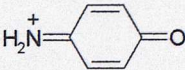
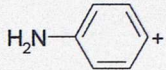
#### The Fragmentation Pathway of Amino-Sulphonamides

The structures of the amino-sulphonamides studied are shown in **Appendix 3, Table 1**. All molecules followed a common dissociation route. Common fragment ions were formed at  $m/z$  156,  $m/z$  108 and  $m/z$  92, together with neutral losses due to 66, 75, 93 and 155 Da. *E.g.* the ES-MS/MS spectrum of 4-amino-*N*-(5-methyl-2-pyridinyl)-benzenesulphonamide is shown in **Figure 45**.



**Figure 45:** The ES-MS/MS spectrum of 4-amino-*N*-(5-methyl-2-pyridinyl)-benzenesulphonamide.

Analysis of the compounds by FTICRMS allowed calculation of the elemental composition for most of the  $m/z$  values present in the spectra. These, together with Mass Frontier and literature reports available for this class of molecules<sup>50,113,122,151-196</sup>, were used to assign structures to the common fragment ions observed. (**Table 5**) The ion at  $m/z$  156 is known to be formed due to cleavage of the sulphonamide bond. Further loss of  $\text{SO}_2$  leads to the ion at  $m/z$  92, whilst  $m/z$  108 is known to be formed *via* a rearrangement. Complimentary ions to  $m/z$  156 and  $m/z$  92 were observed due to the losses of 155 Da and 93 Da respectively, while the loss of 66 Da suggests the loss of  $\text{H}_2\text{SO}_2$ , this requiring a complex rearrangement to take place.

Fragment Ion	Molecular Formula	Proposed Structure
m/z 156	$C_6H_6NO_2S^+$	
m/z 108	$C_6H_6NO^+$	
m/z 92	—	
loss of 66 Da	loss of $H_2SO_2$	Further investigation required.
loss of 93 Da	loss of $C_6H_7N$	$X-NH_2-SO_2^+$
loss of 155 Da	loss of $C_6H_5NO_2S$	$X-NH_3^+$

**Table 5:** Structures proposed for the common fragment ions and neutral losses produced by the amino-sulphonamides.

The ion due to the loss of 75 Da was reported in literature as an adduct of the fragment ion due to the loss of 93 Da, with water.<sup>180,182,189</sup> In order to confirm this, studies were carried out on three amino-sulphonamides, sulphamerazine, sulphadiazine and sulphamethazine, for which the loss of 75 Da resulted in a prominent fragment ion in their ES-MS/MS spectra. The three compounds were initially analysed on the LCQ ion trap and pairs of fragment ions, either 18 or 32 Da apart, were identified. (**Figures 46, 47 and 48**) The m/z values indicated that, a large number of ions present in the spectra of the three compounds could be explained as solvent adducts of some of the common fragment ions produced by all the amino-sulphonamides.

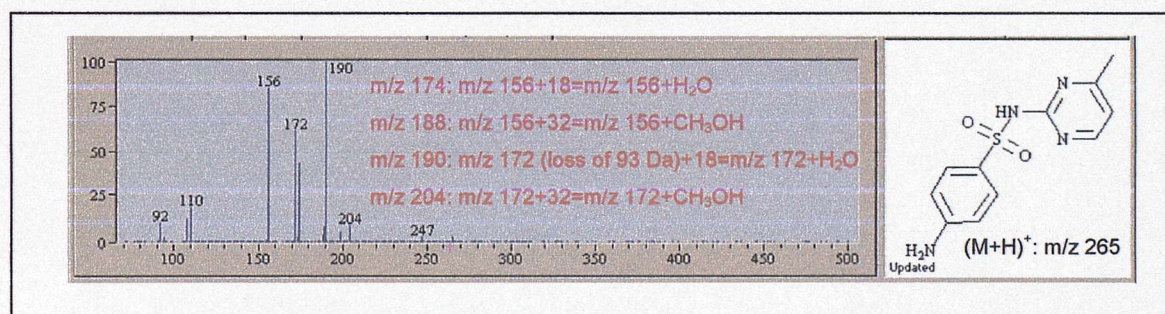


**Figure 46:** The ES-MS/MS spectrum of sulphamerazine, acquired on the LCQ ion trap.

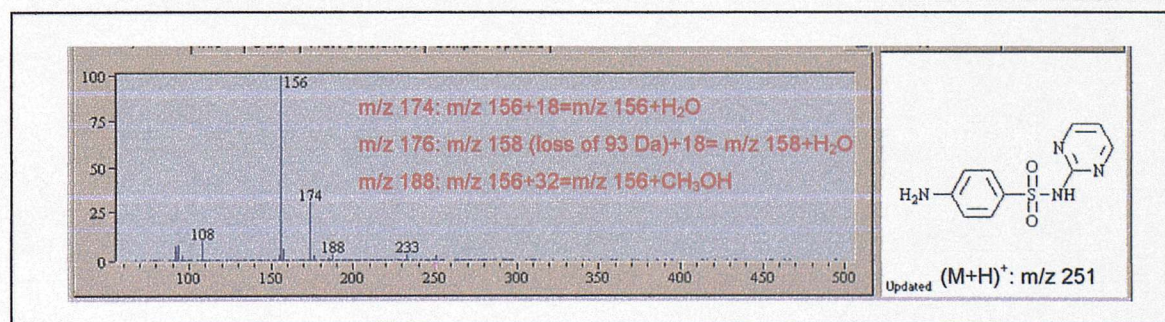


**Figure 47:** The ES-MS/MS spectrum of sulphadiazine, acquired on the LCQ ion trap.

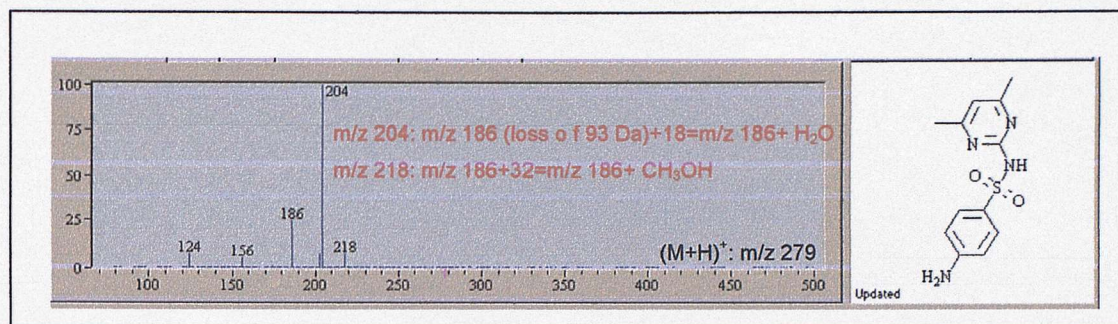


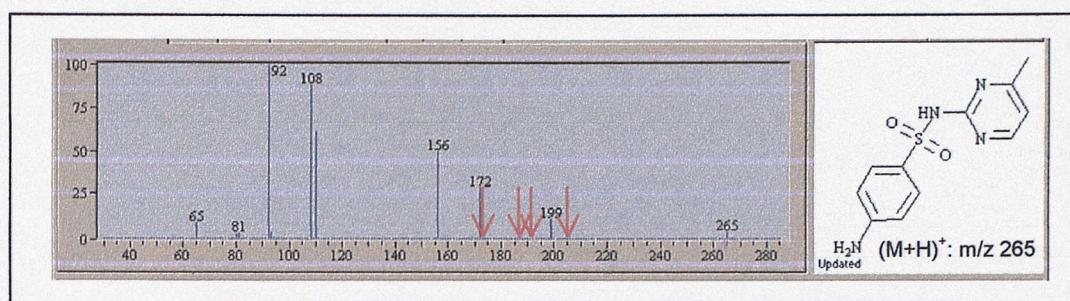
**Figure 48:** The ES-MS/MS spectrum of sulphamethazine, acquired on the LCQ ion trap.

In order to identify the fragment ions of interest as highlighted in the spectra shown in **Figures 46, 47 and 48**, the three amino-sulphonamides were analysed by FTMS and the exact masses of the ions under investigation were obtained. The molecular formulae calculated for each fragment ion pair revealed the formation of H<sub>2</sub>O adducts. **(Table 6)** Adducts due to the presence of methanol were not observed.

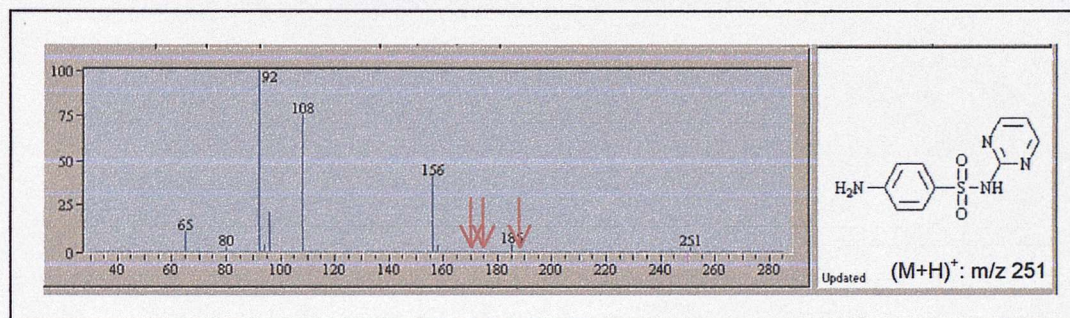
Compound	Fragment Ion and Molecular Formula	Fragment Ion and Molecular Formula	Conclusion
sulfamethazine	m/z 186 C <sub>6</sub> H <sub>8</sub> N <sub>3</sub> O <sub>2</sub> S <sup>+</sup>	m/z 204 C <sub>6</sub> H <sub>10</sub> N <sub>3</sub> O <sub>3</sub> S <sup>+</sup>	m/z 204 = m/z 186 + H <sub>2</sub> O
sulfamerazine	m/z 156 C <sub>6</sub> H <sub>6</sub> N <sub>1</sub> O <sub>2</sub> S <sup>+</sup>	m/z 174 C <sub>6</sub> H <sub>8</sub> N <sub>1</sub> O <sub>3</sub> S <sup>+</sup>	m/z 174 = m/z 156 + H <sub>2</sub> O
	m/z 172 C <sub>5</sub> H <sub>6</sub> N <sub>3</sub> O <sub>2</sub> S <sup>+</sup>	m/z 190 C <sub>5</sub> H <sub>8</sub> N <sub>3</sub> O <sub>3</sub> S <sup>+</sup>	m/z 190 = m/z 172 + H <sub>2</sub> O
sulfadiazine	m/z 156 C <sub>6</sub> H <sub>6</sub> N <sub>1</sub> O <sub>2</sub> S <sup>+</sup>	m/z 174 C <sub>6</sub> H <sub>8</sub> N <sub>1</sub> O <sub>3</sub> S <sup>+</sup>	m/z 174 = m/z 156 + H <sub>2</sub> O

**Table 6:** Summary of the results of the exact mass analysis carried out on sulphamerazine, sulphadiazine and sulphamethazine.

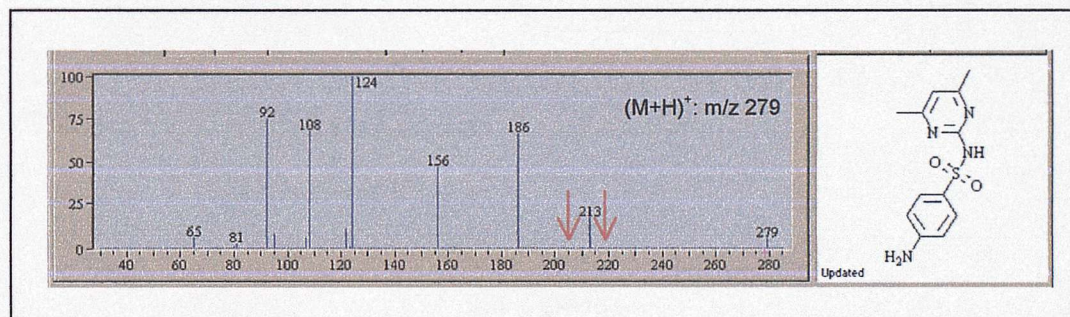
Further confirmation of the existence of solvent adducts was obtained from the analysis of the three amino-sulphonamides on a triple quadrupole instrument. The ES-MS/MS spectra acquired are shown in **Figures 49, 50 and 51**. The compound specific ions present in the LCQ spectra were not observed. This is in agreement with the fact that the set-up of the triple quadrupole instrument does not allow for solvent adduct formation in the analyser. The generation of adducts of fragment ions with H<sub>2</sub>O and CH<sub>3</sub>OH is valid for the ion trap and is limited to this type of instrument only. This is due to the design of the trap that allows neutral solvent molecules to remain inside the trap cavity after quenching.



**Figure 49:** The ES-MS/MS spectrum of sulphamerazine, acquired on the TSQ triple quadrupole.



**Figure 50:** The ES-MS/MS spectrum of sulphadiazine, acquired on the TSQ triple quadrupole.

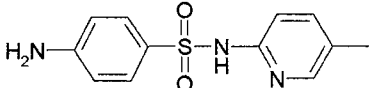
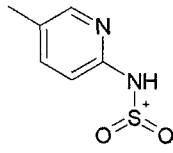
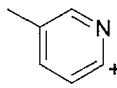
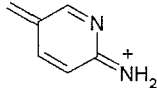
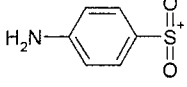
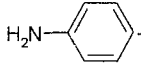
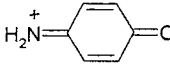


**Figure 51:** The ES-MS/MS spectrum of sulphamethazine, acquired on the TSQ triple quadrupole.

A further investigation was carried out with the aim to determine the origin of the H<sub>2</sub>O and CH<sub>3</sub>OH molecules resulting in the formation of adducts. These could either come from the solvents used for sample preparation or from any residual solvent molecules remaining in the interior of the trap, after the trap was quenched. To differentiate between the two possibilities, two sets of samples of sulphamerazine, sulphadiazine and sulphamethazine, prepared separately in acetonitrile and formic acid and in methanol and formic acid, were analysed on the LCQ. The three sets of data acquired are shown in **Appendix 3, Figures 3, 4 and 5**. CH<sub>3</sub>OH adducts were not formed when the compounds were dissolved in acetonitrile. On the other hand, fragment ion pairs, 32 mass units apart, re-appeared in the spectra when the methanol samples were analysed. This suggests that the H<sub>2</sub>O and CH<sub>3</sub>OH molecules that form solvent adducts with the common fragment ions produced by the amino-sulphonamides, originate from the solvents used to make up the samples and not from the interior of the ion trap.

Once all the common fragment ions present in the spectra of the amino-sulphonamides were identified, studies were carried out aiming to determine the mechanisms taking place, resulting in their formation. MS<sup>3</sup> experiments were carried out on 4-amino-*N*-(5-methyl-2-pyridinyl)-benzenesulphonamide, in order to obtain information about its major dissociation routes. The same experiments were also carried out on a methyl and a non-substituted benzenesulphonamide with the same substituent X, so that the effect of the various functionalities of the benzene ring could be determined. The results obtained for the methyl and the non-substituted compounds are discussed in the following sections of this chapter.

The three main fragment ions of 4-amino-*N*-(5-methyl-2-pyridinyl)-benzenesulphonamide were dissociated. (**Table 7**) The losses of NH<sub>3</sub> and CH<sub>3</sub><sup>•</sup> were observed following dissociation of the ion formed due to the loss of H<sub>2</sub>SO<sub>2</sub>, indicating that the substituents of the benzene ring and on the pyridine ring of the ion were cleaved. Fragmentation of the ion at *m/z* 156 resulted in the formation of the known ions at *m/z* 92 and *m/z* 108, thus proving that these ions are formed after the sulphonamide bond is broken. Loss of SO<sub>2</sub> leads to the ion at *m/z* 92, while a rearrangement leading to the loss of SO occurs in the case of *m/z* 108. Finally, the ion X-NH-SO<sub>2</sub><sup>+</sup>, due to the loss of 93 Da was also dissociated and two fragment ions were observed at *m/z* 92 and *m/z* 107. Both structures are related to the methylated pyridine ring.

Sulphonamide	MS/MS fragment ions	MS <sup>3</sup> fragment ions	
	loss of H <sub>2</sub> SO <sub>2</sub>	loss of NH <sub>3</sub> and CH <sub>3</sub> <sup>•</sup>	
	 loss of 93 Da	 C <sub>6</sub> H <sub>6</sub> N <sup>+</sup> m/z 92	 C <sub>6</sub> H <sub>7</sub> N <sub>2</sub> <sup>+</sup> m/z 107
	 m/z 156	 C <sub>6</sub> H <sub>6</sub> N <sup>+</sup> m/z 92	 C <sub>6</sub> H <sub>6</sub> NO <sup>+</sup> m/z 108

**Table 7:** Summary of the results of the MS<sup>3</sup> experiments carried out on 4-amino-*N*-(5-methyl-2-pyridinyl)-benzenesulphonamide.

The MS<sup>3</sup> experiments carried out revealed that the rearrangement resulting in the formation of the ion at *m/z* 108, takes place after the sulphonamide bond is fragmented. Additionally, after the loss of H<sub>2</sub>SO<sub>2</sub>, the two rings, pyridine and benzene, re-join *via* the NH group, while the functionalities attached to them remain free and are subsequently cleaved. The origin of the hydrogens lost in H<sub>2</sub>SO<sub>2</sub> was then determined using d-labelling experiments. The ES-MS/MS spectrum of the fully labelled 4-amino-*N*-(5-methyl-2-pyridinyl)-benzenesulphonamide is shown in **Figure 52**. Only the loss of 68 Da, corresponding to D<sub>2</sub>SO<sub>2</sub> was observed, which shows that exchangeable hydrogens are involved in the loss of H<sub>2</sub>SO<sub>2</sub>.

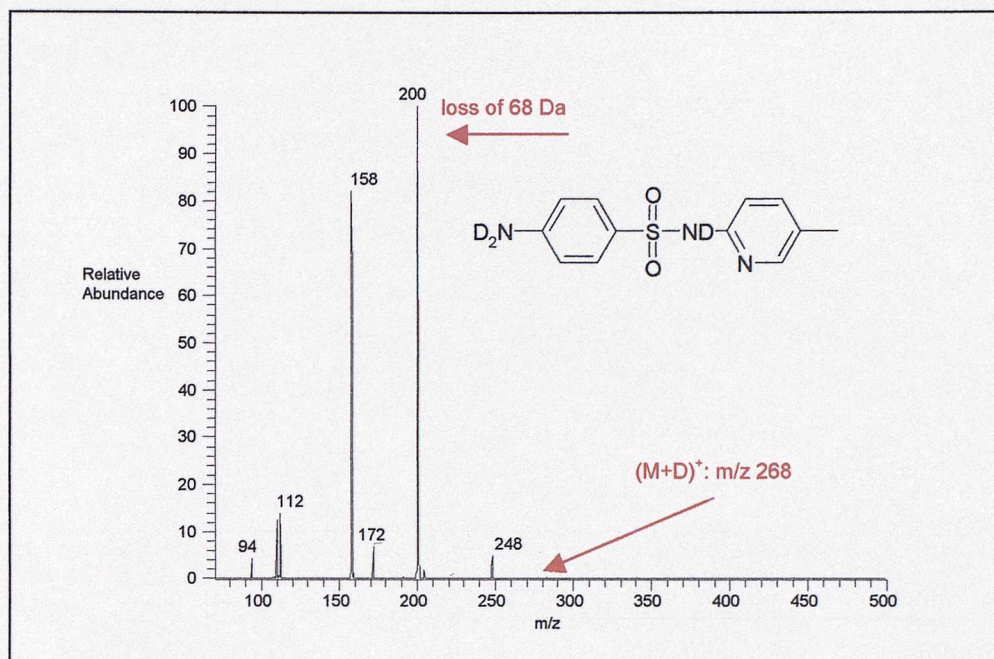


**Figure 52:** The ES-MS/MS spectrum of the fully labelled 4-amino-*N*-(5-methyl-2-pyridinyl)-benzenesulphonamide.

Based on the studies carried out on the sub-group of the amino-sulphonamides and with the aid of publications available in literature,<sup>50,194-196</sup> mechanistic routes can now be proposed for the formation of some of the main fragment ions produced by this group under ES-MS/MS conditions. (Figure 53)

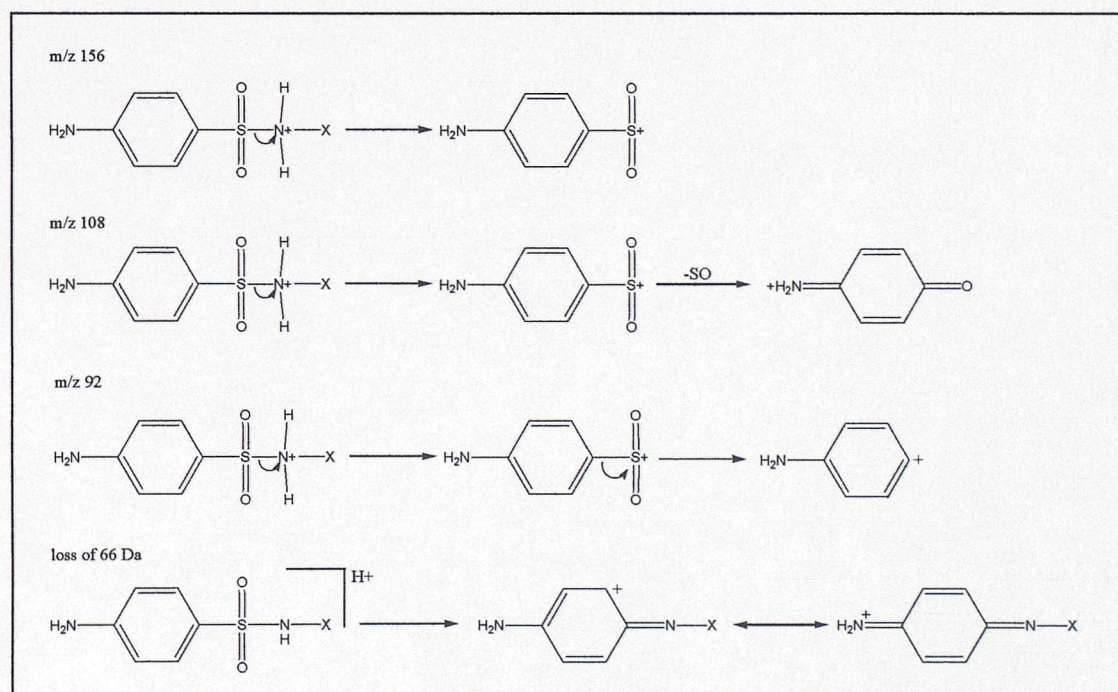


**Figure 53:** Mechanisms proposed for the formation of some of the common fragment ions of the amino-sulphonamides.

### The Fragmentation Pathway of Acetylated Amino-Sulphonamides

The acetylated molecules (**Appendix 3, Table 2**) also followed the same pattern as the one determined for the amino-sulphonamides, but this time the common fragment ions appeared at higher  $m/z$  values due to the presence of the acetyl group. *E.g.* the spectrum of *N*-[4-[[5-methyl-2-pyridinyl)amino)sulphonyl]phenyl]-acetamide is shown in **Figure 54**. The ion at  $m/z$  198 is formed due to cleavage of the sulphonamide bond, while further loss of  $\text{SO}_2$  results in an ion at  $m/z$  134. The ion at  $m/z$  108, formed *via* a rearrangement and the ion due to the loss of  $\text{H}_2\text{SO}_2$  (66 Da) were observed in the same way as in the spectra of the amino-sulphonamides. Finally, the loss of 197 Da, that leads to the complimentary ion of  $m/z$  198,  $\text{X-NH}_3^+$ , also took place.

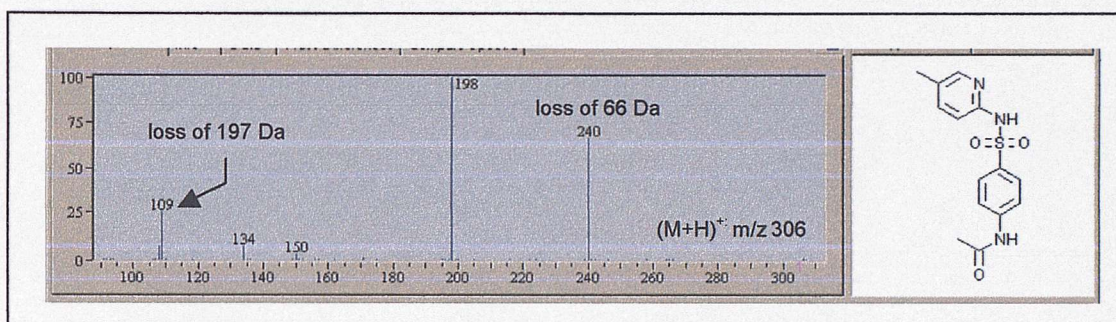


**Figure 54:** The ES-MS/MS spectrum of *N*-[4-[[5-methyl-2-pyridinyl)amino)sulphonyl]phenyl]-acetamide.

Analysis of the acetylated sulphonamides by FTMS allowed calculation of the molecular formulae of most fragment ions present in the spectra. With the aid of Mass Frontier and literature reports available for the acetylated compounds,<sup>182,187,190</sup> structures were assigned to the majority of the  $m/z$  values observed. (**Table 8**)

Fragment Ion	Molecular Formula	Proposed Structure
$m/z$ 198	$\text{C}_8\text{H}_8\text{NO}_3\text{S}^+$	
$m/z$ 134	—	
$m/z$ 108	—	
loss of 66 Da	loss of $\text{H}_2\text{SO}_2$	
loss of 197 Da	loss of $\text{C}_8\text{H}_7\text{NO}_3\text{S}$	$\text{X-NH}_3^+$

**Table 8:** Structures proposed for the main fragment ions and neutral losses produced by the acetylated amino-sulphonamides.

Due to the similarities in the fragmentation pathways of the amino-sulphonamides and the corresponding acetylated molecules, mechanistic studies were not carried out for the acetylated compounds. The mechanisms resulting in the formation of the main fragment ions of the amino-sulphonamides appear to remain valid, when an acetyl group is also present in the structure.

#### The Fragmentation Pathway of Methyl-Sulphonamides

The spectra of thirteen sulphonamides with a methyl group attached on the benzene ring (**Appendix 3, Table 3**) were investigated. It was established, that the compounds followed a similar dissociation pattern to that previously established for the amino-group. Common fragment ions for the methyl-sulphonamides appeared at  $m/z$  155,  $m/z$  109 and at  $m/z$  91, while neutral losses of 66, 67, 92 and 155 Da were also observed. *E.g.* the spectrum of 4-*N*-(5-methyl-2-pyridinyl)-benzenesulphonamide is shown in **Figure 55**.

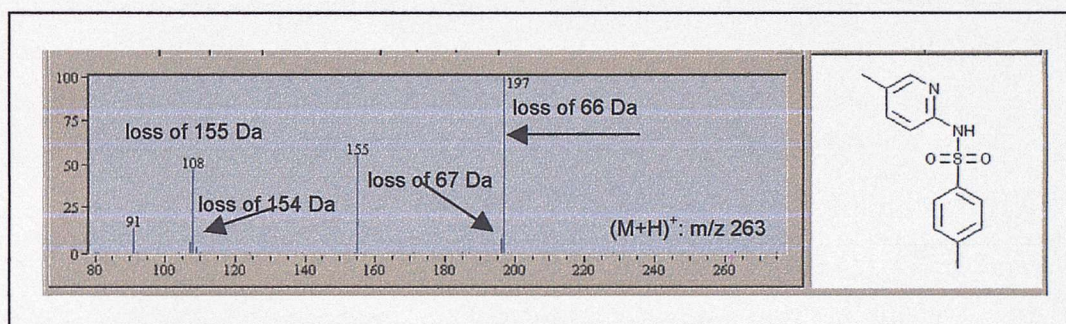


**Figure 55:** The ES-MS/MS spectrum of 4-methyl-*N*-(5-methyl-2-pyridinyl)-benzenesulphonamide.

Analysis of the molecules by FTMS allowed calculation of the molecular formulae and the number of double bond equivalents of all the fragment ions observed. Then, with the aid of Mass Frontier structures were assigned to the fragment ions in the spectra. (**Table 9**) The ion at  $m/z$  155 was shown to be the one generated after the sulphonamide bond was cleaved, whilst the additional loss of  $\text{SO}_2$  resulted in the ion at  $m/z$  91. The loss of  $\text{H}_2\text{SO}_2$  (66 Da) was present in most spectra and the loss of 92 Da resulted in the formation of the known fragment ion  $\text{X-NH-SO}_2^+$ , also observed for the amino-sulphonamides. The fragment ion,  $\text{X-NH}_3^+$ , was present in the spectra of the amino-sulphonamides due to the loss of 155 Da. For the methyl-sulphonamides, the same ion,  $\text{X-NH}_3^+$ , is formed due to the loss of 154 Da and when the substituent X is a methylated pyridine ring, as in the case of a few of the compounds studied, the ion appears at  $m/z$  109. The loss of 155 Da also occurs but the fragment ion obtained is a radical cation corresponding to  $\text{X-NH}_2^{+\bullet}$ . In a similar manner, the loss of 67 Da, observed in the spectra of the methyl-sulphonamides was shown to be the loss of  $\text{H}_3\text{SO}_2^\bullet$ .

Fragment Ion	Molecular Formula	Proposed Structure
m/z 155	$C_7H_7O_2S^+$	
m/z 91	—	
loss of 66 Da	loss of $H_2SO_2$	Further investigation required.
loss of 67 Da	loss of $H_3SO_2^+$	Further investigation required.
loss of 92 Da	loss of $C_7H_8$	$X-NH_2-SO_2^+$
loss of 155 Da	loss of $C_7H_7O_2S^+$	$X-NH_2^+$
loss of 154 Da (m/z 109)	loss of $C_7H_6O_2S$	$X-NH_3^+$

**Table 9:** Structures proposed for the common fragment ions and neutral losses produced by the methyl-sulphonamides.

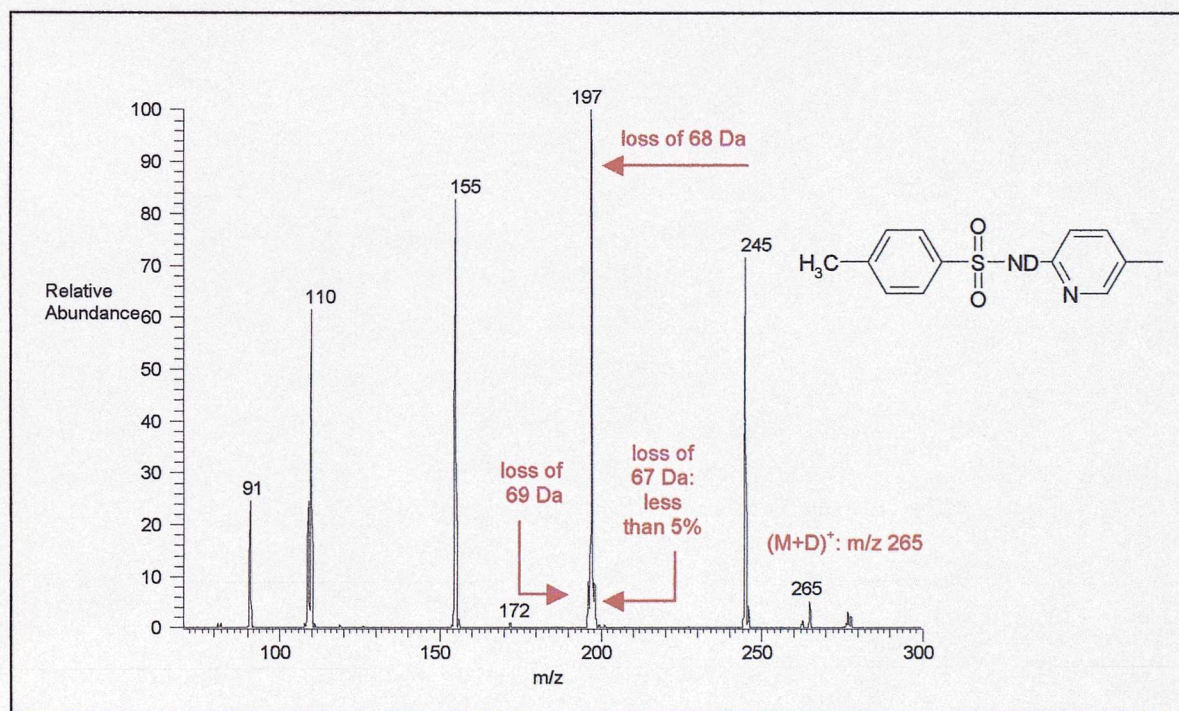
Information about the dissociation routes leading to the main fragment ions observed in the spectra of this group of compounds was gained using  $MS^3$  experiments. The prominent ions in the spectrum of 4-methyl-*N*-(5-methyl-2-pyridinyl)-benzenesulphonamide were dissociated and similar results, as in the case of the amino-sulphonamide, were obtained. (**Table 10**) Dissociation of the fragment ion due to the loss of  $H_2SO_2$  produced the losses of  $CH_4$  and  $CH_3^+$ . Again, the functional groups attached to the benzene ring and the pyridine ring appeared to be cleaved. The ions generated from m/z 155, were present at m/z 91, due to further loss of  $SO_2$ , and at m/z 109, because of a rearrangement following the cleavage of the sulphonamide bond. Finally, dissociation of the radical cation  $X-NH_2^+$  resulted in an even-electron species at m/z 107. The same ion was previously observed in the case of the amino-sulphonamide studied.

Sulphonamide	MS/MS fragment ions	$MS^3$ fragment ions
	loss of $H_2SO_2$	loss of $CH_4$ and $CH_3^+$
	 loss of 155 Da	 $C_6H_7N_2^+$ m/z 107
	 m/z 155	 $C_6H_7^+$ m/z 91 $C_7H_9O^+$ m/z 109

**Table 10:** Summary of the results of the  $MS^3$  experiments carried out on 4-methyl-*N*-(5-methyl-2-pyridinyl)-benzenesulphonamide.

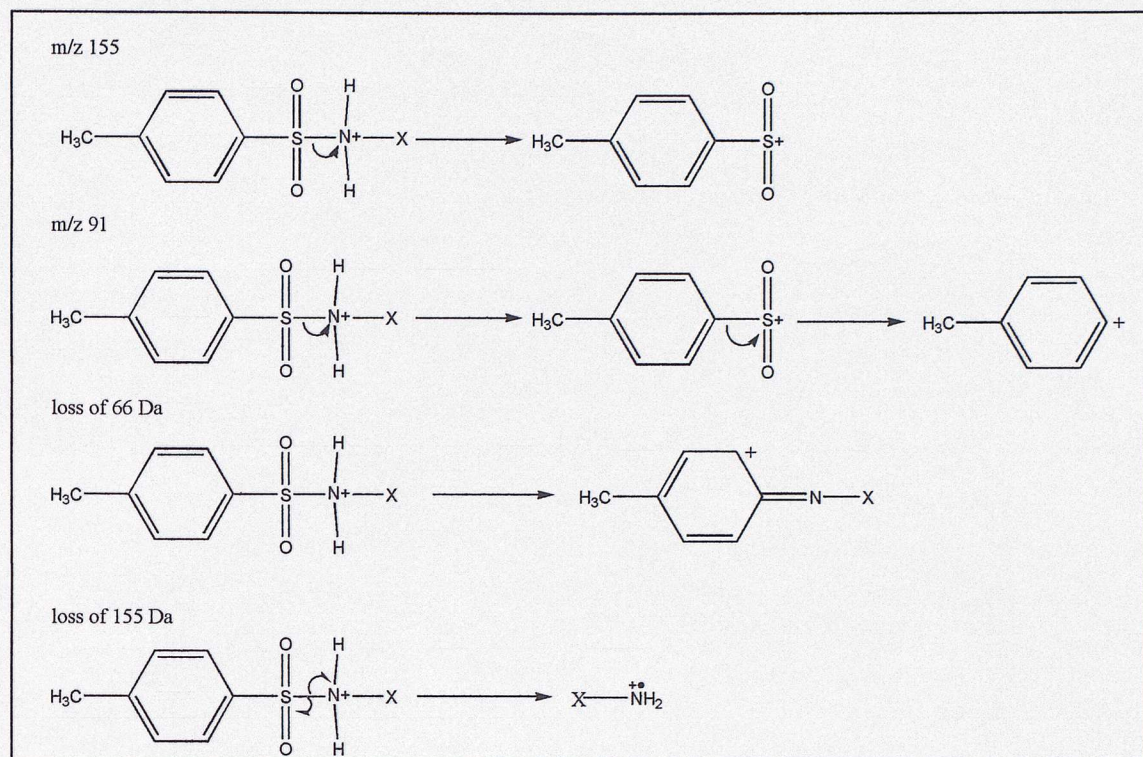
The MS<sup>3</sup> experiments showed that after H<sub>2</sub>SO<sub>2</sub> is lost from the compounds, the two-ring system reconnects in the same manner as for the amino-sulphonamides, *via* the NH group. In that way, the substituents on the pyridine ring and on the benzene ring remain free to be cleaved. In the case of the amino-sulphonamide, a rearrangement, that occurs after the sulphonamide bond is fragmented, results in the formation of the ion at *m/z* 108. For the methyl-sulphonamides a rearrangement also takes place and a fragment ion at *m/z* 109 is formed. Finally, it appears that the ion at *m/z* 107, due to the methylated pyridine ring, can be formed both from the even electron species X-NH-SO<sub>2</sub><sup>+</sup>, present in the spectra of the amino sulphonamides and from the radical cation X-NH<sub>2</sub><sup>•+</sup> observed for the methyl compounds.

The origin of the hydrogens lost in H<sub>2</sub>SO<sub>2</sub> was once more investigated using d-labelling experiments and the ES-MS/MS spectrum obtained for the fully labelled 4-methyl-*N*-(5-methyl-2-pyridinyl)-benzenesulphonamide is shown in **Figure 56**. The previously observed loss of 66 Da for the un-labelled compound is now shifted to 68 Da, indicating the loss of exchangeable hydrogens only. This result is in agreement with the d-labelling results produced by the amino-sulphonamide.



**Figure 56:** The ES-MS/MS spectrum of the fully labelled 4-methyl-*N*-(5-methyl-2-pyridinyl)-benzenesulphonamide.

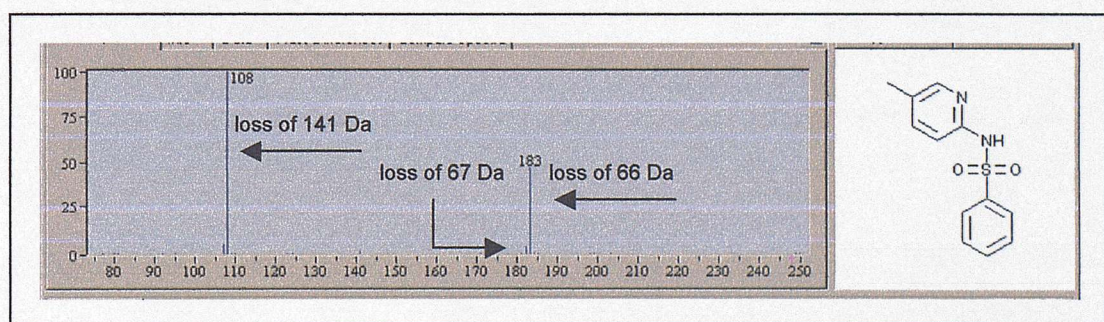
The mechanisms proposed for the generation of some of the fragment ions for methyl-sulphonamides are shown in **Figure 57**.



**Figure 57:** Mechanisms proposed for the formation of some of the common fragment ions of the methyl-sulphonamides.

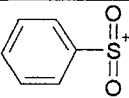
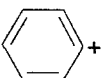
#### The Fragmentation Pathway of Non-Substituted Benzenesulphonamides

A group of sulphonamides with no substituents on the benzene ring of the molecules (**Appendix 3, Table 4**) was investigated. It was observed that all compounds followed a dissociation pathway that closely resembles the fragmentation route established for the methyl-sulphonamides. Ions appeared at  $m/z$  141, due to cleavage of the sulphonamide bond, and at  $m/z$  77, due to the subsequent loss of  $\text{SO}_2$ . The losses of 66 and 67 Da known to correspond to  $\text{H}_2\text{SO}_2$  and  $\text{H}_3\text{SO}_2^+$  were also observed. Finally, the loss of 141 Da, that results in the formation of the radical cation  $\text{X}-\text{NH}_2^+$  was present in most spectra at high abundance. *E.g.* the spectrum of *N*-(5-methyl-2-pyridinyl)-benzenesulphonamide is shown in **Figure 58**.



**Figure 58:** The ES-MS/MS spectrum of *N*-(5-methyl-2-pyridinyl)-benzenesulphonamide.

Confirmation of the structures proposed for the fragment ions in the spectra of the non-substituted benzenesulphonamides was obtained again by exact mass analysis by FTMS. Molecular formulae and the number of double bond equivalents were calculated for most of the  $m/z$  values observed in the spectra of these compounds and the structures assigned to the related fragment ions are shown in **Table 11**.

Fragment Ion	Molecular Formula	Proposed Structure
$m/z$ 141	$C_6H_5O_2S^+$	
$m/z$ 77	—	
loss of 66 Da	loss of $H_2SO_2$	Further investigation required.
loss of 67 Da	loss of $H_3SO_2^{\bullet}$	Further investigation required.
loss of 141 Da	loss of $C_6H_5O_2S^{\bullet}$	$X-NH_2^{+\bullet}$

**Table 11:** Structures proposed for the common fragment ions and neutral losses produced by the non-substituted benzenesulphonamides.

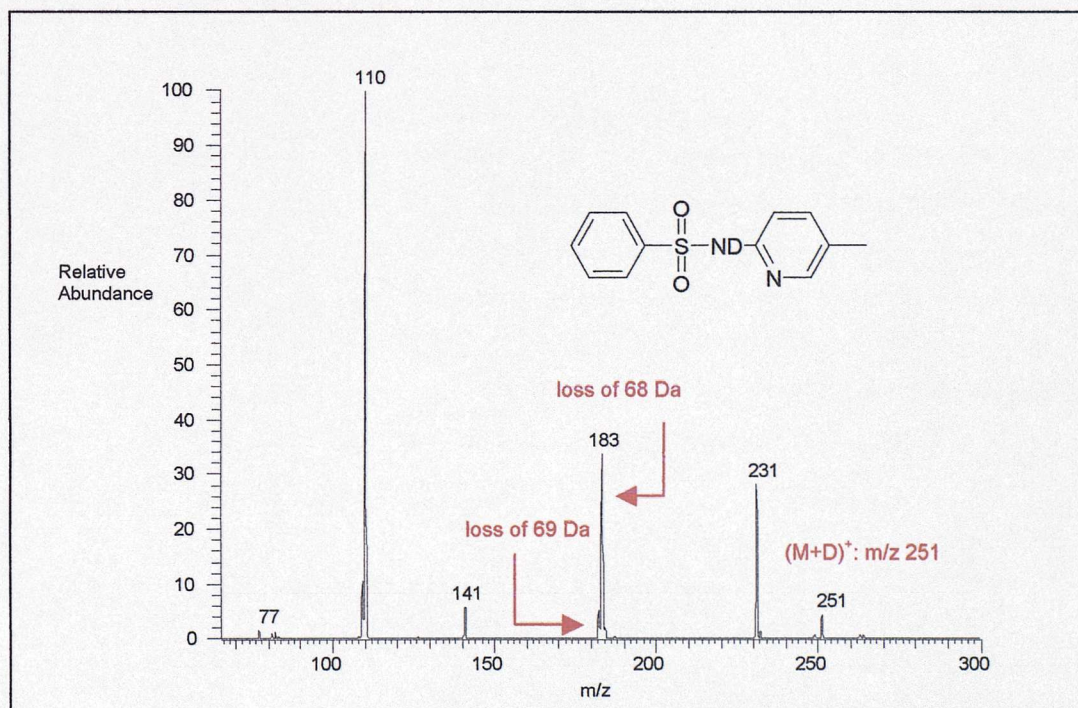
*N*-(5-methyl-2-pyridinyl)-benzenesulphonamide was used as the model compound in order to study the fragmentation processes occurring for this type of sulphonamides and compare the results with those previously obtained for the amino and the methyl sub-groups. The main fragment ions produced by *N*-(5-methyl-2-pyridinyl)-benzenesulphonamide were dissociated using  $MS^3$  experiments. The ion due to the loss of  $H_2SO_2$  after dissociation produced the additional losses of  $H^{\bullet}$  and  $CH_3^{\bullet}$ . This once more confirmed that only the substituents on the benzene ring and on the pyridine ring of the ion are cleaved. The radical cation,  $X-NH_2^{+\bullet}$  led to the generation of the ion at  $m/z$  107, previously observed for both the amino and the methyl-sulphonamides. Finally, the ion due to cleavage of the sulphonamide bond, at  $m/z$  141, was of low abundance in the MS/MS spectrum acquired on the FTICRMS and useful  $MS^3$  spectra were not observed. (**Table 12**)

The  $MS^3$  experiments carried out on *N*-(5-methyl-2-pyridinyl)-benzenesulphonamide confirmed the observations previously made for the amino and the methyl-sulphonamides. The structure of the ion due to the loss of  $H_2SO_2$  involves reconnection of the benzene ring and the pyridine ring *via* the NH group. The same ion appears to be formed by all types of sulphonamides. In addition, the fragment ion at  $m/z$  107, that corresponds to the methylated pyridine ring, is formed after dissociation of both even electron species such as the  $X-NH-SO_2^+$  present in the spectra of the amino-sulphonamides and of radical cations such as the  $X-NH_2^{+\bullet}$  observed for the methyl and non-benzene substituted molecules.

Sulphonamide	MS/MS fragment ions	MS <sup>3</sup> fragment ions
	loss of H <sub>2</sub> SO <sub>2</sub>	loss of H <sup>+</sup> and CH <sub>3</sub> <sup>•</sup>
	 loss of 141 Da	 C <sub>6</sub> H <sub>7</sub> N <sub>2</sub> <sup>+</sup> m/z 107

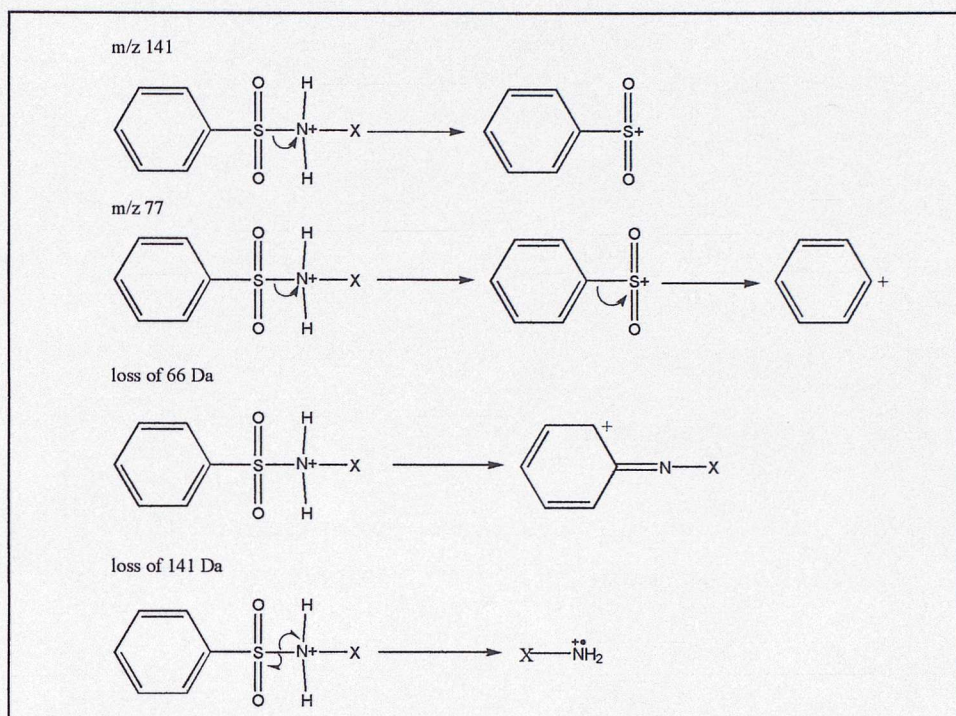
**Table 12:** Summary of the results of the MS<sup>3</sup> experiments carried out on *N*-(5-methyl-2-pyridinyl)-benzenesulphonamide.

The hydrogens involved in the loss of H<sub>2</sub>SO<sub>2</sub> were identified for the amino and the methylsulphonamides to be exchangeable Hs. This was also confirmed for the non-substituted molecules and the ES-MS/MS spectrum of the fully labelled *N*-(5-methyl-2-pyridinyl)-benzenesulphonamide is shown in **Figure 59**. The loss of 68 Da that corresponds to D<sub>2</sub>SO<sub>2</sub> results to one of the main fragment ions observed. According to the results of the d-labelling experiments carried out on the three sulphonamides, the hydrogens involved in the loss of H<sub>2</sub>SO<sub>2</sub> from the methyl and the non-substituted benzenesulphonamides are the hydrogen of the NH group and the proton gained during ionisation. In the case of the amino-sulphonamides, the hydrogens could also originate from the NH<sub>2</sub> group attached on the benzene ring.



**Figure 59:** The ES-MS/MS spectrum of the fully labelled *N*-(5-methyl-2-pyridinyl)-benzenesulphonamide.

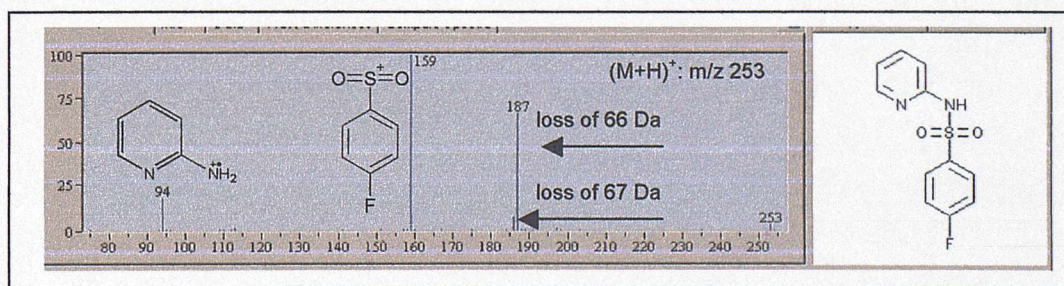
Based on all the experiments carried out in the non-substituted sulphonamides, mechanisms can be proposed leading to the formation of some of the main fragment ions observed for this group. (**Figure 60**)



**Figure 60:** Mechanisms proposed for the formation of some of the common fragment ions of the non-substituted benzenesulphonamides.

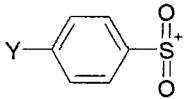
#### The Fragmentation Pathway of a Group of Various Sulphonamides

The final sub-group of sulphonamides investigated, consisted of five compounds with various substituents attached on the benzene ring. (**Appendix 3, Table 5**) The ES-MS/MS spectra of the compounds were studied and it was established that the group followed a dissociation pathway similar to that identified for the methyl and the non-substituted benzene sulphonamides. Fragment ions were again observed due to cleavage of the sulphonamide bond, due to the losses of 66 and 67 Da and also corresponding to  $\text{X-NH}_2^+$ . The  $m/z$  values in the spectra varied, depending on the substituents  $\text{X}$  and  $\text{Y}$  attached on the molecules. *E.g.* the spectrum of 4-trifluoromethyl-*N*-2-pyridinylbenzenesulphonamide is shown in **Figure 61**.



**Figure 61:** The ES-MS/MS spectrum of 4-fluoro-*N*-2-pyridinyl-benzenesulphonamide.

Exact mass analysis by FTMS was carried out on all the fragment ions generated by the five molecules and elemental compositions were assigned to the  $m/z$  values present in the spectra. In accordance with the results obtained, the structures proposed for the fragment ions of this sub-group are shown in **Table 13**.

Fragment Ion	Molecular Formula	Proposed Structure
cleavage of the sulphonamide bond	various	
radical cation due to X	various	$X-NH_2^{+\bullet}$
loss of 66 Da	loss of $H_2SO_2$	Further investigation required.
loss of 67 Da	loss of $H_3SO_2^\bullet$	Further investigation required.

**Table 13:** Structures proposed for the main fragment ions and neutral losses produced by the five sulphonamides studied with various groups attached on the benzene ring.

It was shown that the five compounds followed the dissociation pathway previously established for the methyl and the non-substituted benzene sulphonamides. Hence the mechanisms proposed for the formation of fragment ions for those two sub-groups were expected to be maintained in the case of this group of molecules. For this reason, additional mechanistic studies were not carried out for this group.

#### 4d. Molecular Modelling Calculations

The potential of *ab initio* calculations with respect to fragment ion prediction was explored using a “model” sulphonamide. *N*-(5-methyl-2-pyridinyl)-benzenesulphonamide was used with the aim to study the effects of protonation in the structure and to determine whether the sites most likely to be cleaved can be predicted. The energetically favoured conformers of the neutral sulphonamide and all its possible protonated forms were identified and optimised. Protonation was proposed on the  $SO_2$  group ( $OH^+$  benzenesulphonamide), on the NH group of the sulphonamide bond ( $NH_2^+$  benzenesulphonamide) and on the nitrogen of the pyridine ring (ring  $NH^+$  benzenesulphonamide). The results of the calculations carried out are summarised in **Appendix 3, Figure 6**.

Comparison between the energies of the protonated molecules shows that the  $OH^+$  and the ring  $NH^+$  protonated compounds are more stable than the  $NH_2^+$  benzenesulphonamide. In addition, the structure of the neutral compound does not change significantly, with respect to the length of the major bonds, after protonation takes place on the  $SO_2$  group or on the pyridine ring. On the other hand, the addition of a proton to the sulphonamide bond causes important alterations to the initial neutral structure. The sulphonamide bond elongates significantly and becomes the easiest bond to break. This is in agreement with the fragment ions observed in the ES-MS/MS spectra, where it

was proven that many ions were formed after the sulphonamide bond was cleaved. It, therefore, appears that the  $\text{NH}_2^+$  benzenesulphonamide can be a starting point for dissociation in ES-MS/MS.

The structure of the neutral molecule and of the cations resulting after protonation is not planar, but the angle created between the benzene ring and the sulphonamide bond is close to  $100^\circ$ . This indicates that the molecule would dissociate to form fragment ions with a more planar structure that would be energetically favoured. This could be the reason why the loss of  $\text{H}_2\text{SO}_2$  is a major fragmentation process. To confirm this and also obtain further information about the driving forces leading to the dissociation of sulphonamides under ES-MS/MS conditions, additional calculations and comparisons need to be carried out for the neutral molecule, the protonated forms and the resulting fragment ions. These would provide reasons behind fragment ion formation and would also reveal the favoured site for ionisation. Additional potential protonation sites would have to be considered in the case of the amino-sulphonamides and for any compounds with electronegative groups on the substituent Y.

The calculations described above, however, require a high level of theory and interpretation of the results can only be addressed by the highly experienced expert in the field of molecular modelling. Here, only the potential of *ab initio* calculations is demonstrated and the observations made were extensively discussed with molecular modellers to confirm their validity. Further use of this technique by experts could be a great advantage for the improvement of mass spectra interpretive packages.

#### 4e. Conclusion

The fragmentation pathway of a library of sulphonamides was investigated. It was observed that all sub-groups of the library followed a common dissociation route and a fragmentation pattern was established. This proves that fragmentation patterns can be identified for large combinatorial libraries and are not limited to small groups of molecules only.

Structures were assigned to most of the fragment ions observed and some of the mechanisms taking place for fragment ion formation were explored. In the same way, as it was previously observed in the case of the amino acids, mechanisms could be postulated for the entire group and were not limited to certain molecules only. The presence of radical cations under ES-MS/MS conditions was reported. This widens the range of possible dissociation routes that are known to take place when ES-MS/MS is used. The formation of solvent adducts of fragment ions in the ion trap was also confirmed. Incorporation of this feature into AI software packages should prevent misinterpretation of fragment ions and together with an option for radical cation formation should improve the fragment ion prediction mode.

Finally, *ab initio* studies carried out on a "model" sulphonamide showed that the behaviour of molecules under ES-MS/MS conditions can be predicted. Important observations were made with respect to the sites of ionisation and the effects of protonation to the initial structure of the neutral molecule. The bonds more likely to be cleaved were identified and the results were in agreement with the fragment ions observed in the ES-MS/MS spectra. It appears that, molecular modelling

can find enormous applications in the field of mass spectrometry and could become a powerful tool for fragment ion prediction.

## 5. Identification of Unknown Non-Peptidic Molecules From Their ES-MS/MS Spectra: Automated Approach and Limitations

### 5a. Introduction

The studies carried out so far, have shown that different classes of non-peptidic molecules follow distinct dissociation pathways when analysed by ES-MS/MS. This was proven to be the case for small groups of molecules, (**Chapter 2**) arrays of monomers, as demonstrated by the amino acids, (**Chapter 3**) and combinatorial libraries such as sulphonamides. (**Chapter 4**)

These findings were not surprising, since the common fragment ions produced by the different classes of drug molecules were often reported in literature for their use in detection and quantification studies carried out on the corresponding compounds. However, the proof that fragmentation in ES-MS/MS is structure dependant was a critical step in moving towards an improved, automated system that is capable of reliably handling the data interpretation.

The patterns observed are now further used to identify an unknown molecule from its MS/MS spectrum, in two stages: initially its substructure is identified from the general pattern and then in more detail, the functionalities present in its structure are recognised. The first step, carried out for substructure identification can also be automated using pattern recognition methods available from multivariate statistics. The two-step method developed for structure identification of unknowns and its limitations are discussed below.

### 5b. Experimental

#### Materials

- The fragmentation pathways of the ergopeptine alkaloids and the aflatoxins were determined using spectra available in the MS/MS library.<sup>52</sup>
- The library of sulphonylureas was purchased from Qmx Laboratories Ltd, Thaxted, UK.
- The group of sulphonamides was synthesised in house and used without further purification.
- Methanol, HPLC grade, was purchased from Fisher, Loughborough, UK.
- Formic acid, analytical grade 98-100%, was purchased from Sigma-Aldrich, Gillingham, UK.

#### Sample Preparation

- Solutions of all compounds analysed were prepared in methanol and 0.1% formic acid. Concentration: 10 µg/mL.

#### Instrumentation and Conditions Used

- ES-MS/MS spectra for the sulphonylureas and the sulphonamides were obtained from an LCQ Deca Ion Trap (Thermo Finnigan, San Jose, CA, USA) under standard conditions: Capillary Temperature: 200 °C, Sheath Gas Flow: 35 au, Auxiliary Gas Flow: 10 au, Source Voltage: 4.5 kV. Nitrogen was used as the sheath and the auxiliary gas and helium was the collision gas. MS/MS parameters: Isolation Width: 1, Collision Energy: 35%.

- The MS<sup>3</sup> experiments on the group of sulphonamides were carried out using an Apex III FTICRMS (Bruker, Billerica, MA, USA): Capillary: -4.5 kV, End Plate: -3.8 kV, Capillary Exit: 102 V, Skimmer 1: 8.26 V, Skimmer 2: 7.64 V, Offset: 1.00, Rf Amplitude: 550.00 Hz, Dry Gas Temperature: 130°C. Nitrogen was used as the drying gas and argon was used as the collision gas.

MS/MS parameters: corr sweep pulse length: 1000  $\mu$ sec, corr sweep attenuation: 30.0 dB, ejection safety belt: 3000 Hz, user pulse length: 5000  $\mu$ sec, ion activation pulse length: 250000  $\mu$ sec, ion activation attenuation: 49.5 dB, frequency offset from activation mass: -500 Hz, user delay length: 3 sec.

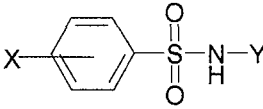
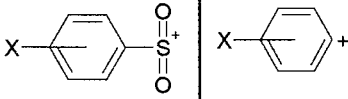
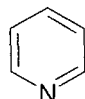
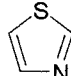
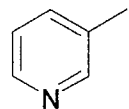
MS/MS/MS parameters: corr sweep pulse length: 500  $\mu$ sec, corr sweep attenuation: 30.0 dB, ejection safety belt: 0 Hz, user pulse length: 5000  $\mu$ sec, ion activation pulse length: 250000  $\mu$ sec, ion activation attenuation: 49.5 dB, frequency offset from activation mass: -500 Hz, user delay length: 6 sec.

### 5c. Results and Discussion

As described in **Chapters 2, 3 and 4**, approximately 200 spectra of different libraries of compounds were studied. It was observed that each of the libraries produced specific fragment ions and neutral mass losses, depending on the functional groups present in the structures of the molecules. The fragmentation patterns established for each class of molecule can subsequently be used to identify an unknown, providing it belongs to one of these classes of compounds. This can be done in two steps.

In first instance, the class of compound can be identified from the general pattern of specific ions observed in its respective MS/MS spectrum. *E.g.* loss of 66 Da and ions at  $m/z$  156, 108 and 92 are indicative of an amino-sulphonamide. For carnitines representative fragment ions at  $m/z$  85 and 144 together with loss of 59 Da are observed. Similarly characteristic ions are observed for the other sub-groups studied.

Once the substructure of the unknown has been revealed, identification of the functionalities present in the structure can be achieved using the specific  $m/z$  values present in the spectrum. *E.g.*, the components of the library of sulphonamides can be identified by combining the information provided by the fragment ions observed in the spectra. **(Table 14)** Fragment ions present at  $m/z$  156 and  $m/z$  92, suggest there is an amino functionality attached to the benzene ring. If the fragment ions observed, appear at  $m/z$  155 and  $m/z$  91 instead, then the functional group attached to the aromatic ring is a methyl group. Similarly, fragment ions at  $m/z$  141 and  $m/z$  77, correspond to no substituent present on the benzene ring. Information about the substituent Y can be obtained from the ion due to the loss of 155 Da. In the case of an amino-sulphonamide this corresponds to the charged substituent. If Y is a pyridine ring, the fragment ion due to the loss of 155 Da is observed at  $m/z$  95. Similarly, a methylated pyridine shows the analogous ion at  $m/z$  109. If Y is a thiazole ring then the corresponding fragment ion appears at  $m/z$  101. Combination of the information obtained from all the fragment ions in the spectra of each molecule results in identification of the individual compounds and aids characterisation of the library.

<div style="text-align: center;">  <p>core structure of sulphonamide library</p> </div>			
Step 1: Identification of Substituent X		Step 2: Identification of Substituent Y	
Fragment Ions Used:	Functionality:	Fragment Ions Used:	Functionality:
		Y-NH <sub>3</sub> <sup>+</sup>	
m/z 156 and m/z 92 <div style="display: inline-block; vertical-align: middle; text-align: center;"> <math>\xrightarrow{X}</math> </div>	NH <sub>2</sub>	m/z 95 <div style="display: inline-block; vertical-align: middle; text-align: center;"> <math>\xrightarrow{Y}</math> </div>	
m/z 155 and m/z 91 <div style="display: inline-block; vertical-align: middle; text-align: center;"> <math>\xrightarrow{X}</math> </div>	CH <sub>3</sub>	m/z 101 <div style="display: inline-block; vertical-align: middle; text-align: center;"> <math>\xrightarrow{Y}</math> </div>	
m/z 144 and m/z 77 <div style="display: inline-block; vertical-align: middle; text-align: center;"> <math>\xrightarrow{X}</math> </div>	H	m/z 109 <div style="display: inline-block; vertical-align: middle; text-align: center;"> <math>\xrightarrow{Y}</math> </div>	

**Table 14:** Identification of the functionalities present in the structure of an unknown sulphonamide based on the m/z values observed in its spectrum.

The process of substructure identification, which is the first step of the method developed, can be automated using AI software packages like Mass Frontier. Classification methods such as PCA (Section 1c) are employed in order to achieve automatic pattern recognition. *E.g.* **Figure 62** displays the projection of the ES-MS/MS spectra of the three largest sets of compounds available for this study, the amino acids, the sulphonamides and the carnitines, that have been classified using PCA. Based on the three coordinate system shown, three clusters are separated in space. The three different groups can be distinguished based on their ES-MS/MS spectra only. This projection is a clear demonstration of the close relationship between the structures of molecules and the fragment ions formed under ES-MS/MS conditions. Identification of the library of an unknown can be achieved following insertion of its spectrum into the projection plane. The position of the new spectrum on the projection plane is indicative of the substructure of the molecule in question. Classification by PCA or by other classification methods, such as Neural Networks, which are available in the latest version of Mass Frontier, can be applied to large numbers of libraries consisting of many compounds.<sup>197</sup>

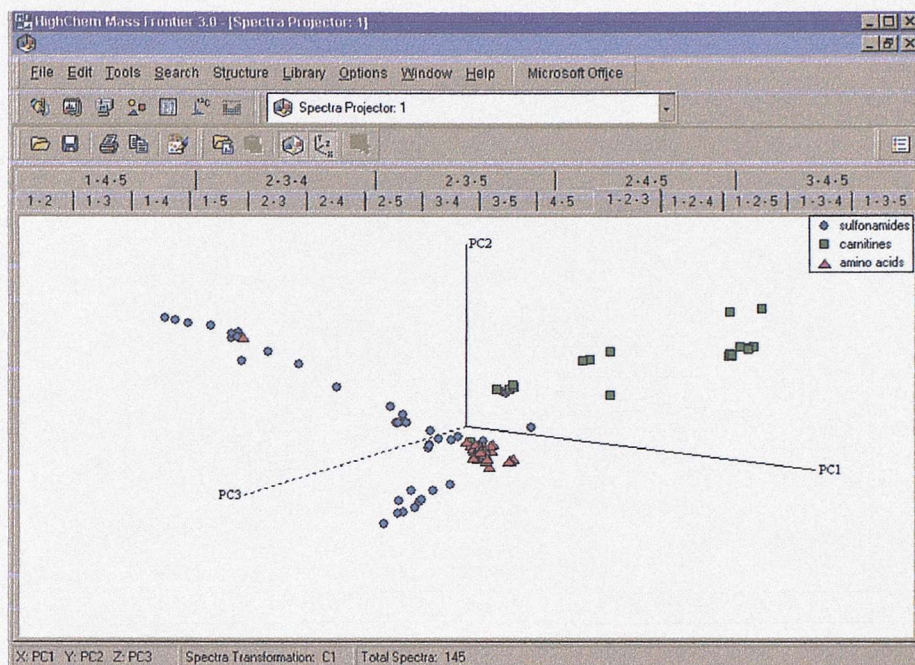


**Figure 62:** Classification of three groups of compounds using PCA.

Based on the two-step method developed for the identification of unknowns using ES-MS/MS, recognition of the functionalities present in the structures of the compounds is achieved using the  $m/z$  values present in their spectra. This approach does not currently allow identification between isomeric molecules. The spectra of three isomeric sulphonamides are shown in **Figure 63**. The only difference in the structures of the three compounds is the position of the methyl group on the pyridine ring. The spectra produced by the three molecules are very similar and the same predominant  $m/z$  values are observed in all of them. Using the method developed, the compounds would be successfully identified as benzenesulphonamides with a methylated pyridine ring attached, but the position of the methyl group on the pyridine ring could not be determined.

In literature, successful differentiation between isomers is reported using compound specific ions and the differences in the abundances of the main fragment ions observed.<sup>164,196,198</sup> The use of MS<sup>3</sup> experiments in order to achieve differentiation was also reported.<sup>173</sup> Correlation between the structure of the precursor ion and the abundances of the fragment ions requires an in-depth study on each set of compounds and it is not within the scope of this investigation. MS<sup>3</sup> experiments were carried out on the three sulphonamides in order to determine whether differentiation between them could be achieved. The fragment ion at  $m/z$  108 corresponding to the methylated pyridine was isolated for each compound and dissociated. The results are summarised in **Table 15**. The same MS<sup>3</sup> fragment ions were obtained for all sulphonamides and therefore the experiments did not aid in distinguishing between the isomers. The process of complete structure elucidation with respect to isomeric compounds analysed by ES-MS/MS using CID remains a challenge.

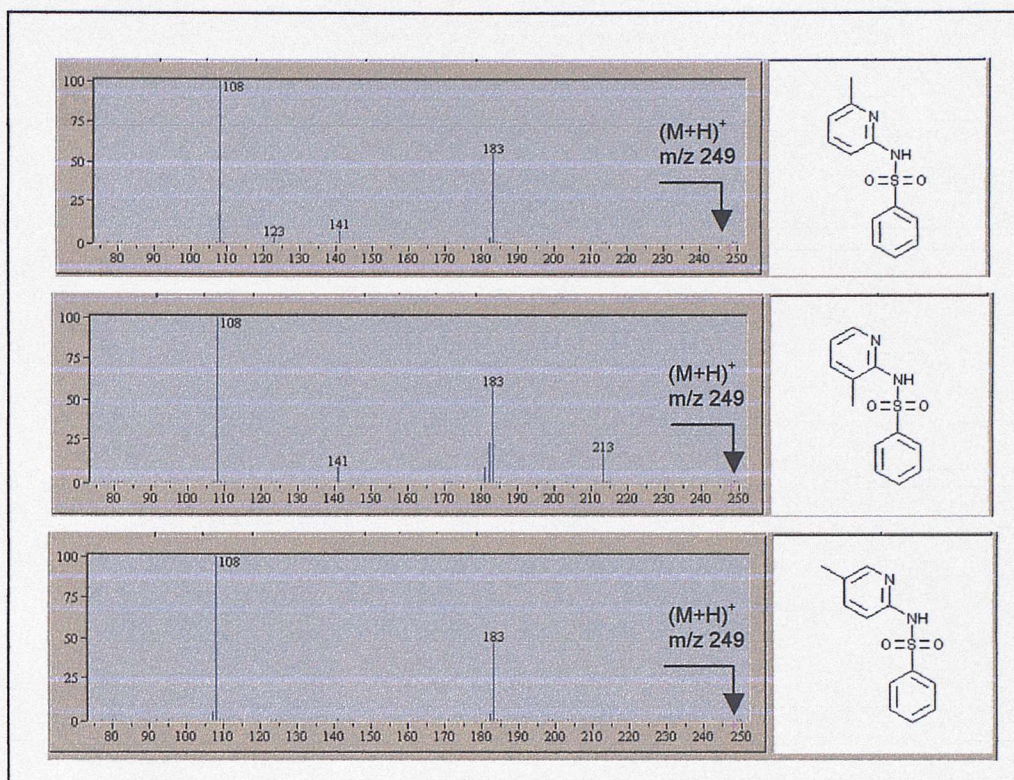


**Figure 63:** The ES-MS/MS spectra of three isomeric sulphonamides.

Fragment Ion Isolated	Molecular Formula	MS <sup>3</sup> Fragment Ions		
	$C_6H_8N_2^{+•}$	m/z 107 $C_6H_7N_2^+$	m/z 81 $C_5H_7N^{+•}$	m/z 80 $C_5H_6N^+$
	$C_6H_8N_2^{+•}$		m/z 81 $C_5H_7N^{+•}$	m/z 80 $C_5H_6N^+$
	$C_6H_8N_2^{+•}$	m/z 107 $C_6H_7N_2^+$	m/z 81 $C_5H_7N^{+•}$	m/z 80 $C_5H_6N^+$

**Table 15:** Summary of results of the MS<sup>3</sup> experiments carried out on the isomeric sulphonamides.

A further limitation of the method developed for the identification of unknowns is that the types of compounds that can be currently identified in two steps are limited to combinatorial molecules only. The method cannot be applied to fused ring systems, *e.g.* aflatoxins, where identification of the structures of the fragment ions is very complex. The dissociation patterns of two groups of compounds consisting of fused ring systems were investigated and although a common

dissociation route was observed for all compounds within each group, only general observations could be made about the sites of dissociation. Identification of the structures of the fragment ions produced was not possible without stable isotope experiments.

The core structure of ergopeptine alkaloids is shown in **Figure 64** and the individual structures of all the compounds studied are shown in **Appendix 4, Table 1**. Dissociation for these molecules mainly occurs around the amide bond<sup>199-205</sup> and the non-aromatic heterocycles. General observations were made with respect to the roles of the X, Y and R groups in dissociation under ES-MS/MS conditions.

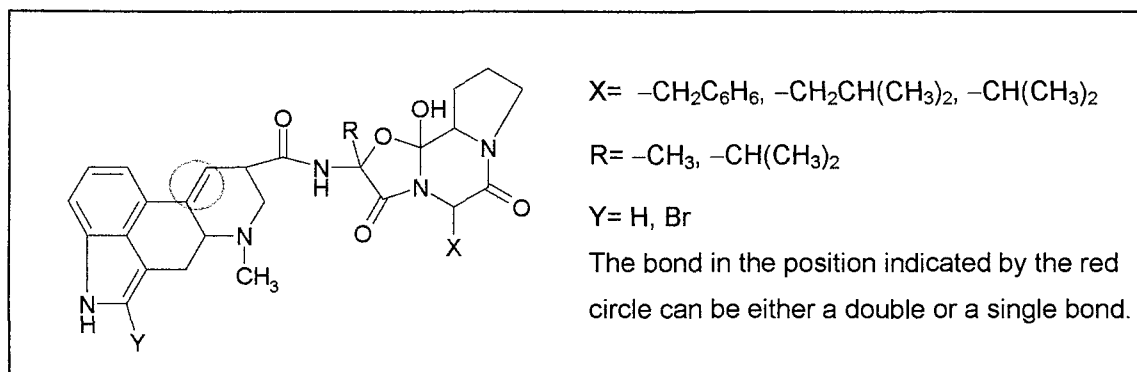


**Figure 64:** The core structure of the ergopeptine alkaloids studied.

The MS/MS spectra of this library are shown in **Appendix 4, Figure 1**. The first comparison carried out involved ergocryptine, ergocornine and ergocristine, whose structures differ only with respect to the substituent X. The spectra produced by the three molecules are very similar and the same  $m/z$  values are observed for all of them. This indicates that the substituent X is cleaved during dissociation and that the non-aromatic heterocyclic part of the molecules is the major site, where fragmentation occurs.<sup>206</sup> Comparison between ergotamine and ergocristine reveals that the substituent R remains on most of the fragment ions formed. Predominant ions 28 mass units apart, as well as at the same  $m/z$  values are present in the two spectra. Comparison between ergocryptine and bromocryptine showed that the Y group is not cleaved during dissociation. This time, fragment ions 78 mass units apart are observed in the two spectra due to the presence of the bromine atom in the bromocryptine structure. This confirms that the aromatic part of the molecules remains intact when fragment ions are formed.<sup>205</sup> Finally the spectra of ergocristine and ergocornine were compared with those of dihydroergocristine and dihydroergocornine. The spectra of the two dihydro compounds are very similar, but significantly different from those of the other two compounds containing the double bond. Comparison of the high mass regions showed that common fragment ions are present, but at  $m/z$  values that are two mass units apart, because of the bond difference in the structures.<sup>207</sup> Common fragment ions were not observed in the low mass region. The most abundant ion in the spectra of dihydroergocristine and dihydroergocornine appears at  $m/z$  270 and corresponds to the protonated aromatic substructure. The same ion is also present at  $m/z$  268 in the spectra of ergocornine and ergocristine, as well as in the spectra of ergotamine and ergocryptine, but its intensity is lower. For these molecules the most abundant

fragment ion appears at  $m/z$  305 possibly after a rearrangement has occurred. The presence or the absence of the double bond at the indicated position in the core structure (**Figure 64**) affects the dissociation route of the molecules significantly and causes considerable changes in the resulting spectra.

General observations were also made on the dissociation pathways of a group of aflatoxins. (**Appendix 4, Table 2**) Again, structure assignment of all the fragment ions in the spectra was not possible unless stable isotope experiments were undertaken. Studies carried out using Mass Frontier predictions and literature references<sup>208-214</sup> resulted in the following comments to be made.

The spectra of the aflatoxins studied are shown **Appendix 4, Figure 2**. All aflatoxins produce the loss of 28 Da that corresponds to the loss of CO, possibly from the coumarin part of the structures.<sup>208</sup> In the case of aflatoxins B1 and B2 additional fragment ions were formed due to the losses of 29 Da, as CHO, from the difuran rings<sup>208</sup> and 56 Da. In the spectra of aflatoxin G1 and G2 prominent fragment ions are observed due to the losses of 86 Da and 46 Da, due to dissociation taking place at more than one site of the structures. The fragmentation of the compounds is significantly affected by the double bond on the furan ring.<sup>208</sup> An increased number of fragment ions are observed in the spectra of aflatoxins B2 and G2 compared to those of B1 and G1, especially in the case of aflatoxin G2. The type of rings present on the coumarin part of the molecules does not affect the dissociation. Fragment ions 16 mass units apart are observed in the spectra of aflatoxins B1 and G1, as well as B2 and G2. This is a further indication that dissociation occurs mainly on the difuran rings rather than in the coumarin substructure.

The investigation carried out on the two sets of compounds consisting of fused ring systems showed that the two-step method developed for the identification of unknowns using ES-MS/MS is better suited for studies carried out on non-peptidic, combinatorial compounds. Although the groups of aflatoxins and ergopeptine alkaloids followed a common dissociation pattern respectively, the complexity of their ES-MS/MS spectra renders identification of the fragment ions difficult and application of the method developed for recognition of unknowns impossible. The Fragments and Mechanisms module in Mass Frontier generates an enormous number of possible fragment ions for these types of molecules and uses complex reaction schemes to predict their formation, as shown in **Figure 65**. This results in isotope labelling experiments being necessary for confirmation of the structures. The process of identification of this type of unknown compounds is currently not amenable to automation using AI predictive packages.

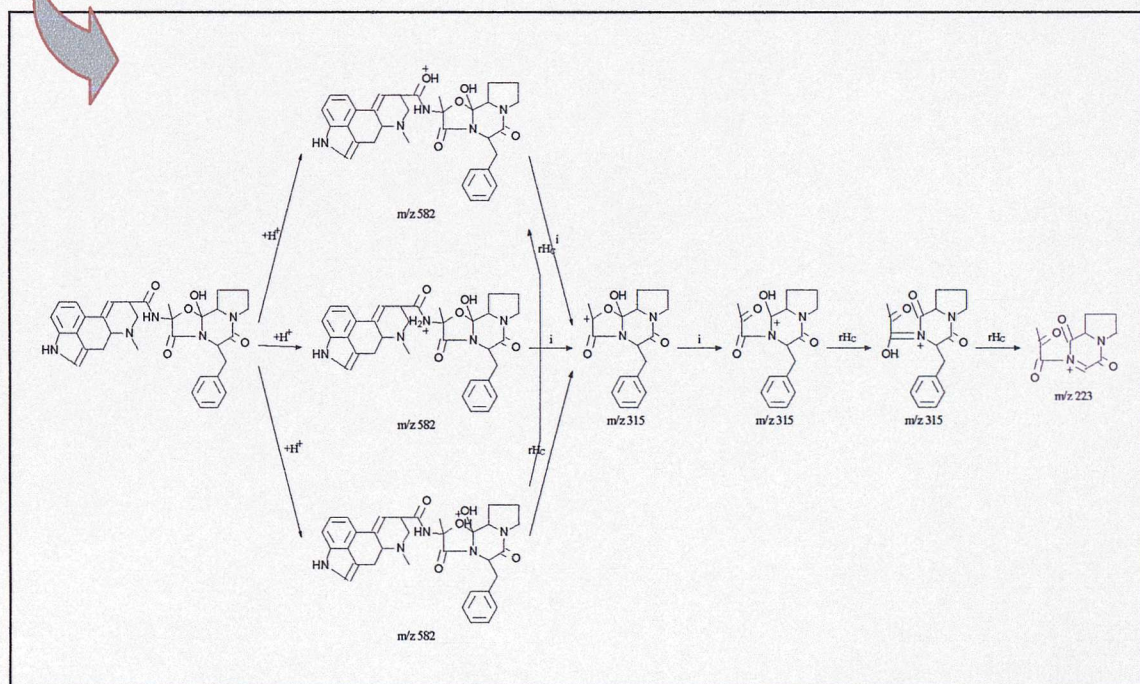
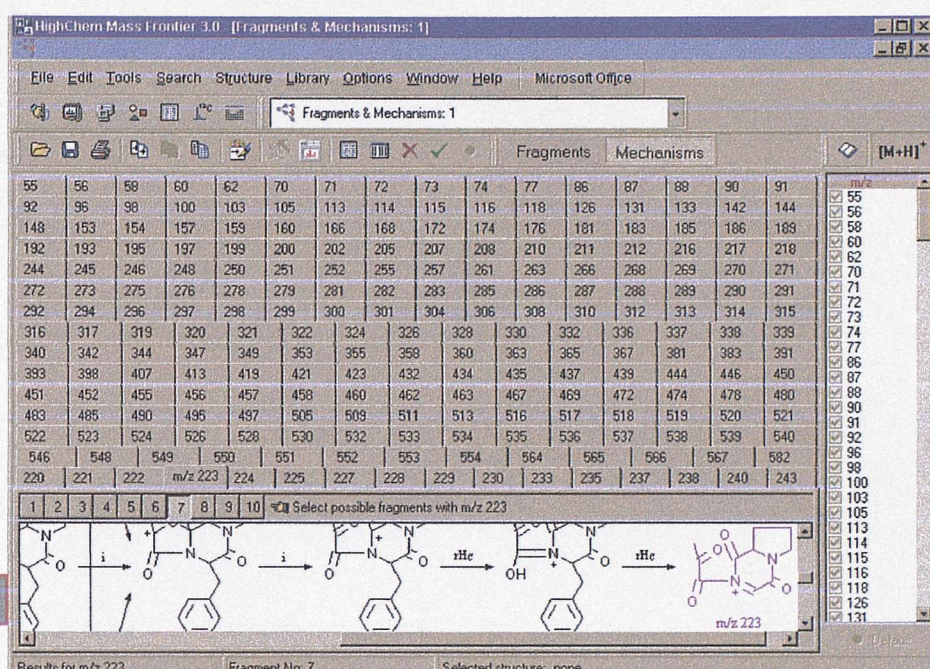


**Figure 65:** Example of the types of fragment ions and mechanisms generated by Mass Frontier to interpret the spectra of fused ring systems.

The last drawback of the method developed for the identification of unknowns from their ES-MS/MS spectra is the fact that fragmentation patterns can only be established from libraries, *i.e.* small structural variation between the compounds within a group is necessary for the formation of common fragment ions. This is demonstrated by comparison of two structurally similar sets of

compounds, the sulphonamides and the sulphonylureas, whose core structures are shown in **Figure 66**. The fragmentation pattern followed by the sulphonamides has been extensively studied and it was shown that the dominant site for dissociation in ES-MS/MS was the sulphonamide bond. (**Chapter 4**) Although sulphonylureas also contain a sulphonyl moiety in their structures, their dissociation pathway differs from that of the sulphonamides.

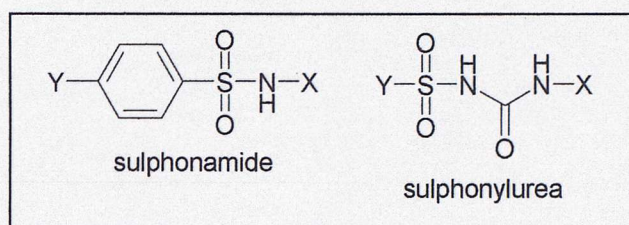


**Figure 66:** The core structures of sulphonamides and sulphonylureas.

The sulphonylureas used for this investigation are shown in **Appendix 4, Table 3**. A common fragmentation pattern is followed by all compounds. Fragment ions are observed due to cleavages around the amide bond and the  $m/z$  values observed in the spectra vary depending on the substituents X and Y.<sup>215-229</sup> The loss of  $\text{CH}_3\text{OH}$  or  $\text{CH}_3\text{CH}_2\text{OH}$  also occurs from any compounds with the corresponding ester substituents attached on the aromatic rings. *E.g.* the spectrum of metsulphuron methyl is shown in **Figure 67**.

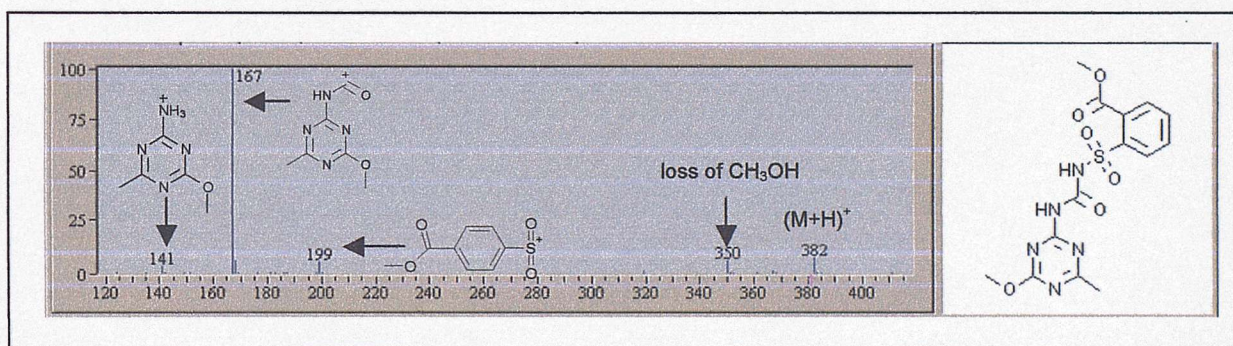


**Figure 67:** The ES-MS/MS spectrum of metsulphuron methyl.

The amide bond in the structure of sulphonylureas is the dominant functionality under ES-MS/MS conditions. Although some of the compounds produced additional compound specific ions, possibly due to the other functional groups present in the structures, these are usually of low abundance. Fragment ion prediction based on knowledge that cleavages occur around the amide bond results in identification of an estimated 80% of the fragment ions produced by this class of molecules. Ions common with the sulphonamide library were not observed. The difference in the structures of the two groups is significant enough that, under ES-MS/MS conditions different fragmentation routes are observed.

#### 5d. Conclusion

The fragmentation patterns established for the different groups of molecules using ES-MS/MS were applied to demonstrate that identification of an unknown from its ES-MS/MS spectrum is possible. The pattern of the fragment ions present in the spectrum indicates the class of the unknown, whilst the  $m/z$  values of each fragment ion can reveal the functional groups present in its structure. Classification methods currently available in AI predictive software packages enable automation of the process of class identification. Although the method described was developed using a small data set and limitations are known to exist, the results obtained suggest that this strategy has great merit and potential to aid high-throughput data interpretation.

## 6. Comparison of the Fragmentation Patterns Observed for Three Sets of Compounds on Different Trap Instruments

### 6a. Introduction

Throughout this investigation, the ES-MS/MS spectra used for the determination of the fragmentation patterns of various classes of non-peptidic molecules were always acquired on an LCQ Deca ion trap. The distinct dissociation routes established for each group led to the development of a method for the identification of unknowns based on the MS/MS spectra only. To ensure the wide applicability of the new strategy, it was important to determine that the compounds followed the same fragmentation routes under ES-MS/MS conditions on all trap systems regardless of the manufacturer. To prove this, three sets of molecules, whose fragmentation patterns were previously identified, were analysed on three trap systems other than the LCQ and the spectra acquired were compared.

### 6b. Experimental

#### Materials

- The library of sulphonylureas (**Appendix 5, Table 1**) was purchased from Qmx Laboratories Ltd, Thaxted, UK.
- The group of sulphonamides (**Appendix 5, Table 2**) was synthesised in house and used without further purification.
- The group of benzimidazoles (**Appendix 5, Table 3**) was purchased from Sigma-Aldrich, Gillingham, UK.
- Methanol, HPLC grade, was purchased from Fisher, Loughborough, UK.
- Formic acid, analytical grade 98-100%, was purchased from Sigma-Aldrich, Gillingham, UK.

#### Sample Preparation

- Solutions of all compounds analysed were prepared in methanol and 0.1% formic acid. Concentration: 10 µg/mL.

#### Instrumentation and Conditions Used

ES-MS/MS analysis of the three sets of molecules was carried out using the following instruments:

- LCQ Deca Ion Trap (Thermo Finnigan, San Jose, CA, USA)

Capillary Temperature: 200 °C, Sheath Gas Flow: 35 au, Auxiliary Gas Flow: 10 au, Source Voltage: 4.5 kV. Nitrogen was used as the sheath and the auxiliary gas and helium was the collision gas.

MS/MS parameters: Isolation Width: 1, Collision Energy: 35%.

- Esquire 3000 Plus Ion Trap (Bruker, Billerica, MA, USA)

Dry Temperature: 325 °C, Nebulizer: 25.00 psi, Dry Gas: 8 L/min, Capillary: 4 kV. Nitrogen was used as the sheath and the auxiliary gas and helium was the collision gas.

MS/MS parameters: Isolation Width: 1, Collision Energy: 35%.

- Apex III FTICRMS (Bruker, Billerica, MA, USA)

Capillary: -4.5 kV, End Plate: -3.8 kV, Capillary Exit: 102 V, Skimmer 1: 8.26 V, Skimmer 2: 7.64 V, Offset: 1.00, Rf Amplitude: 550.00 Hz, Dry Gas Temperature: 130°C. Nitrogen was used as the drying gas and argon was used as the collision gas.

MS/MS parameters: corr sweep pulse length: 1000  $\mu$ sec, corr sweep attenuation: 30.0 dB, ejection safety belt: 3000 Hz, user pulse length: 5000  $\mu$ sec, ion activation pulse length: 250000  $\mu$ sec, ion activation attenuation: 49.5 dB, frequency offset from activation mass: -500 Hz, user delay length: 3 sec.

- Q TRAP Linear Trap (MDS Sciex, Concord, ON, Canada)

Ion Spray Voltage: 5.5 kV, Curtain Gas: 20 psi, Gas 1: 10 psi, Declustering Potential: 40 V, Collision Energy: 20 eV. Nitrogen was used as the ion spray gas and the collision gas. Data were acquired using three scan modes:

- Product Ion Scan Mode: the instrument is used as a triple quadrupole MS, equivalent to the API 2000 (MDS Sciex, Concord, ON, Canada).
- Enhanced Product Ion Scan Mode: the instrument operates as a linear trap and trapping of the ions takes place in Q3.
- Enhanced Product Ion Scan Mode with Q0 Trap On: the instrument operates as a linear trap with ion trapping occurring both in Q0 and Q3.

### 6c. Theory of Operation of the Linear Trap<sup>230,231</sup>

The linear trap instrumentation is based on the triple quadrupole mass spectrometer. (**Figure 68**) Sample ions, generated in the ionisation source, travel through a curtain gas, *via* an orifice into the Q0 chamber. The Q0 chamber consists of a skimmer and a set of quadrupole rods (Q0) that can be used for ion accumulation and as an ion guide. During experiments, trapping can take place in Q0 in order to increase the concentration of the ions and enhance the sensitivity of the instrument. Confinement of the ions is achieved with the application of RF voltages to the quadrupole rods and the lens (IQ1) placed just after them. From Q0 the ions are then directed into the analyser chamber.

In the analyser chamber, the role of the first quadrupole (Q1) depends upon the types of experiments carried out. For single MS experiments, Q1 acts as an ion guide only and transmits ions to Q2 and Q3. During tandem MS experiments, Q1 is used for the selection of the precursor ion of interest. RF and direct current (DC) voltages are applied to the rods in order to allow only the ion of the desired  $m/z$  value to pass through the quadrupole. The isolated precursor ion enters then the collision cell, Q2, which is an enclosed linear quadrupole rod array, filled with nitrogen gas used for Collision Induced Dissociation (CID). The ion can enter and exit the cell through small orifices in the centre of the lenses IQ1 and IQ2, which are situated approximately 2 mm from the Q2 rods. For single MS experiments, Q2 is used in the same manner as Q1, for the transmission of the ions to Q3. For MS/MS, the collision cell is the area, where the fragmentation of the ions occurs. The fragment ions formed by CID or the ions guided through the different components of

the instrument during single MS experiments, finally enter the third quadrupole Q3, which is used as the linear trap.

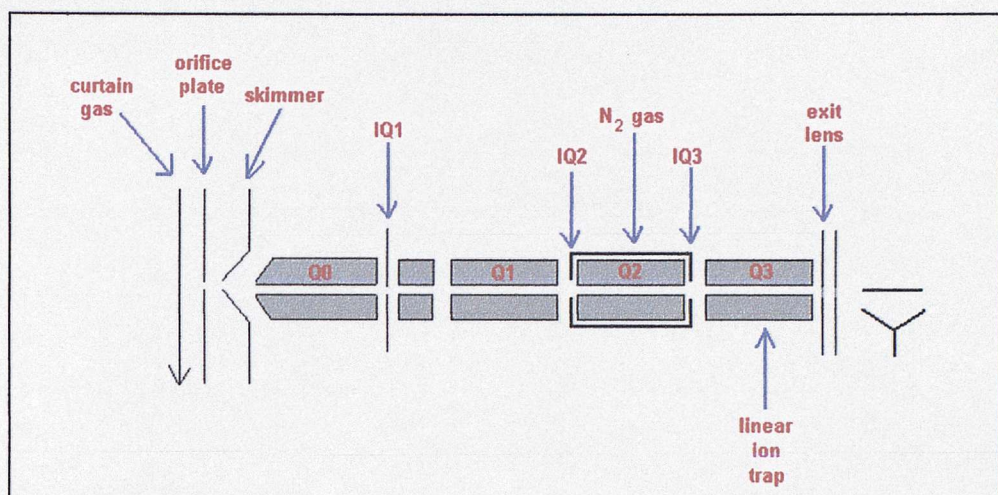


**Figure 68:** Schematic representation of the linear trap.

Trapping in the linear trap is achieved using the Q3 quadrupole rods and the lenses IQ3 and exit lens. **(Figure 69)** When RF voltages are applied on the rods, the ions become trapped in the radial direction. In addition, the application of alternating current (AC) to the lenses causes axial trapping of the ions to take place. As a result, the ions oscillate in the radial and axial directions and because the frequency of the axial motion is much higher than the frequency of the radial one, they eventually arrange themselves in a linear string. The ions finally exit Q3 via a grid placed in the centre of the exit lens, they pass through a final lens and are detected with the use of an electron multiplier.

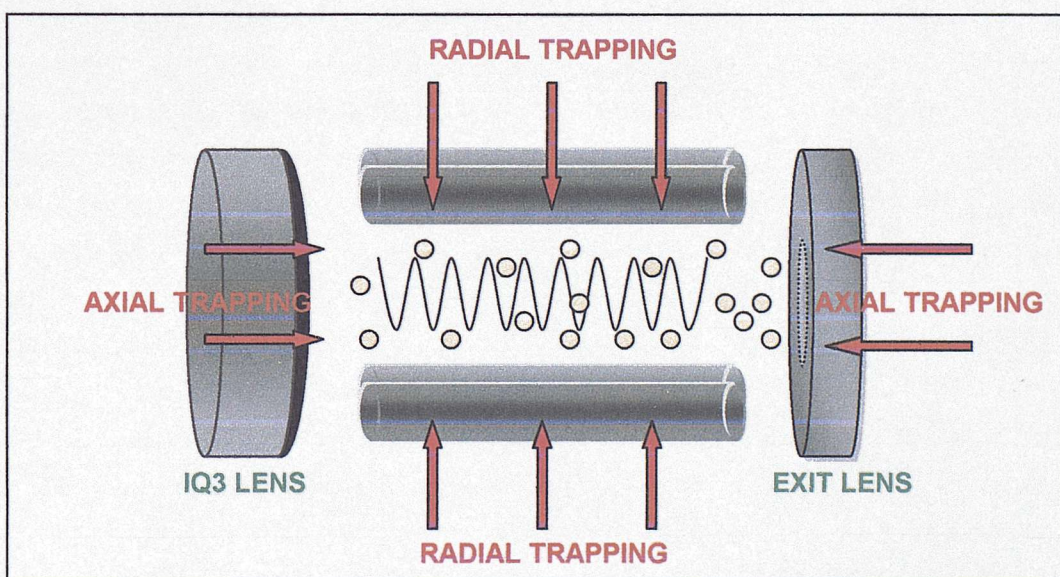


**Figure 69:** Axial and radial trapping of the ions in the linear trap.

## 6d. Results and Discussion

ES-MS/MS spectra were obtained for the sulphonamides, sulphonylureas and benzimidazoles on each of the trap instruments. The main fragment ions and neutral losses formed in every instrument for each group were identified and the spectra were compared with those obtained on the LCQ.

There were no significant differences in the results from the LCQ and the Esquire. The same prominent fragment ions were observed and the same fragmentation patterns were established using either trap. This was also the case for the FTICRMS data. Differences in the three sets of spectra were only observed with respect to the abundances of the fragment ions. Generally, fragment ions of low intensity formed in the LCQ did not appear in the Esquire and the FTMS under the conditions used. Variations as such were expected, since the conditions employed for analysis on each instrument were not optimised for each set of molecules. **Figures 1, 2 and 3 in Appendix 5** provide an example of the type of spectra obtained on the trap instruments discussed, for the three groups of compounds.

Three sets of data were also obtained from the Q Trap for each class of molecules. MS/MS spectra were acquired using the instrument as a triple quadrupole, as a linear trap and finally as a linear trap with concurrent trapping at Q0 and Q3 for enhanced sensitivity of the system. An initial comparison was carried out between the spectra obtained using the three different scan modes. The triple quadrupole fragmentation patterns were maintained when the system was used as a linear trap, but sharper ion profiles and better mass accuracy than on the triple quadrupole analyser were observed. Trapping in Q0 to increase the ion concentration, did not cause significant changes in the spectra. The ES-MS/MS spectra acquired for a methyl-sulphonamide using the three different scan modes performed on the Q Trap are shown in **Figure 70**.

A final comparison was carried out between the fragmentation patterns established for the three groups of compounds on the linear trap and those observed on the conventional trap instruments. The main difference detected was the fact, that more fragment ions were present in the spectra obtained from the linear trap. This is due to two reasons. In the linear trap, the triple quadrupole fragmentation patterns are maintained. This involves the ions undergoing multiple collisions, which means that as soon as they are formed, are reactivated by collision with the neutral gas molecules and can fragment further, resulting in additional fragment ions to be formed.<sup>70</sup> In the spherical trap only the isolated precursor ion is excited using the appropriate voltages and fragmented. The product ions are usually too cool to fragment further. In addition, in conventional quadrupole traps only ions with a mass of 70% below the precursor ion can be stabilised in the trap and subsequently detected. As a result, spectra with many fragment ions, especially in the low mass region, were obtained for the three sets of molecules studied only from the linear trap. This does not imply that the fragmentation patterns previously established on the conventional traps were completely changed. The same fragment ions and neutral mass losses as before were observed, but new fragment ions also appeared. *E.g.* the spectra of some of the compounds analysed on the LCQ and the Q Trap, with concurrent trapping in Q3 and Q0, are shown in **Appendix 5, Figures 4, 5 and 6**.

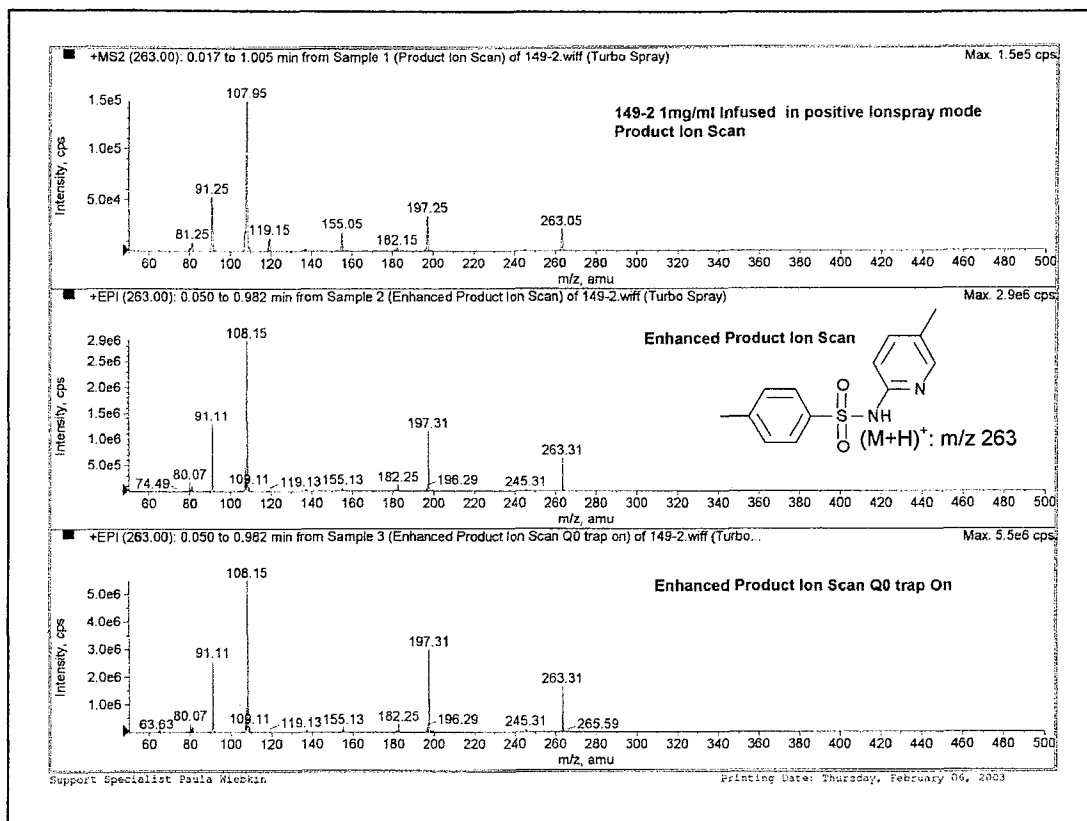


**Figure 70:** The ES-MS/MS spectra of a methyl-sulphonamide obtained on the Q Trap using three different scan modes.

The presence of additional fragment ions in the spectra acquired on the linear trap can be an advantage when ES-MS/MS is used with the aim of structure elucidation. As described in **Chapter 5**, classification using PCA can be applied for automatic identification of the class of an unknown compound. According to PCA, the position of a spectrum in the  $n$ -dimensional space depends upon the  $m/z$  values present in the spectrum and their intensities. A spectrum becomes better defined, when the number of co-ordinates specifying its place increases, *i.e.* the number of fragment ions increases. Spectra from the various classes of compounds acquired on the linear trap, when classified by PCA should result in the formation of well-spaced clusters. This would assist in efficient substructure identification of unknowns and could overcome problems sometimes encountered with spectra obtained from conventional traps, containing only a few fragment ions. The drawback of large numbers of fragment ions is the time that must be invested for fragment ion identification and structure assignment. Pattern recognition can become difficult due to the increased complexity of the spectra.

## 6e. Conclusion

It was proven that the ES-MS/MS fragmentation patterns established for the various classes of non-peptidic compounds on the Thermo Finnigan LCQ ion trap are reproducible in most trap instruments regardless of their design. This implies that the two-step method developed for the identification of unknowns from their ES-MS/MS spectra can be widely applied to spectra acquired

on most trap systems. Spectra obtained from the linear trap can also be used for the identification of unknowns but the process of establishing an initial dissociation pathway can be time-consuming, due to the increased number of fragment ions observed.

## 7. Conclusion and Further Applications

During the investigation into the dissociation processes of non-peptidic molecules under ES-MS/MS conditions, a total of approximately 300 spectra were studied. A distinct dissociation pathway was identified for each different class and it was shown that fragmentation by ES-MS/MS is indeed structure dependant. An additional observation was that certain functional groups have a greater influence on the fragmentation processes, allowing a hierarchy of influence to be determined. Based on this, the following statements can be made:

- Molecules with aliphatic substituents usually fragment by straightforward bond cleavage, while cyclic compounds favour rearrangements.
- Functionalisation of aliphatic chains, e.g. the addition of hydroxyl or carbonyl substituents, results in fragmentation *via* rearrangement processes.
- Amines and in particular quaternary amines are easily cleaved and when present in the structure the corresponding loss is often observed.
- When molecules contain amino acid functionalities, the loss of 46 Da is usually observed. When the acid functionality is protected, the protected group is cleaved first, followed by the loss of the acid group.
- The presence of the sulphone and the cyano moieties in the structure causes rearrangements to occur.
- Heterocycles are usually unstable and many fragment ions are formed due to fragmentation taking place at the heterocyclic ring. In contrast to this, aromatic rings are very stable and remain intact under ES-MS/MS conditions.
- The presence of substituents on aromatic rings such as hydroxyl groups and halogens does not appear to have any influence on the dissociation of the molecules.
- Hydrogen rearrangements generally involve only exchangeable hydrogens.

These observations show that non-peptidic molecules follow general trends when analysed by ES-MS/MS and therefore fast spectral prediction and interpretation is possible.

General trends were also observed with respect to the mechanisms that take place for the formation of fragment ions. The studies carried out on various groups showed that mechanisms can be postulated for classes of molecules and that they are not compound specific. The mechanisms leading to the formation of fragment ions for different types of compounds under EI conditions have been explored<sup>49-51</sup> and are already used by AI packages for fragment ion prediction. Similar studies can now be carried out for the mechanisms involved in ES-MS/MS. The identified mechanistic routes can eventually be applied towards fragment ion generation for non-peptidic molecules by applications, such as Mass Frontier.

The success rate of fragment ion prediction could be further increased, if data obtained from *ab initio* calculations were employed. The studies carried out on the library of sulphonamides showed that, molecular modelling can assist in recognising the driving forces that lead to dissociation. The primary sites of ionisation can be identified. Then the differences in bond lengths before and after protonation can reveal the sites of the molecules more likely to be cleaved. Steric effects resulting in the elimination of fractions of the compounds can also be explored. The combination of

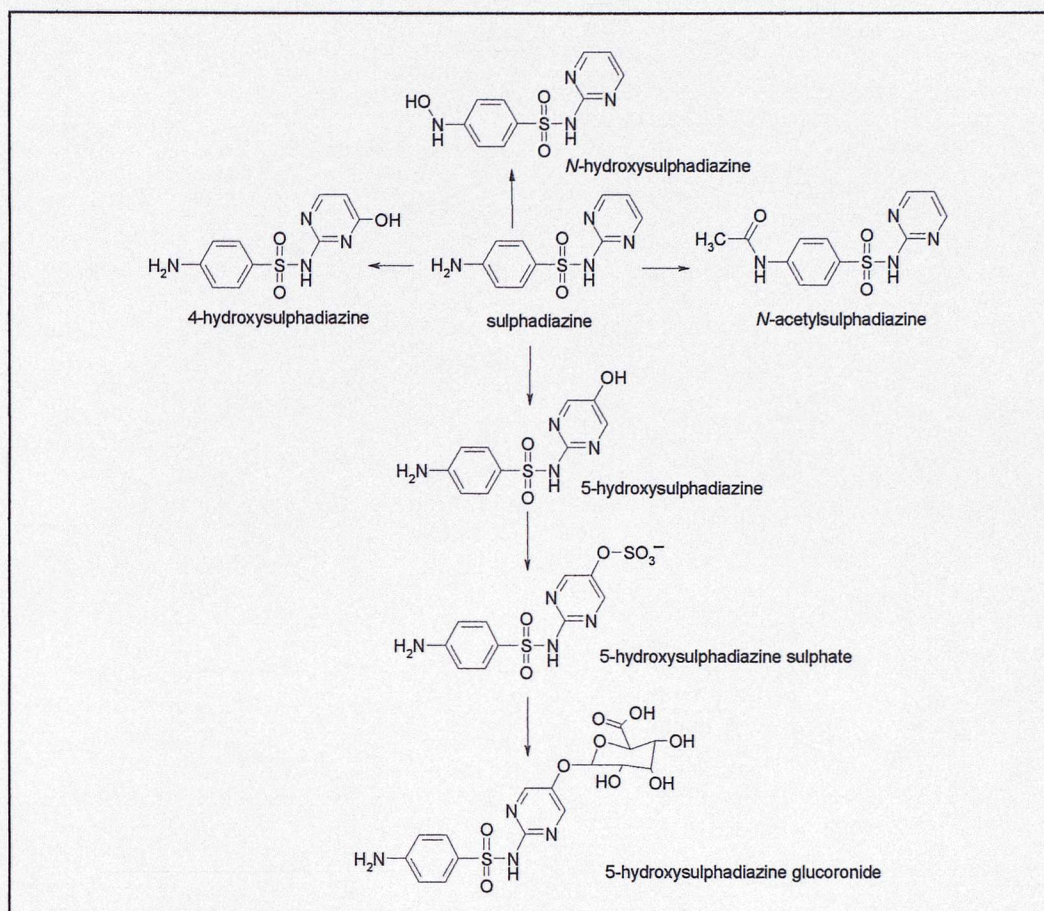
molecular modelling applications with software packages that are used for mass spectra interpretation will result in a powerful tool that will aid the fragment ion prediction under ES-MS/MS conditions.

The key in improving software packages like Mass Frontier is to combine expertise in the areas of mass spectrometry, artificial intelligence and molecular modelling. The potential for improvement has been demonstrated and a method for the identification of unknowns has been developed. Incorporation of the information gained regarding the dominant functionalities in ES-MS/MS, the fragmentation patterns established and the mechanisms involved in fragment ion formation should improve the fragment ion prediction modes of the AI packages. With the input from experts in AI systems, algorithms leading to automation of both steps of the method developed could be produced. Also more powerful pattern recognition techniques, such as Neural Networks, could be explored. Such improvements would allow application of the new strategy towards the classification of corporate libraries from pharmaceutical companies. These would provide an enormous range of chemical structures to be processed in minimum time, allowing identification of any type of unknown. Eventually, automated interpretation of ES-MS/MS spectra of non-peptidic molecules will become possible and the automatic characterisation of the components of non-peptidic, pharmaceutical, combinatorial libraries using ES-MS/MS could eventually become a routine application.

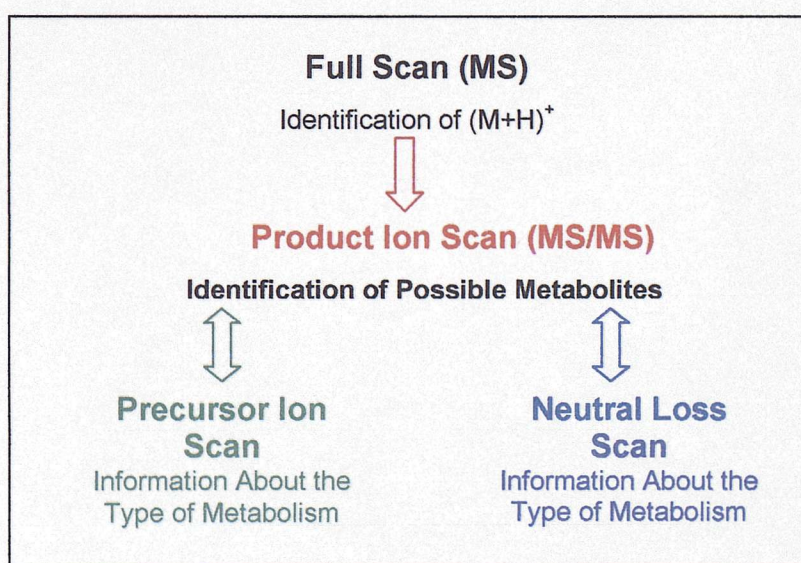
This new strategy for structure characterisation is not limited to the field of combinatorial chemistry only, but could also be applied for the identification of drug metabolites. The efficacy of a drug, the duration of its action and its toxicity are critically dependant upon the drug's metabolic pathway in the body. The study of drug metabolism plays a key role in the drug discovery process and structure elucidation of metabolites provides vital information that guides selection and drug optimisation of drug candidates.<sup>21,232</sup> Typically, metabolism tends to be an alteration to the drug molecule that results in a more polar chemical structure and the difference between the parent drug and the metabolite is usually one functional group. *E.g.* the known metabolites of one of the sulphonamides studied, sulphadiazine, are shown in **Figure 71**.<sup>233</sup>

Detection and identification of metabolites is routinely carried out using LC-MS/MS and the general methodology is shown schematically in **Figure 72**. A full scan mass spectrum displays all masses detected over the desired mass range. The ions of interest are then dissociated to give the MS/MS spectrum and structural information about the compounds detected in the simple MS experiment is obtained from the resulting fragment ions. The fragment ions of a metabolite should either resemble those of the original parent drug or differ by the mass of the metabolic modification. The type of modification can be elucidated using the mass differences in the fragment ions observed. Additional information can be obtained using precursor ion scans. In this case, a characteristic product ion is specified and all precursor ions that dissociate to form this product ion are monitored. In this manner, all possible metabolites that might produce the same ion can be identified. Finally, neutral loss scans can also be carried out. These are similar to the precursor ion scans, except that a characteristic neutral mass loss is selected rather than a

product ion. Certain metabolites, such as sulphates, give characteristic neutral losses when fragmented and therefore detection becomes easier when this type of scan is employed.<sup>35,234-236</sup>



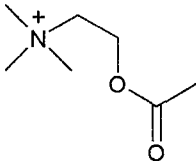
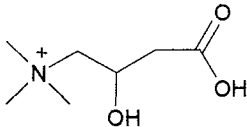
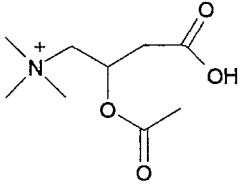
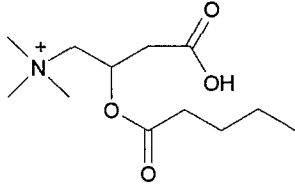
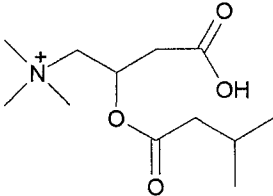
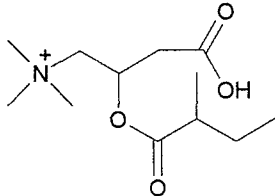
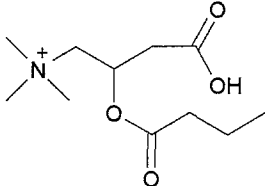
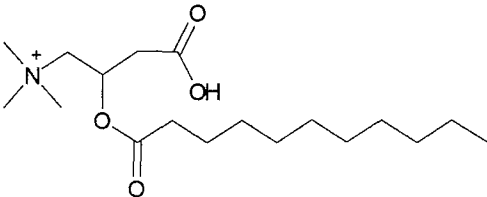
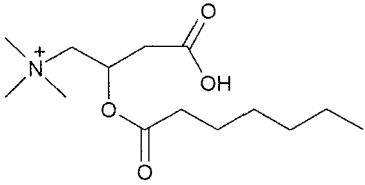
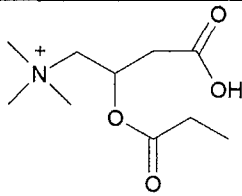
**Figure 71:** The known metabolites of sulphadiazine.<sup>233</sup>

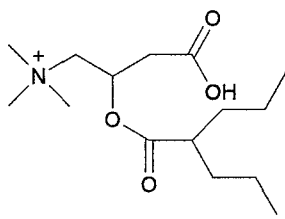
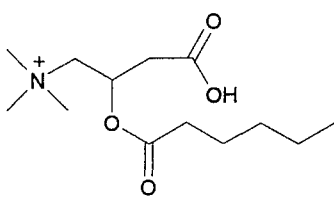


**Figure 72:** General strategy for the use of MS/MS for the detection and identification of metabolites.<sup>234</sup>

Data interpretation is usually the largest bottleneck in metabolite identification.<sup>236</sup> Physical handling of the MS/MS spectra by expert analysts is required for the same reasons as in the case of MS/MS spectra from combinatorial libraries. Existing software packages perform certain functions that accelerate spectra processing, such as isotope cluster analysis for Cl or Br containing compounds, but complete spectra interpretation and structure assignment of metabolites is not possible when ES-MS/MS is used. Software packages that can reduce operator workload by using a series of criteria to analyse data and report apparent metabolites will significantly improve throughput in metabolite identification. Evolution of existing programmes can be achieved using the findings of this investigation in the same way as proposed for the combinatorial libraries. By applying general trends for the dissociation of molecules under ES-MS/MS, together with an automated strategy for structure elucidation of unknowns, the metabolites of drugs will be identified efficiently and in a short amount of time. This approach will accelerate the process of metabolite identification and will make it amenable to the high-throughput needs of the drug discovery process, in the same way as for non-peptidic combinatorial compounds.

## Appendix 1

 <p>2-Acetyloxy-<i>N,N,N</i>-trimethyl-ethanaminium (Acetylcholine) RMM: 146 <math>C_7H_{16}NO_2^+</math></p>	 <p>3-Carboxy-2-hydroxy-<i>N,N,N</i>-trimethyl-1-propanaminium (Carnitine) RMM: 162 <math>C_7H_{16}NO_3^+</math></p>
 <p>2-Acetyloxy-3-carboxy-<i>N,N,N</i>-trimethyl-1-propanaminium (Acetylcarnitine) RMM: 204 <math>C_9H_{18}NO_4^+</math></p>	 <p>3-Carboxy-<i>N,N,N</i>-trimethyl-2-[(1-oxopentyl)oxy]-1-propanaminium (Valerylcarnitine) RMM: 246 <math>C_{12}H_{24}NO_4^+</math></p>
 <p>3-Carboxy-<i>N,N,N</i>-trimethyl-(3-methyl-1-oxobutoxy)-1-propanaminium (Isovalerylcarnitine) RMM: 246 <math>C_{12}H_{24}NO_4^+</math></p>	 <p>3-Carboxy-<i>N,N,N</i>-trimethyl-2-(2-methyl-1-oxobutoxy)-1-propanaminium (2-Methylbutyrylcarnitine) RMM: 246 <math>C_{12}H_{24}NO_4^+</math></p>
 <p>3-Carboxy-<i>N,N,N</i>-trimethyl-2-(1-oxobutoxy)-1-propanaminium (Butyrylcarnitine) RMM: 232 <math>C_{11}H_{22}NO_4^+</math></p>	 <p>3-Carboxy-<i>N,N,N</i>-trimethyl-2-[(1-oxoundecyl)oxy]-1-propanaminium (Undecylcarnitine) RMM: 330 <math>C_{18}H_{36}NO_4^+</math></p>
 <p>3-Carboxy-<i>N,N,N</i>-trimethyl-2-[(1-oxoheptyloxy)]-1-propanaminium (Heptanoylcarnitine) RMM: 274 <math>C_{14}H_{28}NO_4^+</math></p>	 <p>3-Carboxy-<i>N,N,N</i>-trimethyl-2-[(1-oxopropoxy)]-1-propanaminium (Propionylcarnitine) RMM: 218 <math>C_{10}H_{20}NO_4^+</math></p>

 <p>3-Carboxy-<i>N,N,N</i>-trimethyl- 2-[(1-oxo-2-propylpentyl)oxy]-1-propanaminium (Valpropylcarnitine) RMM: 288 <math>C_{15}H_{30}NO_4^+</math></p>	 <p>3-Carboxy-<i>N,N,N</i>-trimethyl-2- [(1-oxohexyl)oxy]-1-propanaminium (Hexanoylcarnitine) RMM: 260 <math>C_{13}H_{26}NO_4^+</math></p>
--	--

**Table 1:** The structures of the carnitines studied.

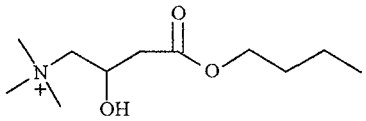
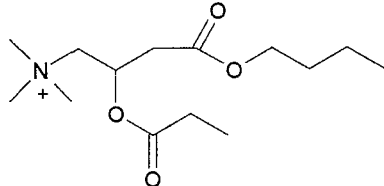
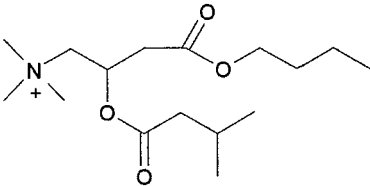
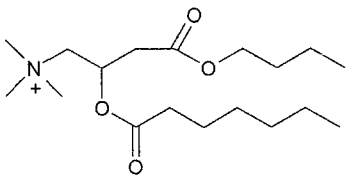
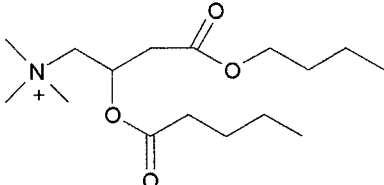
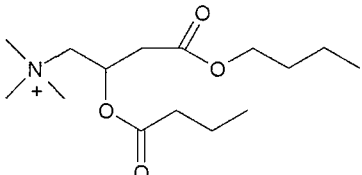
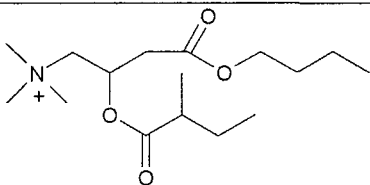
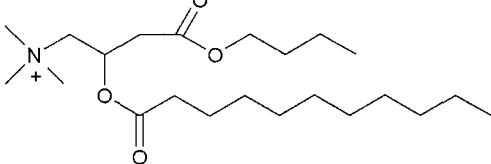
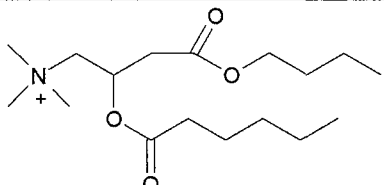
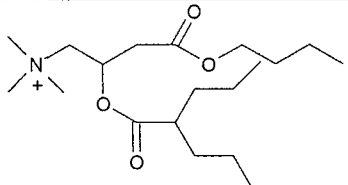
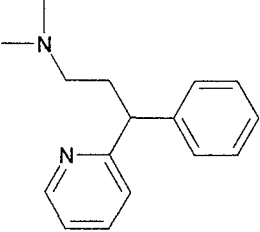
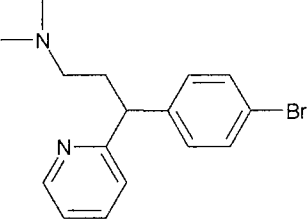
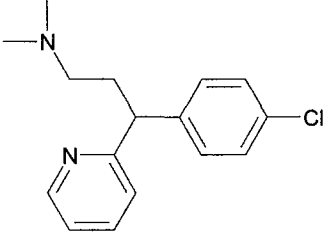
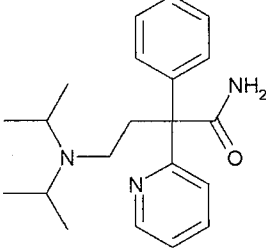
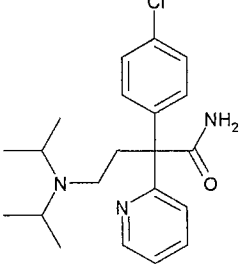
 <p>4-Butoxy-2-hydroxy-<i>N,N,N</i>-trimethyl-4-oxo-1-butaniminium (Carnitine butyl ester) RMM: 146 <math>C_7H_{16}NO_2^+</math></p>	 <p>4-Butoxy-<i>N,N,N</i>-trimethyl-2-(1-oxopropoxy)-4-oxo-1-butaniminium (Propionylcarnitine butyl ester) RMM: 274 <math>C_{14}H_{28}NO_4^+</math></p>
 <p>4-Butoxy-<i>N,N,N</i>-trimethyl-2-(3-methyl-1-oxobutoxy)-4-oxo-1-butaniminium (Isovalerylcarnitine butyl ester) RMM: 302 <math>C_{16}H_{32}NO_4^+</math></p>	 <p>4-Butoxy-<i>N,N,N</i>-trimethyl-2-[(1-oxoheptyloxy)]-4-oxo-1-butaniminium (Heptanoylcarnitine butyl ester) RMM: 330 <math>C_{18}H_{36}NO_4^+</math></p>
 <p>4-Butoxy-<i>N,N,N</i>-trimethyl-2-[(1-oxopentyl)oxy]-4-oxo-1-butaniminium (Valerylcarnitine butyl ester) RMM: 302 <math>C_{16}H_{32}NO_4^+</math></p>	 <p>4-Butoxy-<i>N,N,N</i>-trimethyl-2-(1-oxobutoxy)-4-oxo-1-butaniminium (Butyrylcarnitine butyl ester) RMM: 288 <math>C_{15}H_{30}NO_4^+</math></p>
 <p>4-Butoxy-<i>N,N,N</i>-trimethyl-2-[2-methyl-1-oxobutoxy]-4-oxo-1-butaniminium (2-Methylbutyrylcarnitine butyl ester) RMM: 302 <math>C_{16}H_{32}NO_4^+</math></p>	 <p>4-Butoxy-<i>N,N,N</i>-trimethyl-2-[(1-oxoundecyl)oxy]-4-oxo-1-butaniminium (Undecylcarnitine butyl ester) RMM: 386 <math>C_{22}H_{44}NO_4^+</math></p>
 <p>4-Butoxy-<i>N,N,N</i>-trimethyl-2-[(1-oxohexyl)oxy]-4-oxo-1-butaniminium (Hexanoylcarnitine butyl ester) RMM: 316 <math>C_{17}H_{34}NO_4^+</math></p>	 <p>4-Butoxy-<i>N,N,N</i>-trimethyl-2-[(1-oxo-2-propylpentyl)oxy]-4-oxo-1-butaniminium (Valpropylcarnitine butyl ester) RMM: 344 <math>C_{19}H_{38}NO_4^+</math></p>

Table 2: The structures of the carnitine butyl esters studied.

 <p><i>N,N</i>-Dimethyl-<math>\gamma</math>-phenyl-2-pyridinepropanamine (Pheniramine) RMM: 240 <math>C_{16}H_{20}N_2</math></p>	 <p><math>\gamma</math>-(4-Bromophenyl)-<i>N,N</i>-dimethyl-2-pyridinepropanamine (Brompheniramine) RMM: 318 <math>C_{16}H_{19}N_2Br</math></p>
 <p><math>\gamma</math>-(4-Chlorophenyl)-<i>N,N</i>-dimethyl-2-pyridinepropanamine (Chlorpheniramine) RMM: 274 <math>C_{16}H_{19}N_2Cl</math></p>	 <p><math>\alpha</math>-[2-Bis(1-methylethyl)amino]ethyl]-<math>\alpha</math>-phenyl-2-pyridineacetamide (Disopyramide) RMM: 339 <math>C_{21}H_{29}N_3O</math></p>
 <p><math>\alpha</math>-[2-Bis(1-methylethyl)amino]ethyl]-<math>\alpha</math>-(4-chlorophenyl)-2-pyridineacetamide (<i>p</i>-Chlorodisopyramide) RMM: 373 <math>C_{21}H_{28}N_3OCl</math></p>	

**Table 3:** The structures of the pheniramines and disopyramides studied.

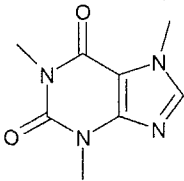
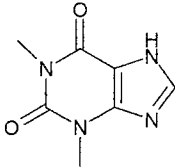
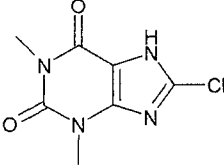
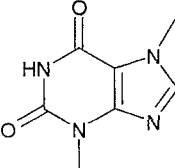
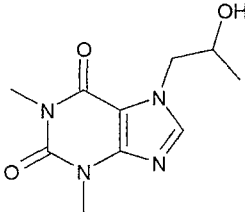
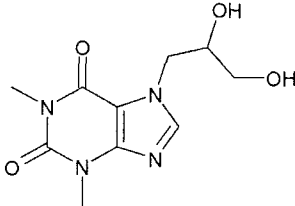
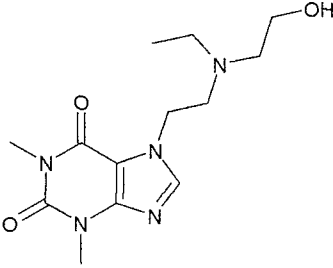
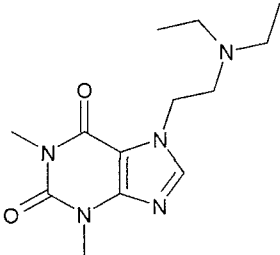
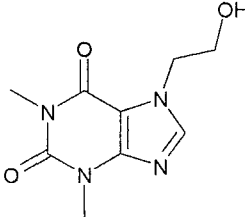
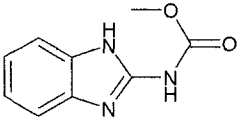
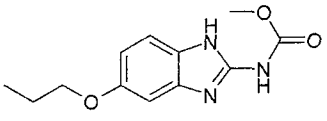
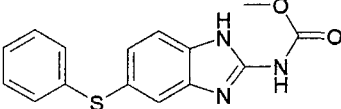
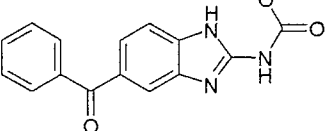
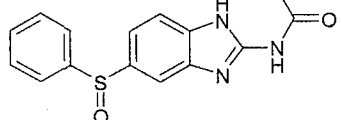
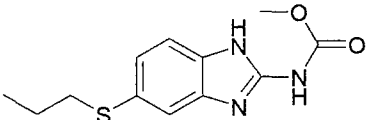
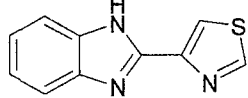
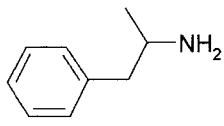
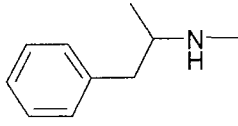
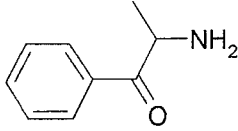
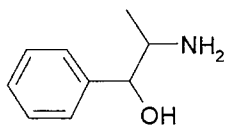
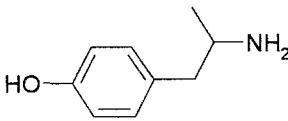
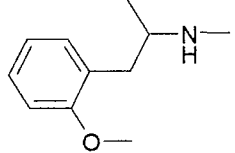
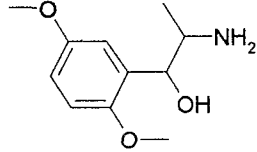
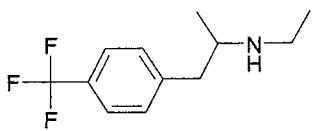
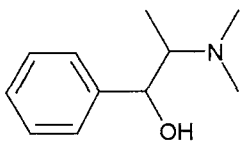
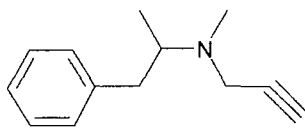
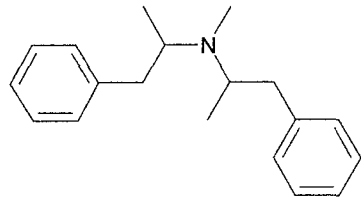
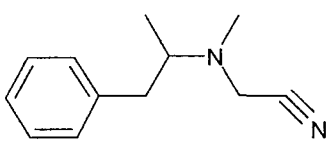
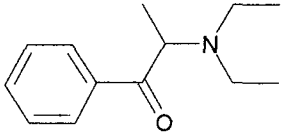
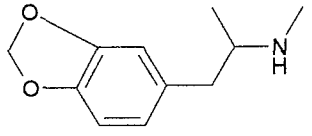
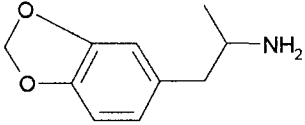
 <p>3,7-Dihydro-1,3,7-trimethyl-1H-purine-2,6-dione (Caffeine) RMM: 194 <math>C_8H_{10}N_4O_2</math></p>	 <p>3,7-Dihydro-1,3-dimethyl-1H-purine-2,6-dione (Aminophylline) RMM: 180 <math>C_7H_8N_4O_2</math></p>
 <p>8-Chloro-3,7-dihydro-1,3-dimethyl-1H-purine-2,6-dione (8-Chlorotheophylline) RMM: 214 <math>C_7H_7N_4O_2Cl</math></p>	 <p>3,7-Dihydro-3,7-dimethyl-1H-purine-2,6-dione (Theobromine) RMM: 180 <math>C_7H_8N_4O_2</math></p>
 <p>3,7-Dihydro-7-(2-hydroxypropyl)-1,3-dimethyl-1H-purine-2,6-dione (Proxyphylline) RMM: 238 <math>C_{10}H_{14}N_4O_3</math></p>	 <p>7-(2,3-Dihydroxypropyl)-3,7-dihydro-1,3-dimethyl-1H-purine-2,6-dione (Diprophylline) RMM: 254 <math>C_{10}H_{14}N_4O_4</math></p>
 <p>7-[2-Ethyl(2-hydroxyethyl) amino]ethyl]-3,7-dihydro-1,3-dimethyl-8-(phenylmethyl)-1H-purine-2,6-dione (Bamiphylline) RMM: 385 <math>C_{20}H_{27}N_5O_3</math></p>	 <p>7-[2-Diethylamino]ethyl]-3,7-dihydro-1,3-dimethyl-1H-purine-2,6-dione (Etamiphylline) RMM: 279 <math>C_{13}H_{21}N_5O_2</math></p>
 <p>3,7-Dihydro-7-(2-hydroxyethyl)-1,3-dimethyl-1H-purine-2,6-dione (Etophylline) RMM: 224 <math>C_9H_{10}N_4O_3</math></p>	

Table 4: The structures of the purines studied.

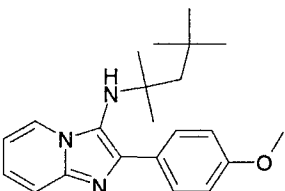
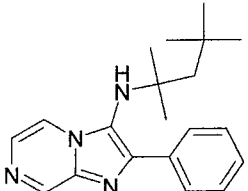
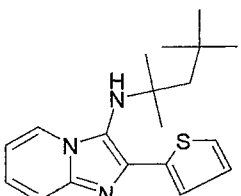
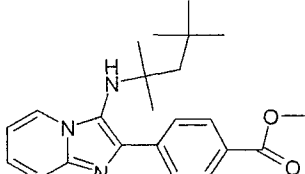
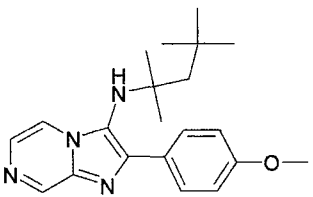
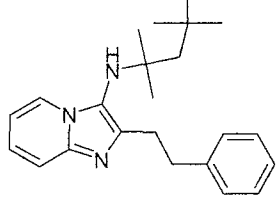
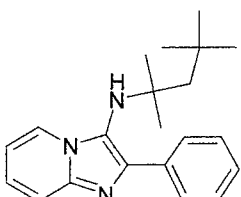
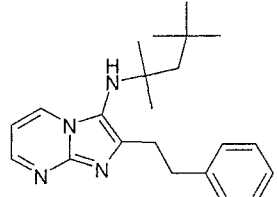
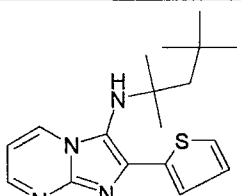
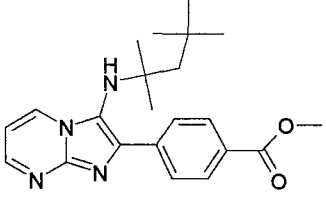
 <p>1H-Benzimidazol-2-yl-carbamic acid methyl ester (Carbendazim) RMM: 191 <math>C_9H_9N_3O_2</math></p>	 <p>(5-Propoxy-1H-benzimidazol-2-yl)-carbamic acid methyl ester (Oxibendazole) RMM: 249 <math>C_{12}H_{15}N_3O_3</math></p>
 <p>[(5-Phenylthio)-1H-benzimidazol-2-yl]-carbamic acid methyl ester (Fenbendazole) RMM: 299 <math>C_{15}H_{13}N_3O_2S</math></p>	 <p>(5-Benzoyl-1H-benzimidazol-2-yl)-carbamic acid methyl ester (Mebendazole) RMM: 295 <math>C_{16}H_{13}N_3O_3</math></p>
 <p>(5-Phenylsulphonyl-1H-benzimidazol-2-yl)- carbamic acid methyl ester (Oxfendazole) RMM: 315 <math>C_{15}H_{13}N_3O_3S</math></p>	 <p>(5-Propylthio-1H-benzimidazol-2-yl)-carbamic acid methyl ester (Albendazole) RMM: 265 <math>C_{12}H_{15}N_3O_2S</math></p>
 <p>2-(4-Thiazolyl)-1H-benzimidazole (Thiabendazole) RMM: 201 <math>C_{10}H_7N_3S</math></p>	

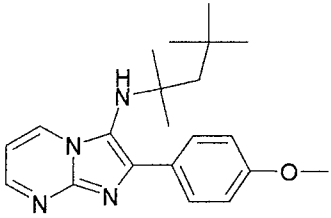
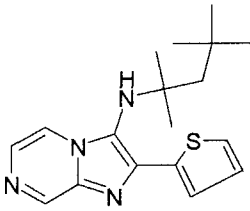
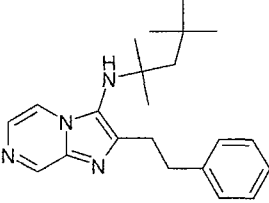
**Table 5:** The structures of the benzimidazoles studied.

 <p><b>α-Methyl-benzeneethanamine</b> (Amphetamine) <u>RMM:</u> 135 C<sub>9</sub>H<sub>13</sub>N</p>	 <p><b>N-α-Dimethyl-benzeneethanamine</b> (Methamphetamine) <u>RMM:</u> 149 C<sub>10</sub>H<sub>15</sub>N</p>
 <p><b>2-Amino-1-phenyl-1-propanone</b> (Cathinone) <u>RMM:</u> 149 C<sub>9</sub>H<sub>11</sub>NO</p>	 <p><b>α-(1-Aminoethyl)-benzenemethanol</b> (Phenylpropanolamine) <u>RMM:</u> 151 C<sub>9</sub>H<sub>13</sub>NO</p>
 <p><b>4-(2-Aminopropyl)-phenol</b> (Paredrine) <u>RMM:</u> 151 C<sub>9</sub>H<sub>13</sub>NO</p>	 <p><b>2-Methoxy-N,α-dimethyl-benzeneethanamine</b> (Methoxyphenamine) <u>RMM:</u> 179 C<sub>11</sub>H<sub>17</sub>NO</p>
 <p><b>α-(1-Aminoethyl)-2,5-dimethoxy-benzenemethanol</b> (Methoxamine) <u>RMM:</u> 211 C<sub>11</sub>H<sub>17</sub>NO<sub>3</sub></p>	 <p><b>N-Ethyl-α-methyl-3-(trifluoromethyl)-benzeneethanamine</b> (Fenfluramine) <u>RMM:</u> 231 C<sub>12</sub>H<sub>16</sub>NF<sub>3</sub></p>
 <p><b>α-[(1-Dimethylamino)ethyl]-benzenemethanol</b> (N-Methyl-Pseudoephedrine) <u>RMM:</u> 179 C<sub>11</sub>H<sub>17</sub>NO</p>	 <p><b>N-α-Dimethyl-N-2-propynyl-benzeneethanamine</b> (Deprenyl) <u>RMM:</u> 187 C<sub>13</sub>H<sub>17</sub>N</p>
 <p><b>N-α-Dimethyl-N-(phenylmethyl)-benzeneethanamine</b> (Benzphetamine) <u>RMM:</u> 267 C<sub>17</sub>H<sub>21</sub>N</p>	 <p><b>[Methyl(1-methyl-2-phenylethyl)amino]-acetonitrile</b> <u>RMM:</u> 188 C<sub>12</sub>H<sub>16</sub>N<sub>2</sub></p>

 <p>2-(Diethylamino)-1-phenyl-1-propanone (Diethylpropion) RMM: 205 C<sub>13</sub>H<sub>19</sub>NO</p>	 <p><i>N</i>-<math>\alpha</math>-Dimethyl-1,3-benzodioxole-5-ethanamine (MDMA) RMM: 193 C<sub>11</sub>H<sub>15</sub>NO<sub>2</sub></p>
 <p><math>\alpha</math>-Methyl-1,3-benzodioxole-5-ethanamine (MDA) RMM: 179 C<sub>10</sub>H<sub>13</sub>NO<sub>2</sub></p>	

**Table 6:** The structures of the amphetamines studied.

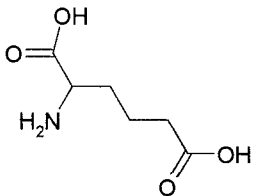
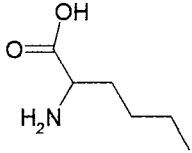
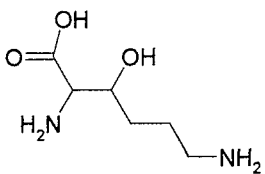
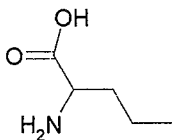
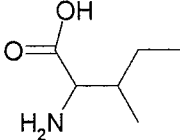
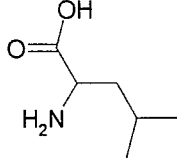
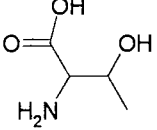
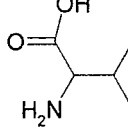
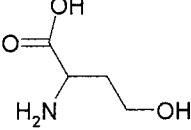
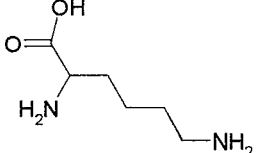
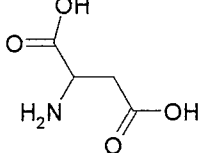
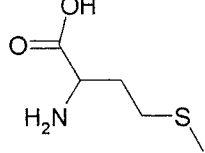
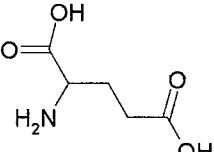
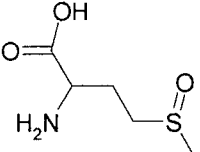
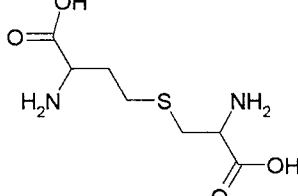
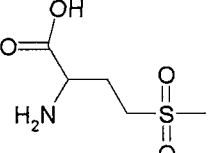
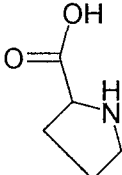
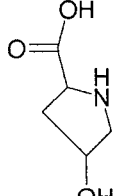
 <p>2-(4-Methoxyphenyl)-<i>N</i>-(1,1,3,3-tetramethylbutyl)imidazo[1,2-<math>\alpha</math>]-pyridin-3-amine  <u>RMM:</u> 351  <math>C_{22}H_{29}N_3O</math></p>	 <p>2-Phenyl-<i>N</i>-(1,1,3,3-tetramethylbutyl)imidazo[1,2-<math>\alpha</math>]-pyrazin-3-amine  <u>RMM:</u> 322  <math>C_{20}H_{26}N_4</math></p>
 <p><i>N</i>-(1,1,3,3-Tetramethylbutyl)-2-(2-thienyl)imidazo[1,2-<math>\alpha</math>]-pyridin-3-amine  <u>RMM:</u> 327  <math>C_{19}H_{25}N_3S</math></p>	 <p>4-{3-[(1,1,3,3-Tetramethylbutyl)amino]imidazo[1,2-<math>\alpha</math>]-pyridin-2-yl}-benzoate  <u>RMM:</u> 379  <math>C_{23}H_{29}N_3O_2</math></p>
 <p>2-(4-Methoxyphenyl)-<i>N</i>-(1,1,3,3-tetramethylbutyl)imidazo[1,2-<math>\alpha</math>]-pyrazin-3-amine  <u>RMM:</u> 352  <math>C_{21}H_{28}N_4O</math></p>	 <p>2-(2-Phenylethyl)-<i>N</i>-(1,1,3,3-tetramethylbutyl)imidazo[1,2-<math>\alpha</math>]-pyridin-3-amine  <u>RMM:</u> 349  <math>C_{23}H_{31}N_3</math></p>
 <p>2-Phenyl-<i>N</i>-(1,1,3,3-tetramethylbutyl)imidazo[1,2-<math>\alpha</math>]-pyridin-3-amine  <u>RMM:</u> 321  <math>C_{21}H_{27}N_3</math></p>	 <p>2-(2-Phenylethyl)-<i>N</i>-(1,1,3,3-tetramethylbutyl)imidazo[1,2-<math>\alpha</math>]-pyrimidin-3-amine  <u>RMM:</u> 350  <math>C_{22}H_{30}N_4</math></p>
 <p><i>N</i>-(1,1,3,3-Tetramethylbutyl)-2-(2-thienyl)imidazo[1,2-<math>\alpha</math>]-pyrimidin-3-amine  <u>RMM:</u> 328  <math>C_{18}H_{24}N_4S</math></p>	 <p>4-{3-[(1,1,3,3-Tetramethylbutyl)amino]imidazo[1,2-<math>\alpha</math>]-pyrimidin-2-yl}benzoate  <u>RMM:</u> 380  <math>C_{22}H_{28}N_4O_2</math></p>

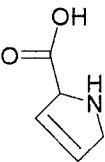
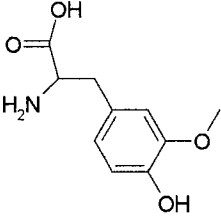
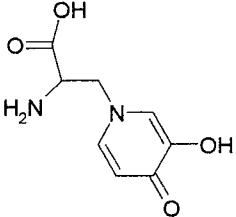
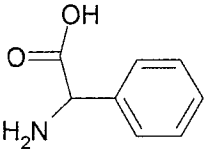
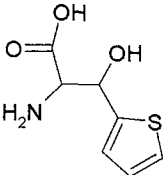
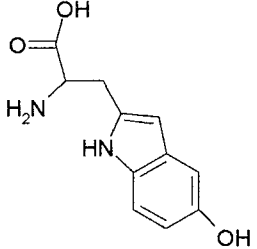
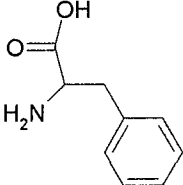
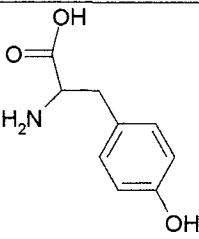
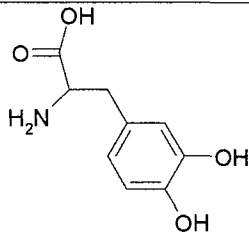
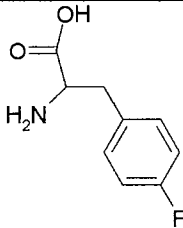
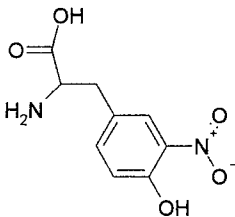
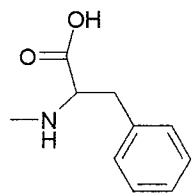
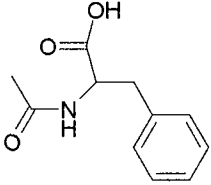
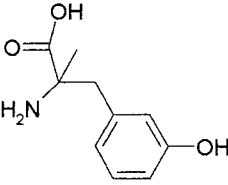
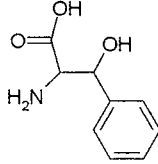
 <p>2-(4-Methoxyphenyl)-<i>N</i>-(1,1,3,3-tetramethylbutyl)imidazo[1,2-<math>\alpha</math>]pyrimidin-3-amine  RMM: 352  C<sub>21</sub>H<sub>28</sub>N<sub>4</sub>O</p>	 <p><i>N</i>-(1,1,3,3-Tetramethylbutyl)-2-(2-thienyl)imidazo[1,2-<math>\alpha</math>]pyrazin-3-amine  RMM: 328  C<sub>18</sub>H<sub>24</sub>N<sub>4</sub>O<sub>2</sub>S</p>
 <p>2-(2-Phenylethyl)-<i>N</i>-(1,1,3,3-tetramethylbutyl)imidazo[1,2-<math>\alpha</math>]pyrazin-3-amine  RMM: 350  C<sub>22</sub>H<sub>30</sub>N<sub>4</sub></p>	

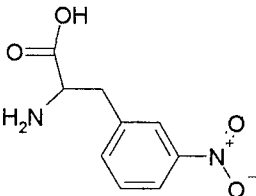
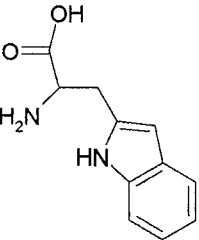
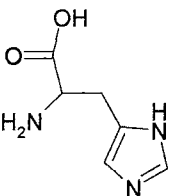
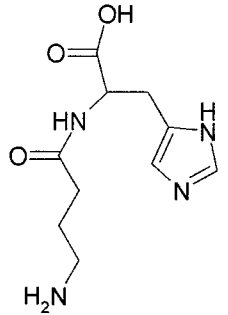
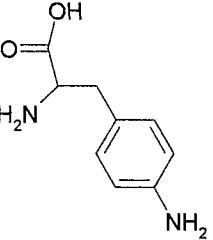
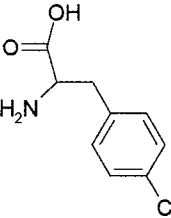
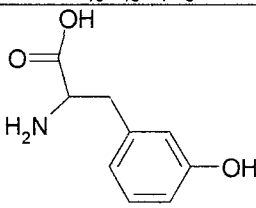
**Table 7:** The structures of the 3-alkylamino-imidazo-[1,2- $\alpha$ ]azines studied.



## Appendix 2

 <p>2-Aminoadipic acid RMM: 161 <math>C_6H_{11}NO_4</math></p>	 <p>Norleucine RMM: 131 <math>C_6H_{13}NO_2</math></p>	 <p><math>\alpha</math>-Hydroxylysine RMM: 162 <math>C_6H_{14}N_2O_3</math></p>
 <p>Norvaline RMM: 117 <math>C_5H_{11}NO_2</math></p>	 <p>Isoleucine RMM: 131 <math>C_6H_{13}NO_2</math></p>	 <p>Leucine RMM: 131 <math>C_6H_{13}NO_2</math></p>
 <p>Threonine RMM: 119 <math>C_4H_9NO_3</math></p>	 <p>Valine RMM: 117 <math>C_5H_{11}NO_2</math></p>	 <p>Homoserine RMM: 119 <math>C_4H_9NO_3</math></p>
 <p>Lysine RMM: 146 <math>C_6H_{14}N_2O_2</math></p>	 <p>Asparagine RMM: 133 <math>C_4H_7NO_4</math></p>	 <p>Methionine RMM: 149 <math>C_5H_{11}NO_2S</math></p>
 <p>Glutamic acid RMM: 147 <math>C_5H_9NO_4</math></p>	 <p>Methionine sulfoxide RMM: 165 <math>C_5H_{11}NO_3S</math></p>	 <p>Cystathionine RMM: 222 <math>C_7H_{14}N_2O_4S</math></p>
 <p>Methionine sulphone RMM: 181 <math>C_5H_{11}NO_4S</math></p>	 <p>Proline RMM: 115 <math>C_5H_9NO_2</math></p>	 <p>4-Hydroxyproline RMM: 131 <math>C_5H_9NO_3</math></p>

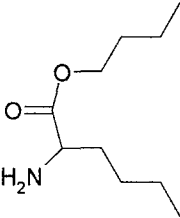
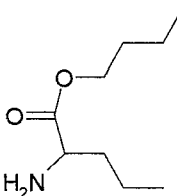
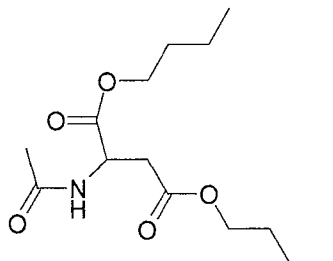
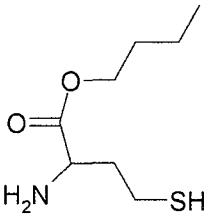
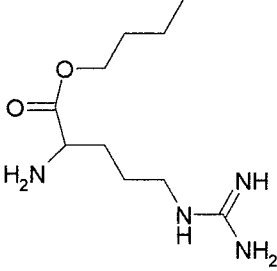
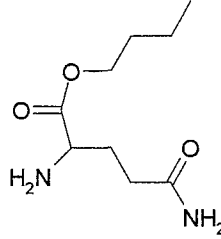
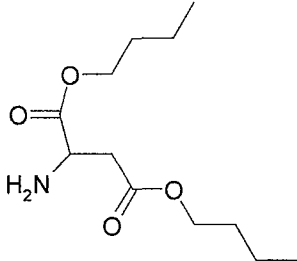
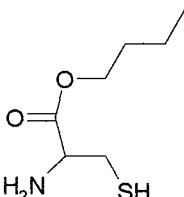
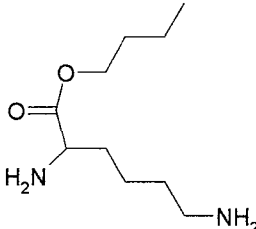
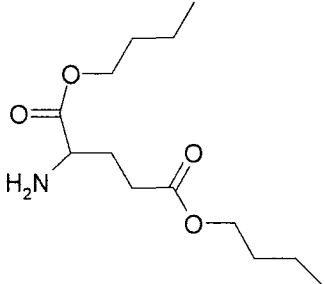
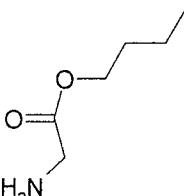
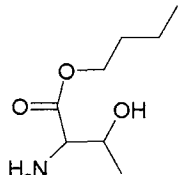
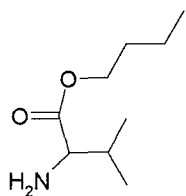
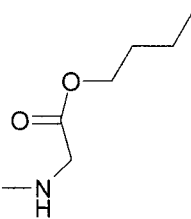
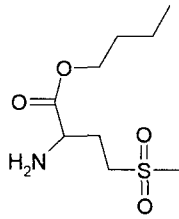
 <p>3,4-Dihydroproline RMM: 113 C<sub>5</sub>H<sub>7</sub>NO<sub>2</sub></p>	 <p>3-Methoxytyrosine (3-O-Methyldopa) RMM: 211 C<sub>10</sub>H<sub>13</sub>NO<sub>4</sub></p>	 <p>Mimosine RMM: 198 MF: C<sub>8</sub>H<sub>10</sub>N<sub>2</sub>O<sub>4</sub></p>
 <p>Phenylglycine RMM: 151 C<sub>8</sub>H<sub>9</sub>NO<sub>2</sub></p>	 <p><math>\beta</math>-2-Thienyl-serine RMM: 187 C<sub>7</sub>H<sub>9</sub>NO<sub>3</sub>S</p>	 <p>5-Hydroxytryptophan RMM: 220 C<sub>11</sub>H<sub>12</sub>N<sub>2</sub>O<sub>3</sub></p>
 <p>Phenylalanine RMM: 165 C<sub>9</sub>H<sub>11</sub>NO<sub>2</sub></p>	 <p>Tyrosine RMM: 181 C<sub>9</sub>H<sub>11</sub>NO<sub>3</sub></p>	 <p>3,4-Dihydroxyphenylalanine RMM: 197 C<sub>9</sub>H<sub>11</sub>NO<sub>4</sub></p>
 <p><i>p</i>-Fluorophenylalanine RMM: 183 C<sub>9</sub>H<sub>10</sub>FNO<sub>2</sub></p>	 <p>3-Nitrotyrosine RMM: 226 C<sub>9</sub>H<sub>10</sub>N<sub>2</sub>O<sub>5</sub></p>	 <p><i>N</i>-Methylphenylalanine RMM: 179 C<sub>10</sub>H<sub>13</sub>NO<sub>2</sub></p>
 <p><i>N</i>-Acetylphenylalanine RMM: 207 C<sub>11</sub>H<sub>13</sub>NO<sub>3</sub></p>	 <p><math>\alpha</math>-Methyl-<i>m</i>-tyrosine RMM: 195 C<sub>10</sub>H<sub>13</sub>NO<sub>3</sub></p>	 <p><math>\beta</math>-Phenylserine RMM: 181 C<sub>9</sub>H<sub>11</sub>NO<sub>3</sub></p>

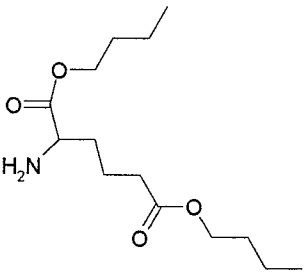
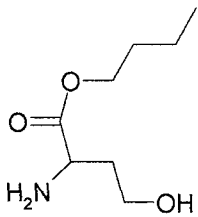
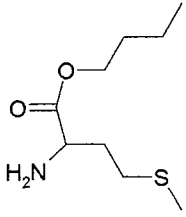
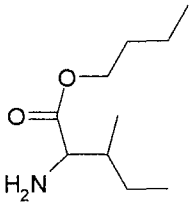
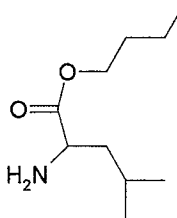
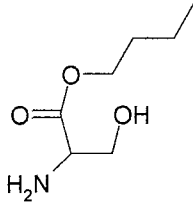
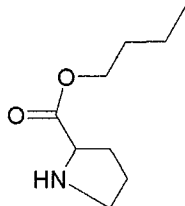
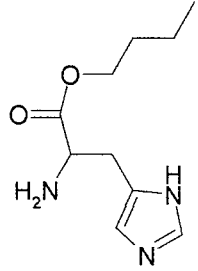
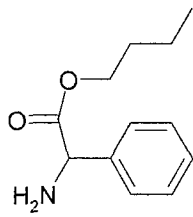
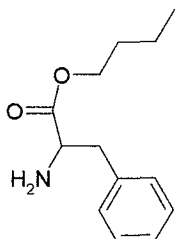
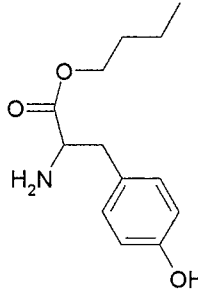
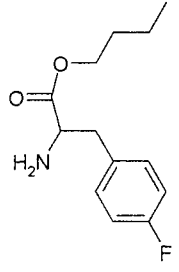
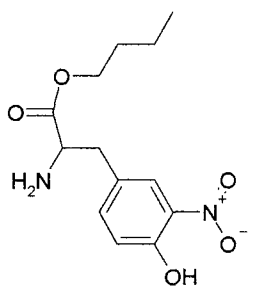
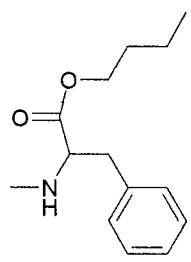
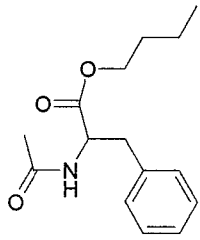
 <p><i>p</i>-Nitrophenylalanine RMM: 210 C<sub>9</sub>H<sub>10</sub>N<sub>2</sub>O<sub>4</sub></p>	 <p>Tryptophan RMM: 204 C<sub>11</sub>H<sub>12</sub>N<sub>2</sub>O<sub>2</sub></p>	 <p>Histidine RMM: 155 C<sub>6</sub>H<sub>9</sub>N<sub>3</sub>O<sub>2</sub></p>
 <p>Homocarnosine RMM: 240 C<sub>10</sub>H<sub>16</sub>N<sub>4</sub>O<sub>3</sub></p>	 <p><i>p</i>-Aminophenylalanine RMM: 180 C<sub>9</sub>H<sub>12</sub>N<sub>2</sub>O<sub>2</sub></p>	 <p><i>p</i>-Chlorophenylalanine RMM: 199 C<sub>9</sub>H<sub>10</sub>ClNO<sub>2</sub></p>
 <p><i>m</i>-Tyrosine RMM: 181 C<sub>9</sub>H<sub>11</sub>NO<sub>3</sub></p>		

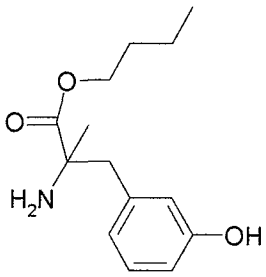
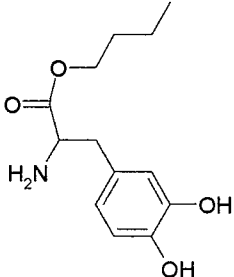
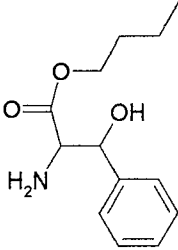
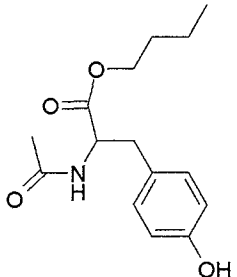
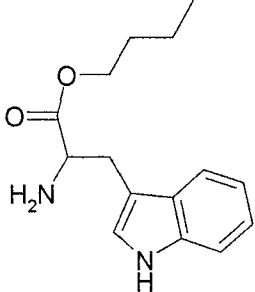
**Table 1:** The structures of the unprotected amino acids studied.

Common Neutral Losses Observed	Loss as identified by FTMS	Error
loss of 35 Da	loss of H <sub>5</sub> NO ≡ H <sub>2</sub> O and NH <sub>3</sub> (observed for tyrosine)	0.02 ppm
loss of 46 Da	loss of H <sub>2</sub> CO <sub>2</sub> (observed for all compounds)	Methionine: 0.4 ppm Phenylalanine: 0.3 ppm Tyrosine: 0.2 ppm
loss of 59 Da	C <sub>2</sub> H <sub>5</sub> NO (observed for tyrosine)	0.5 ppm
loss of 63 Da	loss of CH <sub>5</sub> NO <sub>2</sub> ≡ H <sub>2</sub> CO <sub>2</sub> and NH <sub>3</sub> (observed for tyrosine and phenylalanine)	Phenylalanine: 0.3 ppm Tyrosine: 0.6 ppm

**Table 2:** Summary of the exact mass analysis results for the unprotected amino acids.

 <p>Norleucine butyl ester RMM: 187 C<sub>10</sub>H<sub>21</sub>NO<sub>2</sub></p>	 <p>Norvaline butyl ester RMM: 173 C<sub>9</sub>H<sub>19</sub>NO<sub>2</sub></p>	 <p>N-Acetylaspartic acid dibutyl ester RMM: 287 C<sub>14</sub>H<sub>25</sub>NO<sub>5</sub></p>
 <p>Homocysteine butyl ester RMM: 191 C<sub>8</sub>H<sub>17</sub>NO<sub>2</sub>S</p>	 <p>Arginine butyl ester RMM: 230 C<sub>10</sub>H<sub>22</sub>N<sub>4</sub>O<sub>2</sub></p>	 <p>Glutamine butyl ester RMM: 202 C<sub>9</sub>H<sub>18</sub>N<sub>2</sub>O<sub>3</sub></p>
 <p>Aspartic acid dibutyl ester RMM: 245 C<sub>12</sub>H<sub>23</sub>NO<sub>4</sub></p>	 <p>Cysteine butyl ester RMM: 177 C<sub>7</sub>H<sub>15</sub>NO<sub>2</sub>S</p>	 <p>Lysine butyl ester RMM: 202 C<sub>10</sub>H<sub>22</sub>N<sub>2</sub>O<sub>2</sub></p>
 <p>Glutamic acid dibutyl ester RMM: 259 C<sub>13</sub>H<sub>25</sub>NO<sub>4</sub></p>	 <p>Glycine butyl ester RMM: 131 C<sub>6</sub>H<sub>13</sub>NO<sub>2</sub></p>	 <p>Threonine butyl ester RMM: 175 C<sub>8</sub>H<sub>17</sub>NO<sub>3</sub></p>
 <p>Valine butyl ester RMM: 173 C<sub>9</sub>H<sub>19</sub>NO<sub>2</sub></p>	 <p>Sarcosine butyl ester RMM: 145 C<sub>7</sub>H<sub>15</sub>NO<sub>2</sub></p>	 <p>Methionine sulphone butyl ester RMM: 237 C<sub>9</sub>H<sub>19</sub>NO<sub>4</sub>S</p>

 <p><math>\alpha</math>-Aminiadipic acid dibutyl ester RMM: 273 C<sub>14</sub>H<sub>27</sub>NO<sub>4</sub></p>	 <p>Homoserine butyl ester RMM: 175 C<sub>8</sub>H<sub>17</sub>NO<sub>3</sub></p>	 <p>Methionine butyl ester RMM: 205 C<sub>9</sub>H<sub>19</sub>NO<sub>2</sub>S</p>
 <p>Isoleucine butyl ester RMM: 187 C<sub>10</sub>H<sub>21</sub>NO<sub>2</sub></p>	 <p>Leucine butyl ester RMM: 187 C<sub>10</sub>H<sub>21</sub>NO<sub>2</sub></p>	 <p>Serine butyl ester RMM: 161 C<sub>7</sub>H<sub>15</sub>NO<sub>3</sub></p>
 <p>Proline butyl ester RMM: 171 C<sub>9</sub>H<sub>17</sub>NO<sub>2</sub></p>	 <p>Histidine butyl ester RMM: 211 C<sub>10</sub>H<sub>17</sub>N<sub>3</sub>O<sub>2</sub></p>	 <p>Phenylglycine butyl ester RMM: 207 C<sub>12</sub>H<sub>17</sub>NO<sub>2</sub></p>
 <p>Phenylalanine butyl ester RMM: 221 C<sub>13</sub>H<sub>19</sub>NO<sub>2</sub></p>	 <p>Tyrosine butyl ester RMM: 237 C<sub>13</sub>H<sub>19</sub>NO<sub>3</sub></p>	 <p><i>p</i>-Fluorophenylalanine butyl ester RMM: 239 C<sub>13</sub>H<sub>18</sub>FNO<sub>2</sub></p>
 <p>3-Nitrotyrosine butyl ester RMM: 282 C<sub>13</sub>H<sub>18</sub>N<sub>2</sub>O<sub>5</sub></p>	 <p><i>N</i>-Methylphenylalanine butyl ester RMM: 235 C<sub>14</sub>H<sub>21</sub>NO<sub>2</sub></p>	 <p><i>N</i>-Acetylphenylalanine butyl ester RMM: 263 C<sub>15</sub>H<sub>21</sub>NO<sub>3</sub></p>

 <p><math>\alpha</math>-Methyl-<i>m</i>-tyrosine butyl ester RMM: 251 C<sub>14</sub>H<sub>21</sub>NO<sub>3</sub></p>	 <p>3,4-Dihydroxyphenylalanine butyl ester RMM: 253 C<sub>13</sub>H<sub>19</sub>NO<sub>4</sub></p>	 <p>3-Phenylserine butyl ester RMM: 237 C<sub>13</sub>H<sub>19</sub>NO<sub>3</sub></p>
 <p><i>N</i>-Acetyltyrosine butyl ester RMM: 279 C<sub>15</sub>H<sub>21</sub>NO<sub>4</sub></p>	 <p>Tryptophan butyl ester RMM: 260 C<sub>15</sub>H<sub>20</sub>N<sub>2</sub>O<sub>2</sub></p>	

**Table 3:** The structures of the protected amino acids studied.

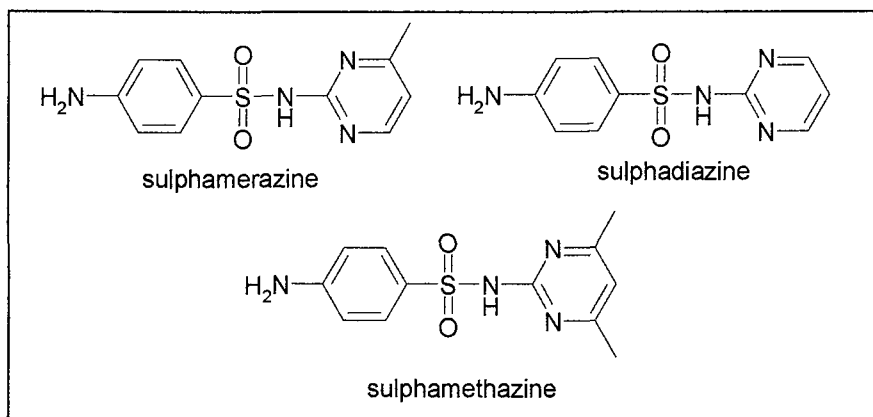
Amino Acid	m/z Value in Spectrum	Corresponding Neutral Loss	Equivalent Losses in the Spectra of the Methyl Ester and Butyl Ester Protected Amino Acids
Threonine methyl ester	m/z 116	loss of 18 Da	loss of 32 Da $\equiv$ loss of 74 Da loss of 50 Da $\equiv$ loss of 92 Da loss of 60 Da $\equiv$ loss of 102 Da
	m/z 102	loss of 32 Da	
	m/z 84	loss of 50 Da	
	m/z 74	loss of 60 Da	
Threonine butyl ester	m/z 120	loss of 56 Da	
	m/z 102	loss of 74 Da	
	m/z 84	loss of 92 Da	
	m/z 74	loss of 102 Da	
Methionine methyl ester	m/z 147	loss of 17 Da	loss of 60 Da $\equiv$ loss of 102 Da
	m/z 104	loss of 60 Da	
Methionine butyl ester	m/z 150	loss of 56 Da	
	m/z 104	loss of 102 Da	
Phenylalanine methyl ester	m/z 164	loss of 17 Da	loss of 60 Da $\equiv$ loss of 102 Da
	m/z 131	loss of 49 Da	
	m/z 120	loss of 60 Da	
Phenylalanine butyl ester	m/z 166	loss of 56 Da	
	m/z 149	loss of 73Da	
	m/z 120	loss of 102 Da	
Tyrosine methyl ester	m/z 179	loss of 17 Da	loss of 49 Da $\equiv$ loss of 91 Da loss of 60 Da $\equiv$ loss of 102 Da
	m/z 147	loss of 49 Da	
	m/z 136	loss of 60 Da	
Tyrosine butyl ester	m/z 179	loss of 56 Da	
	m/z 182	loss of 59 Da	
	m/z 165	loss of 73 Da	
	m/z 147	loss of 91 Da	
	m/z 136	loss of 102 Da	

**Table 4:** Correlation between the spectra of the butyl ester and the methyl ester amino acids.

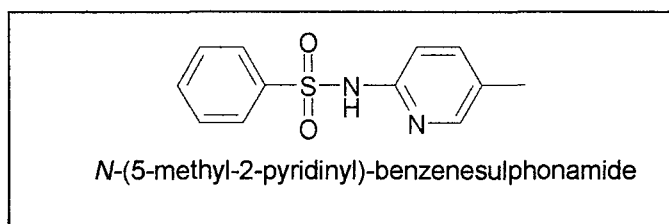
Common Neutral Losses Observed	Loss as identified by FTMS	Error
loss of 49 Da	loss of $\text{CH}_7\text{ON} \equiv \text{CH}_3\text{OH} + \text{NH}_3$ (observed for tyrosine m.e)	0.5 ppm
loss of 60 Da	loss of $\text{C}_2\text{H}_4\text{O}_2 \equiv \text{HCOOCH}_3$ (observed for all compounds)	Threonine methyl ester: 0.4ppm Methionine methyl ester: 0.3 ppm Phenylalanine methyl ester: 0.4 ppm Tyrosine methyl ester: 0.3 ppm

**Table 5:** Summary of the exact mass analysis results for the methyl ester amino acids.

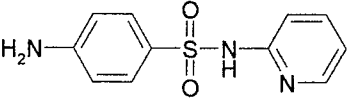
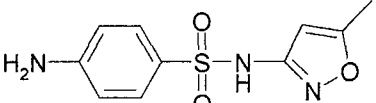
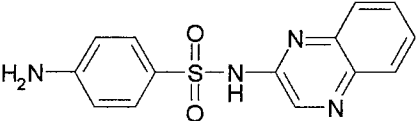
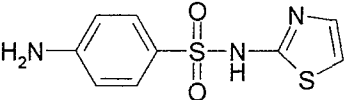
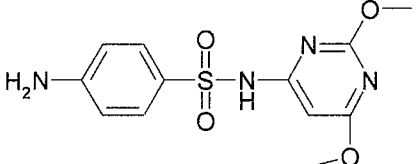
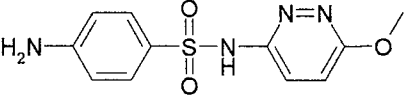
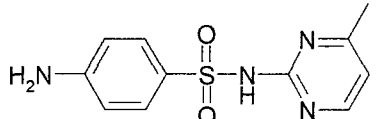
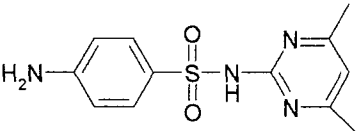
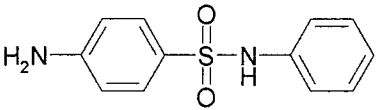
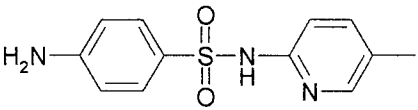
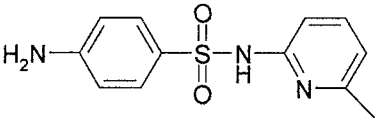
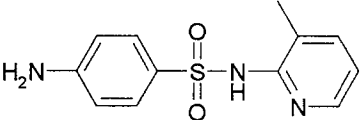
## Appendix 3

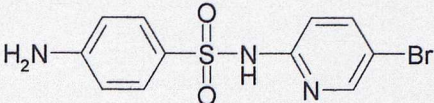
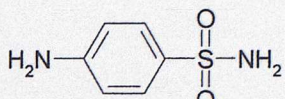
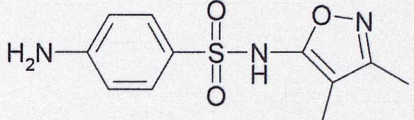
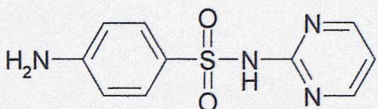
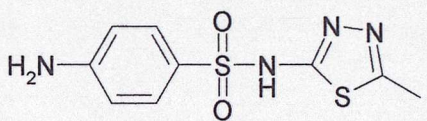
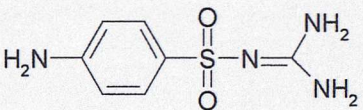


**Figure 1:** The structures of sulphamerazine, sulphadiazine and sulphamethazine.

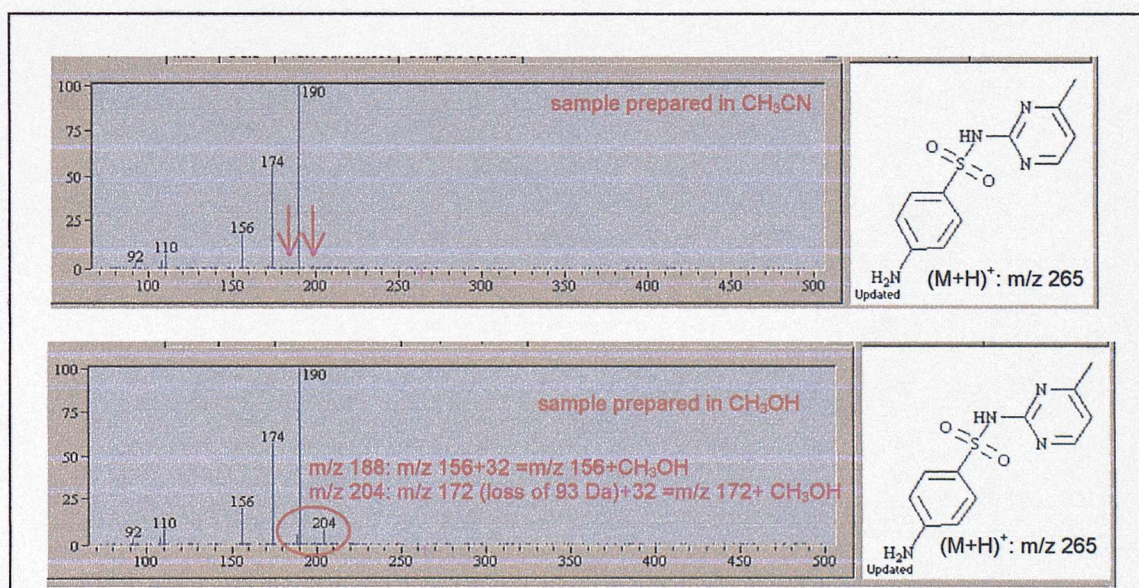


**Figure 2:** The structure of the "model" sulphonamide used to carry out *ab initio* calculations.

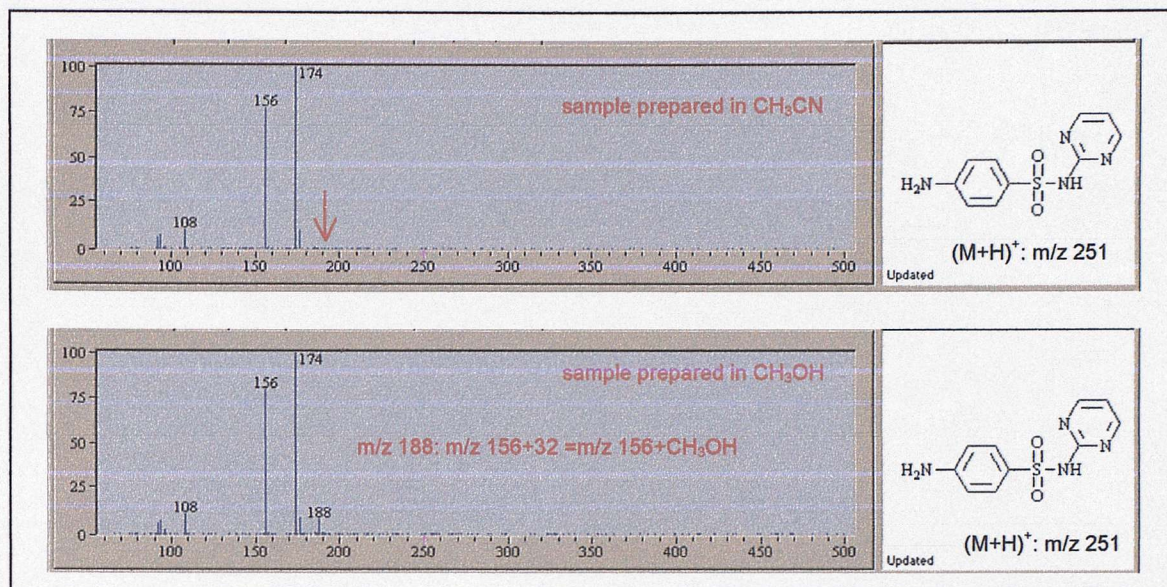
 <p>4-Amino-<i>N</i>-2-pyridinyl-benzenesulphonamide (Sulphapyridine) RMM: 249 C<sub>11</sub>H<sub>11</sub>N<sub>3</sub>O<sub>2</sub>S<sub>2</sub></p>	 <p>4-Amino-<i>N</i>-(5-methyl-3-isoxazolyl)-benzenesulphonamide (Sulphamethoxazole) RMM: 253 C<sub>10</sub>H<sub>11</sub>N<sub>3</sub>O<sub>3</sub>S</p>
 <p>4-Amino-<i>N</i>-2-quinoxaliny-benzenesulphonamide (Sulphaquinoxaline) RMM: 300 C<sub>14</sub>H<sub>12</sub>N<sub>4</sub>O<sub>2</sub>S</p>	 <p>4-Amino-<i>N</i>-2-thiazolyl- benzenesulphonamide (Sulphathiazole) RMM: 255 C<sub>9</sub>H<sub>9</sub>N<sub>3</sub>O<sub>2</sub>S<sub>2</sub></p>
 <p>4-Amino-<i>N</i>-(2,6-dimethoxy-4-pyrimidinyl)-benzenesulphonamide (Sulphadimethoxine) RMM: 310 C<sub>12</sub>H<sub>14</sub>N<sub>4</sub>O<sub>4</sub>S</p>	 <p>4-Amino-<i>N</i>-(6-methoxy-3-pyridazinyl)-benzenesulphonamide (Sulphamethoxypyridazine) RMM: 280 C<sub>11</sub>H<sub>12</sub>N<sub>4</sub>O<sub>3</sub>S</p>
 <p>4-Amino-<i>N</i>-(4-methyl-2-pyrimidinyl)-benzenesulphonamide (Sulphamerazine) RMM: 264 C<sub>11</sub>H<sub>12</sub>N<sub>4</sub>O<sub>2</sub>S</p>	 <p>4-Amino-<i>N</i>-(4,6-dimethyl-2-pyrimidinyl)-benzenesulphonamide (Sulphamethazine) RMM: 278 C<sub>12</sub>H<sub>14</sub>N<sub>4</sub>O<sub>2</sub>S</p>
 <p>4-Amino-<i>N</i>-phenyl- benzenesulphonamide (Sulphabenzene) RMM: 248 C<sub>12</sub>H<sub>11</sub>NO<sub>2</sub>S</p>	 <p>4-Amino-<i>N</i>-(5-methyl-2-pyridinyl)-benzenesulphonamide RMM: 263 C<sub>12</sub>H<sub>13</sub>N<sub>3</sub>O<sub>2</sub>S</p>
 <p>4-Amino-<i>N</i>-(6-methyl-2-pyridinyl)-benzenesulphonamide RMM: 263 C<sub>12</sub>H<sub>13</sub>N<sub>3</sub>O<sub>2</sub>S</p>	 <p>4-Amino-<i>N</i>-(3-methyl-2-pyridinyl)-benzenesulphonamide RMM: 263 C<sub>12</sub>H<sub>13</sub>N<sub>3</sub>O<sub>2</sub>S</p>

 <p>4-Amino-<i>N</i>-(5-bromo-2-pyridinyl)-benzenesulphonamide (5-Bromosulphapyridine) RMM: 327 C<sub>11</sub>H<sub>10</sub>N<sub>3</sub>O<sub>2</sub>SBr</p>	 <p>4-Amino-benzenesulphonamide (Sulphanilamide) RMM: 172 C<sub>6</sub>H<sub>8</sub>N<sub>2</sub>O<sub>2</sub>S</p>
 <p>4-Amino-<i>N</i>-(3,4-dimethyl-5-isoxazolyl)-benzenesulphonamide (Sulphisoxazole) RMM: 267 C<sub>11</sub>H<sub>13</sub>N<sub>4</sub>O<sub>3</sub>S</p>	 <p>4-Amino-<i>N</i>-2-pyrimidinyl- benzenesulphonamide (Sulphadiazine) RMM: 250 C<sub>10</sub>H<sub>10</sub>N<sub>4</sub>O<sub>2</sub>S</p>
 <p>4-Amino-<i>N</i>-(5-methyl-1,3,4-thiadiazol-2-yl)-benzenesulphonamide (Sulphamethizole) RMM: 270 C<sub>9</sub>H<sub>10</sub>N<sub>4</sub>O<sub>2</sub>S<sub>2</sub></p>	 <p>4-Amino-<i>N</i>-(aminoiminomethyl)-benzenesulphonamide (Sulphaguanidine) RMM: 214 C<sub>7</sub>H<sub>10</sub>N<sub>4</sub>O<sub>2</sub>S</p>

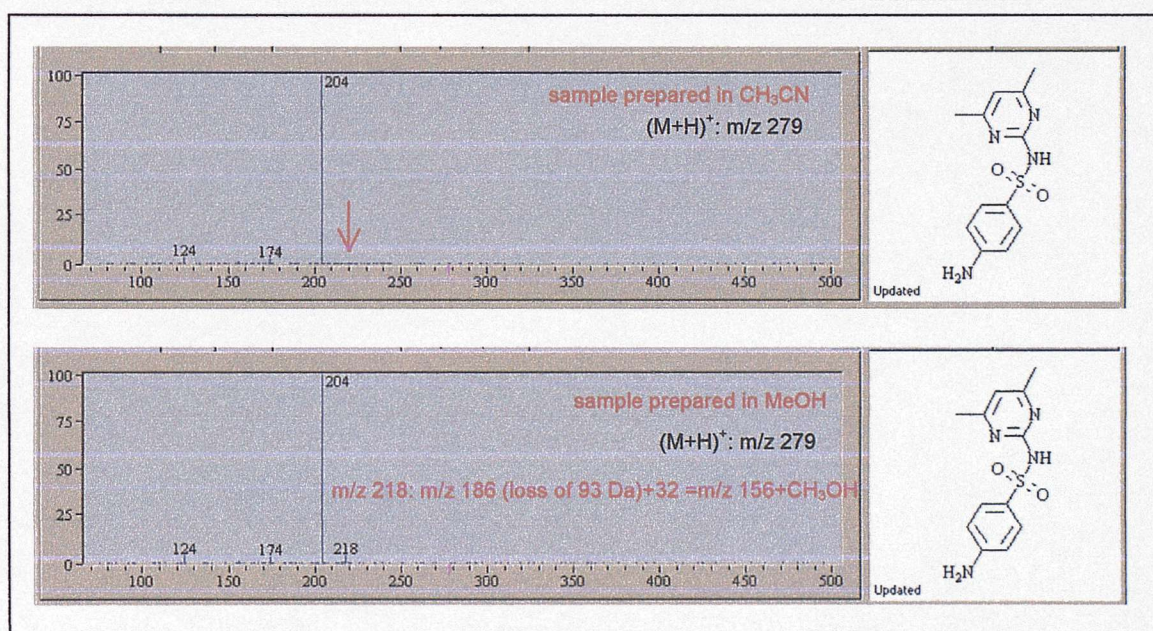
**Table 1:** The structures of the amino sulphonamides studied



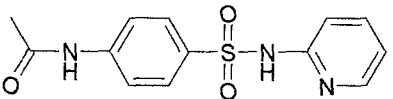
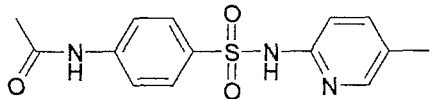
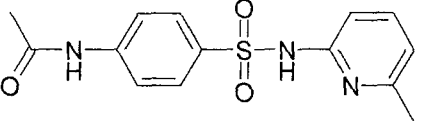
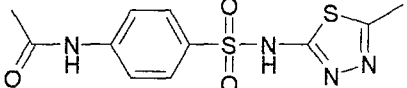
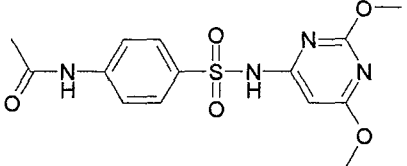
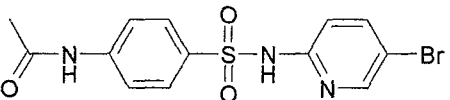
**Figure 3:** ES-MS/MS spectra obtained on the LCQ ion trap for samples of sulphamerazine prepared in acetonitrile and methanol.



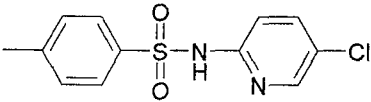
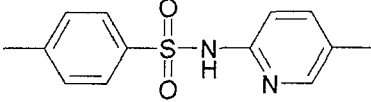
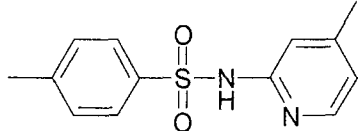
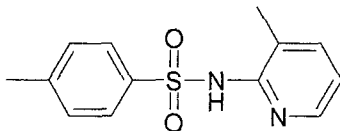
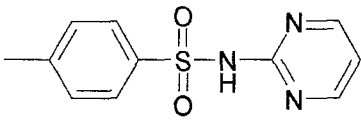
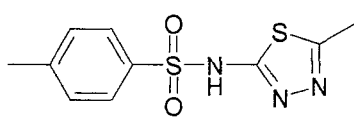
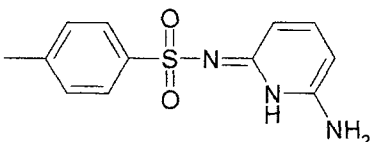
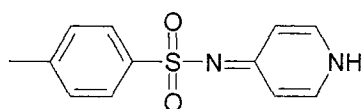
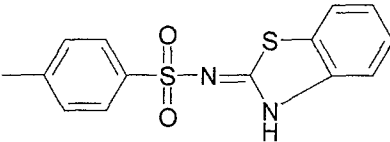
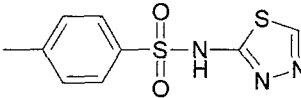
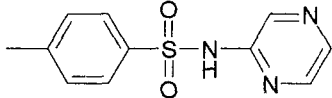
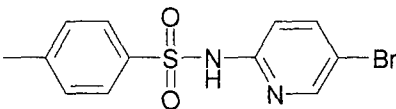
**Figure 4:** ES-MS/MS spectra obtained on the LCQ ion trap for samples of sulphadiazine prepared in acetonitrile and methanol.



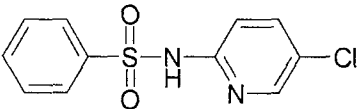
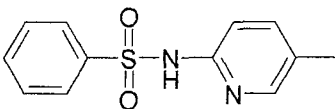
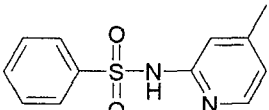
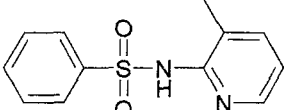
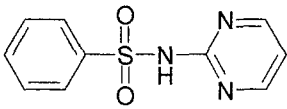
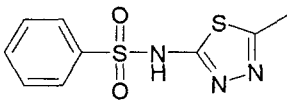
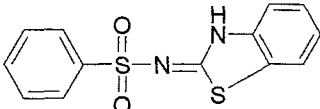
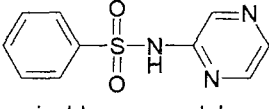
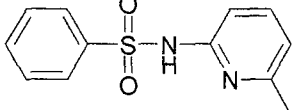
**Figure 5:** ES-MS/MS spectra obtained on the LCQ ion trap for samples of sulphamethazine prepared in acetonitrile and methanol.

 <p><i>N</i>-[4-[(2-Pyridinylamino)sulphonyl]phenyl]-acetamide RMM: 291 C<sub>13</sub>H<sub>13</sub>N<sub>3</sub>O<sub>2</sub>S</p>	 <p><i>N</i>-[4-[(5-Methyl-2-pyridinyl)amino]sulphonyl]phenyl]-acetamide RMM: 305 C<sub>14</sub>H<sub>15</sub>N<sub>3</sub>O<sub>3</sub>S</p>
 <p><i>N</i>-[4-[(6-Methyl-2-pyridinyl)amino]sulphonyl]phenyl]-acetamide RMM: 305 C<sub>14</sub>H<sub>15</sub>N<sub>3</sub>O<sub>3</sub>S</p>	 <p><i>N</i>-[4-[(5-Methyl-1,3,4-thiadiazol-2-yl)amino]sulphonyl]phenyl]-acetamide RMM: 305 C<sub>11</sub>H<sub>12</sub>N<sub>4</sub>O<sub>3</sub>S<sub>2</sub></p>
 <p><i>N</i>-[4-[(2,6-Dimethoxy-pyrimidinyl)amino]sulphonyl]phenyl]-acetamide RMM: 352 C<sub>14</sub>H<sub>16</sub>N<sub>4</sub>O<sub>5</sub>S</p>	 <p><i>N</i>-[4-[(5-Bromo-2-pyridinyl)amino]sulphonyl]phenyl]-acetamide RMM: 369 C<sub>13</sub>H<sub>12</sub>N<sub>3</sub>O<sub>3</sub>SBr</p>

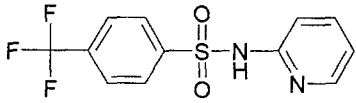
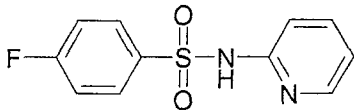
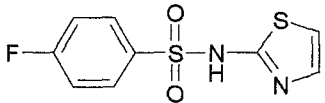
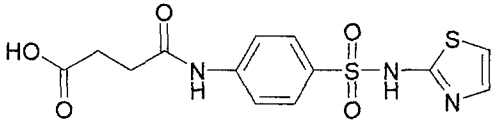
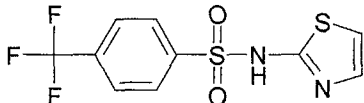
**Table 2:** The structures of the acetylated amino-sulphonamides studied.

 <p><i>N</i>-(5-Chloro-2-pyridinyl)-4-methylbenzenesulphonamide  <u>RMM:</u> 282  <math>C_{12}H_{11}N_2O_2S</math></p>	 <p>4-Methyl-<i>N</i>-(5-methyl-2-pyridinyl)benzenesulphonamide  <u>RMM:</u> 262  <math>C_{13}H_{14}N_2O_2S</math></p>
 <p>4-Methyl-<i>N</i>-(4-methyl-2-pyridinyl)benzenesulphonamide  <u>RMM:</u> 262  <math>C_{13}H_{14}N_2O_2S</math></p>	 <p>4-Methyl-<i>N</i>-(3-methyl-2-pyridinyl)benzenesulphonamide  <u>RMM:</u> 262  <math>C_{13}H_{14}N_2O_2S</math></p>
 <p>4-Methyl-<i>N</i>-2-pyrimidinylbenzenesulphonamide  <u>RMM:</u> 249  <math>C_{11}H_{11}N_3O_2S</math></p>	 <p>4-Methyl-<i>N</i>-(5-methyl-1,3,4-thiadiazol-2-yl)benzenesulphonamide  <u>RMM:</u> 269  <math>C_{10}H_{11}N_3O_2S_2</math></p>
 <p>4-Methyl-<i>N</i>-(3-amino-2-pyridinyl)benzenesulphonamide  <u>RMM:</u> 263  <math>C_{12}H_{13}N_3O_2S</math></p>	 <p>4-Methyl-<i>N</i>-4-pyridinylbenzenesulphonamide  <u>RMM:</u> 248  <math>C_{12}H_{12}N_2O_2S</math></p>
 <p><i>N</i>-2-benzothiazolyl-4-methylbenzenesulphonamide  <u>RMM:</u> 304  <math>C_{14}H_{12}N_2O_2S_2</math></p>	 <p>4-Methyl-<i>N</i>-(1,3,4-thiadiazol-2-yl)benzenesulphonamide  <u>RMM:</u> 255  <math>C_9H_9N_3O_2S_2</math></p>
 <p>4-Methyl-<i>N</i>-pyrazinylbenzenesulphonamide  <u>RMM:</u> 249  <math>C_{11}H_{11}N_3O_2S</math></p>	 <p><i>N</i>-(5-Bromo-2-pyridinyl)-4-methylbenzenesulphonamide  <u>RMM:</u> 326  <math>C_{12}H_{11}N_2O_2S</math>Br</p>

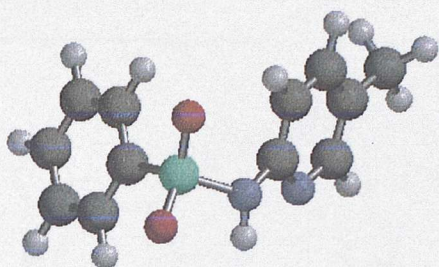
**Table 3:** The structures of the methyl-sulphonamides studied.

 <p><i>N</i>-(5-Chloro-2-pyridinyl)- benzenesulphonamide RMM: 268 <math>C_{11}H_9N_2O_2S</math></p>	 <p><i>N</i>-(5-Methyl-2-pyridinyl)- benzenesulphonamide RMM: 248 <math>C_{12}H_{12}N_2O_2S</math></p>
 <p><i>N</i>-(4-Methyl-2-pyridinyl)- benzenesulphonamide RMM: 248 <math>C_{12}H_{12}N_2O_2S</math></p>	 <p><i>N</i>-(3-Methyl-2-pyridinyl)- benzenesulphonamide RMM: 248 <math>C_{12}H_{12}N_2O_2S</math></p>
 <p><i>N</i>-2-Pyrimidinyl- benzenesulphonamide RMM: 235 <math>C_{10}H_9N_3O_2S</math></p>	 <p><i>N</i>-(5-Methyl-1,3,4-thiadiazol-2-yl)- benzenesulphonamide RMM: 255 <math>C_9H_9N_3O_2S_2</math></p>
 <p><i>N</i>-2-benzothiazolyl-4-benzenesulphonamide RMM: 290 <math>C_{13}H_{10}N_2O_2S_2</math></p>	 <p><i>N</i>-Pyrazinyl-benzenesulphonamide RMM: 235 <math>C_{10}H_9N_3O_2S</math></p>
 <p><i>N</i>-(6-Methyl-2-pyridinyl)- benzenesulphonamide RMM: 248 <math>C_{12}H_{12}N_2O_2S</math></p>	

**Table 4:** The structures of the non-substituted benzenesulphonamides studied.

 <p>4-Trifluoromethyl-<i>N</i>-2-pyridinyl- benzenesulphonamide RMM: 302 C<sub>12</sub>H<sub>9</sub>N<sub>2</sub>O<sub>2</sub>SF</p>	 <p>4-Fluoro-<i>N</i>-2-pyridinyl-benzenesulphonamide RMM: 252 C<sub>11</sub>H<sub>9</sub>N<sub>2</sub>O<sub>2</sub>SF</p>
 <p>4-Fluoromethyl-<i>N</i>-2-thiazolyl- benzenesulphonamide RMM: 258 C<sub>9</sub>H<sub>7</sub>N<sub>2</sub>O<sub>2</sub>S<sub>2</sub>F</p>	 <p>4-Oxo-4-[[4-[(2- thiazolylamino)sulphonyl]phenyl]amino]- butanoic acid RMM: 355 C<sub>13</sub>H<sub>13</sub>N<sub>3</sub>O<sub>5</sub>S<sub>2</sub></p>
 <p>4-Trifluoromethyl-<i>N</i>-2-thiazolyl- benzenesulphonamide RMM: 308 C<sub>10</sub>H<sub>7</sub>N<sub>2</sub>O<sub>2</sub>S<sub>2</sub>F<sub>3</sub></p>	

**Table 5:** The structures of the five sulphonamides studied with various substituents attached on the benzene ring.

**Neutral benzenesulphonamide**

E= -1122.58332 au = -704421.03 Kcal/mol

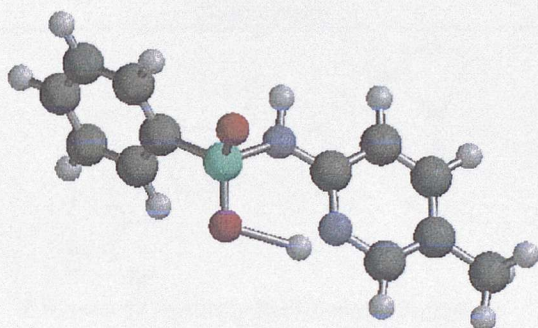
C-S bond: 1.798 Å

S-N bond: 1.699 Å

N-C bond: 1.417 Å

S=O bond: 1.461 Å

C-S-N angle: 106.7°

**OH<sup>+</sup> benzenesulphonamide**

E= -1122.96986 au = -704663.6 Kcal/mol

C-S bond: 1.769 Å

S-N bond: 1.767 Å

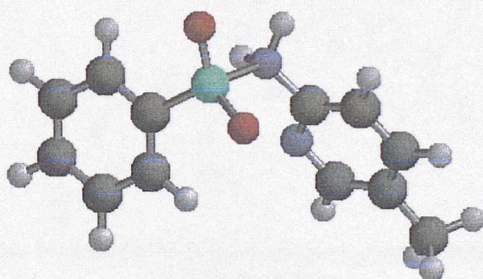
N-C bond: 1.375 Å

S=O bond: 1.454 Å

S=O bond: 1.471 Å

O-H bond: 1.825 Å

C-S-N angle: 101.6°

**NH<sub>2</sub><sup>+</sup> benzenesulphonamide**

E= -1122.93872 au = -704644.05 Kcal/mol

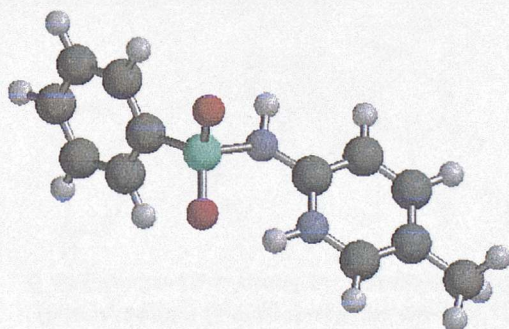
C-S bond: 1.760 Å

S-N bond: 2.058 Å

N-C bond: 1.451 Å

S=O bond: 1.450 Å

C-S-N angle: 102.52°

**Ring NH<sup>+</sup> benzenesulphonamide**

E= -1122.96979 au = -704663.5 Kcal/mol

C-S bond: 1.770 Å

S-N bond: 1.767 Å

N-C bond: 1.375 Å

S=O bond: 1.454 Å

S=O bond: 1.471 Å

C-S-N angle: 101.6°

**Figure 6:** Summary of the results of the *ab initio* calculations carried out on *N*-(5-methyl-2-pyridinyl)-benzenesulphonamide.

## Appendix 4

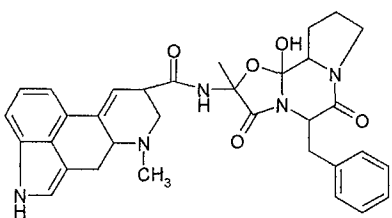
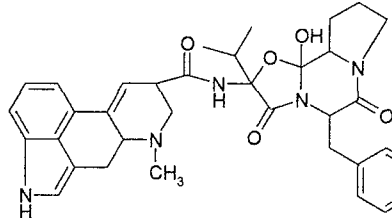
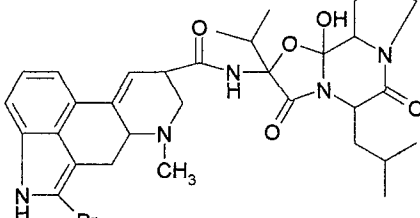
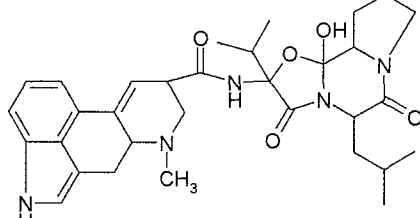
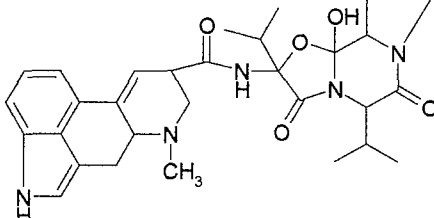
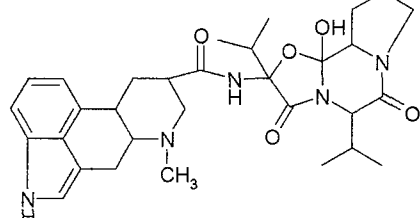
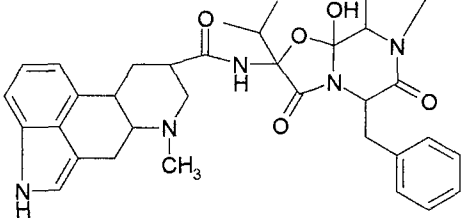
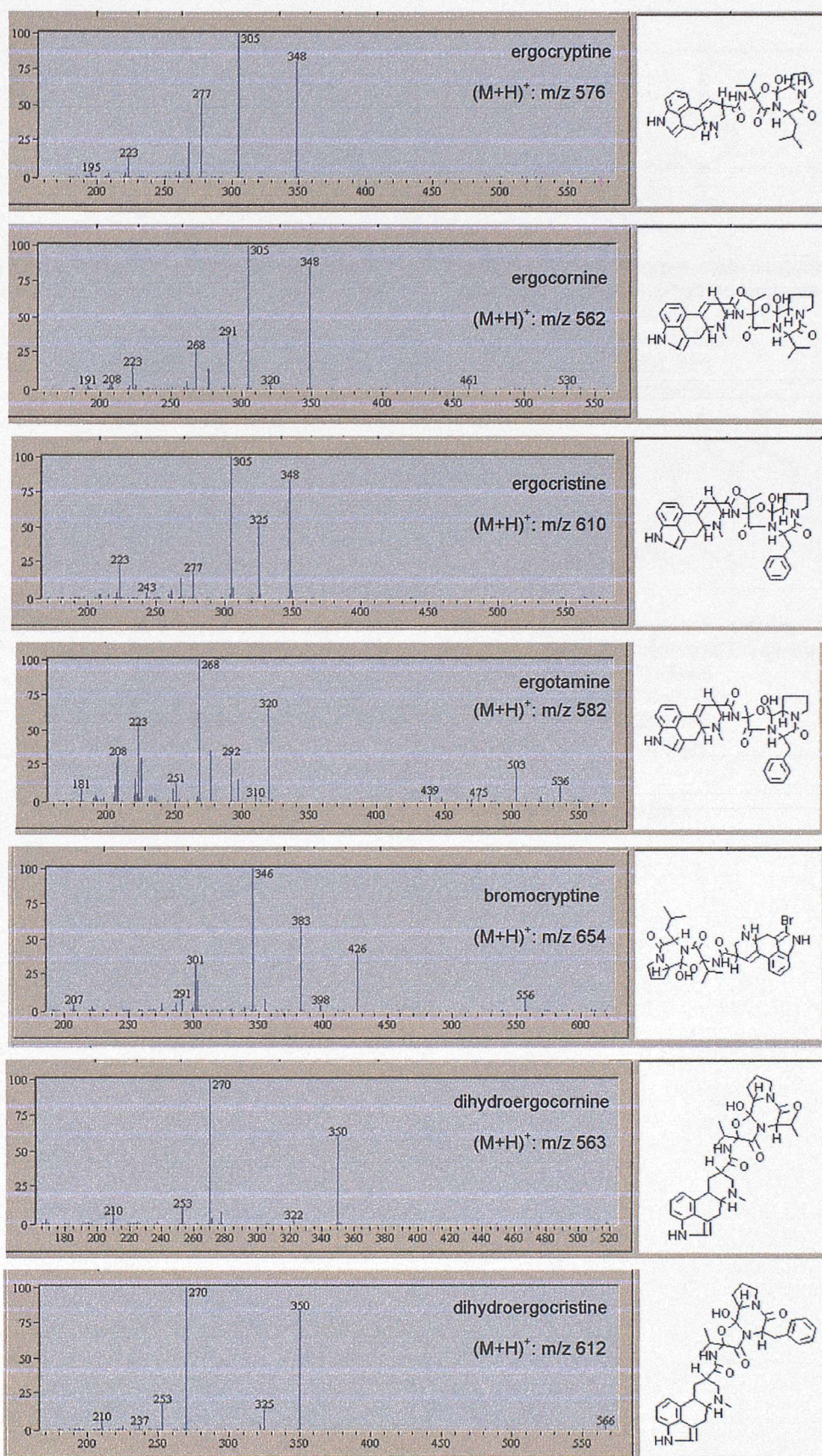
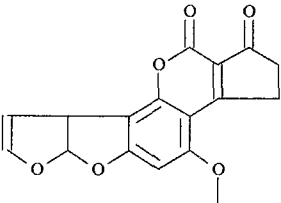
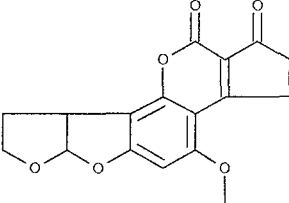
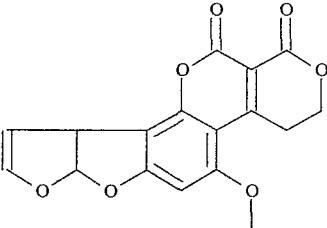
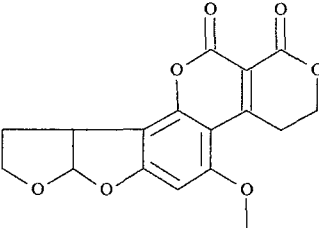
 <p>12'-Hydroxy-2'-methyl-5'-(phenylmethyl)- (5'α)-ergotaman-3',6',18-trione (Ergotamine) <u>RMM:</u> 581 <math>C_{33}H_{35}N_5O_5</math></p>	 <p>12'-Hydroxy-2'-(1-methylethyl)-5'-( phenylmethyl)-(5'α)-ergotaman-3',6',18-trione (Ergocristine) <u>RMM:</u> 609 <math>C_{35}H_{39}N_5O_5</math></p>
 <p>2-Bromo-12'-hydroxy-2'-(1-methylethyl)-5'-(2- methylpropyl)-(5'α)-ergotaman-3',6',18-trione (Bromocryptine) <u>RMM:</u> 653 <math>C_{32}H_{40}N_5O_5Br</math></p>	 <p>12'-Hydroxy-2'-(1-methylethyl)-5'-(2-methylpropyl)- (5'α)-ergotaman-3',6',18-trione (Ergocryptine) <u>RMM:</u> 575 <math>C_{32}H_{41}N_5O_5</math></p>
 <p>12'-Hydroxy-2',5'-bis(1-methylethyl)-ergotaman- (5'α)-3',6',18-trione (Ergocornine) <u>RMM:</u> 561 <math>C_{31}H_{39}N_5O_5</math></p>	 <p>9,10-Dihydro-12'-hydroxy-2',5'-bis(1-methylethyl)- (5'α,10α)-ergotaman-3',6',18-trione (Dihydroergocornine) <u>RMM:</u> 563 <math>C_{31}H_{41}N_5O_5</math></p>
 <p>9,10-Dihydro-12'-hydroxy-2'-(1-methylethyl)-5'- (phenylmethyl)-(5'α,10α)-ergotaman-3',6',18- trione (Dihydroergocristine) <u>RMM:</u> 611 <math>C_{35}H_{41}N_5O_5</math></p>	

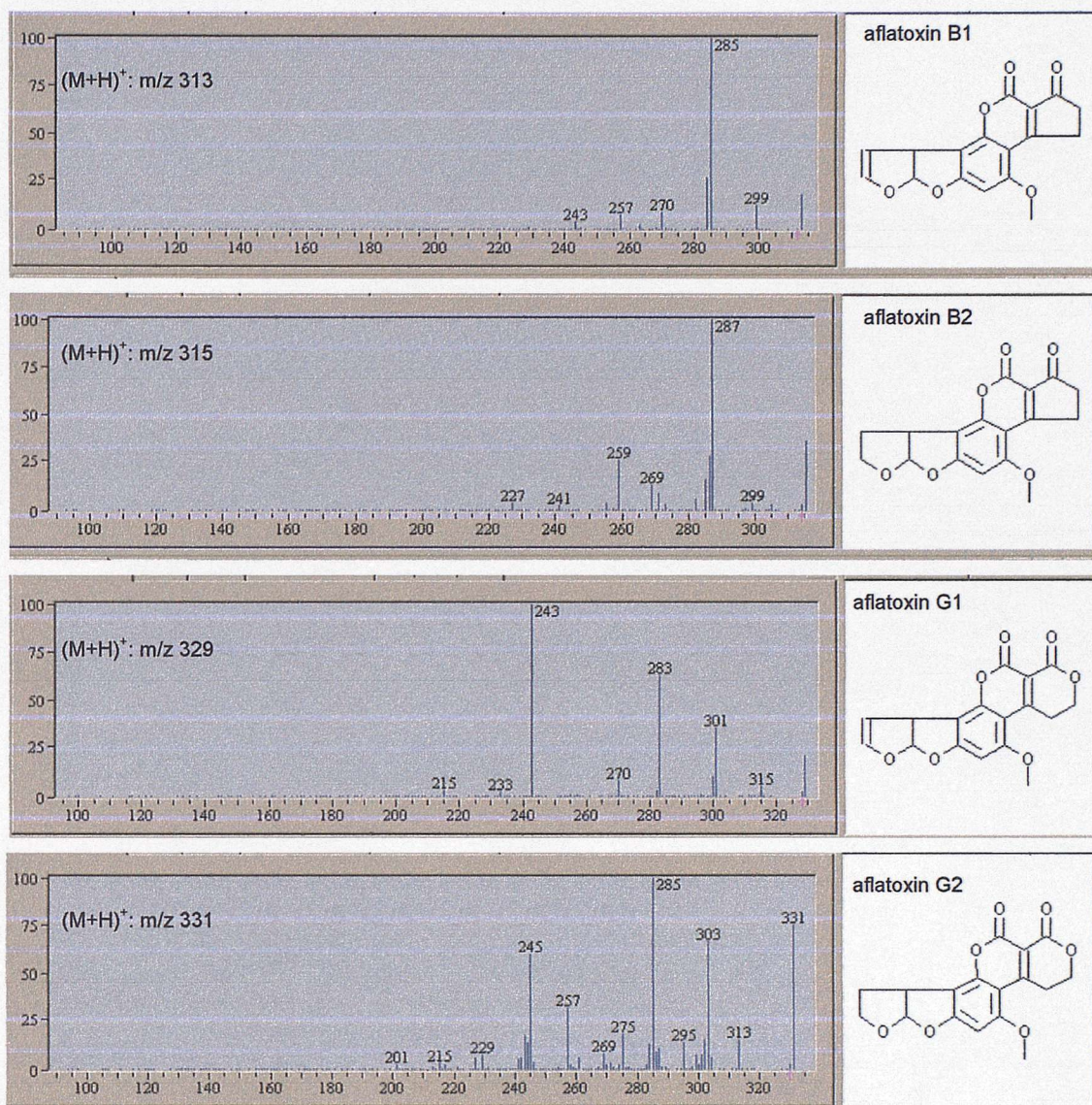
Table 1: The structures of the library of ergopeptine alkaloids studied.



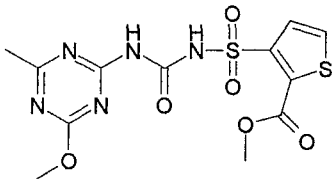
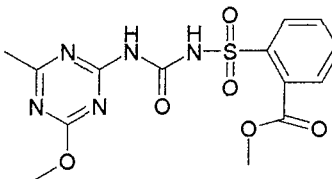
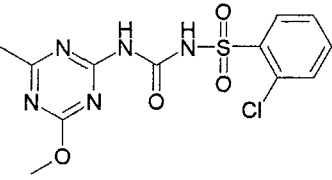
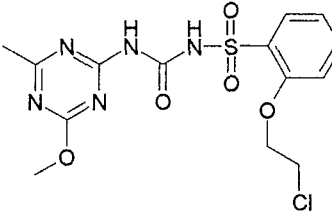
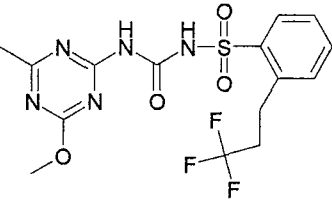
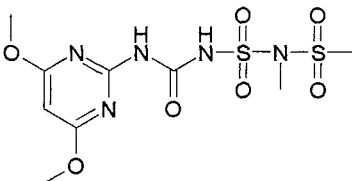
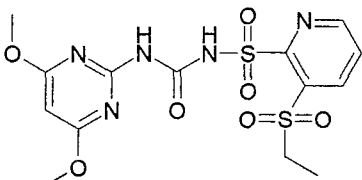
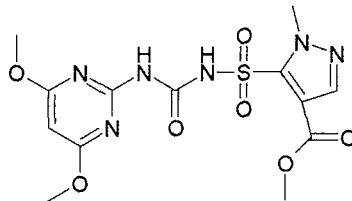
**Figure 1:** The ES-MS/MS spectra of the library of ergopeptine alkaloids studied.

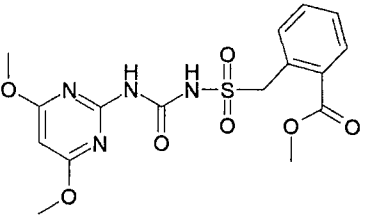
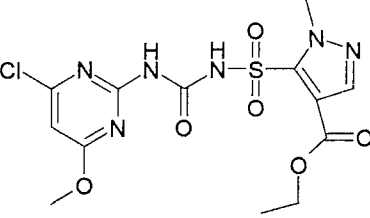
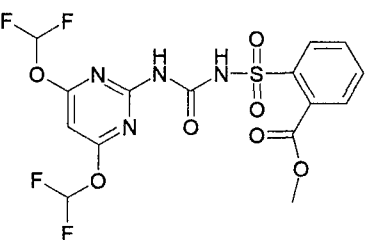
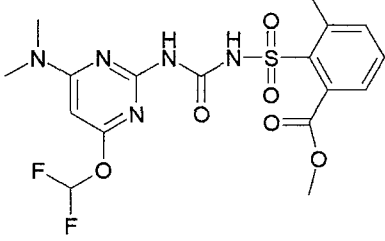
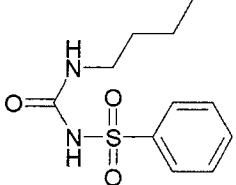
 <p>2,3,6a,9a-Tetrahydro-4-methoxy-cyclopenta [c]furo[3',2':4,5]furo[2,3-h][1]benzopyran-1,11- dione (Aflatoxin B1) <u>RMM:</u> 312 C<sub>17</sub>H<sub>12</sub>O<sub>6</sub></p>	 <p>2,3,6a,8,9,9a-Hexahydro-4-methoxy-cyclopenta [c]furo[3',2':4,5]furo[2,3-h][1]benzopyran-1,11- dione (Aflatoxin B2) <u>RMM:</u> 314 C<sub>17</sub>H<sub>14</sub>O<sub>6</sub></p>
 <p>3,4,7a,10a-Tetrahydro-5-methoxy-1H,12H-furo [3',2':4,5]furo[2,3-h]pyrano[3,4-c][1]benzopyran- 1,12-dione (Aflatoxin G1) <u>RMM:</u> 328 C<sub>17</sub>H<sub>14</sub>O<sub>7</sub></p>	 <p>3,4,7a,9,10,10a-Hexahydro-5-methoxy-1H,12H- furo [3',2':4,5]furo[2,3-h]pyrano[3,4-c]benzopyran- 1,12-dione (Aflatoxin G2) <u>RMM:</u> 330 C<sub>17</sub>H<sub>16</sub>O<sub>7</sub></p>

**Table 2:** The structures of the four aflatoxins studied.



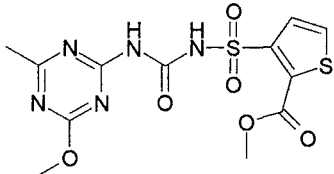
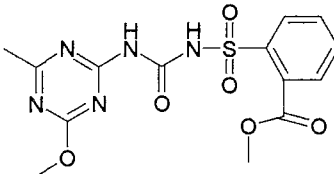
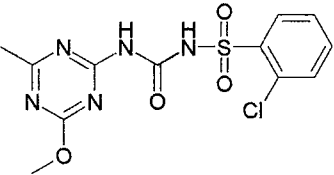
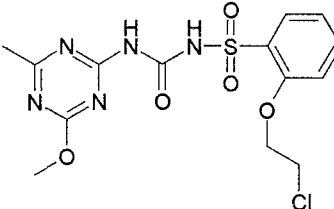
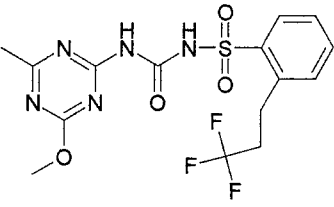
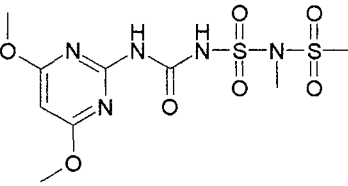
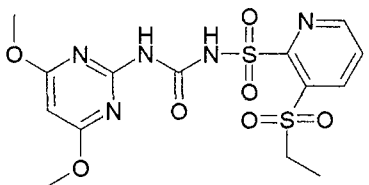
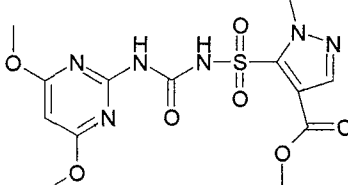
**Figure 2:** The ES-MS/MS spectra of the four aflatoxins studied.

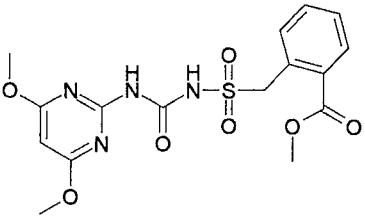
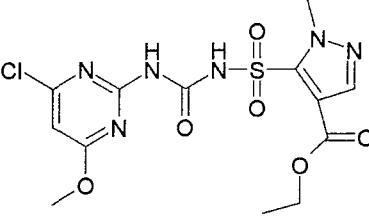
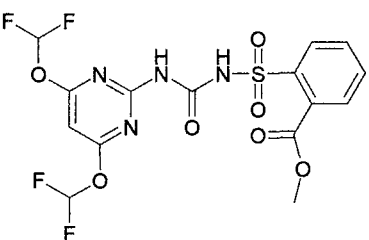
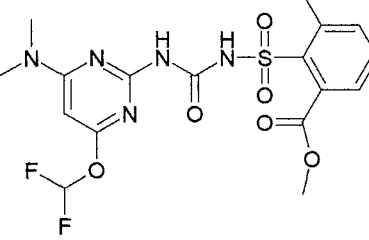
 <p>3-[[[(4-Methoxy-6-methyl-1,3,5-triazin-2-yl)amino]carbonyl]amino]sulphonyl]-2-thiophenecarboxylic acid methyl ester (Thiophensulphuron methyl) RMM: 387 C<sub>12</sub>H<sub>13</sub>N<sub>5</sub>O<sub>6</sub>S<sub>2</sub></p>	 <p>2-[[[(4-Methoxy-6-methyl-1,3,5-triazin-2-yl)amino]carbonyl]amino]sulphonyl]-2-benzoic acid methyl ester (Metsulphuron methyl) RMM: 381 C<sub>14</sub>H<sub>15</sub>N<sub>5</sub>O<sub>6</sub>S</p>
 <p>2-Chloro-<i>N</i>-[[[(4-methoxy-6-methyl-1,3,5-triazin-2-yl)amino]carbonyl]-benzenesulphonamide (Chlorsulphuron) RMM: 357 C<sub>12</sub>H<sub>12</sub>N<sub>5</sub>O<sub>4</sub>SCl</p>	 <p>2-(2-Chloroethoxy)-<i>N</i>-[[[(4-methoxy-6-methyl-1,3,5-triazin-2-yl)amino]carbonyl]-benzenesulphonamide (Triasulphuron) RMM: 401 C<sub>14</sub>H<sub>16</sub>N<sub>5</sub>O<sub>5</sub>SCl</p>
 <p><i>N</i>-[[[(4-Methoxy-6-methyl-1,3,5-triazin-2-yl)amino]carbonyl]-2-(3,3,3-trifluoropropyl)-benzenesulphonamide (Prosulphuron) RMM: 419 C<sub>15</sub>H<sub>16</sub>N<sub>5</sub>O<sub>4</sub>SF<sub>3</sub></p>	 <p><i>N</i>-(4,6-Dimethoxy-2-pyrimidinyl)-3-methyl-2,4-dithia-3,5-diazahexan-6-amide-2,2,4,4-tetraoxide (Amidosulphuron) RMM: 369 C<sub>9</sub>H<sub>15</sub>N<sub>5</sub>O<sub>7</sub>S<sub>2</sub></p>
 <p><i>N</i>-[[[(4,6-Dimethoxy-2-pyrimidinyl)amino]carbonyl]-3-(ethylsulphonyl)-2-pyridinesulphonamide (Rimsulphuron) RMM: 431 C<sub>14</sub>H<sub>17</sub>N<sub>5</sub>O<sub>7</sub>S<sub>2</sub></p>	 <p>5-[[[(4,6-Dimethoxy-2-pyrimidinyl)amino]carbonyl]amino]sulphonyl]-1-methyl-1H-pyrazole-4-carboxylic acid ethyl ester (Pyrazosulphuron ethyl) RMM: 414 C<sub>14</sub>H<sub>18</sub>N<sub>6</sub>O<sub>7</sub>S</p>

 <p>2-[[[(4,6-Dimethoxy-2-pyrimidinyl)amino]carbonyl]amino]sulphonyl]methyl]-benzoic acid methyl ester (Bensulfuron methyl) <u>RMM:</u> 410 <math>C_{16}H_{18}N_4O_7S</math></p>	 <p>2-[[[(4-Chloro-6-methoxy-2-pyrimidinyl)amino]carbonyl]amino]sulphonyl]benzoic acid ethyl ester (Chlorimuron ethyl) <u>RMM:</u> 414 <math>C_{15}H_{15}N_4O_6SCl</math></p>
 <p>2-[[[(4,6-Bis(difluoromethoxy)-2-pyrimidinyl)amino]carbonyl]amino]sulphonyl]-benzoic acid methyl ester (Primisulphuron methyl) <u>RMM:</u> 468 <math>C_{15}H_{12}N_4O_7SF_4</math></p>	 <p>2-[[[(4-(dimethylamino)-6-(2,2,2-trifluoroethoxy)-1,3,5-triazin-2-yl)amino]carbonyl]amino]sulphonyl]-3-methylbenzoic acid methyl ester (Triflusulphuron methyl) <u>RMM:</u> 492 <math>C_{17}H_{19}N_6O_6SF_3</math></p>
 <p><i>N</i>-[(Butylamino)carbonyl-4-methylbenzenesulphonamide (Tolbutamide) <u>RMM:</u> 270 <math>C_{12}H_{18}N_2O_3S</math></p>	

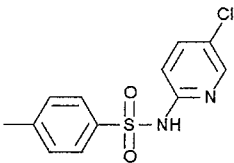
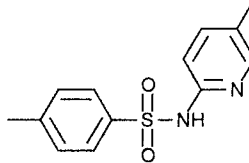
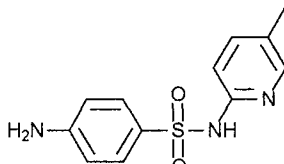
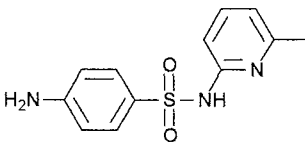
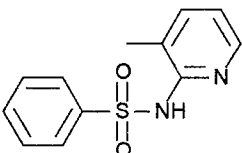
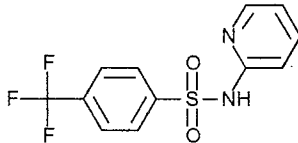
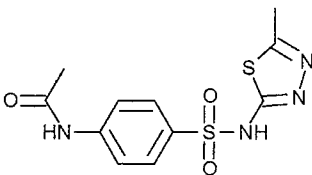
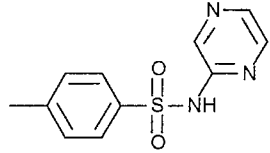
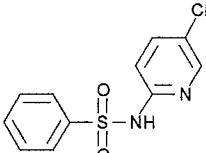
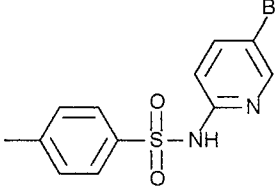
**Table 3:** Structures of the library of sulphonylureas studied.

## Appendix 5

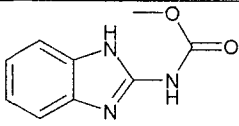
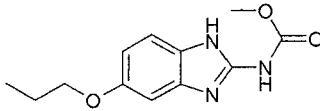
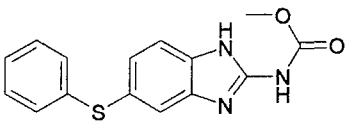
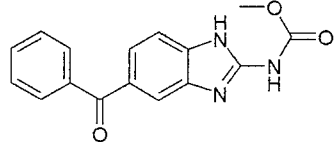
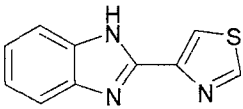
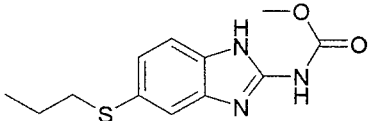
 <p>3-[[[(4-Methoxy-6-methyl-1,3,5-triazin-2-yl)amino]carbonyl]amino]sulphonyl]-2-thiophenecarboxylic acid methyl ester (Thiphensulphuron methyl) RMM: 387 C<sub>12</sub>H<sub>13</sub>N<sub>5</sub>O<sub>6</sub>S<sub>2</sub></p>	 <p>2-[[[(4-Methoxy-6-methyl-1,3,5-triazin-2-yl)amino]carbonyl]amino]sulphonyl]-2-benzoic acid methyl ester (Metsulphuron methyl) RMM: 381 C<sub>14</sub>H<sub>15</sub>N<sub>5</sub>O<sub>6</sub>S</p>
 <p>2-Chloro-<i>N</i>-[[[(4-methoxy-6-methyl-1,3,5-triazin-2-yl)amino]carbonyl]-benzenesulphonamide (Chlorsulphuron) RMM: 357 C<sub>12</sub>H<sub>12</sub>N<sub>5</sub>O<sub>4</sub>SCl</p>	 <p>2-(2-Chloroethoxy)-<i>N</i>-[[[(4-methoxy-6-methyl-1,3,5-triazin-2-yl)amino]carbonyl]-benzenesulphonamide (Triasulphuron) RMM: 401 C<sub>14</sub>H<sub>16</sub>N<sub>5</sub>O<sub>5</sub>SCl</p>
 <p><i>N</i>-[[[(4-Methoxy-6-methyl-1,3,5-triazin-2-yl)amino]carbonyl]-2-(3,3,3-trifluoropropyl)-benzenesulphonamide (Prosulphuron) RMM: 419 C<sub>15</sub>H<sub>16</sub>N<sub>5</sub>O<sub>4</sub>SF<sub>3</sub></p>	 <p><i>N</i>-(4,6-Dimethoxy-2-pyrimidinyl)-3-methyl-2,4-dithia-3,5-diazahexan-6-amide-2,2,4,4-tetraoxide (Amidosulphuron) RMM: 369 C<sub>9</sub>H<sub>15</sub>N<sub>5</sub>O<sub>7</sub>S<sub>2</sub></p>
 <p><i>N</i>-[[[(4,6-Dimethoxy-2-pyrimidinyl)amino]carbonyl]-3-(ethylsulphonyl)-2-pyridinesulphonamide (Rimsulphuron) RMM: 431 C<sub>14</sub>H<sub>17</sub>N<sub>7</sub>O<sub>7</sub>S<sub>2</sub></p>	 <p>5-[[[(4,6-Dimethoxy-2-pyrimidinyl)amino]carbonyl]amino]sulphonyl]-1-methyl-1H-pyrazole-4-carboxylic acid ethyl ester (Pyrazosulphuron ethyl) RMM: 414 C<sub>14</sub>H<sub>18</sub>N<sub>8</sub>O<sub>7</sub>S</p>

 <p>2-[[[[(4,6-Dimethoxy-2-pyrimidinyl)amino]carbonyl]amino]sulphonyl]methyl]-benzoic acid methyl ester (Bensulfuron methyl) RMM: 410 C<sub>16</sub>H<sub>18</sub>N<sub>4</sub>O<sub>7</sub>S</p>	 <p>2-[[[[(4-Chloro-6-methoxy-2-pyrimidinyl)amino]carbonyl]amino]sulphonyl]benzoic acid ethyl ester (Chlorimuron ethyl) RMM: 414 C<sub>15</sub>H<sub>15</sub>N<sub>4</sub>O<sub>6</sub>SCl</p>
 <p>2-[[[[(4,6-Bis(difluoromethoxy)-2-pyrimidinyl)amino]carbonyl]amino]sulphonyl]-benzoic acid methyl ester (Primisulphuron methyl) RMM: 468 C<sub>15</sub>H<sub>12</sub>N<sub>4</sub>O<sub>7</sub>SF<sub>4</sub></p>	 <p>2-[[[[(4-(dimethylamino)-6-(2,2,2-trifluoroethoxy)-1,3,5-triazin-2-yl)]amino]carbonyl]amino]sulphonyl]-3-methylbenzoic acid methyl ester (Triflusulphuron methyl) RMM: 492 C<sub>17</sub>H<sub>19</sub>N<sub>6</sub>O<sub>6</sub>SF<sub>3</sub></p>

**Table 1:** The structures of the sulphonylureas analysed.

 <p><i>N</i>-(5-Chloro-2-pyridinyl)-4-methylbenzenesulphonamide RMM: 282 <math>C_{12}H_{11}N_2O_2SCl</math></p>	 <p>4-Methyl-<i>N</i>-(5-methyl-2-pyridinyl)benzenesulphonamide RMM: 262 <math>C_{13}H_{14}N_2O_2S</math></p>
 <p>4-Amino-<i>N</i>-(5-methyl-2-pyridinyl)benzenesulphonamide RMM: 263 <math>C_{12}H_{13}N_3O_2S</math></p>	 <p>4-Amino-<i>N</i>-(6-methyl-2-pyridinyl)benzenesulphonamide RMM: 263 <math>C_{12}H_{13}N_3O_2S</math></p>
 <p><i>N</i>-(3-Methyl-2-pyridinyl)benzenesulphonamide RMM: 248 <math>C_{12}H_{12}N_2O_2S</math></p>	 <p>4-Trifluoromethyl-<i>N</i>-2-pyridinylbenzenesulphonamide RMM: 302 <math>C_{12}H_9N_2O_2SF</math></p>
 <p><i>N</i>-[4-[(5-Methyl-1,3,4-thiadiazol-2-yl) amino]sulphonyl]phenyl]-acetamide RMM: 312 <math>C_{11}H_{12}N_4O_3S_2</math></p>	 <p>4-Methyl-<i>N</i>-pyrazinylbenzenesulphonamide RMM: 249 <math>C_{11}H_{11}N_3O_2S</math></p>
 <p><i>N</i>-(5-Chloro-2-pyridinyl)benzenesulphonamide RMM: 268 <math>C_{11}H_9N_2O_2SCl</math></p>	 <p><i>N</i>-(5-Bromo-2-pyridinyl)-4-methylbenzenesulphonamide RMM: 326 <math>C_{12}H_{11}N_2O_2SBr</math></p>

**Table 2:** The structures of the sulphonamides analysed.

 <p>1H-Benzimidazol-2-yl-carbamic acid methyl ester (Carbendazim) RMM: 191 <math>C_9H_9N_3O_2</math></p>	 <p>(5-Propoxy-1H-benzimidazol-2-yl)-carbamic acid methyl ester (Oxibendazole) RMM: 249 <math>C_{12}H_{15}N_3O_3</math></p>
 <p>[(5-Phenylthio)-1H-benzimidazol-2-yl]-carbamic acid methyl ester (Fenbendazole) RMM: 299 <math>C_{15}H_{13}N_3O_2S</math></p>	 <p>(5-Benzoyl-1H-benzimidazol-2-yl)-carbamic acid methyl ester (Mebendazole) RMM: 295 <math>C_{16}H_{13}N_3O_3</math></p>
 <p>2-(4-Thiazolyl)-1H-benzimidazole (Thiabendazole) RMM: 201 <math>C_{10}H_7N_3S</math></p>	 <p>(5-Propylthio-1H-benzimidazol-2-yl)-carbamic acid methyl ester (Albendazole) RMM: 265 <math>C_{12}H_{15}N_3O_2S</math></p>

**Table 3:** The structures of the benzimidazoles analysed.

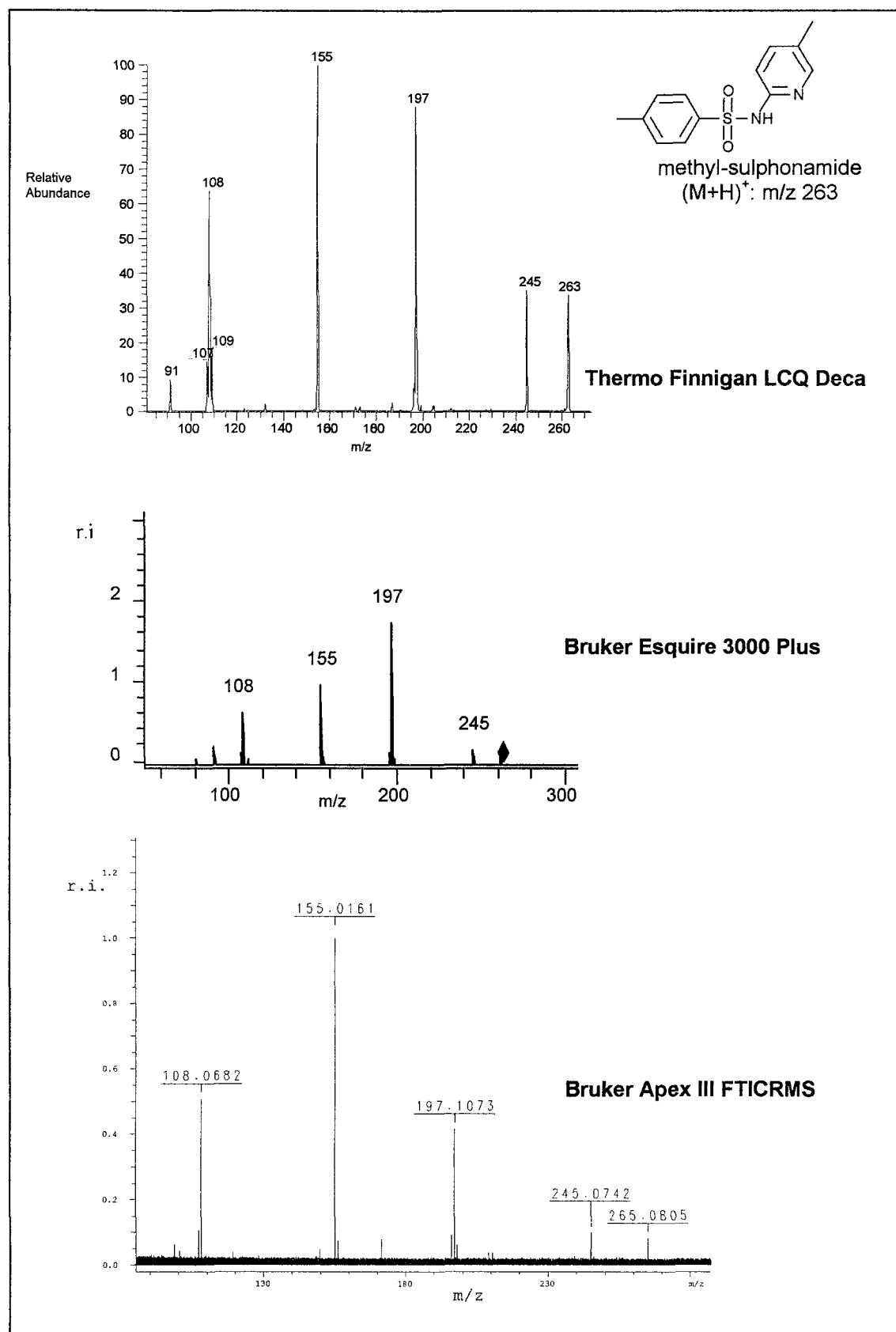


**Figure 1:** ES-MS/MS spectra obtained for a methylsulphonamide from the two conventional bench-top ion traps and the FTMS.

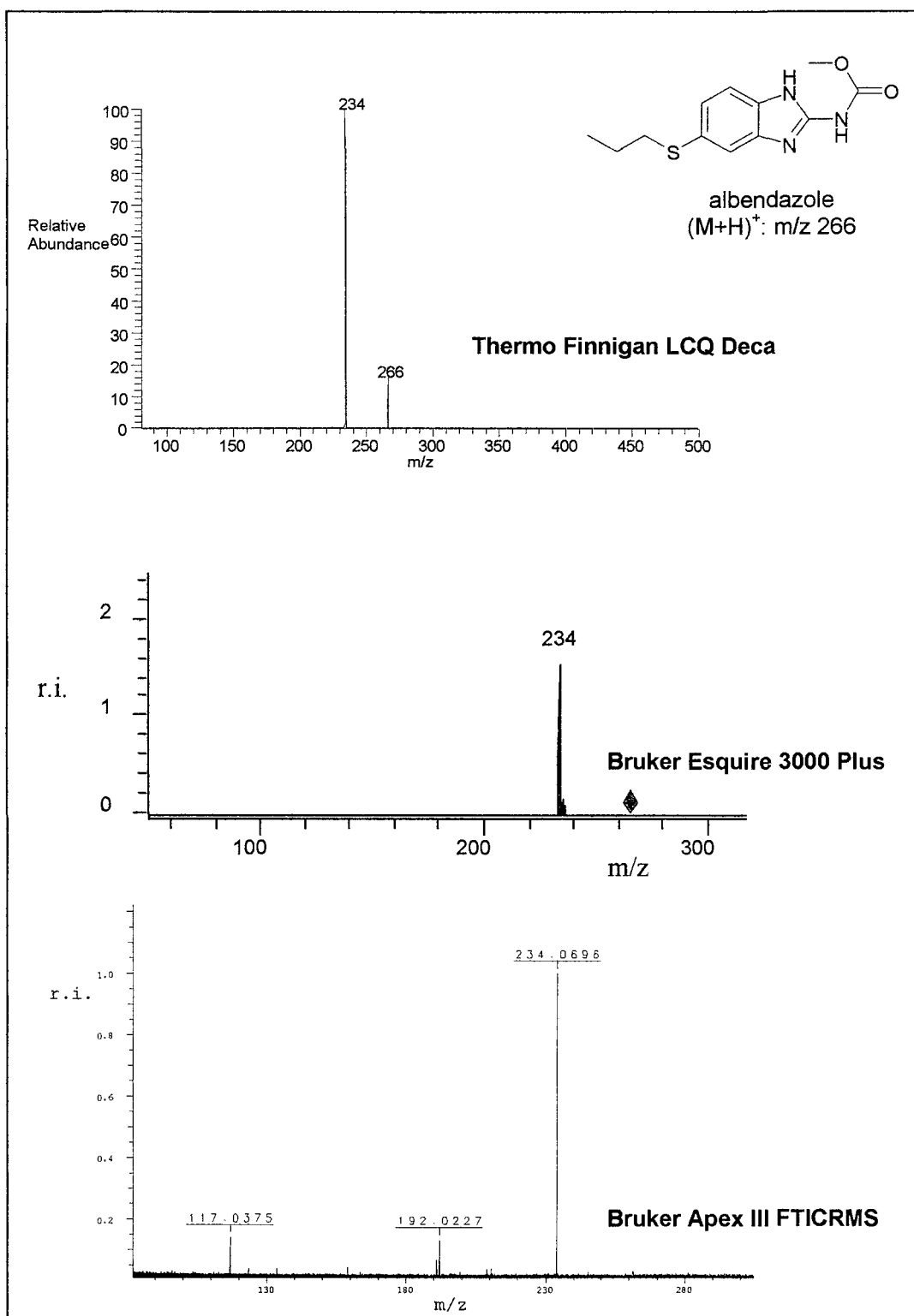


**Figure 2:** ES-MS/MS spectra obtained for albendazole from the two conventional bench-top ion traps and the FTMS.

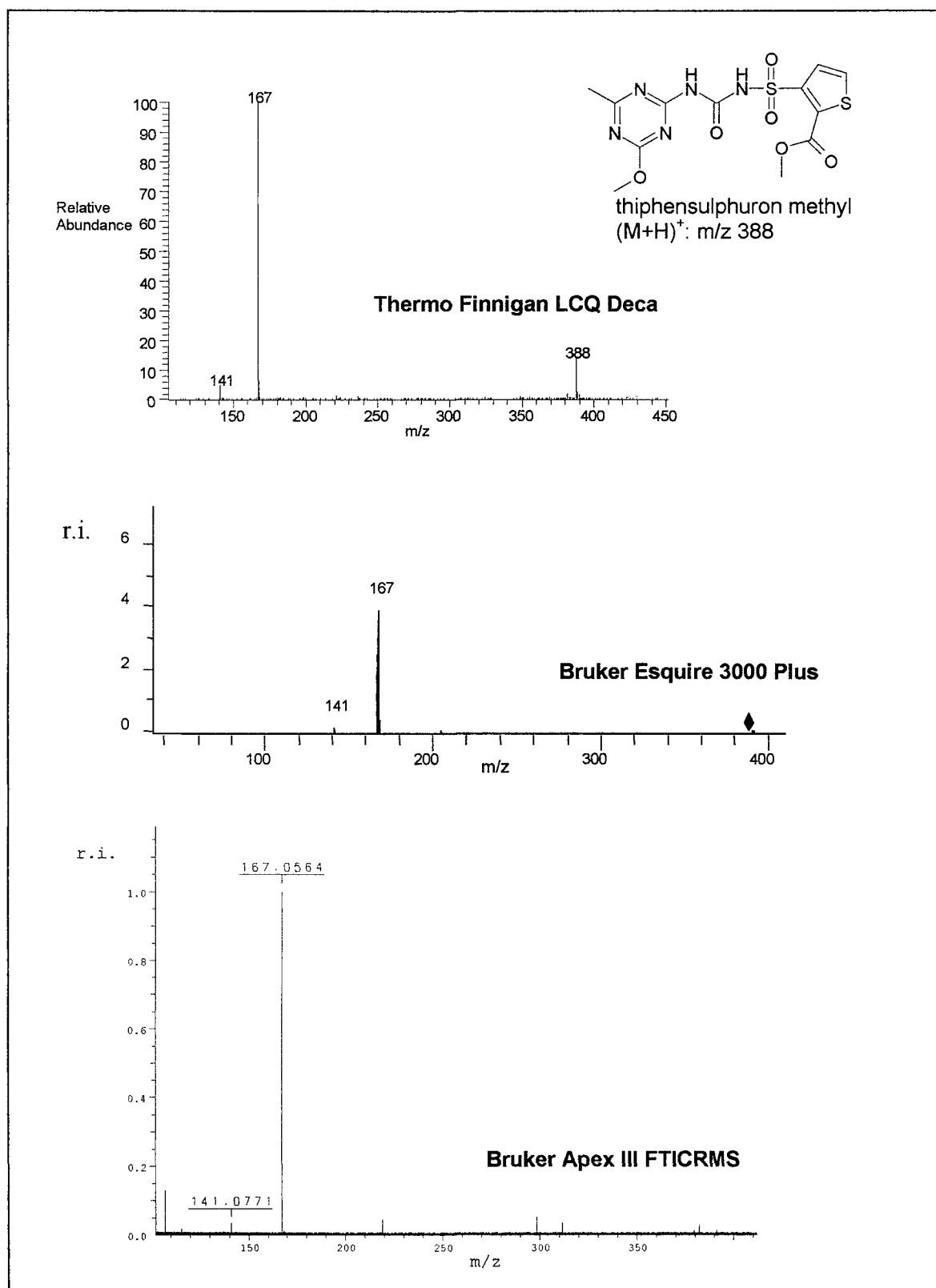


**Figure 3:** ES-MS/MS spectra obtained for thiphen sulphuron methyl from the two conventional bench-top ion traps and the FTMS.

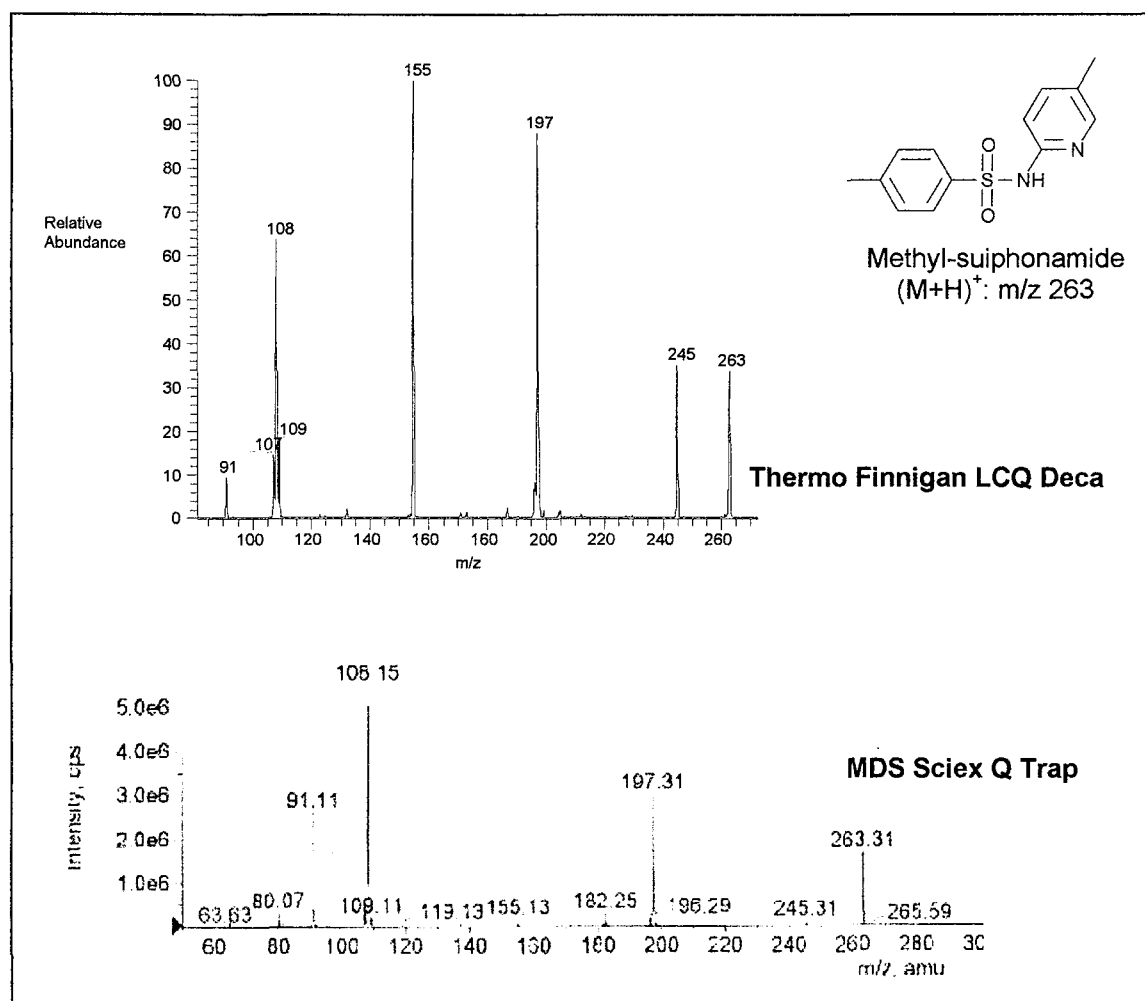


**Figure 4:** Comparison between the ES-MS/MS spectra obtained for a methyl-sulphonamide on a conventional, spherical, quadrupole ion trap and the linear ion trap.

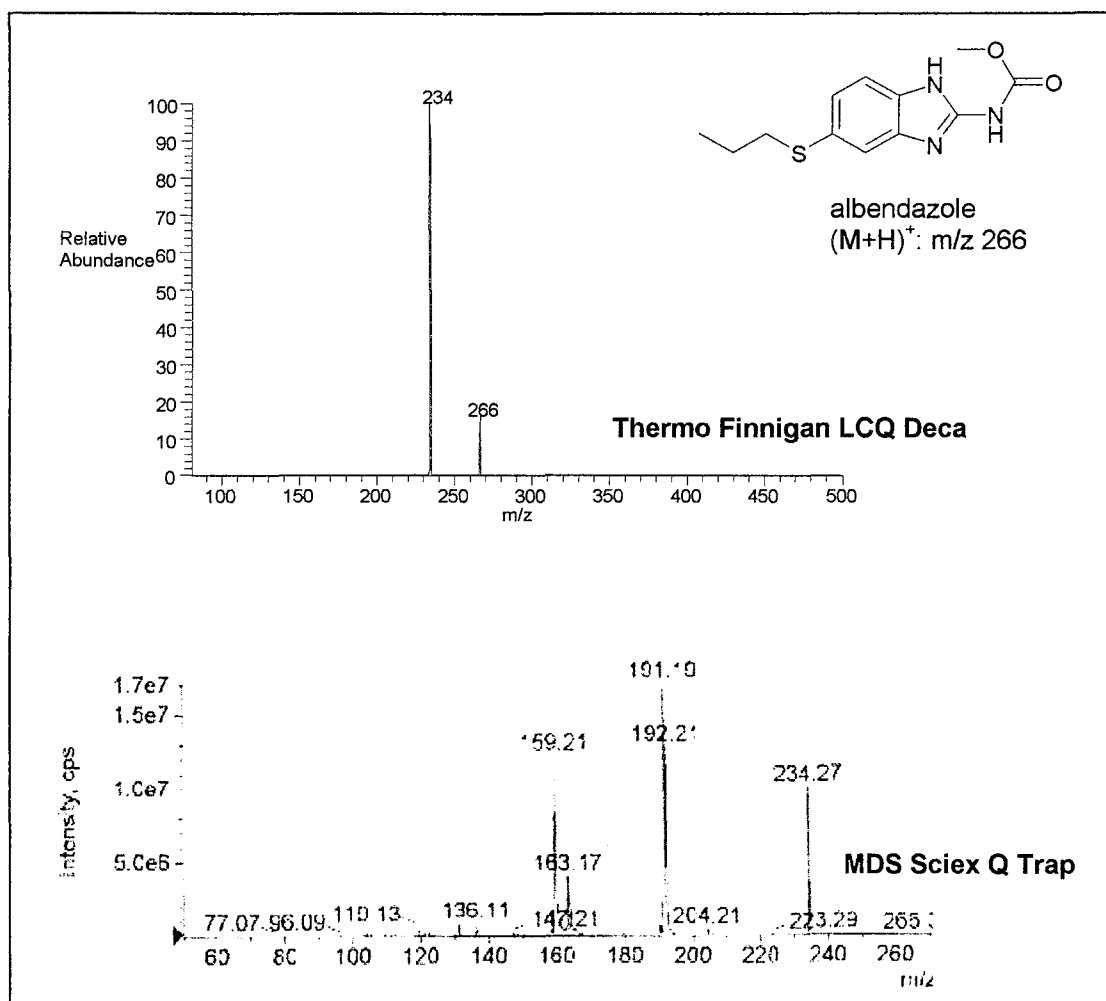


**Figure 5:** Comparison between the ES-MS/MS spectra obtained for albendazole on a conventional, spherical, quadrupole ion trap and the linear ion trap.

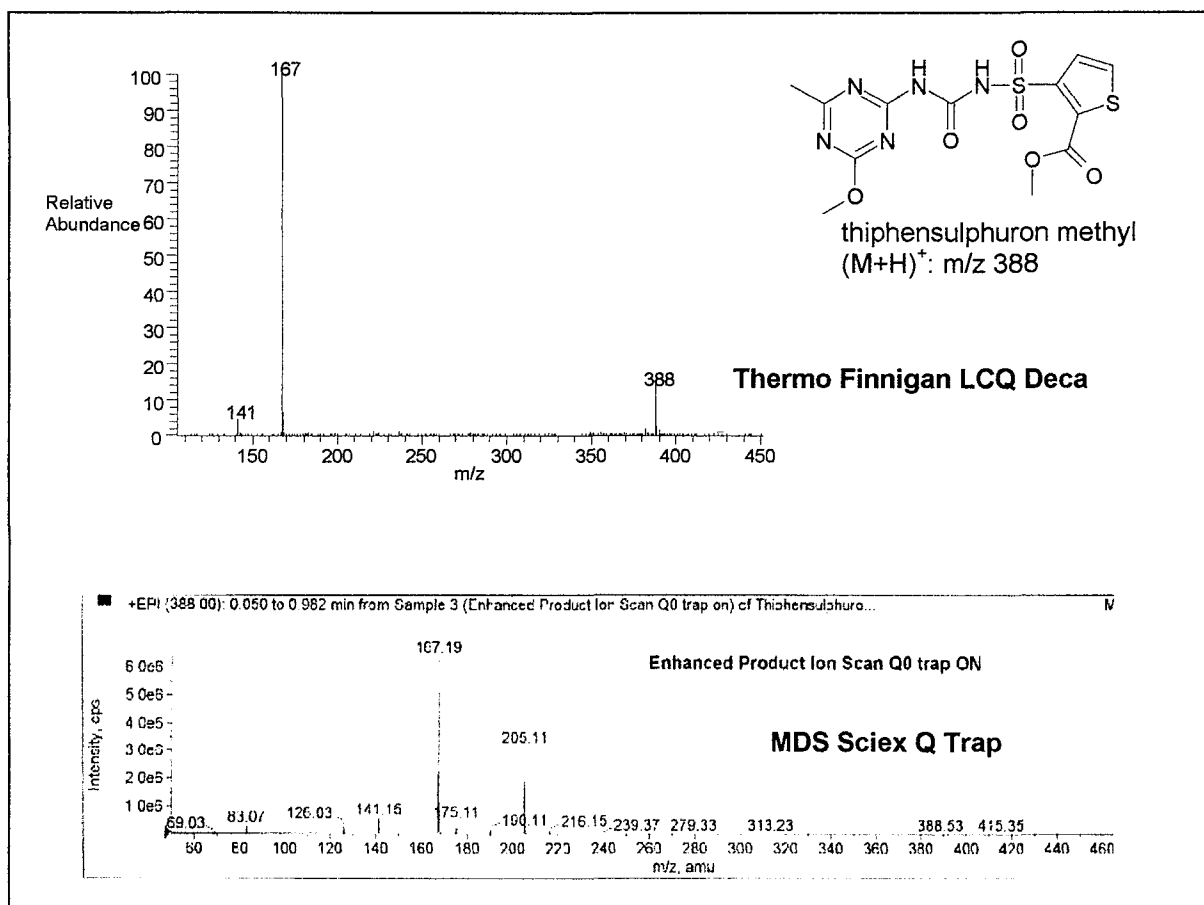


**Figure 6:** Comparison between the ES-MS/MS spectra obtained for thiphen sulphuron methyl on a conventional, spherical, quadrupole ion trap and the linear ion trap.

---

References

1. Young RN. *Pure Appl. Chem.* 1999; **71**: 1655.
2. Grayson MA. *Measuring Mass*. 2002; 1<sup>st</sup> Edition.
3. Van Hijfte L, Marciniac G, Froloff N. *J. Chromatogr. B.* 1999; **725**: 3.
4. Triolo A, Altamura M, Cardinali F, Sisto A, Maggi CA. *J. Mass Spectrom.* 2001; **36**: 1249.
5. Landro JA, Taylor ICA, Stirtan WG, Osterman DG, Kristie J, Hunnicutt EJ, Rae PMM, Sweetnam PM. *J. Pharmacol. Toxicol. Method.* 2000; **44**: 273.
6. Venton DL, Woodbury CP. *Chemometr. Intell. Lab. Syst.* 1999; **48**: 131.
7. Thorpe DS. *Comb. Chem. High Throughput Scr.* 2000; **3**: 421.
8. Ripka WC, Barker G, Krakover J. *Drug Discov. Today.* 2001; **6**: 471.
9. Lambert P-H, Bertin S, Fauchère J-L, Volland J-P. *Comb. Chem. High Throughput Scr.* 2001; **4**: 317.
10. Adang AEP, Hermkens PHH. *Curr. Medicinal. Chem.* 2001; **8**: 985.
11. Myers PL. *Curr. Opin. Biotechnol.* 1997; **8**: 701.
12. Enjalbal C, Martinez J, Aubagnac J-L. *Mass Spectrom. Rev.* 2000; **19**: 139.
13. Kassel DB. *Chem. Rev.* 2001; **101**: 255.
14. Fauchère J-L, Boutin JA, Henlin J-M, Kucharczyk N, Ortuno J-C. *Chemometr. Intell. Lab. Syst.* 1998; **43**: 43.
15. Merrifield RB. *J. Am. Chem. Soc.* 1963; **85**: 2149.
16. Geysen HM, Meloen RH, Barteling S. *J. Proc. Natl. Acad. Sci. USA.* 1984; **81**: 3998.
17. Furka A, Sebestyen F, Asgedom M, Dibo G. *Int. J. Pept. Protein Res.* 1991; **37**: 487.
18. Houghten RA, Pinilla C, Blondelle SE, Appel JR, Dooley CT, Cuervo J. *Nature.* 1991; **354**: 84.
19. Lam KS, Salmon SE, Hersh EM, Hruby VJ, Kazmierski WM, Knapp RJ. *Nature.* 1991; **354**: 82.
20. Furka A. *Drug Develop. Res.* 1995; **36**: 1.
21. Hoke II SH, Morand KL, Greis KD, Baker TR, Harbol KL, Dobson RLM. *Int. J. Mass Spectrom.* 2001; **212**: 135.
22. Shin YG, van Breemen RB. *Biopharm. Drug Dispos.* 2001; **22**: 353.
23. Lee MS, Kerns EH. *Mass Spectrom. Rev.* 1999; **18**: 187.
24. Bauser M. *J. Chromatogr. Sci.* 2002; **40**: 292.
25. Swali V, Langley GJ, Bradley M. *Curr. Opin. Chem. Biol.* 1999; **3**: 337.
26. Niessen WMA. *J. Chromatogr. A.* 1999; **856**: 179.
27. Lim C-K, Lord G. *Biol. Pharm. Bull.* 2002; **25**: 547.
28. Plumb RS, Dear GJ, Mallett DN, Higton DM, Pleasance S, Biddlecombe RA. *Xenobiotica.* 2001; **31**: 599.
29. Siuzdak G, Lewis JK. *Biotechnol. Bioeng.* 1998; **61**: 127.
30. Kyranos JN, Cai H, Wei D, Goetzinger WK. *Curr. Opin. Biotechnol.* 2001; **12**: 105.
31. Hughes I, Hunter D. *Curr. Opin. Chem. Biol.* 2001; **5**: 243.

- 
32. Yates N, Wislocki D, Roberts A, Berk S, Klatt T, Shen D-M, Willoughby C, Rosauer K, Chapman K, Griffin P. *Anal. Chem.* 2001; **73**: 2941.
  33. Süßmuth RD, Jung G. *J. Chromatogr. B.* 1999; **725**: 49.
  34. Cheng X, Hochlowski J. *Anal. Chem.* 2002; **74**: 2679.
  35. Papac DI, Shahrokh Z. *Pharmaceut. Res.* 2001; **18**: 131.
  36. Loo JA. *Eur. Mass Spectrom.* 1997; **3**: 93.
  37. Enjalbal C, Maux D, Martinez J, Combarieu R, Aubagnac J-L. *Comb. Chem. High Throughput Scr.* 2001; **4**: 363.
  38. Pullen FS, Perkins GL, Burton KJ, Ware RS, Teague MS, Kiplinger JP. *J. Am. Soc. Mass Spectrom.* 1995; **6**: 394.
  39. Taylor LCE, Johnson RL, Raso L. *J. Am. Soc. Mass Spectrom.* 1995; **6**: 387.
  40. Tong H, Bell D, Tabei K, Siegel MM. *J. Am. Soc. Mass Spectrom.* 1999; **10**: 1174.
  41. Niessen WMA. *J. Chromatogr. A.* 1998; **794**: 407.
  42. Trauger SA, Webb W, Siuzdak G. *Spectroscopy.* 2002; **16**: 15.
  43. Sadagopan N, Watson JT. *J. Am. Soc. Mass Spectrom.* 2000; **11**: 107.
  44. Falick AM, Hines WM, Medzihradzsky KF, Baldwin MA, Gibson BW. *J. Am. Soc. Mass Spectrom.* 1993; **4**: 882.
  45. Roepstorff P, Fohlmann J. *Biomed. Mass Spectrom.* 1984; **11**: 601.
  46. Johnson RS, Biemann K. *Biomed. Environ. Mass Spectrom.* 1989; **18**: 945.
  47. Ashcroft A. Personal Communication.
  48. Jonsson AP. *Cell. Mol. Life Sci.* 2001; **58**: 868.
  49. McLafferty FW. *Interpretation of Mass Spectra.* 1966; 1<sup>st</sup> Edition.
  50. Budzikiewicz H, Djerassi C, Williams DH. *Mass Spectrometry of Organic Compounds.* 1967; 1<sup>st</sup> Edition.
  51. Porter QN. *Mass Spectrometry of Heterocyclic Compounds.* 1985; 2<sup>nd</sup> Edition.
  52. Baumann C, Cintora MA, Eichler M, Lifante E, Cooke M, Przyborowska A, Halket JM. *Rapid Commun. Mass Spectrom.* 2000; **14**: 349.
  53. Gaskell SJ. *J. Mass Spectrom.* 1997; **32**: 677.
  54. Bakhtiar R, Nelson RW. *Biochem. Pharmacol.* 2000; **59**: 891.
  55. Hop CECA, Bakhtiar R. *Biospectroscopy.* 1997; **3**: 259.
  56. Mosi AA, Eigendorf GK. *Curr. Org. Chem.* 1998; **2**: 145.
  57. Siuzdak G. *Mass Spectrometry for Biotechnology.* 1996; 1<sup>st</sup> Edition.
  58. De Hoffmann E, Stroobant V. *Mass Spectrometry: Principles and Applications.* 2002; 2<sup>nd</sup> Edition.
  59. Kebarle P. *J. Mass Spectrom.* 2000; **35**: 804.
  60. Dole M, March LL, Hines RL, Mobley RC, Ferguson LD, Alice MB. *J. Chem. Phys.* 1968; **49**: 2240.
  61. Iribarne JV, Thomson BA. *J. Chem. Phys.* 1976; **64**: 2287.
  62. Catinella S, Pelizzi N, Barbosa S, Favretto D, Seraglia R, Traldi P. *Rapid Commun. Mass Spectrom.* 2002; **16**: 1897.
-

- 
63. March RE. *J. Mass Spectrom.* 1997; **32**: 351.
  64. Wong PSH, Cooks RG. *CurrentSeparations.com*. 1997; **16(3)**.
  65. Hao C, March RE. *Int. J. Mass Spectrom.* 2001; **212**: 337.
  66. March RE. *Rapid Commun. Mass Spectrom.* 1998; **12**: 1543.
  67. Todd JFJ, March RE. *Int. J. Mass Spectrom.* 1999; **190/191**: 9.
  68. Creaser CS, Stygall JW. *Trends Anal. Chem.* 1998; **17**: 583.
  69. Thermo Electron Corporation. *Finnigan LCQ Advantage: Instructions Manual*. 2002.
  70. De Hoffmann E. *J. Mass Spectrom.* 1996; **31**: 129.
  71. Shukla AK, Futrell JH. *J. Mass Spectrom.* 2000; **35**: 1069.
  72. Futrell JH. *Int. J. Mass Spectrom.* 2000; **200**: 495.
  73. Marshall AG. *Int. J. Mass Spectrom.* 2000; **200**: 331.
  74. Amster IJ. *J. Mass Spectrom.* 1996; **31**: 1325.
  75. Schmid DG, Grosche P, Bandel H, Jung G. *Biotechnol. Bioeng.* 2000; **71**: 149.
  76. Marshall AG, Guan S. *Phys. Scri.* 1995; **T59**: 155.
  77. Marshall AG, Hendrickson CL, Jackson GS. *Mass Spectrom. Rev.* 1998; **17**: 1.
  78. Hendrickson CL, Emmett MR. *Annu. Rev. Phys. Chem.* 1990; **50**: 517.
  79. Laude Jr DA, Johlman CL, Brown RS, Weil DA, Wilkins CL. *Mass Spectrom. Rev.* 1986; **5**: 107.
  80. Johlman CL, White RL, Wilkins CL. *Mass Spectrom. Rev.* 1983; **2**: 389.
  81. Mistrik R. *Finnigan Xcalibur™, HighChem®: Mass Frontier™ Software, Revision B XCALI-97012*, 2000.
  82. Kowalski BR. *Chemometrics-Mathematics and Statistics in Chemistry*. 1983; 1<sup>st</sup> Edition.
  83. Brereton RG. *Chemometrics: Applications of Mathematics and Statistics to Laboratory Systems*. 1990; 1<sup>st</sup> Edition.
  84. Miller JC, Miller JN. *Statistics for Analytical Chemistry*. 1993. 3<sup>rd</sup> Edition.
  85. Mandair GS, Light M, Russell A, Hursthouse M, Bradley M. *Tetrahedron Lett.* 2002; **43**: 4267.
  86. Zhu Y, Wong PSH, Cregor M, Gitzen JF, Coury LA, Kissinger PT. *Rapid Commun. Mass Spectrom.* 2000; **14**: 1695.
  87. Heinig K, Henion J. *J. Chromatogr. B.* 1999; **735**: 171.
  88. Möder M, Löster H, Herzsuh R, Popp P. *J. Mass Spectrom.* 1997; **32**: 1195.
  89. Gaskell SJ, Guenat C, Millington DS, Maltby DA, Roe CR. *Anal. Chem.* 1986; **58**: 2801.
  90. Deng Y, Henion J, Li J, Thibault P, Wang C, Harrison DJ. *Anal. Chem.* 2001; **73**: 639.
  91. Cheng KN, Rosankiewicz J, Tracey BM, Chalmers RA. *Biomed. Environ. Mass Spectrom.* 1989; **18**: 668.
  92. Vernez L, Hopfgartner G, Wenk M, Krähenbühl S. *J. Chromatogr. A.* 2003; **984**: 203.
  93. Tallarico C, Pace S, Longo A. *Rapid Commun. Mass Spectrom.* 1998; **12**: 403.
  94. Briand G, Fontaine M, Schubert R, Ricart G, Degand P, Vamecq J. *J. Mass Spectrom.* 1995; **30**: 1731.
  95. McCellan JE, Quarmby ST, Yost RA. *Anal. Chem.* 2002; **74**: 5799.
-

- 
96. Bourcier S, Hoppilliard Y, Pechiné YM, Perez F. *Eur. J. Mass Spectrom.* 2000; **6**: 175.
97. Mueller P, Schulze A, Schindler I, Ethofer T, Buehrdel P, Ceglarek U. *Clin. Chim. Acta.* 2003; **327**: 1.
98. Carpenter KH, Wiley V. *Clin. Chim. Acta.* 2002; **322**: 1.
99. Rashed MS. *J. Chromatogr. B.* 2001; **758**: 27.
100. Rolinski B, Arnecke R, Dame T, Kreischer J, Olgemöller B, Wolf E, Balling R, Hrabé de Angelis M, Roscher AA. *Mamm. Genome.* 2000; **11**: 547.
101. Rashed MS, Ozand PT, Harrison ME, Watkins PJF, Evans S. *Rapid Commun. Mass Spectrom.* 1994; **8**: 129.
102. Kodo N, Millington DS, Norwood DL, Roe CR. *Clin. Chim. Acta.* 1989; **186**: 383.
103. Celma C, Allué JA, Pruñonosa J, Peraire C, Obach R. *J. Chromatogr. A.* 2000; **870**: 77.
104. Josephs JL. *Rapid Commun. Mass Spectrom.* 1995; **9**: 1270.
105. Liguori A, Mascaro P, Porcelli B, Sindona G, Uccella N. *Org. Mass Spectrom.* 1991; **26**: 608.
106. Hieda Y, Kashimura S, Hara K, Kageura M. *J. Chromatogr. B.* 1995; **667**: 241.
107. Catinella S, Rovatti L, Hamdan M, Porcelli B, Frosi B, Marinello E. *Rapid Commun. Mass Spectrom.* 1997; **11**: 869.
108. Todi F, Mendonca M, Ryan M, Herskovits P. *J. Vet. Pharmacol. Therap.* 1999; **22**: 333.
109. Tuomi T, Johnsson T, Reijula K. *Clin. Chem.* 1999; **45**: 2164.
110. Ternes T, Bonerz M, Schmidt T. *J. Chromatogr. A.* 2001; **938**: 175.
111. Schneider H, Ma L, Glatt H. *J. Chromatogr. B.* 2003; **789**: 227.
112. Cannavan A, Haggan SA, Kennedy DG. *J. Chromatogr. B.* 1998; **718**: 103.
113. Casetta B, Cozzani R, Cinquina AL, di Marzio S. *Rapid Commun. Mass Spectrom.* 1996; **10**: 1497.
114. Bean KA, Henion JD. *J. Chromatogr. A.* 1997; **791**: 119.
115. Balizs G. *J. Chromatogr. B.* 1999; **727**: 167.
116. Hogendoorn EA, Westhuis K, Dijkman E, Heusinkveld HAG, Chamraskul P, Biadul P, Baumann RA, Cornelese AA, Van Der Linden MA. *Int. J. Environ. Anal. Chem.* 2000; **78**: 67.
117. Moghaddam MF, Trubey RK, Anderson JJ. *J. Agric. Food Chem.* 2000; **48**: 5195.
118. Jeannot R, Sabik H, Sauvard E, Genin E. *J. Chromatogr. A.* 2000; **879**: 51.
119. De Ruyck H, Daeseleire E, De Ridder H. *Analyst.* 2001; **126**: 2144.
120. De Ruyck H, Daeseleire E, Grijspeerd K, De Ridder H, Van Renterghem R. Huyghebaert G. *J. Agric. Food Chem.* 2001; **49**: 610.
121. De Ruyck H, Daeseleire E, De Ridder H, Van Renterghem R. *J. Chromatogr. A.* 2002; **976**: 181.
122. Van Rhijn JA, Lasaroms JJP, Berendsen BJA, Brinkman UAT. *J. Chromatogr. A.* 2002; **960**: 121.
123. Steiner WE, Clowers BH, Fuhrer K, Gonin M, Matz LM, Siems WF, Schultz AJ, Hill HH Jr. *Rapid Commun. Mass Spectrom.* 2001; **15**: 2221.
-

- 
124. Van Berkel GJ, Goeringer DE. *Anal. Chim. Acta*. 1993; **277**: 41.
125. Hideg ZS, Dinya Z. *Anal. Lett.* 1993; **26(12)**: 2637.
126. Kargar T, Bourcier S, Hoppilliard Y. *Rapid Commun. Mass Spectrom.* 1995; **9**: 413.
127. Mortier KA, Maudens KE, Lambert WE, Clauwaert KM, Van Bocxlaer JF, Deforce DL, Van Peteghem CH, De Leenheer AP. *J. Chromatogr. B*. 2002; **779**: 321.
128. Slawson MH, Taccogno JL, Foltz RL, Moody DE. *J. Anal. Toxicol.* 2002; **26**: 430.
129. Milne GWA, Axenrod T, Fales HM. *J. Am. Chem. Soc.* 1970; **92**: 5170.
130. Leclercq PA, Desiderio DM. *Org. Mass Spectrom.* 1973; **7**: 515.
131. Tsang CW, Harrison AG. *J. Am. Chem. Soc.* 1976; **98**: 1301.
132. Van der Greef J, Ten Noever de Brauw MC, Zwinselman JJ, Nibbering NMM. *Org. Mass Spectrom.* 1982; **17**: 274.
133. Kulik W, Heerma W. *Biomed. Environ. Mass.* 1988; **15**: 419.
134. Bouchonnet S, Denhez J-P, Hoppilliard Y, Mauriac C. *Anal. Chem.* 1992; **64**: 743.
135. Dookeran NN, Yalcin T, Harrison AG. *J. Mass Spectrom.* 1996; **31**: 500.
136. Rogalewicz F, Hoppilliard Y, Ohanessian G. *Int. J. Mass Spectrom.* 2000; **196/196**: 565.
137. Meot-Ner M, Field FH. *J. Am. Chem. Soc.* 1973; **95**: 7207.
138. Parker CD, Hercules DM. *Anal. Chem.* 1985; **57**: 698.
139. Bouchoux G, Bourcier S, Hoppilliard Y, Mauriac C. *Org. Mass Spectrom.* 1993; **28**: 1064.
140. Beranová S, Cai J, Wesdemiotis C. *J. Am. Chem. Soc.* 1995; **117**: 9492.
141. Fan TP, Hardin ED, Vestal ML. *Anal. Chem.* 1984; **56**: 1870.
142. Aubagnac IL, Devienne FM, Combarieu R. *Org. Mass Spectrom.* 1985; **20**: 428.
143. Parker CD, Hercules DM. *Anal. Chem.* 1986; **58**: 25.
144. Voigt D, Schmidt J. *Biomed. Mass Spectrom.* 1978; **5**: 44.
145. Chase HC, Kalas TA, Naylor EW. *Annu. Rev. Genomics Hum. Genet.* 2000; **3**: 17.
146. Vazquez S, Truscott RJW, O'Hair RAJ, Weimann A, Sheil MM. *J. Am. Soc. Mass Spectrom.* 2001; **12**: 786.
147. Butcher CPG, Dyson PJ, Johnson BFG, Langridge-Smith PRR, McIndoe JS, Whyte C. *Rapid Commun. Mass Spectrom.* 2002; **16**: 1595.
148. Rogalewicz F, Hoppilliard Y. *Int. J. Mass Spectrom.* 2000; **199**: 235.
149. O'Hair AJR, Broughton PS, Styles ML, Frink BT, Hadad CM. *J. Am. Soc. Mass Spectrom.* 2000; **11**: 687.
150. Johnson DW. *Rapid Commun. Mass Spectrom.* 2001; **15**: 2198.
151. Garland W, Miwa B, Weiss G, Chen G, Saperstein R, MacDonald A. *Anal. Chem.* 1980; **52**: 842.
152. Roach JAG, Sphon JA, Hunt DF, Crow FW. *J. Assoc. Off. Anal. Chem.* 1980; **63**: 452.
153. Henion JD, Thomson BA, Dawson PH. *Anal. Chem.* 1982; **54**: 451.
154. Stout SJ, Steller WA, Manuel AJ, Poeppel MO, DACuncha AR. *J. Assoc. Off. Anal. Chem.* 1984; **67**: 142.
155. Simpson RM, Suhre FB, Shafer JW. *J. Assoc. Off. Anal. Chem.* 1985; **68**: 23.
156. Paulson GD, Mitchell AD, Zaylskie RG. *J. Assoc. Off. Anal. Chem.* 1985; **68**: 1000.
-

- 
157. Gilbert J, Startin JR, Shepherd MJ, Mitchell JC. *J. Chromatogr.* 1986; **356**: 206.
158. Finlay EMH, Games DE, Startin JR, Gilbert J. *Biomed. Environ. Mass Spectrom.* 1986; **13**: 633.
159. Matusik JE, Sternal RS, Barnes CJ, Sphon JA. *J. Assoc. Off. Anal. Chem.* 1990; **73**: 529.
160. Takatsuki K, Kikuchi T. *J. Assoc. Off. Anal. Chem.* 1990; **73**: 886.
161. Carignan G, Carrier K. *J. Assoc. Off. Anal. Chem.* 1991; **74**: 479.
162. Perkins JR, Games DE, Startin JR, Gilbert J. *J. Chromatogr.* 1991; **540**: 239.
163. Johansson IM, Pavelka R, Henion JD. *J. Chromatogr.* 1991; **559**: 515.
164. Perkins JR, Parker CE, Tomer KB. *J. Am. Soc. Mass Spectrom.* 1992; **3**: 139.
165. Doerge DR, Bajic S, Lowes S. *Rapid Commun. Mass Spectrom.* 1993; **7**: 1126.
166. Mooser AE, Koch H. *J. AOAC. Int.* 1993; **76**: 976.
167. Abián J, Churchwell MI, Korfmacher WA. *J. Chromatogr.* 1993; **629**: 267.
168. Porter S. *Analyst.* 1994; **119**: 2753.
169. Kristiansen GK, Brock R, Bojesen G. *Anal. Chem.* 1994; **66**: 3253.
170. Boison JO, Keng LJ-Y. *J. AOAC. Int.* 1995; **78**: 651.
171. Volmer DA. *Rapid Commun. Mass Spectrom.* 1996; **10**: 1615.
172. Gehring TA, Rushing LG, Churchwell MI, Doerge DR, McErlane KM, Thompson Jr HC. *J. Agric. Food Chem.* 1996; **44**: 3164.
173. Bateman KP, Locke SJ, Volmer DA. *J. Mass Spectrom.* 1997; **32**: 297.
174. Niessen WMA. *J. Chromatogr. A.* 1998; **812**: 53.
175. Kennedy DG, McCracken RJ, Cannavan A, Hewitt SA. *J. Chromatogr. A.* 1998; **812**: 77.
176. Hirsch R, Ternes TA, Haberer K, Mehlich A, Ballwanz F, Kratz K-L. *J. Chromatogr. A.* 1998; **815**: 213.
177. Hartig C, Storm T, Jekel M. *J. Chromatogr. A.* 1999; **854**: 163.
178. Combs MT, Ashraf-Khorassani M, Taylor LT. *J. Pharm. Biomed. Anal.* 1999; **19**: 301.
179. Reeves VB. *J. Chromatogr. A.* 1999; **723**: 127.
180. De Baere S, Baert K, Croubels S, De Busser J, De Wasch K, De Backer P. *Analyst.* 2000; **125**: 409.
181. Dost K, Jones DC, Davidson G. *Analyst.* 2000; **125**: 1243.
182. Bartolucci G, Pieraccini G, Villanelli F, Moneti G, Triolo A. *Rapid Commun. Mass Spectrom.* 2000; **14**: 967.
183. Van Eeckhoot N, Perez JC, Van Peteghem. *Rapid Commun. Mass Spectrom.* 2000; **14**: 2331.
184. Ito Y, Oka H, Ikai Y, Matsumoto H, Miyazaki Y, Nagase H. *J. Chromatogr. A.* 2000; **898**: 95.
185. Lindsey ME, Meyer M, Thurman EM. *Anal. Chem.* 2001; **73**: 4640.
186. Kaufmann A, Roth S, Bianca R, Widmer M, Guggisberg D. *J. AOAC Int.* 2002; **85**: 853.
187. Haller MY, Müller SR, Mc Ardell CS, Alder AC, Suter MJ-F. *J. Chromatogr. A.* 2002; **952**: 111.
-

- 
188. Heller DN, Ngoh MA, Donoghue D, Podhorniak L, Righter H, Thomas MH. *J. Chromatogr. B.* 2002; **774**: 39.
189. Verzeegnassi L, Savoy-Perroud M-C, Stadler RH. *J. Chromatogr. A.* 2002; **977**: 77.
190. Pfeifer T, Tuerk J, Bester K, Spiteller M. *Rapid Commun. Mass Spectrom.* 2002; **16**: 663.
191. Bononi M, De Dominicis E, Fossati A, Tateo F. *Ital. J. Food Sci.* 2002; **14**: 295.
192. Cavaliere C, Curini R, Di Corcia A, Nazzari M, Samperi R. *J. Agric. Food Chem.* 2003; **51**: 558.
193. Bogialli S, Curini R, Di Corcia A, Nazzari M, Sergi M. *Rapid Commun. Mass Spectrom.* 2003; **17**: 1146.
194. Suhre FB, Simpson RM, Shafer JW. *J. Agric. Food Chem.* 1981; **29**: 727.
195. Brumley WC, Min Z, Matusik JE, Roach JAG, Barnes CJ, Sphon JA, Fazio T. *Anal. Chem.* 1983; **55**: 1405.
196. Pleasance S, Blay P, Quilliam MA, O'Hara G. *J. Chromatogr.* 1991; **558**: 155.
197. Ramirez-Molina C, Lane S, Taylor N, Langley GJ. Unpublished data.
198. Pleasance S, Thibault P, Kelly J. *J. Chromatogr.* 1992; **591**: 325.
199. Eckers C, Games DE, Mallen DNB, Swann BP. *Biomed. Mass Spectrom.* 1982; **9**: 162.
200. Porter JK, Bacon CW, Robbins JD, Betowski D. *J. Agric. Food. Chem.* 1981; **29**: 653.
201. Barber M, Weisbach JA, Douglas B, Dudek GO. *Chem. Ind. (London).* 1965; 1073.
202. Porter JK, Betowski D. *J. Agric. Food. Chem.* 1981; **29**: 650.
203. Plattner RD, Yates SG, Porter JK. *J. Agric. Food. Chem.* 1983; **31**: 785.
204. Halada P, Jegorov A, Ryska M, Havlíček V. *Chem. Listy.* 1998; **92**: 538.
205. Ardrey RE, Moffat AC. *J. Forens. Sci. Soc.* 1979; **19**: 253.
206. Shelby RA, Olsovská J, Havlíček V, Flieger M. *J. Agric. Food. Chem.* 1997; **45**: 4674.
207. Chen X, Zhong D, Xu H, Schug B, Blume H. *J. Chromatogr. B.* 2002; **768**: 267.
208. Plattner RD, Bennett GA, Stubblefield RD. *J. Assoc. Off. Anal. Chem.* 1984; **67**: 734.
209. Uyakul D, Isobe M, Goto T. *J. Assoc. Off. Anal. Chem.* 1989; **72**: 491.
210. Hurst WJ, Martin RA, Vestal CH. *J. Liq. Chromatogr.* 1991; **14**: 2541.
211. Coppiello A, Famiglini G, Tirrillini V. *Chromatographia.* 1995; **40**: 411.
212. Kussak A, Nilsson C-A, Andersson B, Langridge J. *Rapid Commun. Mass Spectrom.* 1995; **9**: 1234.
213. Vahl M, Jorgensen K. *Z. Lebensm. Unters. Forsch. A.* 1998; **206**: 243.
214. Schatzki TF, Haddon WF. *J. Agric. Food Chem.* 2002; **50**: 3062.
215. Barefoot AC, Reiser RW. *J. Chromatogr.* 1987; **398**: 217.
216. Reiser RW, Barefoot AC, Dietrich RF, Fogiel AJ, Johnson WR, Scott MT. *J. Chromatogr.* 1991; **554**: 91.
217. Garcia F, Henion J. *J. Chromatogr.* 1992; **606**: 237.
218. Shalaby LM, Bramle, Jr FQ, Lee PW. *J. Agric. Food Chem.* 1992; **40**: 513.
219. Klaffenbach P, Holland PT. *J. Agric. Food Chem.* 1993; **41**: 396.
220. Volmer D, Wilkes JG, Levsen K. *Rapid Commun. Mass Spectrom.* 1995; **9**: 767.
221. Dietrich RF, Reiser RW, Stieglitz B. *J. Agric. Food Chem.* 1995; **43**: 531.
-

- 
222. Marek LJ, Koskinen WC. *J. Agric. Food Chem.* 1996; **44**: 3878.
223. Li LYT, Campbell DA, Bennett PK, Henion J. *Anal. Chem.* 1996; **68**: 3397.
224. Di Corcia A, Crescenzi C, Samperi R, Scappaticcio L. *Anal. Chem.* 1997; **69**: 2819.
225. Krynitsky AJ. *J. AOAC. Int.* 1997; **80**: 392.
226. Rodriguez M, Orescan DB. *Anal. Chem.* 1998; **70**: 2710.
227. Shimamura Y, Tomiyama N, Murakoshi M, Kobayashi H, Matano O. *J. Pesticide Sci.* 1998; **23**: 241.
228. Bossi R, Seiden P, Andersen SM, Jacobsen CS, Streibig JC. *J. Agric. Food Chem.* 1999; **47**: 4462.
229. Dost K, Jones DC, Auerbach R, Davidson G. *Analyst.* 2000; **125**: 1751.
230. Hager JW. *Rapid Commun. Mass Spectrom.* 2002; **16**: 512.
231. Wiebkin PF. *Personal Communication.*
232. Bu H-Z, Poglod M, Micetich RG, Khan JK. *J. Chromatogr. B.* 2000; **738**: 259.
233. Vree TB, Schoondermark-van de Ven E, Verwey-van Wissen CPWGM, Baars AM, Swolfs A, van Galen PM, Amatdjais-Groenen H. *J. Chromatogr. B.* 1995; **670**: 111.
234. Korfmacher WA, Cox KA, Bryant MS, Veals J, Ng K, Watkins R, Lin C-C. *Drug Discov. Today.* 1997; **2**: 532.
235. Liu DQ, Xia Y-Q, Bakhtiar R. *Rapid Commun. Mass Spectrom.* 2002; **16**: 1330.
236. Clarke NJ, Rindgen D, Korfmacher WA, Cox KA. *Anal. Chem.* 2001; **73**: 430A.